Letter from the Editors

The regular world congress of the International Union of Biochemistry and Molecular Biology (IUBMB) was held in Shanghai in august 2009. This forum takes place regularly every three years and brings together thousands of scientists from all over the world. The sweep of considered questions is broad and covers almost every possible topic, which can be brought under the general umbrella of Life Sciences. It is worth admitting that the World and European International versions of the congress have become less attractive. This is mostly because of the absence of the "stars," the researchers who have initiated the development of dramatically new trends in science. Scientists with great interest attend more specialized forums, and the ability of the Internet and modern telecommunication often eliminate the necessity for personal communication. In the present case, the Shanghai congress was a pleasant exception. Suffice to say that plenary lectures were given by four Nobel Prize winners – Kurt Wüthrich, Aaron Ciechanover, Sidney Altman, and Luc Montagnier. Three of them made their reports a summary of their work for the Nobel Prize discovery, namely NMR proteins, ubiquitin-dependent processing of proteins, and the world of RNA. Luc Montagnier, the man who discovered the human immunodeficiency virus (2008 prize in physiology and medicine), disappointed the audience because he did not speak on immunodeficiencies but chose to lecture on electromagnetic waves conduction through DNA.

The slogan of the congress "Biomolecules for the Quality of Life" defined the plenary and symposium sessions. Biomedical research was the overriding theme. It was conclusively shown, using several examples, that the discovery of the new signal transduction pathway, enzyme, receptor-ligand low-molecular weight bioregulator inevitably leads to the target-pointed search of a new therapeutic reagent. Not only is the direct work of the research groups devoted to this aim, but the patent and innovation departments of the company working with these researchers are as well. Everything is devoted to achieving efficiency in the work of scientists, could realize in biomedicine. Actually the final states of any research are preclinical and clinical investigations. Such an adequate mechanism has resulted in the introduction of dozens of new revolutionary drugs, whose existence we couldn't have suspected several decades ago. In this connection, the plenary lecture by Japanese scientist Shinya Yamanaka should be considered revolutionary. It centered on the induction of cells pluripotency with the determination of cell factors. In all probability, conditions for cells "reprogramming" will be created soon. Today, the combination of the factors influencing stem cells "reprogramming" and subsequent differentiation has been determined. A separate symposium was dedicated to the problem of genetic reprogramming and signal transduction. There is no doubt that progress in this area will bring mankind closer to a solution to the problem of "cell" and "tissue" therapy.

A separate symposium was dedicated to the molecular basis of socially significant diseases. The revolutionary success in drug design, with the use of combinatorial chemistry methods, leads to the creation of effective cells kinase active receptors' inhibitors. This trend evaluated the basis for new anticancer compounds. This research was summarized in the reports of pioneers in this sphere, Axel Ulrich (Germany) and Joseph Jordan (Israel). Neurodegenerative diseases took a special place in this section. They were considered in reports dedicated to cells' channels, drugs' compounds, which influence the permeability of these channels, and pathologies of proteins folding were examined. In this connection, animal models in which these pathologies developed were scrutinized. Reports by Susan Ackerman and Marie Chesselet were dedicated to the investigation of the neurodegeneration and therapeutic influence on these processes in animal models.

The glycobiology section was quite interesting. There is no doubt that intercellular contacts and signal transduction depend on the cells' "carbohydrates environment." Reports on cutting-edge proteomic investigations deserved praise. It is possible to say that human proteomic portrait creation is really in process.

The number of reports from Russia has greatly fallen due to the economic difficulties in Russian science. Several forums are held with no Russian participation, and of course this fact doesn't reflect today's condition in life sciences research. The Shanghai forum was a pleasant exception. P.G. Georgiev, E.S. Gromova, S.M. Deyev, O.A. Dontsova, A.M. Egorov, S.A. Nedospasov and the authors of this letter were invited to speak at the symposium.

It is important to mention the developments in Chinese science. Some ten years ago, such a forum with the participation of a great number of Chinese scientists was unimaginable. The right policies of the Chinese government in attracting Chinese scientists living in the U.S. and Europe have yielded results. Institutes and laboratories involved in cutting-edge science have now appeared in China.

A.G. Gabibov
S.N. Kochetkov

Docking approaches are further improved by implementing new algorithms of the conformational search and new scoring functions (methods to estimate the free energy of ligand binding). Scoring functions may include either components of molecular mechanics force fields [2] or empirical terms, e.g. hydrogen bonds described by their geometrical parameters [4]. In this work we studied stacking interactions, which usually are not properly taken into account in widely used scoring functions.

THE PARAMETERS OF STACKING INTERACTIONS

Of all the various types of interactions in biomolecular complexes (such as hydrogen bonds, salt bridges, etc.), the stacking of aromatic substances deserves special attention. Most drugs include aromatic fragments in their chemical structure, and stacking often plays a notable role in their recognition by protein-targets. We have recently shown that an explicit account of stacking in scoring functions increases the efficiency of ATP docking [5]. The aromatic interactions were identified by the mutual orientation of two cycles described by geometrical parameters: the height h and displacement d of one cycle relative to the other, and the angle between their planes (Fig. 1).

However, the range of these parameters, which corresponds to the presence or absence of a stacking contact, is still not very well defined and usually taken as arbitrary [6, 7]. Defining it more accurately would assist in developing more efficient scoring functions and should increase the prediction quality of the spatial structures of protein-ligand complexes by molecular modeling methods. With this aim in view, we performed an analysis of the spatial structures of protein-ligand complexes determined experimentally with atomic resolution where ligands contained adenine or guanine as a substructure.

One well-known example of stacking interactions is the parallel packing of purine and pyrimidine nucleobases in DNA [8, 9]. Some aromatic compounds tend to orient perpendicular to each other (T-shaped stacking), as has been shown for amino acids in proteins [7, 10] and for model systems of carbon aromatic cycles (benzene and naphtalene) [11–14]. Besides, such compounds participate in cation–π interactions, where a positively charged group interacts with the negatively charged cloud of aromatic π-electrons [15–17].

Taking all that into account, we analyzed the distribution of geometrical parameters h, d, and α for contacts of adenine and guanine moieties of ligands with the aromatic side chains of receptor amino acids Phe, Tyr, Trp, and His, as well as with the positively charged guanidine group of Arg and amino group of Lys. The results obtained for guanine are presented in Fig. 2.

It can be seen that two distinct orientations are typical for Phe: parallel and perpendicular to the guanine plane (Fig. 2, shown in red and green, respectively). The displacement d lies in the same range 0–3 Å for both types of contacts. Meanwhile, they clearly differ in the value of height h, which is <4.5 for parallel Å and <5.5 Å for perpendicular orientation. Similar distributions were obtained for Tyr, Trp, and His, though the data are scarcer in these cases. However, the T-shaped contact is not as typical for Tyr, Trp, and His as it is for Phe.

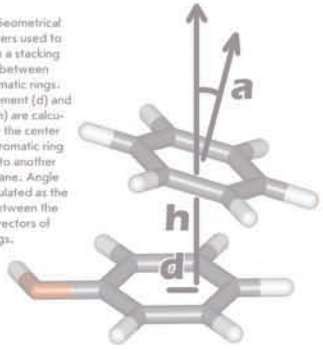

Fig. 1. Geometrical parameters used to describe a stacking contact between two aromatic rings. Displacement (d) and height (h) are calculated for the center of one aromatic ring relative to another ring's plane. Angle (α) is calculated as the angle between the normal vectors of both rings.

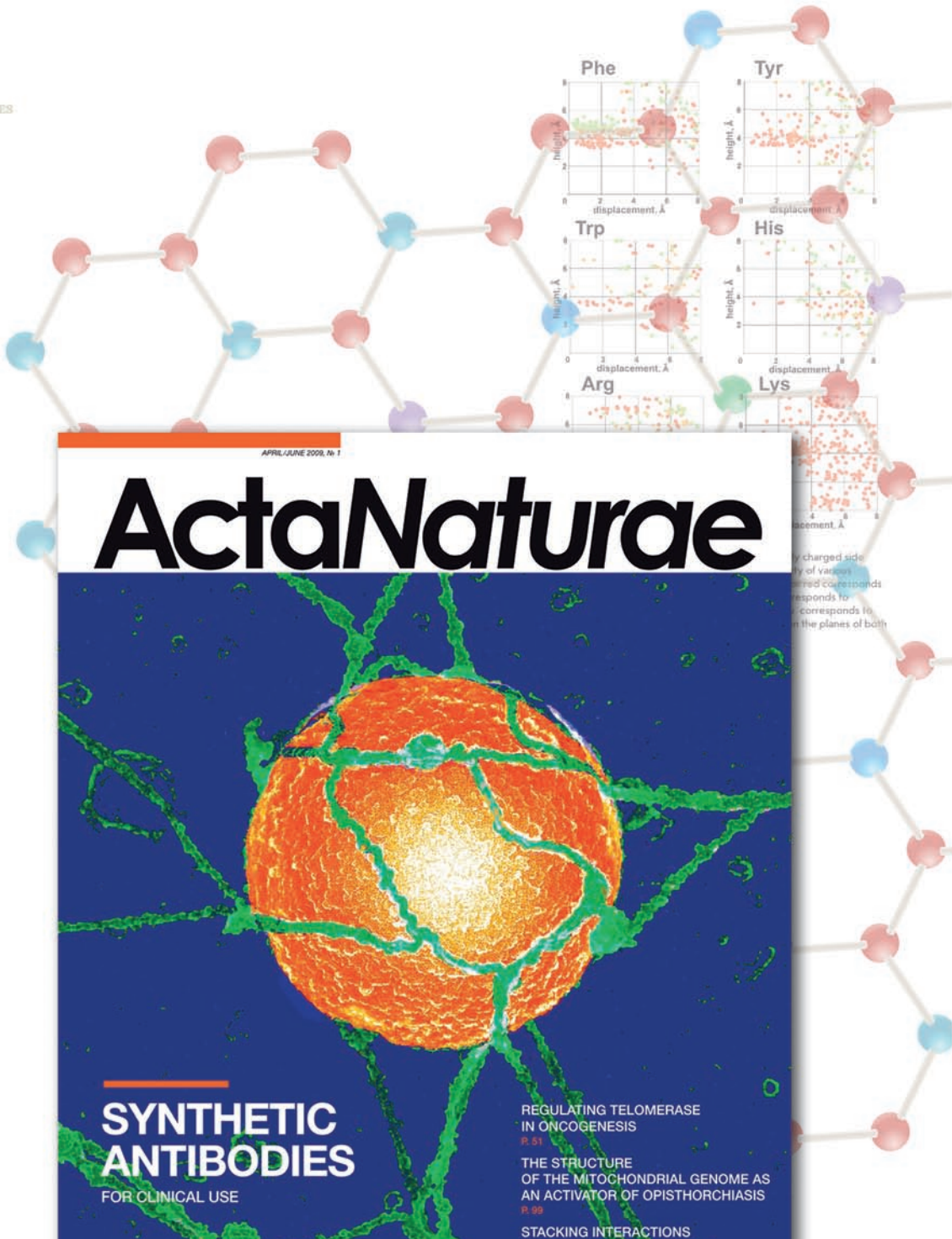

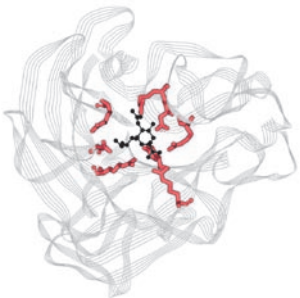

Y.A. Shtyrya, L.V. Mochalova, N.V. Bovin

Influenza Virus Neuraminidase: Structure and Function

Active site of influenza virus A neuraminidase (N2 subtype) in complex with Neu5Ac2en (2-deoxy-2,3-didehydro-N-acetylneuraminic acid). Neu5Ac2en is presented in black, functional a.a. of the active site – red.

O.A. Patutina, N.L. Mironova, V.V. Vlassov, M.A. Zenkova

New Approaches for Cancer Treatment: Antitumor Drugs Based on Gene-Targeted Nucleic Acids

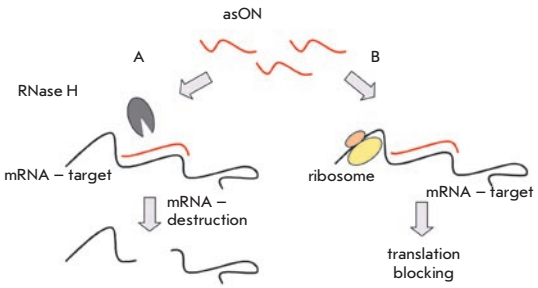

How antisense oligonucleotides (asON) work. (a) RNA is cleaved as a part of a heteroduplex with the asON by RNase H. (b) Block of translation caused by binding of the oligonucleotide onto the mRNA

T. Shcheglova, S.P. Makker, A. Tramontano

Covalent Binding Antibodies Suppress Advanced Glycation: On the Innate Tier of Adaptive Immunity

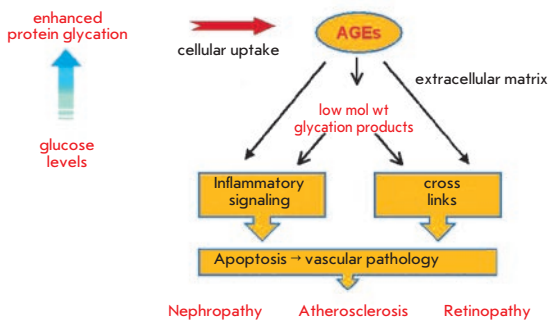

Advanced Glycation Endproducts in Pathology. Protein glycation due to hyperglycemia or normal aging is further modified in the body to advanced glycation endproducts (AGE). These AGE may be further broken down to glycated peptides and low-molecular-weight AGEs. Both high- and low-molecular weight AGEs could be taken up by vascular tissues, by cellular receptors, and by cross-linking of the extracellular matrix. These modifications account for the cytotoxicity and tissue necrosis and ultimately lead to vascular pathologies, as is seen in diabetic complications

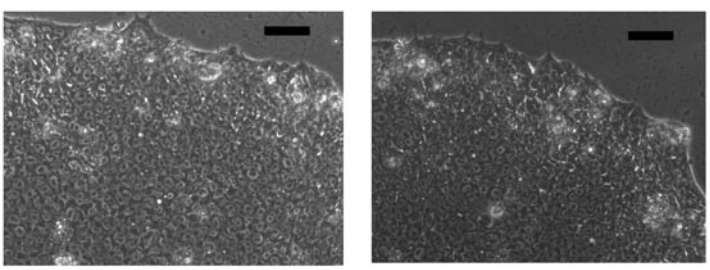

Morphology of iPS derived from an endothelium, feeder-free culture. A – Bright field image of iPS colony. B – Image of ESC colony. Bar scale – 100 mkm

M.V. Shutova, A.N. Bogomazova, M.A. Lagarkova, S.L. Kiselev

Derivation and Characterization of Human Induced Pluripotent Stem Cells

ActaNaturae
JULY-SEPTEMBER 2009, № 2

Founders
Russian Federation Agency
for Science and Innovation,
Lomonosov Moscow State University,
Park Media Ltd

Address: 119991 Moscow, Russia, Leninskiye Gory, Nauchny
Park MGU, vlad.1, stroeniye 75G.
Phone/Fax: +7 (495) 930 80 06
E-mail: knorrevd@gmail.com, rpetrov@strf.ru, vsychev@strf.ru

Номер подписан в печать 28 октября 2009 г.
Тираж 800 экз. Цена свободная.
Отпечатано в типографии ООО «Принт Сэйл»

CONTENTS

Letter from the Editors 1

FORUM

V.T. Ivanov
The 50th Anniversary of the M. M. Shemyakin & Yu. A. Ovchinnikov Institute of Bioorganic Chemistry of the Russian Academy of Sciences 6

A.V. Zelenin and V.L. Karpov
In the Front Line of World Science 9

The Institute of Chemical Biology and Fundamental Medicine of the Siberian Division of the Russian Academy of Sciences (until 2003 the Novosibirsk Institute of Bioorganic Chemistry) 13

REVIEWS

V.A. Stonik
Marine Natural Products: A Way to New Drugs 15

Y.A. Shtyrya, L.V. Mochalova, N.V. Bovin
Influenza Virus Neuraminidase: Structure and Function 26

A.V. Nemukhin, B.L. Grigorenko, A.P. Savitsky
Computer Modeling of the Structure and Spectra of Fluorescent Proteins 33

O.A. Patutina, N.L. Mironova, V.V. Vlassov, M.A. Zenkova
New Approaches for Cancer Treatment: Antitumor Drugs Based on Gene-Targeted Nucleic Acids 44

V.V. Terskikh, Ye. A. Vorotelyak, A.V. Vasiliev
Self-Renewalof Stem Cells 61

T. Shcheglova, S.P. Makker, and A. Tramontano
Covalent Binding Antibodies Suppress Advanced Glycation: On the Innate Tier of Adaptive Immunity 66

RESEARCH ARTICLES

E.G. Salina, H.J. Mollenkopf, S.H.E. Kaufmann, A.S. Kaprelyants
***M. tuberculosis* Gene Expression during Transition to the "Non-Culturable" State** 73

E.S. Knyazhanskaya, M.A. Smolov, O.V. Kondrashina, M.B. Gottikh
Relative Comparison of Catalytic Characteristics of Human Foamy Virus and HIV-1 Integrases 78

D.M. Shcherbakova, M.I. Zvereva, and O.A. Dontsova
Telomerase Complex from Yeast *Saccharomyces cerevisiae* Contains a Biotinylated Component 81

P.V. Spirin, D. Baskaran, P.M. Rubtsov, M.A. Zenkova, V.V. Vlassov, E.L. Chernolovskaya, V.S. Prassolov
A Comparison of Target Gene Silencing using Synthetically Modified siRNA and shRNA That Express Recombinant Lentiviral Vectors 86

M.V. Shutova, A.N. Bogomazova, M.A. Lagarkova, S.L. Kiselev
Derivation and Characterization of Human Induced Pluripotent Stem Cells 91

E.V. Novosadova, E.S. Manuilova, E.L. Arsenieva, A.N. Lebedev, N.V. Khaidarova, V.Z. Tarantul, and I.A. Grivennikov
Influence of *pub* Gene Expression on Differentiation of Mouse Embryonic Stem Cells into Derivatives of Ecto-, Meso-, and Endoderm *in vitro* 93

D.A. Davydova, E.A.Vorotelyak, Yu.A. Smirnova, R.D. Zinovieva, Yu. A. Romanov, N. V. Kabaeva, V.V. Terskikh, and A.V. Vasiliev
Cell Phenotypes in Human Amniotic Fluid 98

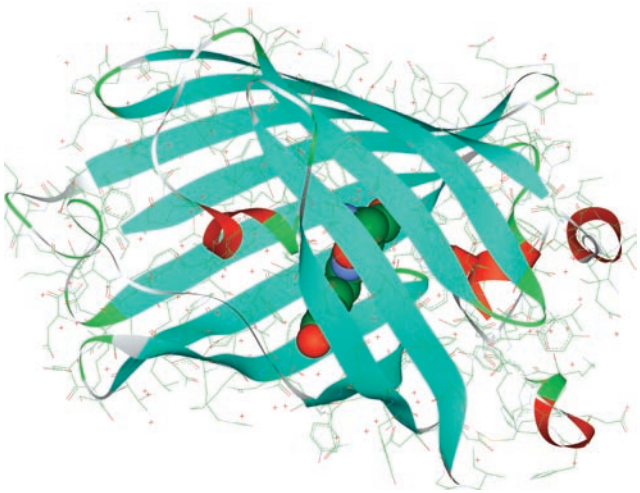

IMAGE ON THE COVER PAGE
Structure of GFP (PDB ID: 1EMA). The chromophore group is emphasized. Fluorescent proteins have a tubby structure consisting of tightly-fitted β-sheets, good shielding from the external environment of a chromophore, based on a hydroxybenzylidene-imidazoline molecule, which is formed in nature from three amino-acid residues inside the protein globule. Transformations occurring with this chromophore group inside the macromolecule upon light illumination at certain wavelengths are the basis of photophysical properties of fluorescent proteins.
The figure was generated with the Discovery Studio 2.5 Visualizer (Accelrys Software Inc.)

The 50th Anniversary of the M. M. Shemyakin & Yu. A. Ovchinnikov Institute of Bioorganic Chemistry of the Russian Academy of Sciences

By Academician V.T. Ivanov, Director of the Institute

Under the February 20, 1959, Resolution of the Presidium of the USSR Academy of Sciences, the Institute for Chemistry of Natural Products was founded within the Academy's Chemical Sciences Division. The institution would go on to play an important part in the development of Russian physical and chemical biology. The founding of the Institute was brought about by the rapid developments in the chemistry of bioactive compounds, the natural products among them, and reflected the growing importance of this field in understanding the mechanisms of biological processes and in development of new medicinal preparations.

The leader of the natonal antibiotics chemistry, academician Mikhail Mikhailovich Shemyakin, was appointed head of the Institute, and he managed to lure the best specialists working in different fields: in the chemistry of carbohydrates, V.N. Orekhovitch and V.M. Stepanov; in the chemistry of antibiotics, future academicians A.S. Khokhlov and M.N. Kolosov, as well as future corresponding member V.K. Antonov; and in the chemistry of lipids, future corresponding member L.D. Bergelson. Recent graduates from higher educational institutions also joined the team and later became members of the USSR Academy of Sciences; they retained, to a significant degree, the scientific identity of the Institute (Yu.A. Ovchinnikov, V.F. Bystrov, E.V. Grishin, V.T. Ivanov, A.I. Miroshnikov and E.D. Sverdlov).

After a short period of time, the Institute became a top scientific establishment in its field in the country, actively interacting with the international community (multiple publications in foreign magazines and broad participation in international symposia).

In the case of depsipeptide antibiotics, the molecular mechanism of the induced cationic permeability of biological and artificial membranes was decoded; the causes of the unique in several cases ionic selectivity were revealed, and the synthesis of a series of new high-performance membrane-active complexons was conducted. A new class of non-glyceride neutral lipids present in a broad variety of different organisms (plants, animals and microorganisms) was discovered, and their role in the biomembranes' functioning was demonstrated. New methods of carbohydrate, steroid and lipid synthesis, as well as selective modification of the nucleic acids, were extensively developed. For the first time, the full synthesis of tetracycline was performed, an antibiotic of practical importance and with a most complicated structure. In a collaborative effort by several laboratories, a new comprehensive approach for establishing the spatial structure of peptides in solution based on the coordinated application of a set of spectral and computational methods was developed. The efficiency of this approach was proved through numerous examples of natural and synthetic peptides, with membrane active antibiotics and toxins among them. A new, so called topochemical approach was developed to design and synthesize of biologically active peptides - hormones, antibiotics, toxins, substrates and enzyme inhibitors.

In 1970, after M.M. Shemyakin's death, academician Yu.A. Ovchinnikov became the head of the Institute and the vice president of the USSR Academy of Sciences from 1974.

The 70s and the 80s were years of rapid development in physico-chemical biology in the USSR and of an intensive effort to narrow the gap in the level of research from the best laboratories in the world. The Government passed a

I.A. Solovey

decision on comprehensive support for this scientific field, whose progress essentially determined progress in the spheres of medicine, agriculture, environmental protection and biosecurity. The Institute was appointed as a leading institution responsible for implementation of the corresponding government decrees. Its main area of activity became investigation of biological problems with the help of the methods of organic chemistry. That trend led to change of name in 1973 to the Institute of Bioorganic Chemistry and, correspondingly, the proportion of biological research in it essentially increased. Institutes under analogous names and similar scientific tasks were founded in Novosibirsk, Vladivostok, Kiev, Minsk, and Tashkent. Beginning from 1975, the *Bioorganic Chemistry Journal* was started, based in the Institute and issued by the publishers Nauka. In the same year, a chair of bioorganic chemistry was founded in the Biological Faculty of Moscow State University and Yu.A. Ovchinnikov became its first Professor. In 1974, construction of a new building for the Institute was started in the south west of Moscow, and the building became operational in 1984. Scientists were provided with a superb set of buildings meeting their needs in specialized facilities and engineering equipment; this equipment has continued to efficiently operate to this day.

As the Institute progressed, the focus of its interest shifted from low molecular bioregulators to the major biopolymers of the cell, primarily to proteins and nucleic acids. In 1972, in a collaborative effort by two Institutes – the Institute of Bioorganic Chemistry and the Institute of Molecular Biology – the full primary structure was established for the porcine cardiac muscle cytoplasmatic aspartate aminontansferase, the first protein sequenced in our country.. It was a significant achievement for that time. During the following years, the number of sequenced proteins grew exponentially. The groundbreaking work on the structure of integral membrane proteins - bacteriorhodopsin (1978) and bovine rhodopsin (1982) deserves special attention. The task was completed under conditions of strong competition with the best foreign laboratories, and this story clearly demonstrated the remarkable progress of biomolecular science in the USSR at that time.

From the early 80s, the Institute became one of the top biotechnological centers in the country. Researchers at the Institute had been extensively developing methods for chemical-enzymatic synthesis of nucleic acids. The latter was further applied as an important component of genetic engineering technologies for the production of recombinant proteins. The interferon a2 strain producer obtained in the Institute served as a basis for the following industrial production of this important medicinal preparation. Beginning from 1985, and after 1988, this time without Yu.A. Ovchinnikov, who passed away untimely, the Institute became the head organization in the structure of the Inter-Industry Scientific and Technological Biogen complex, which united dozens of scientific and manufacturing biotechnological centers in the country. Beginning from 1992, the Institute took the lead in the Novel Methods in Bioengineering national program.

A decision was reached on establishing the Pushchino Branch of the Institute of Bioorganioc Chemistry in 1979, and in 1988 construction work was completed. Facilities for growing plants under controlled conditions and an excellent animal house, as well as pharmacological laboratories for conducting preclinical trials of medicinal preparations, were now available. These facilities significantly enhanced the potential

of the Institute for carrying out work in the sphere of plant biotechnology and for creating new drugs.

Today, the Institute of Bioorganic Chemistry is the largest among the Biology Sciences Branch Institutions of the RAS. The Institute includes 40 independent laboratories and groups conducting research in a wide range of directions. The scientific council of the Institute has approved the following main directions in its work:

- Isolation and structural analysis of new biomolecules. Studies of their structure-functional relations and the mechanisms of action;
- Biocatalysis;
- Structure and function of proteins and peptides;
- Structure and function of nucleic acids.
- Molecular mechanisms of genetic processes;
- Mechanisms of biomolecular recognition and signal transduction in biological systems;
- Molecular and cell immunology;
- Biomedical research;
- Fundamental and applied aspects of biotechnology;
- New reagents, materials and equipment.

In each of the above-mentioned directions, new original results have been obtained and presented in hundreds of publications, patents and reports. Among the achievements of recent years worth mentioning are: discovery of new fluorescent protein families in marine organisms (coral polyps and ratchets), their structure identification and development of genetically coded markers for the visualization of cell processes on their basis. Protein components have been isolated and identified from animal poisons. Several of them display unique selectivity of membrane action and membrane receptor binding, in particular, on pain receptors. These proteins might serve as an instrument for the study of signal transduction mechanisms in biological systems and for the development of new medicinal preparations. New approaches to comparing the full genomes of closely related organisms have been developed.. This method has been used for unraveling genetic differences between humans and chimpanzees, the differences that reflect the integration of endogenous retroviruses. A new direction has been developed in peptide research called peptidomics. Total screening of several biological objects has been carried out in order to detect the presence of endogenous peptides, and it has been shown that any kind of protein can serve as a source of biologically active peptides, including those with a well studied individual function (for example, hemoglobin).

Development of new pharmaceuticals ("Deltaran", "Likopid") registered with the State Register of Medical Products of the Russian Federation, as well as manufacturing of the most important recombinant protein preparations, such as human insulin and human growth hormones, is worth mentioning among work of immediate practical value. At present, our Institute supplies about 15% of the Moscow Health Care system's needs in insulin.

A more comprehensive description of the achievements of the Institute would go far beyond the size of this brief survey. However, even the examples provided here speak to the great potential of the working team and the Institute's perspectives. The work of researchers of the Institute has received two Lenin Prizes, ten State Prizes in the field of science and engineering, five Government of the Russian Federation Prizes in the field of science and engineering, the USSR Academy of Sciences and RAS Prizes named after A.N. Bach, A.O. Kovalesky, Yu.A. Ovchinnikov, and M.M. Shemyakin.

A very significant aspect of the Institute's work is its participation in the teaching and training process in the sphere of bioorganic chemistry and biotechnology. Regular acceptance of talented young people has allowed us to remain scientifically competitive during the period of mass migration of scientists to foreign laboratories. A Scientific Educational center collaborating with several high educational institutions in Moscow, Sankt Petersburg, and Pushchino was founded in the Institute. Leading scientists lecture on specialized topics, and more than 100 undergraduate students on a regular basis join the Institute's laboratories preparing bachelor and master thesis and participating in scientific publications. A series of practical classes have been organized, and corresponding exams and tests have been administered. As a result, the Institute has an opportunity to enroll several graduates annually into post graduate courses and then hire them to work for the Institute. That workforce has a full-scale education and is able to tackle complex scientific problems.

As a whole, the Institute of Bioorganic Chemistry may be considered today as one of the key constituent parts of the system of Institutes in the Biological Sciences Branch of the RAS. The Institute's personnel and its capabilities are ready to fulfill scientific tasks of any degree of complexity. We greatly appreciate the understanding of the necessity of our work by our fellow countrymen and the support of the government. ●

In the Front Line of World Science

A.V. Zelenin and V.L. Karpov

The creation and organization of the Institute of Molecular Biology (in its first six years it was called the Institute of Radiation and Physicochemical Biology, Academy of Sciences of the USSR) is forever connected with the name of Vladimir Alexandrovich Engelhardt, one of the most outstanding biochemists and molecular biologists of the 20th century. Vladimir Alexandrovich won broad fame and international acclaim as far back as the 1930s for discovering oxidative (respiratory) phosphorylation with the participation of ATP. In the beginning of the 1940s, Vladimir Alexandrovich earned fame again, when he and his wife Milicia Nikolaevna Lyubimova discovered the fermentation activity of myosin protein, which allowed him to suggest a theory about the combination of the structure and functions of biological compounds on the level of individual molecules. This scientific body of work became part of a goldmine of science, while Vladimir Alexandrovich began to be justifiably referred to as one of the founders of molecular biology in our country.

ON THE SEMICENTENARY OF THE ENGELHARDT INSTITUTE OF MOLECULAR BIOLOGY, RUSSIAN ACADEMY OF SCIENCES

In the middle the 1950s, Vladimir Alexandrovich progressed up the career ladder and became an Academician-Secretary of the Biological Research Branch, Academy of Sciences of the USSR. Needless to say, he had to immediately join in the reconstruction and consolidation of Russian experimental biology and genetics, which were almost completely in ruins. The most important stage in that process was, in his opinion, the creation of the first specialized Russian molecular biological institute. Vladimir Alexandrovich managed to build that institute with the unwavering support of A.N. Nesmeyanov, president of the Academy of Sciences of the USSR, and a group of outstanding physicists such as I.V. Kurchatov, P.L. Kapitsa, and I.E. Tamma. The Resolution on the Creation of a New Molecular Biological Institute was adopted in April of 1957 by the Presidium of the Academy of Sciences of the USSR, but in fact the institute was launched two years later.

V.A. Engelhardt managed to attract a series of brilliant researchers to the Institute of Molecular Biology (IMB), including biochemists A.E. Brownstein and A.A. Baev, cytogenetics specialist A.A. Prokofieva-Belgovsky, cell biologist M.N. Maisel, biophysicist M.V. Folkenstein, physicist L.A. Tumerman, and crystallographer N.S. Andreeva. At the same time, many young researchers interested in the new science and graduates of different universities also joined the institute.

The young generation of leaders included G.P. Georgiev, A.D. Mirzabekov, A.A. Kraevsky, R.M. Khomutov, and L.L. Kiselev. As a result, in a short period of time, just as the institute received its present name, it had acquired a complete, actively working team involved in investigating a definite range of issues. The researchers investigated the structures and biosynthesis mechanisms of nucleic acids and the primary and space structures of proteins and their complexes, as well as the mechanisms of their functioning on the molecular level in *in vitro* systems, viruses, and cells. That range of problems to tackle predetermined the areas of the institute's activity for many years, though it underwent intensive development and significant modification later on.

The institute became well-known in Russia and abroad. In this connection, it is essential to note first the interpretation of the primary structure of the valine transfer RNA carried out under the guidance of Baev. It was the first structure of biopolymer interpreted in our country and the sixth primary structure of tRNA in the world. In the following years, researchers successfully studied information transfer in eukaryote cells, the mechanisms of gene expressions regulation, and the nature of the mobile genetic elements of drosophila; they also interpreted the chromatin structure and established with high resolution the tertiary structure of pepsin and some other proteins. Great progress was noted in the formulation of the biochemical grounds of protein biosynthesis and the chemical grounds of biocatalysis and the physics of biopolymers, as well as for the creation of new site-directed inhibi-

I.A. Solovey

tors of biological processes. The drug Phosphaside (NIKAVIR), created under the guidance of Kraevsky, became a very important drug that prolongs the life of those suffering from immunodeficiency disorder. Research by a team working under the guidance of Prokofieva-Belgovsky paved the way for medicogenetic service development in our country.

In the late 1980s and early 1990s, the institute underwent significant restructuring. A modern instrumental base was created to intensify work in the sphere of cell molecular biology; investigations in new directions such as immunooncology and immunogenetics were started; and, finally, Mirzabekov initiated the development of biological microchip technology. These investigations have continued to the present day. The bilateral Russian-American Laboratory, which linked the Institute of Molecular Biology in Moscow and the Argonne National Laboratory in Chicago (one of the leading centers in the development of atomic power and for the solution of the most important problems of fundamental science in the United States), gained distinction as well. That international team managed to create the technology of gel microchips on the basis of IMB development work, which is becoming more and more important in the molecular diagnostics of infectious and oncological diseases.

The institute created by V.A. Engelhardt was based on the principle of the three pillars of physics, chemistry, and biology, which formed the basis of molecular biology at that time, although today the talk is about specialists of a new profile, so-called molecular biologists who use the principles and methods of the above-mentioned sciences in their work.

Almost immediately, from the date of its inception, the institute became the center of "crystallization" of the Russian researchers engaged in research and interested in molecular biology. The numerous meetings, conferences, and seminars organized by the institute encouraged that process. As a consequence, the institute took a leading place among the establishments that spearheaded the regeneration of science in our country. It is essential to note the important role that the "Revertase" program and the Soviet (and later Russian) "Human Genome" program played in the development of Russian science.

Today, the main areas of scientific activity at the institute are as follows:

- structure and function of nucleic acids, proteins, and their complexes;
- structural and functional genomics;
- molecular biology of cell;
- molecular immunology;
- bionanotechnologies and the fundamentals of medical diagnostics.

The researchers at the institute have carried out a range of research that has contributed significantly to the development of international molecular biology and spurred current ideas about the physicochemical elements of living systems. It is impossible to consider the whole wide range of investigations carried out at the IMB in this brief review: therefore, let's turn our attention only to the most important issues.

Really cutting-edge discoveries are made at the intersection of disciplines such as immunology, molecular genetics, bioorganic chemistry, biotechnology, and medicine. The focus of interest and primary fields in this direction include physiological functions; the mechanisms of the action and regulation of cytokines; the so-called protein mediators of the immune system; the mechanisms activating cytokines, including the whole chain of signal transfer beginning from the activation of the genetic immunity receptors; and the protective and pathological properties of the TNF family (tumor necrosis factor) cytokines. In particular, researchers have created unique living systems such as mice with the TNF gene silenced in some cells of their immune systems [1] and mice with silenced lymphotoxin genes [2]. Using these mice made it possible to obtain new important results in physiology and medicine [3-5]. The applied aspects of these investigations are related to the characteristics of new human cancer antigens and the possibility of using them for diagnostics and the monitoring of oncological diseases, as well as to create new drugs.

Researchers at the institute have revealed the important prophylactic role played by the p53 gene, which is able to function in a cell as an antioxidant and to decrease the level of oxygen radicals. This effect is achieved thanks to the p53-dependent adaptation of

antioxidant protective systems that save DNA cells from damage caused by physiological stress. Hence, the p53 gene significantly slows the mutation process and, in doing so, prevents malignant diseases and premature aging [6, 7]. The prototype of a new antitumor drug has been created: a small RETRA molecule which selectively kills tumor cells thanks to the activation of the p73 protein [8]. A team at the same laboratory has discovered the fourth nuclear RNA polymerase which performs the partial transcription of mRNA in animal and human cells [9].

Active and successful investigations are ongoing in the sphere of gene transcription regulation by the example of drosophila. Researchers have discovered a new protein complex of drosophila that is related to nuclear pores and responsible for mRNA export from the nucleus. It has been established that the E(y)2 transcription factor, which is a component of this complex, is present in the multiprotein SAGA transcription complex and provides a connection between the transcription and export of mRNA of actively functioning genes; i.e., the researchers have discovered a new mechanism controlling effective gene expression [10–12]. It has been established that the TRF2 transcription activator, which contains a domain homological to the promoter-binding domain of the main TBP transcription activator, plays an important role in maintaining the chromatin structure and its condensation [13].

Investigations in the area of translation mechanisms, traditionally a field of success for the institute, are in progress. In recent years, researchers have developed a system that makes it possible to analyze *in vitro* the contribution of any component of the translation complex at different stages of protein synthesis. It has been established that the GTF hydrolysis precedes the peptidyl-tRNA hydrolysis upon translation termination, while eRF3 significantly accelerates this reaction [14]. In the structure of termination factors of first-class bacteria, the eukaryote and archaeon N-domain are responsible for recognizing the mRNA stop codon, the C-domain is responsible for binding with eRF3, and the M-domain contains a universal GGQ-motive necessary for peptidyl-tRNA hydrolysis in ribosome. The eRF3 protein has been found to be characterized by GTF activity, which depends on eRF1 and ribosomes, and to form an *in vitro* complex with eRF1. The role of guanylic nucleotides in the functioning of the elongation factor of the EF-G translation has been determined [15, 16].

The researchers at IMB have discovered a new class of mobile genetic elements called "Penelope-like elements" [17]. Representatives of this quite ancient class are present in hundreds of animal species, from rotifers to fish and reptiles. The Penelope element has been established to be responsible for the hybrid dysgenesis syndrome of *Drosophila virilis*. The researchers have offered a model of chromosomal speciation, which assigns a leading role to mobile elements that are able, under certain conditions, to cause the "explosion" of mutability.

Work in the sphere of bioinformatics has developed intensively: for instance, researchers have revealed the relation between genome polymorphism phenomena and alternative splicing, which provides multiplicity of the human proteome [18]. A computational method for predicting the substitution of amino acids in proteins has been designed, and a database of the functional protein polymorphisms in the human genome has been created (http://www.snp.imb.ac.ru) [19].

The results of the fundamental scientific research of IMB researchers are used in applied fields. The technology of gel biochips initiated and elaborated under the guidance of Academician Mirzabekov was developed as an innovative product, was patented, and then spread to medical practice, where it helps carry out express diagnostics of socially important infectious, oncological, cardiovascular, and inherited diseases, as well as identify the special danger of infections and biotoxins [20, 21]. A pilot production, where several thousands of biochips were produced every day, was organized. For the Russian Federal Service for the Supervision of Public Health and Social Development, the researchers have developed and registered a biochip analyzer and a range of biochip-based test-systems for different applications in medical diagnostics, including a test-system for the genetic typing of 36 hepatitis C subtypes (International Application for the Patent PCT/RU2007/000438, in partnership with the University and Hospital of Toulouse) [22]. Moreover, they have developed a method for quantitatively estimating proteins on the basis of a combination of biochip technology and time-of-flight mass spectrometry [23].

The biochip-based test-systems make it possible to determine and analyze the sensitivity of tuberculosis microbacteria to medical drugs; viruses of human immunodeficiency (HIV-1); hepatitis B and C (36 subtypes); influenza A (30 subtypes, including bird flu H5N1 and swine flu H1N1); herpetic fever (2 subtypes); pox (6 subtypes); bacillus anthracis; protein markers of oncological diseases (12 tumor markers) and biotoxins (9 types); chromosome aberrations that cause 13 types of leucosis; individual pharmacogenetic status; one's genetic disposition to certain oncological, cardiovascular, and inherited diseases; and personal genetic markers (18 markers which determine more than 1,000 variants of the human genome). Biochips for establishing the causative agent of tuberculosis and identifying its drug-resistant forms allows doctors to reduce the time needed for analysis from 6–10 weeks to a few hours and to choose an adequate treatment quickly. Biochip diagnostics is applied in more than 30 antituberculosis centers in Russia and countries of the CIS. Biochips for typing chromosome aberrations that cause oncological diseases in blood are certified and used for prognosis updating and selecting a treatment strategy at the Russian Children's Health Clinic (Moscow), where samples from 18 regional hematological centers of the Russian Federation are analyzed.

The researchers have created a method of PCR conduction in biochip cells on a real-time basis that allows them not only to detect pathogenic bacteria, viruses, and cancer cells in a sample, but also to simultaneously estimate their number in all samples [24]. An automated device based on replaceable modules is being developed to extract trace amounts of nucleic acids from biological samples. The following integration of this module and system for PCR conduction in biochip cells with real-time detection will lead to the ap-

pearance of a radically new device: the so-called laboratory-on-chip. The appearance of such a device will exclude contact between the object being analyzed and the external environment, which will significantly decrease the probability of personnel infection and contamination.

The Russian Academy of Sciences, along with the Institute of Spectroscopy, has developed analytical systems based on portative dichrometers, which help to detect different compounds in the environments analyzed, and applied for nine patents. Nanoconstructions developed on the basis of liquid-crystalline dispersions of nucleic acids may be used as atom-carriers of heavy elements for neutron-capturing therapy of tumor diseases.

The applied work also includes investigations of the genetic fingerprinting used in the genetic identification of the remains of Nicholas II and the members of his family. The researchers proceeded to successfully develop antivirals based on the original Russian anti-HIV-drug NIKAVIR. A range of new inhibitors of hepatitis C virus replication have been obtained. An analogue of the antiherpetic drug Acyclovir, which allows the replication of strains of the herpes virus resistant to Acyclovir, has been created [25].

For achievements in the sphere of fundamental and applied science, researchers of the Institute of Molecular Biology, Russian Academy of Sciences, have been honored at different times with two Lenin Prizes and eight State Prizes, the Demidov Prize, the Prize of the Federation of European Biochemical Societies, and numerous other prizes and medals. Young scientists have received many Lenin Komsomol prizes and have also been honoured with the State Prize of the Russian Federation in the Sphere of Science and Technology.

In connection with the jubilee of the Institute, foreign scientists have highly rated the contribution of IMB to the development of modern molecular biology; in particular, they have noted that the Engelhardt Institute is famous for its talented researchers and that even in its most difficult years its researchers had continued to believe in the universality of scientific knowledge, ignoring state boundaries and managing to contribute greatly to the development of molecular biology [26].

The Institute of Molecular Biology is celebrating its sixth decade as a first-class scientific establishment that has everything needed to conduct investigations in the sphere of molecular and cellular biology on an international level. Its scientific research is supported by many Russian and foreign grants, while its substantial number of young scientists allow us to face the future with hope and confidence. ●

REFERENCES:

1. Grivennikov S.I., Tumanov A.V., Liepinsh D.J., Kruglov A.A., Marakusha B.I., Shakhov A.N., Murakami T., Drutskaya M.S., Förster I., Clausen B.E., Tessarollo L., Ryffel B., Kuprash D.V., Nedospasov S.A. 2005. Distinct and non-redundant in vivo functions of TNF produced by T cells and macrophages/ neutrophils: protective and deleterious effects. *Immunity*. 22. 93-104.
2. Liepinsh D.J., Grivennikov S.I., Lagarkova M.A., Drutskaya M.S., Klarmann K.D., Lockett S.J., McAuliffe M., Tessarollo L., Keller J.R., Kuprash D.V., Nedospasov S.A. 2006. Novel lymphotoxin alpha knockout mice with unperturbed TNF expression: reassessing LTalpha biological functions. *Mol Cell Biol*. 26. 4214-4225.
3. Cui C.-Y., Hashimoto T., Grivennikov S.I., Piao Y., Nedospasov S.A., and Schlessinger D. 2006. Ectodysplasin activates the lymphotoxin-beta pathway for hair follicle differentiation. *Proc Natl Acad Sci USA*. 103. 9142-9147.
4. Welniak L.A., Kuprash D.V., Tumanov A.V., Panoskaltsis-Mortari A., Blazar B.R., Sun K., Nedospasov S.A., and Murphy W.J. 2006. Peyer's patches are not required for acute lethal graft-versus-host disease after myeloablative conditioning and murine allogeneic bone marrow transplantation. *Blood*. 107. 410-412.
5. Tumanov A.V., Koroleva E.P., Christiansen P.A., Khan M.A., Ruddy M.J., Burnette B., Papa S., Franzoso G., Nedospasov S.A., Fu Y.X., Anders R.A. 2009. T cell-derived lymphotoxin regulates liver regeneration. *Gastroenterology*. 136. 694-704.
6. Sablina A.A., Budanov A.V., Ilyinskaya G.V., Agapova L.S., Kravchenko J.E., Chumakov P.M. 2005. The antioxidant function of the p53 tumor suppressor. *Nat. Medicine*. 11. 1306-1313.
7. Budanov A.V., Sablina A.A., Feinstein E., Koonin E.V., Chumakov P.M. 2004. Regeneration of peroxiredoxins by p53-regulated sestrins, homologs of bacterial AhpD. *Science*. 304. 596-600.
8. Kravchenko J.E., Ilyinskaya G.V., Komarov P.G., Agapova L.S., Kochetkov D.V., Strom E., Frolova E.I., Kovriga I., Gudkov A.V., Feinstein E., Chumakov P.M. 2008. Small molecule RETRA suppresses mutant p53-bearing cancer cells through a p73 dependent salvage pathway. *Proc. Natl. Acad. Sci. USA*. 105. 6302-6307.
9. Kravchenko J.E., Rogozin I.B., Koonin E.V., Chumakov P.M. 2005. Transcription of mammalian mRNAs by a novel nuclear RNA polymerase of mitochondrial origin. *Nature*. 436. 735-739.
10. Shidlovskii Y.V., Krasnov A.N., Nikolenko J.V., Lebedeva L.A., Kopantseva M., Ermolaeva M.A., Ilyin Yu.V., Nabirochkina E.N., Georgiev P.G. and Georgieva S.G. 2005. A novel multidomain transcription coactivator SAYP can also repress transcription in heterochromatin. *EMBO Journal*. 24. 97–107.
11. Kurshakova M., Krasnov A., Kopytova D., Shidlovsky Y., Nikolenko J., Nabirochkina E., Splender D., Schultz P., Tora L., Georgieva S. 2007. SAGA and a novel Drosophila export complex anchor efficient transcription and mRNA export to NPC. *EMBO Journal*. 26. 4956-4965.
12. Krasnov A., Kurshakova M., Ramensky V., Mardanov P., Nabirochkina E., Georgieva S. 2005. A retrocopy of a gene can functionally displace the source gene in evolution. *Nucleic Acids Res*. 33. 6654-6661.
13. Kopytova D., Krasnov A., Kopantceva M., Nabirochkina E., Nikolenko J., Kurshakova M., Lebedeva L., Korochkin L., Tora L., Georgiev P., Georgieva S. 2006. The two isoforms of *Drosophila* TRF2 are essential for embryonic development, premeiotic chromatin condensation and proper differentiation of germ cells of both sexes. *Mol. Cell. Biol*. 26. 7492-7505.
14. Alkalaeva E.Z., Pisarev A.V., Frolova L.Yu., Kisselev L.L., Pestova T.V. 2006. In vitro reconstitution of eukaryotic translation reveals cooperativity between release factors eRF1 and eRF3. *Cell*. 125. 1125-1136.
15. Mitkevich V.A., Kononenko A.V., Petrushanko I.Yu., Yanvarev D.V., Makarov A.A., Kisselev L.L. 2006. Termination of translation in eukaryotes is mediated by the quaternary eRF1·eRF3·GTP·Mg^{2+} complex. The biological roles of eRF3 and prokaryotic RF3 are profoundly distinct. *Nucleic Acids Res*. 34. 3947-3954.
16. Hauryliuk V., Mitkevich V.A., Eliseeva N.A., Petrushanko I.Yu, Ehrenberg M., Makarov A.A. 2008. The pretranslocation ribosome is targeted by GTP-bound EF-G in partially activated form. *Proc. Natl. Acad. Sci. USA*. 105. 15678-15683.
17. Pyatkov K.I., Arkhipova I.R., Malkova N.V., Finnegan D.J., Evgen'ev M.B. 2004. Reverse transcriptase and endonuclease activities encoded by Penelope-like retroelements. *Proc. Natl. Acad. Sci. USA*. 101. 14719-14724.
18. Ramensky V.E, Nurtdinov R.N, Neverov A.D, Mironov A.A, Gelfand M.S. 2008. Positive selection in alternatively spliced exons of human genes. *Am J Hum Genet*. 83. 94-98.
19. Sunyaev S., Kondrashov F.A., Bork P., Ramensky V. 2003. Impact of selection, mutation rate and genetic drift on human genetic variation. *Hum Mol Genet*. 12. 3325-3330.
20. Mikhailovich V., Gryadunov D., Kolchinsky A., Makarov A.A., and Zasedatelev A. 2008. DNA microarrays in the clinic: infectious diseases. *Bioessays*. 30. 673-682.
21. Rubina A.Yu., Kolchinsky A., Makarov A.A., Zasedatelev A.S.. 2008. Why 3D? Gel-Based Microarrays in Proteomics. *Proteomics*. 8. 817-831.
22. Gryadunov D.A., Mikhailovich V.M., Nicot F., Dubois M., Zasedatelev A.S., Izopet J. Method for identifying the genotype and subtype of hepatitis C virus on a biological microchip. *International Application Number* PCT/RU2007/000438.
23. Darii E., Lebeau D., Papin N., Rubina A.Y., Stomakhin A., Tost J., Sauer S., Savvateeva E., Dementieva E., Zasedatelev A., Makarov A.A. and Gut I.G. Quantification of target proteins using hydrogel antibody arrays and MALDI time-of-flight mass spectrometry (A2M2S). 2009. *New Biotechnology*. (in press).
24. Khodakov D.A., Zakharova N.V., Gryadunov D.A., Filatov F.P., Zasedatelev A.S, Mikhailovich V.M. 2008. An oligonucleotide microarray for multiplex real-time PCR identification of HIV-1, HBV, and HCV. *Biotechniques*. 44. 241-248.
25. Karpenko I.L., Jasko M.V., Andropova V.L., Ivanov A.V., Kukhanova M.K., Galegov G.A., Skoblov Y.S. 2003. Synthesis and antiherpetic activity of acyclovir phsphonates. *Nucleosides Nucleotides Nucleic Acids*. 22. 319-328.
26. Jubilee brochure devoted to semicentenary of the Engelhardt Institute of Molecular Biology, Russian Academy of Sciences.

The Institute of Chemical Biology and Fundamental Medicine of the Siberian Division of the Russian Academy of Sciences

(until 2003 the Novosibirsk Institute of Bioorganic Chemistry)

In the spring of 1957, a decree of the Council of Ministers of the USSR founded the Siberian Branch of the USSR Academy of Sciences. At the beginning, this branch included 10 institutes, which were involved in various natural sciences. During the planning of the Siberian Branch of the USSR Academy of Sciences, no provision was made for an institute specializing in physical-chemical problems in biology. This new branch of science remained a pariah, because the leader of the country, N.S. Hrushtschev, was under the influence of the charlatan ideas of T.D. Lysenko. That is why Michael Alexeevich Lavrentyev, the man charged with organizing the Siberian Branch, could only create the Institute of Cytology and Genetics (ICG), headed by Nikolai Petrovich Dubinin, who undoubtedly understood the value of chemical and physical methods in modern biology. Even this veiled attempt at organizing molecular biology research failed as Hrushtschev arrived at the Novosibirsk Academic Town in person and removed Nikolai Dubinin from the post of ICG Director. The institute was saved after Dmitry Konstantinovich Belyaev became the new director. He was a progressive geneticist working with fur-producing animals, a commodity much more understandable to the top officials, rather than the Drosophila fruit-fly, the research of which led to most of the fundamental discoveries in genetics. The future of biology in this country worried many prominent scientists. Among them was Nikolai Nikolaievich Vorozhtsov, a well-known organic chemist, who was appointed to organize the Institute of Organic Chemistry (IOC) under the Siberian Branch. He recruited many of his students, graduates of the Department of Intermediary Products and Dyes and also invited Dmitry Georgievich Knorre, who was very willing to use his knowledge of chemistry in studying life sciences. N.N. Vorozhtsov supported the young scientist in his wish and immediately agreed to create a Laboratory of Natural Polymers. The name was chosen carefully as the black shadow of Lysenko's influence was still not gone from biochemistry, and the use of "heretic" words such as proteins and especially nucleic acids as the name of a laboratory was unsafe. But the idea of creating a new line of scientific research in the Siberian Branch was firmly ingrained in the mind of N.N. Vorozhtsov, and in 1964 he reached an agreement with Michael Alexeevich Lavrentyev, who decided to construct a new building, intended especially for biochemical research. The building was completed in 1969 and it hosted the Biochemistry Department. Thus the Natural Polymer Lab received its true and unmasked name; it became the Nucleic Acid Chemistry Laboratory, and, together with the newly created Ultramicrobiochemistry Lab, it became the Biochemistry Department of the IOC of the Siberian Branch (now Siberian Branch of the Russian Academy of Sciences; SB RAS). It was Vorozhtsov's intention that the new department would combine with the laboratory headed by Rudolph Iosifovich Salganik, a leading biochemist who worked in the ICG SB RAS. This would allow the creation of a new institute. Alas, this intended path to create a new institute did not succeed.

V.V. Luchansky

However, it did not prevent a productive and lasting cooperative relationship between D.G. Knorre and R.I. Salganik, which led to the creation of several biochemical manufacturing facilities, which were very much in need at that time, since the possibilities to buy chemicals and instrumentation with hard currency were very limited.

The issue of creating a new institute was raised again when Yuri Anatolievich Ovchinnikov attained the high post of vice-president of the USSR Academy of Sciences and, no less importantly, gained influence in government and party circles. For a long time, he advocated the creation of such an institute in Siberia. The recently appointed chairman of the Siberian Branch, Valentin Afanasievich Koptyug, also shared this view. As a result, the Decree of the CPSU Central Committee and the USSR Council of Ministers dated June 24, 1981, № 662 On the Further Development of Physical-Chemical Biology and Biotechnology and Their Use in Medicine, Agriculture and Industry had an article that stipulated the creation of the Novosibirsk Institute of Bioorganic Chemistry (NIBC). After several years of preliminary activities, the institute was officially approved in April 1984 and Dmitry Georgievich Knorre was appointed its first director.

The creation of the NIBC SB RAS played an important role in establishing physical-chemical biology in Siberia. A Molecular Biology Division was created in the Novosibirsk State University (NSU) at the Natural Sciences Department on the basis of the NIBC and the laboratory of R.I. Salganik. The division trained several hundred young specialists. This not only allowed to staff the two main biological institutes with young researchers, but also to create new institutions specializing in biochemistry. In particular, this fact played a major role in the choice of location for a large virology center. The Glavmicrobioprom (head organization for microbiological industries) chose a location adjacent to the Novosibirsk Academic Town, which eventually led to the formation of the scientific town of Koltsovo, a center of research and manufacturing of prophylactic drugs against most viral infections, including those deemed extremely dangerous. Now this center is called Vector, the state scientific virology and bacteriology center.

In 1996, D.G. Knorre turned 70 and left the post of director, and the newly elected director was D.G. Knorre's student, a corresponding member of RAS, Valentin Victorovich Vlasov (who became a full member of RAS in 2003). He decided that the most important applications of physical-chemical biology were medical, and so he strengthened this branch of the institute's research and created a division for novel medical technology in the institute. Thus, the institute received a new name in 2003; it became the Institute of Chemical Biology and Fundamental Medicine SB RAS (ICBFM).

Today, ICBFM is the main site for training specialized staff of all levels in the field of physical-chemical biology, starting with college graduates up to PhD. and higher levels of academic research (Doctors of Science). Among the graduates of the Molecular Biology Division are Valentin Victorovich Vlasov, a full member of RAS, and corresponding members Olga Ivanovna Lavrik and Sergey Victorovich Netesov. A very important step in training staff of the highest qualification was the establishment within the institute of a Scientific Council empowered to award PhD degrees. More than 200 PhD. projects have been delivered and defended as of today. The institute continues to be actively involved in the training of students and post-graduates, specializing in the varied fields of chemistry and biology. The institute has post-graduate programs in 3 specialties and trains about 40 people every year.

The Chemical Biology and Fundamental Medicine Institute of SB RAS is well known for the level of its scientific research, and it has a high scientific potential, with a wonderful stock of modern research equipment. The institute is one of the acknowledged leaders among biological institutions in the Siberian Branch of RAS and in all of Russia. Every year, researchers from the institute publish more than 150 articles in leading Russian journals and in international peer-reviewed journals.

At present, the Institute includes 16 laboratories and research groups, and 2 divisions (the Molecular and Cell Biology Division and the Center of Novel Medical Technology). The institute employs about 200 scientists, including 3 full RAS members, 1 corresponding member, 18 Doctors of Science and 78 PhD. researchers. More than half of the scientific staff are young scientists under the age of 35. Several projects completed in the institute have received national prizes, such as the Lenin Prize, two State Prizes in the field of Science and Technology, the Russian Federation State Prize for Education, and a number of other Russian and international prizes, including awards for young scientists.

The main topics of research in the institute are the following:

- Studying the structure and function of biological molecules and supramolecular complexes; creating compounds which have specific effects on genetic structures; bioengineering and synthesis of biopolymers and synthetic biology.
- Biotechnology, including gene therapy, cellular technology for regenerative medicine, and nanobiotechnology.
- Clinical physiology, genetic basis of personalized medicine, molecular basis of immunity and oncogenesis
- The ecology of organisms and communities, communities of extremophilic microorganisms, viral and bacterial agents in mammal organisms.

Among the major scientific results obtained during the quarter century of the institute's existence are the following:

- The establishment of the fundamental basis for obtaining gene-directed bioactive compounds. The development of effective methods for the synthesis of nucleic acid fragments and their analogues and derivatives.
- Development of methods for the analysis of the structure and function of complex biopolymeric supramolecular ensembles.
- Creation of a technological basis for the diagnosis of genetic and infectious diseases and for the sequencing of the genomes of biological objects. The development of novel molecular tools and methods for the diagnosis of oncological, autoimmune, and infectious diseases.

Thus, having passed the stages of establishment and development, after 25 years of productive work, the institute has its own reputation, stands firmly on its feet and is actively conducting research, employing young specialists and the experience of the scientific schools created within the institute itself. ●

Marine Natural Products: A Way to New Drugs

V.A. Stonik
Pacific Institute of Bioorganic Chemistry, Far-eastern Branch of the Russian Academy of Science
Email: Stonik@piboc.dvo.ru

ABSTRACT The investigation of marine natural products (low molecular weight bioregulators) is a rapidly developing scientific field at the intersection of biology and chemistry. Investigations aimed at detecting, identifying, and understanding the structure of marine natural products have led to the discovery of 20,000 new substances, including those characterized by an extremely high physiological activity. Some results and prospects of works aimed at creating new drugs on the basis of marine natural products are discussed herein.
Keywords: marine organisms, natural products, physiological activity, trabectidin, prialt, histochrome, collagenase KK.
Abbreviations: HIV- human immunodeficiency virus, AIDS – acquired immune deficiency syndrome, PIBOC – Pacific Institute of Bioorganic Chemistry, EC_{50} – effective concentration that provokes a response halfway between the baseline and maximum response, IC_{50} – concentration that provokes 50% inhibition, VEGF – vascular endothelial growth factor.

INTRODUCTION

Low molecular natural products are largely referred to the so-called secondary metabolites. In contrast to primary metabolites, these substances are rare in occurrence and may be detected only in some taxa, and occasionally, in one biological species (subspecies, strain). They are formed on the basis of precursor substances participating in primary metabolism, such as acetic acid, amino acids, glucose and are observed mainly as final products of biochemical transformations. Secondary metabolites are quite diverse by chemical structure and include steroids, terpenoids, alkaloids, polyketides, phenolic metabolites, some carbohydrates, lipids, and peptides. On the other hand, secondary metabolites can be classified on the basis of their biological functions as hormones, antibiotics, toxins, pheromones, etc. Among the natural products there are *endo*-metabolites, i.e., substances exercising their biological functions in the organisms-producers, for instance, oxylipins, hormones, phytoalexins, and more numerous exometabolites released into the environment and being of ecological importance, including toxins, antibiotics, and different signal compounds.

The higher terrestrial plants and soil microorganisms were, for a long time, considered to be the major biological sources of natural products. However, when skin-diver equipment was invented and became widely used, different marine organisms began also to be referred to their sources. The study of marine organisms significantly increased the amount of known natural products. In fact, the total number of studied natural products is unlikely to exceed 120-150 thousands, and by the estimates of many scientists, the amount is even lower [1], whereas about 20 thousand natural substances have been segregated. Moreover, the first researchers were surprised by the fact that marine organisms very rarely contained already known compounds. Hence, the biochemistry of their secondary metabolism differs substantially from that of terrestrial organisms. This fact may be explained by significant taxonomic differences between terrestrial and marine animals, plants and microorganisms.

As a whole, the investigation of natural products is of ecological importance. It stimulates the development of organic synthesis, physicochemical and isolation methods, as well as other sciences, such as biochemistry, molecular genetics, biotechnology, and microbiology. Moreover, it is closely related to healthy diet.

Natural products have played and continue to play an important role in the creation of new drugs and development of the pharmaceutical industry around the world. Analgesic preparations based on morphia from opium, cardioactive digitalis glycosides, anti-inflammatory agents created in the course of the investigation of steroid hormones, antibiotics, and many others are included in a list of products developed on the basis of natural drugs or their derivatives and analogues, which contains about 50% of all currently known medical products [5].

Results of the investigation of marine natural products which have been used or are being used now for the creation of new drugs are considered herein.

MARINE NATURAL PRODUCTS WITH ANTITUMOR PROPERTIES.

With the use of an aqualung, natural-product chemists got a chance to study more and more marine organisms. The American scientist Werner Bergmann was one of the first to start their chemical investigation. In 1951, he reported the isolation of unusual nucleosides (spongothymidine (**1**) and spongouridine (**2**) (Fig. 1), and then others) [2-4] from the sponge *Cryptotethia crypta* collected near the coast of Florida. They contained arabinose residues, instead of the ribose and desoxyribose residues observed in most compounds of that class. Those investigations stimulated the appearance of the antimetabolite conception in pharmacology. Antimetabolites are the active substances of drugs, which are characterized by a significant similarity to, and structural difference from, human metabolites. Antimetabolites participate in the biosynthesis of some biopolymers, more often, of DNA, and inhibit its exhibiting antitumor and antiviral properties. Bergmann's discovery was followed by the development of two arabino-

nucleoside drugs: arabinoadenine (**3**) (ara-A, Vidarabine) and arabinocytosine (**4**) (Ara-C, Cytarabine) (Fig. 1), which were used in clinical practice as antitumor and antiviral drugs for tens of years. Several other drugs of a nucleoside nature (azidothymidine, acyclovir, etc.) differ from ordinary nucleosides in other structural features. For instance, azidothymidine has an azide group in its monosaccharide residue, while acyclovir is characterized by an open furanose cycle.

However, further development of antitumor drugs on the basis of marine natural products was not just so successful. The case was not that there were no compounds with high antitumor activity. On the contrary, some marine invertebrates had minor secondary metabolites characterized by extremely high toxicity against tumor cells. By their cytotoxicity, they are hundreds and thousands of times superior to most active antitumor drugs currently in use. For instance, spongistatin (**5**) (Fig. 2) from marine tropic sponges is the most active of all natural and synthetic compounds found over the history of the investigation of antitumor compounds at the National Institute of Cancer (USA). It was initially found in one of the sponges, owing to the biological activity of the corresponding extracts, but for a long time the compound itself could not be obtained in the amount required for a structural investigation. Only after the collection and processing of three tones of sponge did the scientists finally manage to obtain 0.8 mg of spongistatin. Then, another sponge collected near the Maldive Islands was used as a basic material, and after the processing of 400 kg of this sponge, the scientists obtained another 10 mg of spongistatin, shed light on its structure, and began analyzing the physiological action of that macrolide. The inhibitory dose needed to cause the death of 50% of tumor cells (IC_{50}) was 10^{-10} M for colon cancer cells and 10^{-12} M for breast cancer cells. In experiments on animals with deadly malignant tumors, 70% of them survived after the injection of 25 μg/kg of spongistatin.

As a whole, several dozens of marine metabolites, extremely toxic against tumor cells, were detected. It is very important that many of them belong to the fundamentally new structural series of antitumor substances that opens good prospects for synthetic modeling. Until those substances were discovered, all of the natural products applied in chemotherapy were referred to not more than 4-5 structural types.

However, the creation of new-generation medical products based on marine natural products is being slowed down by some complicated issues. Firstly, these substances are difficult to access. It is impossible to harvest a sufficient amount of these substances from marine organisms, because their producers, as a rule, are rare and disseminated species, while the methods for aquaculture of such biological products remain poorly developed. Economically, reasonable syntheses for most of these substances have yet to be developed as well, due to the complexity of their structures and abundance of asymmetric centres in them. Secondly, these compounds, highly toxic against tumor cells, do not always demonstrate good anticancer activity when we are dealing with people or animals. And, thirdly, some of them are characterized by side effects; for instance, they can negatively affect kidneys or other organs and systems, which excludes their clinical application.

Nevertheless, development of another antitumor drug based on marine natural products was successfully completed just recently. In the end of 2007, the drug trabectidin (Yondelis) was approved in European Union countries for treatment of soft tissue sarcoma. The structure of the corresponding active substance, alkaloid ecteinascidin-743 (ET-743) (**6**) (Fig. 1) from the ascidian *Ecteinascidia turbinata,* was elucidated independently by two groups of American scientists 18 years ago [7, 8]. However, the high antitumor activity of extract *E. Turbinate* had been known long before their discovery, since 1969. The toxic concentration of that substance (IC_{50}) against the tumor cells L-1210 was very low (0.5 ng/ml), and in microgram doses (per one kg of test animal weight) it demonstrated a high antitumor activity against different types of mouse cancer.

Multi-stage total syntheses of that substance could not provide researchers with a sufficient amount of material for bioassay. For instance, the total yield in the first such synthesis was less than 1% [9]. As a result, methods of ascidian cultivation were developed, and submarine plantations were created near the coast of Spain. However, that method of production of the basic biological material was also rather inappropriate due to significant variations in the content of ecteinascidins, which were used in clinical testing, in the ascidians cultivated. Finally, after long research, scientists managed to obtain this alcaloid by chemical transformations from antibiotic cyanosafracin B, which is produced with a good yield by the terrestrial bacterium *Pseudomonas fluorescens* [10].

The mechanism of biological action of the trabectidin active substance, ecteinascidin-743, on tumor cells is related to its ability to penetrate the DNA's minor groove and to alkylate guanine residues [11]. Moreover, trabectidin causes

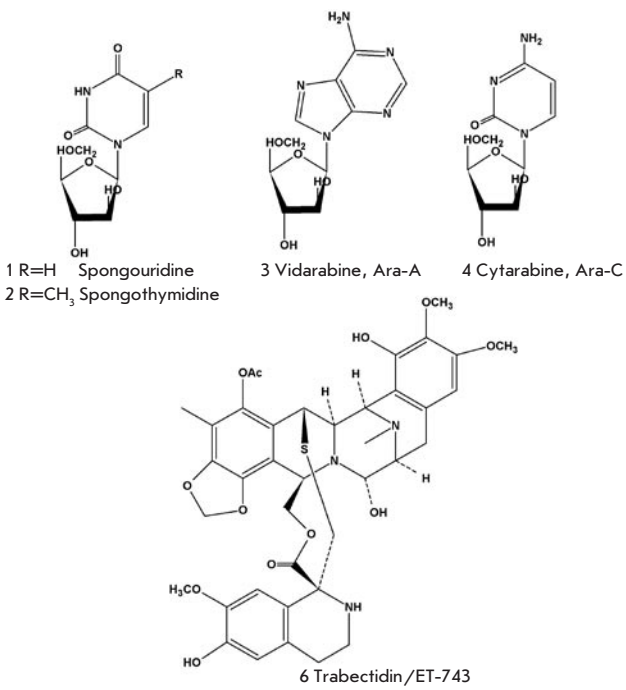

Fig. 1. Antitumor and antiviral drugs created on the basis of marine natural products.

programmed death (apoptosis) of tumor cells and intensifies the antitumor action of some well-know drugs (doxorubicin, paclitaxel (taxol), etc.). In spite of the fact that trabectidin was approved only for the treatment of soft tissue sarcoma, it showed good results in the course of clinical testing for the treatment of other types of malignant tumors. Not long ago, the Pharmamar Company (Spain) that has created trabectidin sold the license to Jonhson&Jonhson/Ortho Biotech to promote that drug on the American market.

A series of other marine natural products possessing extremely high cytotoxicities against tumor cells like spongistatin and ecteinascidin are being studied now as potential antitumor drugs and are subject to different stages of clinical and preclinical testing [12, 13] (Table 1).

For instance, bryostatin-1 (**7**) (Fig. 2), the 26-membered macrocyclic lactone from the bryozoan *Bugula neritina*, a fouling organism that grows in thick colonies on pier pilings and docks in the World Ocean, was detected by Pettit and co-workers from Arizona State University after several samplings of the biological material. Its structure was elucidated with the help of X-ray analysis. The compound (**7**) has 11 asymmetric centres, and it is hardly probable it will be obtained with a sufficient yield by organic synthesis in the years to come. Its content in bryozoan is insignificant (0.00001%), but scientists have managed to obtain 18 g of bryostatin for clinical and preclinical testing from 10,000 gallons of bryozoan collected. This substance has been determined to be a modulator of protein kinase C, a stimulator of the immune system, and an inductor of cell differentiation. It intensifies the antitumor action of some drugs but causes myalgias as a side effect. Currently, this drug is being tested in combination with paclitaxel, vincristine, ara-C, etc. (table 1).

Dolastatin 10 (**8**) (Fig. 2) was discovered after an expedition by Professor Pettit to the Mauritius Island in 1972, when they collected the marine nudibranch *Dolabella auricularia* and discovered the high antitumor activity of its extracts. To obtain the first milligram of the extract's active component – compound (**8**) – the scientists had to collect again a giant amount of that rare mollusk (about 2 tones) due to a low content of the required substance. Dolastatin 10 appeared to be a linear pentapeptide with residues of four previously unknown amino acids: N,N-dimethylvaline, dolaisoleucine, dolaproine, and dolaphenine [14]. In 1989, researchers carried out a total synthesis of that peptide, which confirmed the structure suggested and established its absolute stereochemistry [15]. Dolastatin 10 is extremely toxic against tumor cells, and its semitoxic concentration (IC_{50}) against cells of limphocytic leukemia P388 is 4.5×10^{-5} μg/ml. However, at the first and second stages of clinical testing its high antitumor activity was not confirmed. A while ago, the clinical testing of dolastatin was discontinued.

On the other hand, attempts to create a dolastatin-based antitumor drug were not abandoned. It has been discovered that the synthetic dolastatin derivative TZT-1027, in which the dolaphenine aminoacid is replaced with the phenylalanine group, just like dolastatin, is a strong inhibitor of tubulin polymerization, stops the division of cancer cells in very low concentrations, and reduces blood supply to tumors (inhibits angiogenesis). Currently, TZT-1027 (soblidotine) is undergoing clinical testing in Japan, Europe, and the USA for the

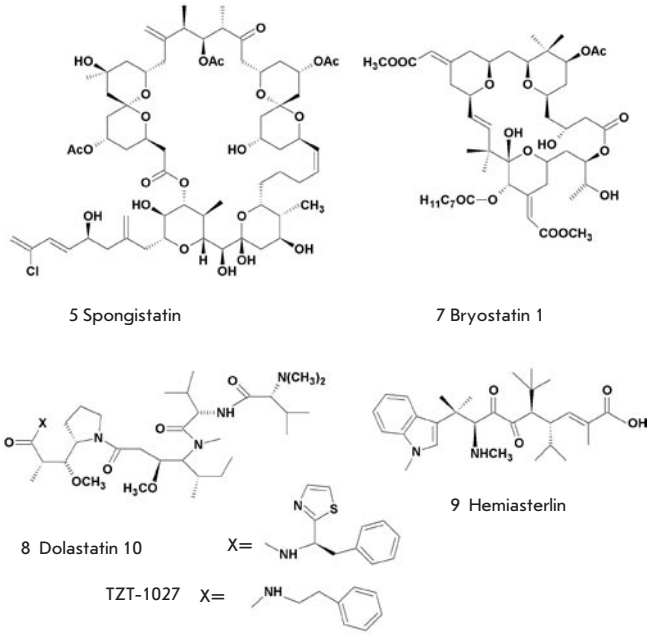

Fig. 2. Some compounds tested as active substances of antitumor drugs.

treatment of solid tumors, including those resistant to other drugs [16].

Hemiasterlin (**9**) (Fig. 2) is a tripeptide that was extracted for the first time from the deep-water sponge *Hemiastrella minor* by Kashman and his co-workers in 1986 [17]. Its synthetic analogue HTI-286, with a phenyl substituent instead of N-methylindol, appeared to be more active and, in nanomolecular concentrations, inhibited cell division binding with the monomeric units of tubulin and complicating its polymerization [18]. In preclinical testing, it showed good activity against tumors resistant to paclitaxel, one of the best antitumor drugs used currently. However, the clinical testing did not confirm that it was active in the case of patients in terminal stages of cancer. Recently, scientists demonstrated the antitumor action of this drug on androgen-dependent tumors, which has inspired renewed interest in further clinical studies of HTI-286 [19].

Discodermolide (**10**) (Fig. 3) was isolated by scientists of the Harbor Branch Oceanographic Institute (Florida, USA) from the rare deep-water sponge *Discodermia disollata* collected in the Bahamas at depths of up to 300 m using a submarine. The chemical structure of the compound (**10**) was elucidated with the help of a thorough analysis of NMR spectra and X-ray analysis, and it was confirmed by syntheses of discodermolide itself [22] and its antipode (-)-discodermolide [21], which in contrast to the natural (+)-isomer appeared to be much less active as a potential antitumor agent. Actually, natural discodermolide was able to stop the development of tumor cells at the G2/M phase of the cell cycle in concentrations of 3-80 nM, whereas the (-)-isomer was 2-20 times weaker. The drug appeared to be a much stronger inhibitor of tubulin polymerizations than paclitaxel; moreover, their combined action was stronger than the action of each one of those

agents. After multiple improvements of different variants of the multistage discodermolide syntheses, researchers of the pharmaceutical company Novartis managed, finally, to obtain 20g of that substance, to complete its preclinical testing in 2004-2005, and to start clinical testing. To date, this testing has been discontinued. In spite of the fact that this drug is relatively low-toxic for patients, it remains insufficiently effective. Nevertheless, it may be used in combination with other antitumor drugs [13].

Tubulin-binding agents also include cryptophycins and related compounds. Cryptophycins are depsipeptides produced by cyanobacteria *Nostoc* spp. [23]. They got their name for strong inhibitory activity against the pathogenic bacteria *Cryptococcus* spp. However, their antitumor properties have attracted even more attention. For instance, cryptophycin-1 (**11**) (Fig. 3) is toxic against tumor cells in concentrations of 1-10 pg/ml. Complete synthesis of cryptophycin-1 [24] has made it possible to pinpoint its structure and allowed the Eli Lilly Company to start the creation of a cryptophycin-based antitumor drug. In particular, a synthetic analogue of cryptophycin-1, the so-called cryptophycin-52, has proved more active against tumor cells than vinca peptides and paclitaxel by 40 and 400 times, respectively. However, in clinical testing it has appeared to be highly toxic for patients. Testing had to be stopped in the end of the 1990s. Later, new derivatives – cryptophycin-309 and -249 – were obtained, which are now undergoing the final stage of preclinical testing [13].

Several highly active depsipeptides from ascidians, including didemnin B from *Tridemnium solidum* [25], were intensely studied for many years as potential antitumor drugs. However, in the mid 1990s, the clinical investigations of didemnin B were discontinued due to significant neuromuscular toxicity and insufficient effectiveness for patients in terminal stages of cancer. However, its analogue aplidin (**12**) (dehydrodidemnin B) (Fig. 3) from the Mediterranean ascidian *Aplidium albicans* initiates oxidative stress with the following apoptosis in tumor cells [26]. Aplidin is also an inhibitor of angiogenesis and disturbs blood supply to tumors. In spite of the fact that aplidin is at the second stage of clinical testing as a drug for myeloma treatment, a good method to produce it has not been developed yet, because neither the technology for the corresponding ascidian cultivation, nor an appropriate synthesis for the production of a sufficient amount of this substance have been elaborated [13].

In 1986, Uemura and Hirata isolated several minor metabolites called halichondrins from the sponge *Halichondria okadai* [27]. Those compounds were strong inhibitors of tumor cell development (IC_{50} 10^{-9} M), bound to tubulin on the same site as the vinca peptides applied in clinical treatment, and were selected for the further investigation of their antitumor properties. However, it was rather difficult to produce halichondrins in sufficient amount. Due to a complex structure, the total synthesis of halichondrin B developed in 1992 [28] consisted of 90 stages and could not solve that problem. Almost at the same time, New Zealand

Table 1. Certain marine natural compounds are potential anticancer drugs

Compound	Biological Source	Chemical nature	Mechanism of action	Company	Status
Bryostatin-1 (**7**)	Bryozoan	Polyketide	Inhibits a protein kinase	GPC Biotech	Phase II clinical trials
Dolastatin-10 (**8**)	Mollusc	Peptide	Inhibits microtubule formation	NCI-Knoll	Phase II clinical trials of the derivative TZT-1027
HTI286 (**9**)	Sponge	Tripeptide	Inhibits microtubule formation	Novartis	Continuing clinical trials
Discodermolid (**10**)	Sponge	Polyketide	Inhibits microtubule formation	Novartis	Phase II clinical trials
Cryptophycin (**11**)	Cyano-bacterium	Cyclic depsipeptide	Inhibits microtubule formation	Eli Lilly	Removed from phase II clinical trials
Aplidin (**12**)	Ascidium	Cyclic depsipeptide	Causes oxidative stress in cells	PharmaMar	Phase II clinical trials
Eribulin mesylate (**13**)	Sponge	Polyester derivative	Inhibits microtubule formation	Esai Company	Phase III clinical trials
Squalamine (**14**)	Shark	Steroid	Inhibits angiogenesis	Genaera	Removed from phase II clinical trials
Kahalalide F (**15**)	Mollusc	Cyclic depsipeptide	Lysosome-tropic effect	PharmaMar	Phase II clinical trials
Salinosporamide A (**16**)	Marine bacterium	Lactam-lactone derivative	Proteasome inhibitor	Nereus	Phase II clinical trials

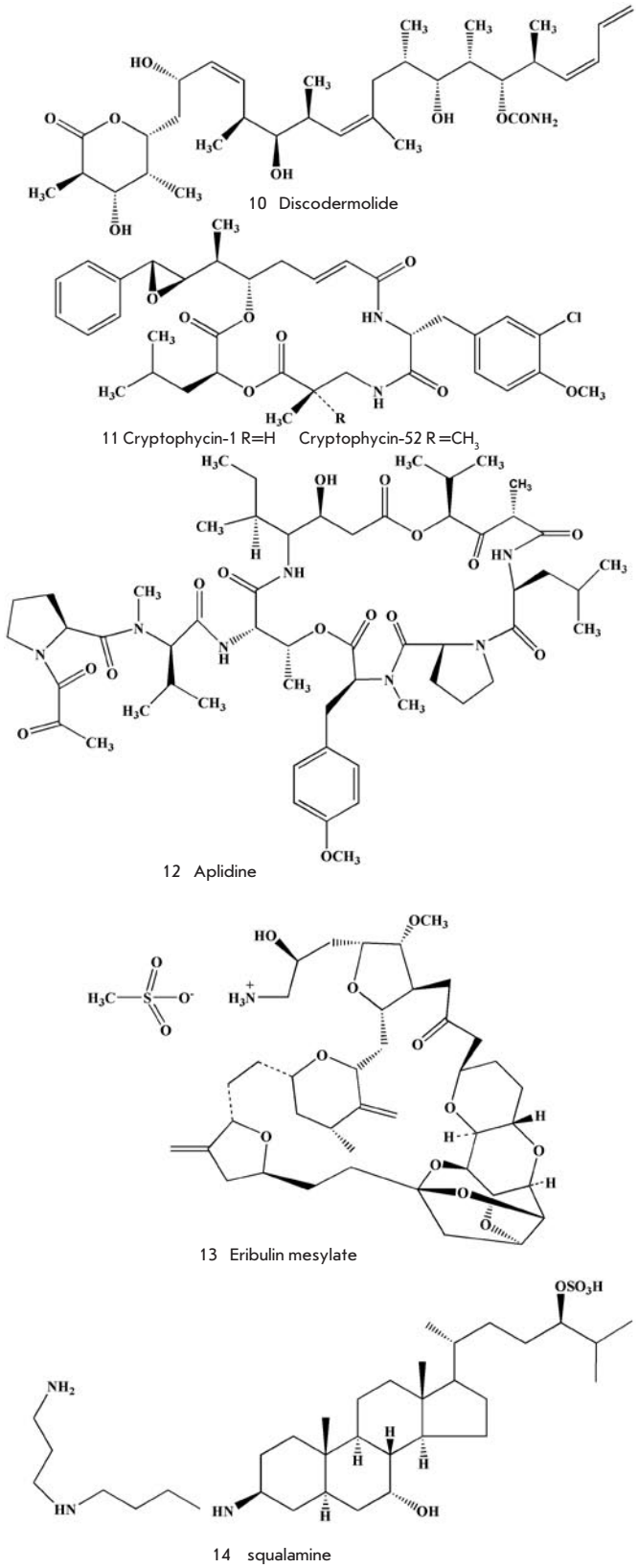

Fig. 3. Some compounds tested as active substances of antitumor drugs

scientists discovered new source of halichondrins, the deep-water sponge *Lissodendoryx* n. sp.1. A ton of that sponge was obtained by dredging. Moreover, plantations of *Lissodendoryx* were created in shallow waters in New Zealand, though the content of the target agents was much lower in the cultivated tube than in the wild one [29]. Those efforts made it possible to obtain 310 mg of halichondrin B and to begin clinical testing in 2002. Then, Japanese scientists, in collaboration with the Esai Company, found out that a much simpler derivative of halichondrin – eribulin mesylate (**13**) (Fig. 3) –was characterized by the same biological activity. Currently, eribulin mesylate is in the third stage of clinical testing as a potential drug for the treatment of breast cancer [13]. Moreover, it is being tested for the treatment of prostate cancer and sarcoma.

Squalamine (**14**) (Fig. 3), a water-soluble aminosteroid, was extracted from the liver of the shark *Squalus acanthis* in 1993. This substance displays strong antimicrobial action [30, 31]. Later, using different types of mouse cancer, squalamine was found to inhibit angiogenesis and to stop the growth of tumors [32]. The Genaera Company organized pharmacological investigations of squalamine, but at the second stage of clinical testing (pulmonary and ovarian cancers), its antitumor properties were found to be insufficient. Nevertheless, squalamine was found to intensify the therapeutic effect of paclitaxel and carboplatin, inhibiting some growth factors, for instance VEGF, and causing a decrease in the amount of blood vessels around the tumor and apoptosis of tumor cells. Moreover, it was established that its physiological effects could be useful in the treatment of diseases characteristic of elderly people and related to vision disorders (macular degeneration) [33, 34].

The investigation of the mollusc *Elysia rufescens* under the guidance of Scheuer at the Hawaiian University in the USA led to the discovery of several new high-active depsipeptides, including kohalalide F (**15**) (Fig. 4) [35]. This mollusc feeds on the algae *Bryopsis* spp., the real producers of kohalalide. The mollusc accumulates this biologically active substance as a chemical protective means against predators. Moreover, the kohalalide content in the mollusc is 5,000 times higher than in the algae. After the solid-phase synthesis of that peptide, its structure and relative stereochemistry were corrected [36] and the PharmaMar company began the preclinical and then clinical investigation.

Kohalalide induces the formation of vacuoles in some tumor cells and stimulates lysosomes. It is several times more toxic against tumor cells than against healthy cells [37]. In spite of the fact that the mechanism of the kohalalide's antitumor action has yet to be pinpointed , currently, it is in the second stage of clinical testing for the treatment of solid tumors resistant to other substances [13].

Salinosporamide A (**16**) (Fig. 4) was isolated in 2003 by Fenical and co-workers (Scripps Institution of Oceanography, California, USA) from the salt-tolerant marine bacterium referred to as a new class of bacteria-actinomycetes called *Salinispora* [38]. It inhibits p26 proteosomes [36]. Not long ago, the pharmaceutical company Nereus Pharmaceuticals (USA) completed the first stage of clinical testing of that substance coded as NPI-0052 for the treatment of multiple myeloma [13].

In addition to the above-mentioned substances, several other marine natural products have been clinically studied as potential antitumor agents: peptide cematidine from moluscs, peptide ILX-65 similar to dolastatin, and tripeptide E-7974 from the sea sponge inhibiting polymerization of tubulin [5, 13, 40] (Knoll Company); derivative of aminoacid LAF389 being an inhibitor of methionine-aminopeptidase (Novartis); synthetic analog of sponge cerebroside KRN7000 characterized by immunostimulatory and strong antitumor action on patients who retained a high level of NK cells. Prospects for the further clinical study of these substances are unclear.

In Russia, alkaloids – polycarpin (**17**) (Fig. 4) [41] and varacin C (**18**) [42], characterized by high toxicity against tumor cells, were isolated from ascidians. Cytotoxicity and activity in the acid environment of varacin C (**18**) are higher than those of well-known doxorubicin: that is why varacin is quite selective as regards tumors, in comparison to normal tissues [43]. In fact, some tumors are known to acidify themselves due to elevated glycolysis. Polycarpin and its numerous synthetic analogues cause apoptosis of tumor cells, intensifying the phosphorylation of protein p53 at the aminoacid residue Ser-15 [44]. However, they have appeared to be rather toxic to animals. Varacin C was synthesized shortly after isolation [43], and a while ago, in Russia, scientists began the synthesis of its analogues and obtained several high-active compounds promising for further investigation as pharmaceutical leads [45].

Hence, most of the substances selected for preclinical and clinical testing are strong inhibitors of tubulin polymerization. Moreover, they include inhibitors of protein kinase C (bryostatin), other enzymes (LAF-389), inhibitors of proteosomes (NPI-0052), agents interacting with DNA (Yondelis), inhibitors of angiogenesis (aplidin, kohalalide, and squalamine), and substances with an undetermined mechanism of action. Taking into consideration the wide diversity in the structures of highly active marine metabolites and the different mechanisms through which they exhibit antitumor action, there is confidence that further efforts aimed at creating antitumor drugs on the basis of marine natural products will be successful.

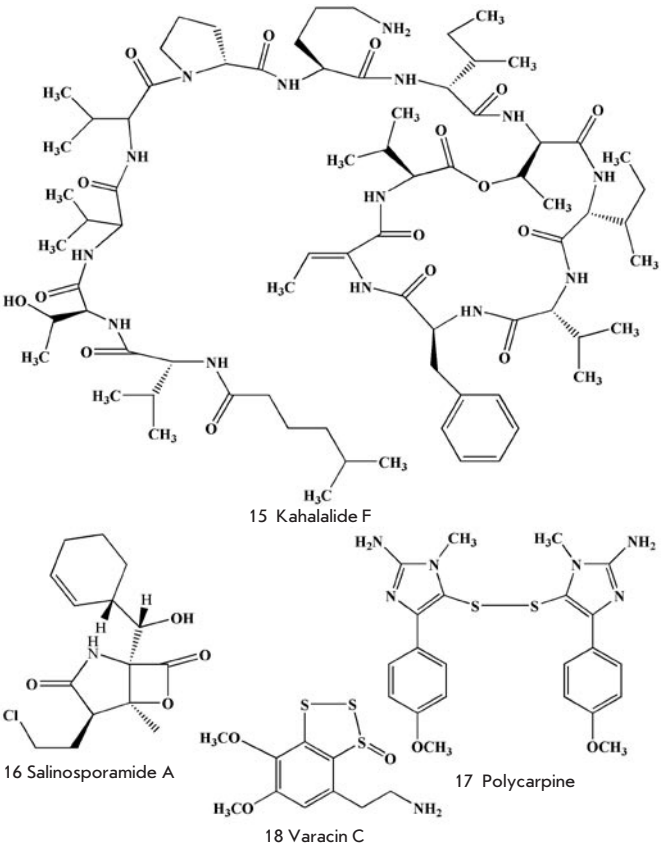

Fig. 4. Some compounds investigated as active substances of antitumor drugs

MARINE NATURAL PRODUCTS WITH ANALGESIC PROPERTIES

The first analgesic drug based on marine natural products was called ziconotide (prialt). It was created after twenty years of investigating toxins from predatory moluscs-gastropods belonging to the *Conus* genus. In the end of 2004, this compound under the commercial name "prialt" was approved for production and clinical use in the USA, and a few months later, in Europe. The name "ziconotide" is more often used for its active substance, ω-conotoxin, obtained with the help of peptide synthesis.

Cone snails, more than 300 species are known, use small fish for food, which snails catch by a harpoon connected by a special channel to their poison gland. The snails' glands biosynthesize hundreds of different peptide toxins [46], which immobilize a victim by affecting the neuromuscular transmission in its organism.

Understanding of the structure of some toxins from different species of cone snails was followed by the synthesis of thousands of their analogues. However, pharmacological trials showed that one of the natural toxins, rather than their synthetic derivatives, was of top interest as a potential drug. That toxin was named ω-conotoxin MVIIA. ω-conotoxin is a linear peptide composed of 25 aminoacid residues, which was isolated for the first time from the Pacific mollusc *Conus magnus*. Six cysteine residues form three disulphide bridges in this compound [47, 48]. The disulphide bridges provide ω-conotoxin with a well-formed and unique space structure, as well as the ability to specifically block the work of N-type voltage-sensitive calcium channels. As a result, the toxin efficiently inhibits the transmission of the pain signal (K_d=9 pM). Clinical investigations of synthetic ω-conotoxin were carried out by the pharmaceutical company Neurex (branch Elan Pharmaceuticals). As an analgesic it appeared to be 1,000 times stronger than morphine [49]. Those investigations showed its high efficiency in the inhibition of pain, including phantom ones. In contrast to morphine, ziconotide (**19**) (Fig. 5) did not cause hallucinogenic effect and addicting property effect and does not cause addiction [50].

Several other conotoxins are now at different stages of investigation as potential drugs. Clinical trials of some compounds of that class were discontinued due to undesirable side effects: for instance, the AM-336 peptide-based drug, which was developed by the AMRAD Company for the treatment of chronic pains.

Recently discovered groups of conotoxins, which specifically block α1–adrenoreceptors, are good model compounds for the creation of new analgesic medical products on their basis [51].

ANTI-INFLAMMATORY AND WOUND-HEALING MARINE NATURAL PRODUCTS

Pseudopterosins, for instance pseudopterosin E (**20**) (Fig. 5), are characterized by strong anti-inflammatory action. Pseudopterosins belong to the group of diterpene glycosides isolated by Fenical and co-workers from the Caribian gorgonian coral *Pseudopterogorgia elisabethae* in the end of the 1980s [52]. The anti-inflammatory action of pseudopterosins is stronger than that of the well-known anti-inflammatory drug indomethacin. They influence the biochemical transformation of arachidonic acid, decreasing the synthesis of eicosanoids [53]. Estee Lauder has created a cosmetic cream for facial skin for commercial realization on the basis of partially purified extracts of *P. elisabethae*, containing pseudopterosin E. To ensure production of the cream with the required amount of pseudopterosins, scientists collected a lot of gorgonian corals along the coast of the Bahamas Islands and, then, studied the regeneration of corals after the removal of some parts of their colonies. Two other ways to produce pseudopterosin were developed to decrease the damage to underwater biocenoses: their aglycons were synthesized by several methods [54–56] and, then, glycosylated: moreover, scientists have discovered new biotechnological ways to produce pseudopterosin from farnesol pyrophosphate under the action of enzymes extracted from *P. elisabethae* [57].

The synthetic derivative of pseudopterosins called methopterosin (OAS 1000) was subjected to clinical testing as an anti-inflammatory agent for the treatment of contact dermatitis. However, those trials were not completed due to the bankruptcy of the OsteoArthritis Sciences Inc. Company [34]. Later, that substance was subjected to the second stage of clinical testing as a wound-healing agent by Tyrosin Group Inc. Company (USA).

Contignasterol (**21**) (Fig. 5) [58], an unusual steroid from the sponges *Petrosia contignata*, was studied under the code IZP 94005 as an anti-inflammatory agent. The structure of contignasterol is characterized by a cis-junction of the C and D cycles. In contrast to drugs with analogous action, this compound (**21**) is not an inhibitor of A_2 phospholipase, but it inhibits the excretion of histamine by leukocytes and is referred to as a leukocyte-selective anti-inflammatory agent [59]. Inflazyme Pharmaceutical Ltd. and Aventis Pharma (USA) were jointly developing a new drug on the basis of contignasterol. However, because of its extremely complicated structure, contignasterol was modified and replaced with the simpler, but highly active, synthetic analogues IPL 576092 and IPL 512602 [60, 61].

This latter compound underwent two stages of clinical testing for the treatment of asthma. In 2004, cooperation between the two companies ended and Inflazyme chose to work independently: several more promising derivatives were obtained, while the testing included not only asthma, but also skin and eye disorders [34]. However, after the sale of this project in 2008 to Orexo Pharmaceuticals Company, information about further investigation of the substance has not appeared.

One more terpenoid – monoalide (**22**) (Fig. 6) – was extracted from sponges *Luffariella variabilis* [62] by Scheuer and co-workers in 1980. Monoalide has two hidden aldehydic groups (hemiacetal and as a γ-lactone derivative) which react with the amino groups of lysine residues on the surface of the substratum binding site in A_2 phospholipase. As a result, monoalide (**22**) inhibits this enzyme and the hydrolytic elimination of arachidonic acid from prospholipide,

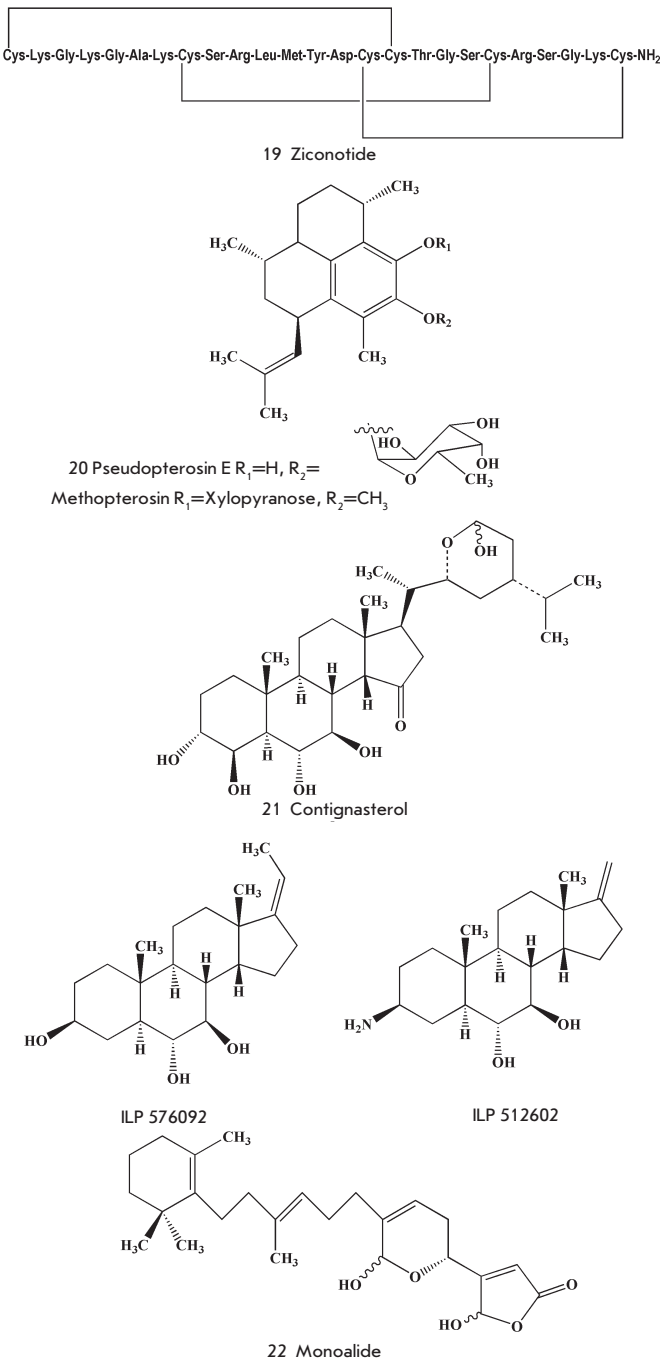

Fig. 5. Some compounds investigated as analgesic and anti-inflammatory agents

demonstrating anti-inflammatory properties. The strong anti-inflammatory action of monoalide [63, 64] has attracted the attention of Allergen Pharmaceutical Company (USA). The company secured a license for the drug and carried out two stages of clinical testing of monoalide as a drug for the treatment of psoriasis. However, problems with the low transport of the active substance through a patient's skin led scientists to stop further clinical investigations. At the same time, monoalide is released as a biochemical reagent, a specific inhibitor of A_2 phospholipase. Moreover, scientists continue to try to obtain such a derivative of monoalide that will be devoid of its disadvantages, with the help of organic synthesis.

The Pacific Institute of Bioorganic Chemistry, Far East Division of the Russian Academy of Scientists, created a new drug called Collagenase KK based on a complex of collagenolytic proteases from the Kamchatka King crab *Paralithodes chamtschaticus*. After preclinical and clinical testing, Collagenase KK was approved for production and use in Russia. The drug was recommended for fermentative wound cleansing in case of pitting, necrosis, chilblains, gangrene, chronic osteomyelitis, and varicose ulcer [65-67]. Experience in the clinical application of Collagenase KK after the release of the first batches shows that this drug, in addition to the above-mentioned areas of medical application, may be useful for the treatment of some other diseases and post-surgery complications. For instance, Collagenase KK was successfully used in endoscopic and plastic surgery and for the treatment of foul peritonitis in children. Collagenase KK may also be used for the destruction of collagen in commissures.

MARINE NATURAL COMPOUNDS WITH ANTIVIRAL AND ANTIMICROBIAL PROPERTIES.

After the discovery of arabinonucleosides characterized by antiviral and antitumor properties in the beginning of the 1950s and after the following synthesis of some nucleoside derivatives, which became the biologically active substances of antiviral drugs, the search for new marine antiviral drugs has been in progress. Compounds with such activity were found among terpenoids, steroids, alkaloids, aliphatic and aromatic derivatives, peptides, polysaccharides, and other secondary metabolites extracted from different marine organisms [68-71].

AIDS remains one of the most dangerous viral diseases affecting a great number of people. The number of people suffering from AIDS approximates 50 million and increases every day by 16 thousand people. By the early 2003, more than 150 highly active marine metabolites were found in the course of testing against HIV [69, 70]. Edible algal polysaccharides, in particular fucoidans, carrageenans, and others, inhibit the penetration of HIV into human mononuclear cells. Some of them inhibit virus replication in very low concentrations (0.1-0.01 μg/ml) and intensify the antiviral action of azidothymidine. However, some specialists believe that their antiviral effects are the result of nonspecific interaction either with viruses, or with cells, while these substances themselves poorly penetrate biological fluids [70]. Hence, the question as to whether these substances can be considered as additional agents that in future may be used for the treatment of AIDS patients remains a matter of debate.

Peptides from some marine invertebrates are one more perspective group of antiviral substances. For instance, peptides composed of 17-18 amino-acid residues from horseshoe crabs *Tachypleus tridentatus* and *Limulus polyphemus* are characterized by strong antiviral effect against HIV-1. Analogous, but simpler in structure compounds were synthesized in the course of a project aimed at creating a new drug on the basis of those peptides. One of the peptides (T144) had IC_{50}=2.6 nM against HIV-1 at low cytotoxicity (IC_{50}=44.6 μM) [72, 73, 69]. The project aimed at creating a T144-based antiviral drug has a fair chance of success.

Among the highly active low-molecular antiviral marine substances it is important to note the above-mentioned didemnin B from ascidians, which when injected every day in a dose of 0.25 μg/kg to mice contaminated with a lethal dose of Rift Valley fever helped save 90% of them. Some hope is related to a relatively simple terpenoquinone avarone (**23**) (Fig. 6) and similar compounds from the sponges *Dysidea*, which inhibit reverse transcriptase from HIV-1 and the virus itself in a concentration of 0.1 μg/ml [70]. Mycalamide B (**24**) (Fig. 6) from the New Zealand *Mycale* sp. may be cited as another example of antiviral metabolite from sponges. Mycalamide B is a strong inhibitor of protein synthesis, which shows inhibiting activity in a dose of 2 ng/band when tested *in vitro* for action on different viruses [70]. The creation of drugs on the basis of these and other highly active compounds is slowed down by the high toxicity of some of them and low accessibility. However, these and other highly active marine substances are good models for syntheses of new less toxic, but highly active, antiviral agents.

Some of the numerous marine antimicrobial compounds displayed high activity against the tuberculosis bacterium *Mycobacterium tuberculosis*. For instance, pseudopteroxazol (**25**) (Fig. 6), benzoxazole diterpene alkaloid from the gorgonian coral *Pseudopterogorgia elisabethae*, inhibits the growth of this mycobacterium by 97% in a concentration of 12.5 μg/ml in the absence of toxic effects [71], while (+)-8-hydroxymanzamine (**26**) (Fig. 7) from the sponge *Pachypellina* sp [71] has a minimum inhibiting concentration of 0.91 μg/ml. Manzamine is even more active against the protozoa *Toxoplasma gondii* (IC_{50}=0.054 μg/ml), an infectious agent which causes such extremely dangerous (especially for pregnant women and children) diseases as toxoplasmosis. Manzamine is not used in medicine due to its low accessibility.

Diterpenoid bromosphaerone (**27**) (Fig. 7) from the red alga *Sphaerococcus coronopifolius* (IC_{50}=0.078 μg/ml), dimeric isoquinoline alkaloid jorumicin (**28**) (Fig. 7) from the Pacific sea hare *Jorunna funebris* (IC_{50}=0.050 μg/ml), and some other marine metabolites [71] are highly active against *Staphylococcus aureus*.

However, most of these substances, as well as fascalkaloid fascaplysin (**29**) (Fig. 7), macrolide forboxazole A (**30**) (Fig.7) and others characterized by strong antifungal action, have appeared too toxic for use in clinical testing.

MARINE NATURAL PRODUCTS WITH OTHER BIOLOGICAL EFFECTS

Two new drugs – Histochrome for ophthalmology and Histochrome for cardiology –have been created in the Pacific Institute of Bioorganic Chemistry, Russian Academy of Sci-

ences, on the basis of sea urchin pigments characterized by antioxidant, antimicrobial and anti-inflammatory properties and then approved for production and use in Russia [74]. Histochrome for ophthalmology has proved highly effective against traumas and blood strokes of different origins and against some other eye diseases. Histochrome for cardiology is a cardioprotector reducing by half the necrosis zone formed due to acute myocardial infarction. Histochrome for cardiology commonly assigned as drop infusion 10 minutes before the thrombolytic therapy decreases the frequency of extrasystoles. Moreover, this drug decreases the number of complications after open-heart surgery. The major constituent active substance of both drugs is the well-known pigment echinochrome (**31**) (Fig. 8). Scientists have found an easily accessible natural source of echinochrome (the sand dollar *Scaphechinus mirabilis*) and have developed new methods of isolation and synthesis of this pigment with a high yield [47].

The clinical application of Histochrome drugs has demonstrated their advantages relative to the analogous drugs used previously. The data obtained on the Histochrome for ophthalmology are of special interest. Histochrome for ophthalmology has been established to be successful in the treatment of hemophthalmos, different child eye pathologies, cataract, as well as in eye surgery.

In 1971, a toxin called anabasein (**32**) (Fig. 8) was extracted from the sea worm hoplonemertea [75]. The synthesis of numerous anabasein analogues has led to the creation of several highly active compounds, including the pharmaceutical lead GTS-21 (**33**) (Fig. 8), which has displayed cytoprotector properties and improved memory in test animals. Competing with the natural ligands, GTS-21 binds to α4β and the α7-subtypes of nicotinic receptors; the latter is considered to be important in control of β-amyloid neurotoxicity. Florida State University sold to the Japanese company Taicho the license for those substances, and they have organized clinical testing in Europe and the U.S. The first stages of testing on patients-volunteers showed the significant cognitive effects of GTS-21 [76]. Currently, substances of this series are being studied as potential drugs for the treatment of Alzheimer's disease.

Holothurians (sea cucumbers), invertebrates belonging to the Holothurioidea class of the phylum Echinodermata, have always attracted the attention of people in Eastern Asian countries due to their biologically active substances. Edible animals of that class (trepangs) are thought to have healing properties, including stimulation, wound-healing, and other

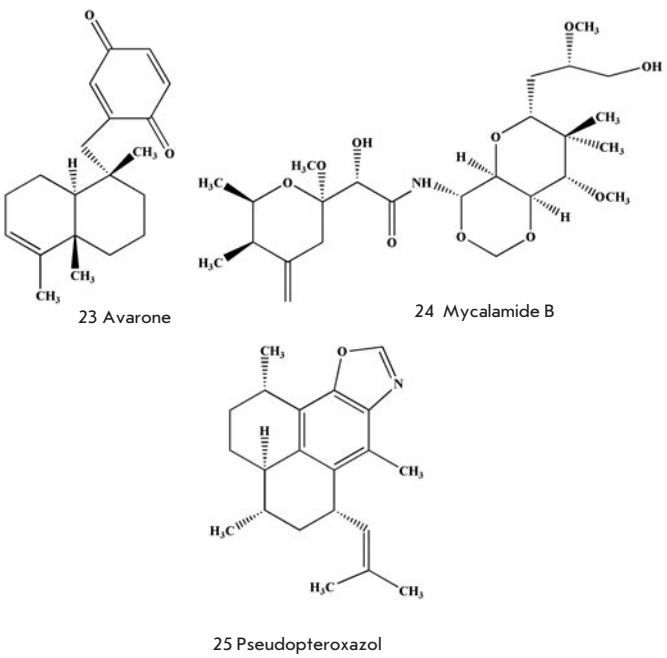

Fig. 6. Marine natural antiviral compounds

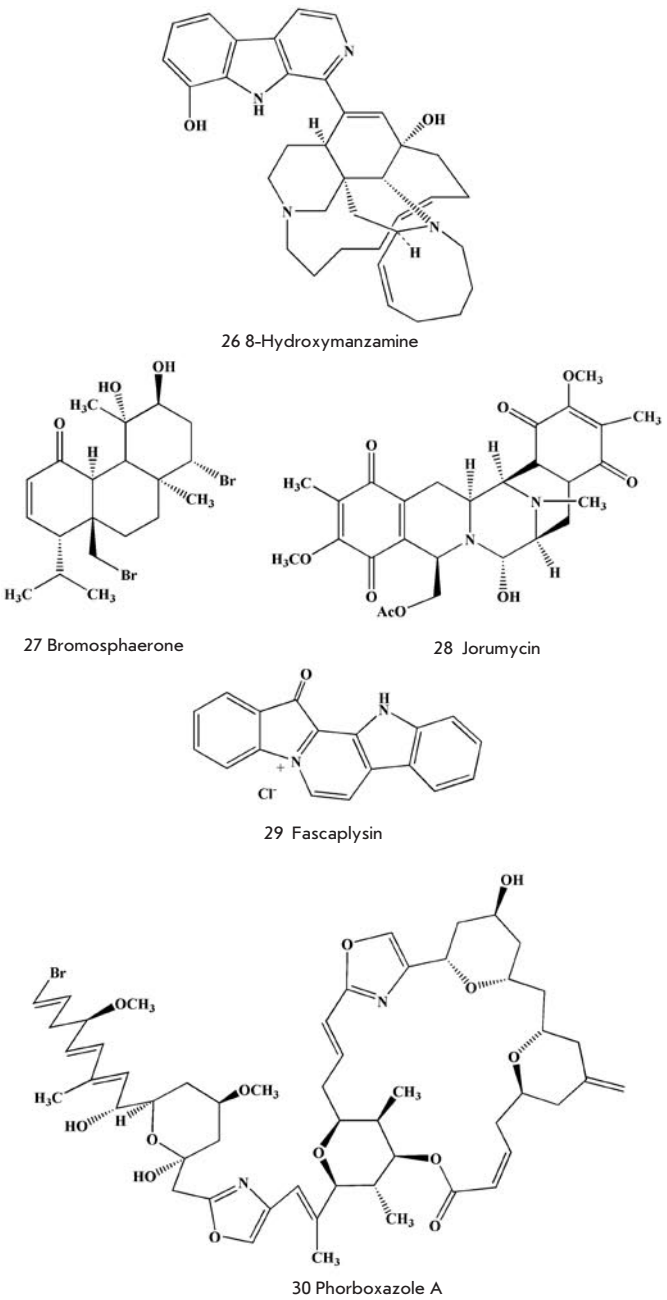

Fig. 7. Marine natural anti-infectious agents

useful effects. However, the substances responsible for the biological activity of trepangs have yet to be studied.

In the course of a multi-year investigation, scientists from the Pacific Institute of Bioorganic Chemistry, Russian Academy of Sciences, have collected about 50 species of holothurians in different parts of the World Ocean and obtained more than 100 new physiologically active triterpene glycosides from their extracts [76]. Some of them have turned out to be strong modulators of cellular immunity. These substances serve as a basis for the development of a potential drug called cumaside, which contains the agents (**34, 35**) (Fig. 8) as an active substance [77]. This drug, in very low concentrations, increases the resistance of test animals to bacterial infections and radiation, stimulates the phagocytic and bactericide activities of macrophages, inhibits tumor growth and intensifies the action of antitumor drugs, without displaying any toxic properties [78, 79]. Cumaside will be subjected to clinical testing in the nearest future.

CONCLUSION

Marine natural products are quite diverse. Every year, the number of known marine natural products increases (between 2007 and 2008, almost by 1,000 compounds every year) [80]. Their biochemical diversity is a result of the high biological diversity in the seas and oceans. According to different estimates, our planet is inhabited by several million species of marine microorganisms, as well as about a million of yet undescribed species of marine invertebrates and other marine organisms.

The investigation of marine natural products has led to the creation of a series of highly efficiency medical products, including antitumor and antiviral drugs (Arabinocytosine, Arbinoadenosine, Trabectidin), the analgesic drug Prialt, two Russian drugs of the Histochrome series, which are able to decrease the necrosis zone after myocardial infarction and to treat the consequences of eye blood stroke of a different ethiology, as well as the Russian burn-treating drug Collagenase KK. More than 40 antitumor, anti-inflammatory, immunostimulatory, and other pharmaceutical leads are at different stages of preclinical and clinical testing. This all became possible thanks to the physiological activity of some marine natural products. Among them are the most potent non-protein toxins (palytoxin, maitotoxin), the most effective inhibitors of tumor cells development (spongistatin, etc.), the strongest analgesic compounds (the toxins of cone snails), and other extremely active substances.

It appears that many marine secondary metabolites extracted from sponges, ascidians, and other marine invertebrates are biosynthesized by symbiont microorganisms [80]. Only 1% of such microorganisms can grow in an artificial environment and may be cultivated. An example is the extraction of the bacterium *Micromonospora* sp from the deep-water sponge by American scientists. It produces manzamine and 8-hydroxymanzamine. As was mentioned before, these substances show very promising anti-parasitogenic and antituberculous activity, but they cannot be obtained in a large amount from the sponges. It is of interest that the biosynthesis of physiologically active alkaloids in this bacterium is possible only in a special environment, while the standard cultivation is not appropriate for their formation [5]. Re-

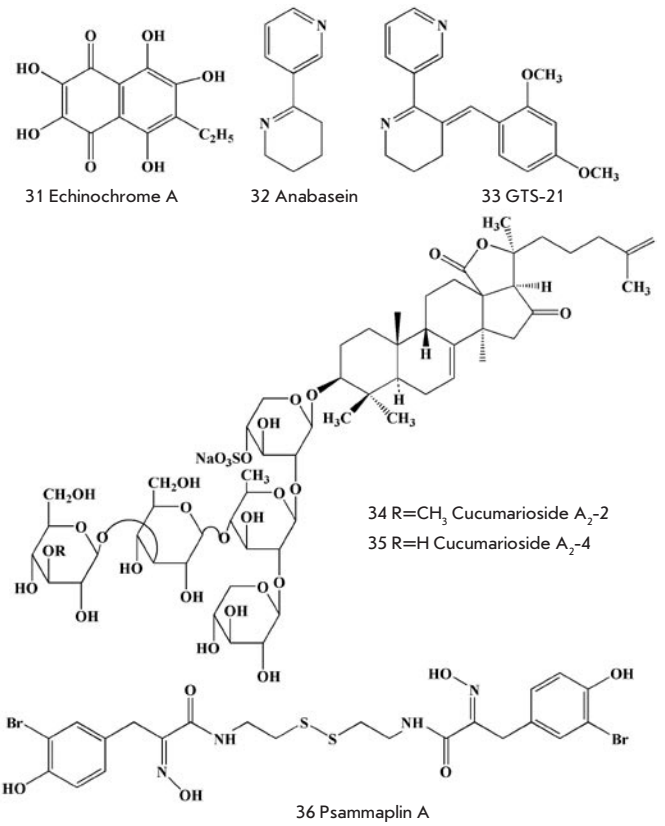

Fig. 8. Other physiologically active marine natural compounds

cently, Fenical and his co-workers selected a medium for the cultivation of marine microorganisms with regard to conditions characteristic of their habitats. As a result, they have managed to cultivate a range of marine actinomycetes and to obtain a series of new secondary metabolites from them [81]. As follows from their investigation of the related species belonging to the new class *Salinispora*, the biosynthesis of secondary metabolites in marine microorganisms is often not strain-specific, but species-specific, which makes these microorganisms an appropriate and reproducible source of highly active compounds. In the opinion of Newman and other scientists from the National Institute of Cancer (USA), the study of bioactive substances from marine microorganisms has just begun [81].

In recent years, a new direction in the search for and study of marine natural products – marine metagenomics – has appeared. Within the framework of this direction, not individual genomes, but a group of genomes from any habitat, for instance from sponges, are analyzed and subjected to manipulations. In addition to the sponge genome, the genomes of numerous microorganisms, largely those hard to cultivate, are investigated. The transfer of big gene clusters to bacteria which are easy to cultivate, followed by the analysis of the metabolite products in some clones, may lead to the creation of producers of useful compounds [82, 83]. However, it is essential to have knowledge about the biosynthesis of these substances to solve the problem of the creation of useful nat-

ural products by this method. A while ago, scientists reported on the transcription of the genes responsible for the biosynthesis of such highly active marine metabolites as bryostatins and some metabolites extracted from sponges [83, 84]. The metagenome projects are being realized now on vast water areas (Monterey Bay, the Sargasso Sea) [85].

Some marine organisms are characterized by high productivity. For instance, the productivity of microalgae is higher than that of agricultural plants. They may be the sources not only of such useful for medicine substances as ω-3 fatty acids and carotenoids, but, likely, of other highly active compounds, as well as biofuel. It is necessary to select the most promising strains of these plants and to develop new-generation phytobioreactors to obtain biomass in an amount sufficient for the solution of these problems [86].

Finally, the study of biologically active marine natural compounds stimulates work aimed at the organic synthesis of these compounds, as well as that of their derivatives and analogues. As a result, extensive libraries of compounds, including those characterized by a higher activity than a substance's prototype, are created. For instance, in the course of the investigation of histone deacetylase inhibitors, the Novartis Company, in cooperation with the group of well-known chemist-synthesist Nikolaou, using the marine natural compound psammaplin A **(36)** (Fig. 8) as a prototype, obtained a library of 3,828 substances through organic synthesis; 6 of those substances were highly active against the methicillin- and vincamycin-resistant strains of *Staphylococcus aureus* [5]. ●

REFERENCES

1. Semenov A. A., Essays of Chemistry of Natural Products, Resp. Red. G. A. Tolstikov, *Nauka*, Novosibirsk, 2000, 664 pp.
2. Bergmann W., Feeney R. J. *//J. Org. Chem.* 1951, **16**, 981-987.
3. Bergmann W., Burke D. C. *// J. Org. Chem.* 1956, **21**, 226-228.
4. Bergmann W., Stempien M. F. *// J. Org. Chem.* 1957, **22**, 1575-1577.
5. Newman D. J., Cragg G. M., *// J. Nat. Prod.*, 2004, **67**, 1216-1258.
6. Newman D. J., Cragg G. M. *// J. Nat. Prod.*, 2007, **70**, 461-477.
7. Rinehart K. L. *et al.*, *// J. Org. Chem.*, 1990, **55**, 4512-4515.
8. Wright A. E. *et al.*, *// J. Org. Chem.*, 1990, **55**, 4508-4512.
9. Corey E. J., Gin D. Y., Kania R. S. *//. J. Am. Chem. Soc.*, 1996, **118**, 9202-9203.
10. Cuevas C, Pérez M, Martín M. J. *et al. //Org. Lett.*, 2000, **2**, 993-996.
11. Pommier Y, Kohlhagen G, Bailly C, *et al. // Biochemistry*, 1996, **35**, 13303-13309.
12. Haefner B*// Drug Discovery To-Day*, 8, 536-544, 2003.
13. Molinski T. F., Dalisay D. S., Lievens S. L., Saludes J. P. // Nat Rev Drug Discov. 2009, 8 January 2009, **8**, 69-85.
14. Pettit G. R. *et al. // J. Am. Chem. Soc.*, 1987, **109**, 6883-6885.
15. Pettit G.R. *et al. // J. Am. Chem. Soc.*, 1989, **111**, 5463-5465.
16. Schöffski P., Thate B., Beutel G., *et al. //Ann. Oncol.*, 2004, **15**, 671-679.
17. Talpir R., Benayahu Y., Kashman Y., Panell L, Schleyer M. *// Tetrahedron Lett.* 1994, **35**, 4453-4456.
18. Niu C, Smith D, Zask A, *et al. // Bioorg. Med. Chem. Lett.* 2004, **14**, 4329-4332.
19. Hadaschik B. A., Ettinger S, Sowery R. D., *et al. // Int. J. Cancer*, 2008, **122**, 2368-2376.
20. Gunasekera S. P., Gunasekera M., Longley R. E., Schulte G. K. *// J. Org. Chem.* 1990, **55**, 4912-4915.
21. Harried S. S., Lee C. P., Yang G., Lee T. I., Myles D. C. *// J. Org. Chem.* 2003, **68**, 6646-6660.
22. Hung D. I., Nerenberg J. B., Schreiber S. I. *// J. Am. Chem. Soc.*, 1993, **115**, 12621-12622.
23. Trimurtulu G. *et al. // J. Am. Chem. Soc.* 1994, **116**, 4729-4737.
24. Barow R. A. *et al. // J. Am. Chem. Soc.* 1995, **117**, 2479-2490.
25. Rinehart K. L., Gloer J. B., Cook J. C., Mizsac S. A., Scahill T. A. *// J. Am. Chem. Soc.* 1981, **103**, 1857-1859.
26. Gajate C., An F., Mollinedo F. *// Clin. Cancer Res.* 2003, **9**, 1535-1545.
27. Hirata Y., Uemura D*// Pure Appl. Chem.*, 1986, **58**, 701-710.
28. Aicher T. D. *et al.*, *// J. Am. Chem. Soc.* 1992, **114**, 3162-3164.
29. Munro M. H., Blunt J. W., Dumdei E. J., *et al. // J. Biotechnol.*, 1990, **70**, 15-25.
30. Moore K. S., Wehrli S., Roder H., *et al. //Proc. Natl. Acad. Sci*, 1993, **90**, 1354-1358.
31. Wehrli S. L., Moore K. C., Roder H., Durell S., Zasloff M. *// Steroids* 1993, **58**, 370-378.
32. Sills A. K. Jr, Williams J. I., Tyler B. M., *et al. // Cancer Res.* 1998, **58**, 2784-2792.
33. Ciulla T. A., Criswell M. H., Danis R. P., Williams J. I., McLane M. P., Holroyd K. J. *// Retina* 2003, **23**, 808-814.
34. Gross H., Konig G. H. *// Phytochem. Rev.*, 2006, **5**, 115-141.
35. Homann M. T., Scheuer P. J. *// J. Am. Chem. Soc.*, 1993, **115**, 5825-5826.
36. Lopez-Macia A., Jimenez J. C., Royo M., Giraet E., Albericio F. *// J. Am. Chem. Soc.*, 2001, **123**, 11398-11401.
37. Suárez Y, González L, Cuadrado A, Berciano M, Lafarga M, Muñoz A. *// Mol. Camcer Ther.* 2003, **2**, 863-872.
38. Feling R. H., Buchanan G. O., Mincer T. J., *et al. // Angew. Chem. Intl. Ed.* 2003, 42, 355-357**.**
39. Chauhan D. L. *et al. // Cancer Cell* 2005, **8**, 407-419.
40. D.J. Newman G. M. Cragg K. M. Snader. *// J. Nat. Prod.*, 2003, **66**, 1022-1037.
41. Radchenko O. S., *et al. // Tetrahedron Lett.* 1997, **38**, 3581-3584.
42. Makarieva T. N., Stonik V. A., Dmitrenok A. S., Grebnev B. B., *et al. // J. Nat. Prod.* 1995, **58**, 254-258
43. Lee A. H., Chen J., Liu D., Leung T. Y., Chan A. S., Li T.//C. *J. Am. Chem. Soc.* 2002, **124**, 13972-13973
44. Fedorov S. N., Bode A. M., Stonik V. A., *et al. // Pharm. Research*, 2004, **21**, 2307-2319,
45. Volcho K. P. Use of Natural Compounds in Catalytic Synthesis of Chiral Biologically Active Substances. *Abstract of Thesis for Degree of Doctor of Chemical Sciences,* Ufa, 2009.
46. Olivera B. M., Gray W. R., Zeikus R., *et al. // Science*, 1985, **230**, 1338-1343.
47. Olivera B. M., Miljanich G. P., Ramachandran J., Adams M.E. *// Ann. Rev. Biochem.* 1994, **63**, 823-867.
48. Chung D., Guar S., Bell J. R., Ramachandran J., Nadasci L. *// Int. J. Pept. Protein Res.* 1995, **46**, 320-325.
49. Wang Y. X., Pettus M., Gao D., Phillips C., Scott Bowersox S. *// Pain*, 2000, **84**, 151-158.
50. Miljanich G. P. *//. Curr. Med. Chem.* 2004, **11**, 3029-3040.
51. Harvey A. L. *// Trend Pharmacol. Sci.* 2002, **5**, 201-203.
52. Roussis V., Wu Z., Fenical W., Strobel S. A., Van Duyne G. D., Clardy J. *// J. Org. Chem.* 1990, **55**, 4916-4922.
53. Potts B. C.M., Faulkner D. J., Jacobs R. C. *// J. Nat. Prod.* 1992, **55**, 1701-1717.
54. Laserwith S. E., Johnson T. W., Corey E. J. *// Org. Lett.* 2000, **2**, 2389-2392.
55. Chow R., *et al. // J. Chem. Soc. Perkin Trans I*, 2001, **19**, 2344-2355.
56. Kocienski P. J., Pontiroli A., Qun L. *// J. Chem. Soc. Perkin Trans I*, 2001, **19**, 2356-2366.
57. Kohl A. C., Kerr R. G. *// J. Ind. Microbiol. Biotechnol.* 2003, **30**, 495-499.
58. Burgoyne D. L., Andersen R. J., Allen T. M. *// J. Org. Chem.* 1992, **57**, 525-528.
59. Takei M., Burgoyne D. L., Andersen R. J. *// J. Pharm. Sci.* 1994, **83**, 1234-1235.
60. Kasserra C. E., Harris P., Stenton G. R., Abraham W., Langlands J. M. *// Pulm. Pharmacol. Ther.* 2004, 17, 309-318.
61. Shen Y., Burgoyne D. L. *// J. Org. Chem.* 2002, **67**, 3908-3910.
62. De Silva E. D., Scheuer P. J. *// Tetrahedron Lett.* 1980, **21**, 1611-1614.
63. Jacobs R. S., Culver P., Langdon R., O'Brien, T, White S. J. *// Tetrahedron*, 1985, **41**, 981-984
64. Soriente A, De Rosa M. M., Scettri A., *et al. // Curr. Med. Chem.* 1999, **6**, 415-431.
65. Kozlovskaya E. P. *et al.* Wound-Healing Multifunctional Agent Collagenase KK. *Patent of the Russian Federation*, 2093166, 1997, *Bulletin, Selection.* 29, 5.
66. Stonik V. A., Mikhailov V. V., Bulgakov V. P., Zhuravlev Yu. N. *// Biotechnol. J.*, 2007, **2**, 818-825.
67. Elyakov G. B., Stonik V.A. *// Russian Chem. Bull.*, 2003, N 1, 1-18.
68. Mayer A. M. S., Rodriguez A. D., Berlinck R. G. S., Hamann M. T. *// Comp. Biochem. Physiol. Part C*, 2007, **145**, 553-581.
69. Gustafson K. R., Oku N., Milanowski D. J. *// Curr. Med. Chem. –Anti-Infective Agents*, 2004, **3**, 233-249.
70. Tzivelka L.-A., Vagias C., Roussis V. *// Curr. Topics in Med. Chem.* 2003, **3**, 1512-1535.
71. Donia M., Hamann M. T. *// Lancet Infect Dis.*, 2003, **3**, 338-348.
72. Morimoto M. *et al. // Chemotherapy*, 1991, **37**, 206-211
73. De Clercq E. *//Med. Res. Revs*, 2000, **20**, 323-349
74. Mishchenko N.P., Fedoreev S.A., Bagirova V.L. *// Chem. Pharm. Journ.*, 2003, **37**, 49-53.
75. Kem W. R., *et al. //Mar. Drugs*, 2006, **4**, 255-273.
76. Martinez A. *// Canc. Opin. Inv. Drugs*, 2007, **8**, 525-530.
77. Aminin D. L., *et al. // Intern. Immunology*, 2006, **6**, 1070–1082.
78. Belousiv M. V. *et al. // Bull. Sib. Med.* 2008, № 2, 20-22.
79. Belousiv M. V. *et al. // Bull. Sib. Med.* 2008, № 3, 9-12.
80. Blunt J. W., Copp B. R., Hu W. P., *et al. // Nat. Prod. Rep.* 2009, **26**, 170-244.
81. Newman, D. J., Hill R. T. *// J. Ind. Microbial. Biotechnol.*, 2006, **33**, 539-544.
82. Piel J., Butzke D., Fusetani N., *et al. // J. Nat. Prod.*, 2005, **68**, 472-479.
83. Schirmer A., Gadkari R., Reeves C.D., *et al. //* 2005, **71**, 4840-4849.
84. Hildebrand M., Waggoner L. E., Liu H., *et al. //Chem. Biol.*, 2004, **11**, 1543-1552.
85. Piel J., Hui D., Wen G., *et al. // Proc. Natl. Acad. Sci. USA*, 2004, **101**, 16222-16227.
86. Venter J. C., Remington K., Heidelberg J. F., *et al. // Science*, 2004, **304**, 66-74.
87. Wijffels R. H. *// Trends in Biotechnology*, 2007, **26**, 26-31.

Influenza Virus Neuraminidase: Structure and Function

Y.A. Shtyrya, L.V. Mochalova, N.V. Bovin#
Shemyakin and Ovchinnikov Institute of Bioorganic Chemistry, RAS
#e-mail: professorbovin@yandex.ru

ABSTRACT The structure of the influenza virus neuraminidases, the spatial organization of their active site, the mechanism of carbohydrate chains desialylation by neuraminidase, and its role in the influenza virus function at different stages of the viral infectious cycle are considered in this review. Data on the neuraminidase substrate specificity and different approaches in studying the activity of this enzyme are summarized. In addition, data on neuraminidase inhibitors (as antivirals) are provided, along with considerations on the mechanisms of resistance of modern influenza viruses to those antivirals.
Keywords: influenza virus, neuraminidase, substrate specificity
Abbreviations: a.a. – amino acid residue; HA – haemagglutinin; NA – neuraminidase; Neu5Ac – N-acetylneuraminic acid; 3`SiaLac – NeuAcα2-3Galβ1-4Glc; 6`SiaLac – NeuAcα2-6Galβ1-4Glc; MU-NANA – methylumbelliferyl-α-neuraminic acid; BODIPY - 6-((4,4-difluoro-5,7- dimethyl -4- bora -3a,4a-diaza-s-indacene-3-propionyl)amino)-hexaonic acid, succinimidyl ester; MDCK – Madin-Darby Canine Kidney Cells; VERO – kidney epithelial cells from African green monkey ; Neu5Gc – N-glycolylneuraminic acid; 3`SiaLacNAc – Neu5Acα2-3Galβ1-4GlcNAc; 6`SiaLacNAc – Neu5Acα2-6Galβ1-4GlcNAc.

The influenza virus is an enveloped (-)RNA containing a virus with a segmented genome, and its genetic material is coded by eight RNA-segments. All RNA segments are packed in a nucleocapsid protein, and a complex of polymerase proteins is attached to each of the genomic segments. Those RNA-protein complexes are packed in a lipoprotein envelope lined from the inside with a matrix protein, with haemagglutinin, neuraminidase, and M2 proteins exposed on the outer surface of the viral particle.

Neuraminidase is an exosialidase (EC 3.2.1.18) which cleaves α-ketosidic linkage between the sialic (N-acetylneuraminic) acid and an adjacent sugar residue [1]. The amino acid sequence of NA is coded by the 6th RNA segment. Nine subtypes of NA are described for influenza A, whereas only one NA subtype was revealed for the influenza viruses B and C [2]. Nine subtypes of influenza A NA are divided into two phylogenic groups. The first group consists of the neuraminidases of N1, N4, N5 and N8 subtypes, and the second one consists of N2, N3, N6 N7 and N9 subtypes [3].

The enzyme of the influenza C virus does not belong to the neuraminidase group. It promotes the O-deacetylation of the N-acetyl-9-O-acetylneuraminic acid, i.e. it belongs to the esterase family and will not be considered in this review.

The influenza virus NA executes several functions. Firstly, its activity is required at the time of the budding of newly formed viral particles from the surface of the infected cell, to prevent aggregation of viral particles. In addition, NA cleaves neuraminic acid residues from the respiratory tract mucins; by doing so, it facilitates viral movement to the target cell. Those functions will be considered further in more detail.

NEURAMINIDASE STURCTURE

The polypeptide chain of the influenza virus NA comprises 470 amino acid residues. The three-dimensional structure of NA consists of several domains: the cytoplasmic, transmembrane, "head," and also "stem," connecting the head to the transmembrane domain.

On the virion surface, NA resembles a homotetramer of a mushroom shape: head of 80*80*40 Å on the thin stem, 15 Å wide and from 60 to 100 Å long [2]. The molecular mass of the monomer is ≈ 60 kDa, and ≈ 240 kDa for the tetramer [1]. One viral particle has approximately 50 tetramers. Tetramers can form clusters on the viral surface [4]. The three-dimensional structure has been revealed for N1, N2, N4, N8, N9 and B NA [1, 3, 5, 6, 7]. Notwithstanding that NA types A and B homology cover only 30 %, their three-dimensional structures are virtually identical [6].

HEAD

The enzyme active site and calcium binding domain, which stabilizes the enzyme structure at low pH values, are situated in the head of NA [2; 8].

Homology between the strains inside one subtype attains about 90%, whereas homology between subtypes is 50%, and 30% between A and B types [9]. A.a. region 74-390 is the most conservative (N2 numbering)[1]. Residues, which account for the catalytic function of the enzyme (Arg118, Asp151, Arg152, Arg224, Glu276, Arg292, Arg371 and Tyr406, Figure 1), are constant for all NA subtypes of influenza A and also for influenza B NA. This works also for amino acids, which form the dimensional structure of the active site: Glu119, Arg156, Trp178, Ser179, Asp198, Ile222, Glu227, Glu277, Asp293, and Glu425. Asparagine residues, which form the glycosylation site, are strictly conservative (specifically, Asn146); proline and cysteine residues, which provide the required folding of the polypeptide chain and stabilize the 3-dimentional structure of the molecule, are also quite conservative [2].

The calcium binding site, which is located inside the molecule (particularly under the active site, if it is placed in accordance with the picture provided) is formed by the oxygen

[1] *As amino acid sequences of different neuraminidases differ from one another by insertions and deletions, it is common practice to highlight NA subtype according to which the numbering of amino acids is done, usually, as in this case N2 subtype numbering is used.*

of the main chain residues 297, 345 and 348, as well as by the oxygen of the side chain of Asp324 [1, 6]. Additionally, this site is formed by a.a. 293, 347, 111-115 and 139-143 [8].

The second neuraminic acid binding site, the so called HB-site, was found in N9 neuraminidases [10]. The a.a. sequence of this site is highly conservative among avian influenza viruses. This site is formed by three NA loops:

367 – 372, which is involved in neuraminic acid binding via serine residues 367, 370 and 372;

400 – 403, which interacts with the substrate via the side chain of asparagine 400, the carbonyl oxygen of the main chain of asparagines, and tryptophan 403;

430 – 433, which interacts with neuraminic acid via the ε-amino group of lysine 432.

All six above-mentioned conservative amino acids were found only in N9 NA. Avian influenza virus NAs of other subtypes usually lack lysine 432, but its absence does not interfere with their haemoadsorption activity. Human influenza virus neuraminidases usually lack the HB-site a.a. sequence. At the same time, two early isolates of human influenza viruses of the H2N2 subtype (RI+/57 and A/Leningrad/134/57) have the HB-site "frame" (serine triplet and tryptophan) [10, 11], which might be indicative of elimination of this site in the course of the influenza virus adaptation to replication in humans.

The function of the HB-site has yet to be clarified. It has been suggested that it may play the role of an alternative neuraminic acid binding site, in other words, function as a surrogate of the influenza virus HA; this assumption is based on the existence of viruses with combined HA and NA functions in one protein molecule, such as the ND virus. The HB-site, described earlier, is common for the NAs of viruses which HA interacts with α2-3-sialylated carbohydrate chains (i.e. avian and equine influenza viruses); at the same time, the key amino acid positions of this site are changed in viruses with α2-6-specificity (human, swine, and poultry H9N2 viruses). It is worth mentioning that the H9N2 influenza viruses isolated from poultry in Hong Kong and viruses of H2N2 and H3N2 subtypes, which caused human pandemics, have similar changes in the HB-site sequence. This data allows one to suggest that some species of poultry may act as intermediate hosts in the influenza virus transfer from its natural reservoir (waterfowl population) to humans [11].

THREE-DIMENSIONAL STRUCTURE

The three-dimensional structure of cytoplasmic, transmembrane and stem domains has not been determined yet (due to the features of the enzymes, which are used for cleavage of this membrane protein from the virion, the crystallized region starts at residues ~74-77) [6]. There is speculation about the presence of an α-helix motif in the uncrystallized structure, which has been supported by cryoelectron microscopy [4]. Therefore, one can unequivocally judge only the chain folding of the head region of the enzyme (as part of the tetrameric structure). The NA's head region consists of one big domain, which is formed by six identical antiparallel β-sheets (motifs) organized in the form of a propeller-like structure. Loops connecting the motifs and loops between every second and third strain of each motif are of ultimate importance for the enzyme [2]. Loops are the most variable parts of the

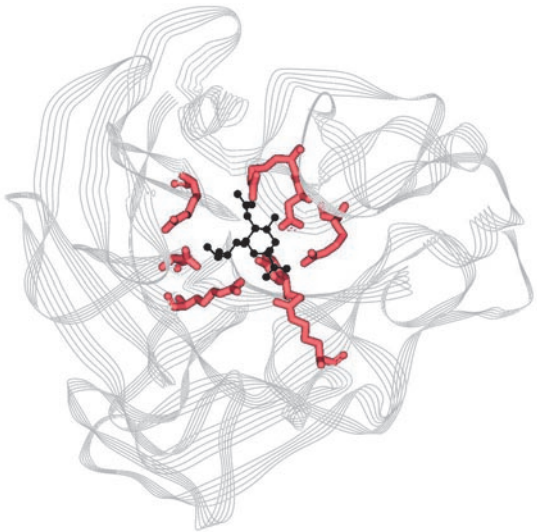

Figure 1. Active site of influenza virus A neuraminidase (N2 subtype) in complex with Neu5Ac2en (2-deoxy-2,3-didehydro-N-acetylneuraminic acid). Neu5Ac2en is presented in black, functional a.a. of the active site – red

structure of all NAs; they vary in length and can even have some arranged elements typical of the secondary structure. For example, loops of N9 NA have some α-helix regions: residues 106 – 110 form one spiral turn (α), located above the C-terminus of the polypeptide chain, which consecutively forms another α-helix turn, and a.a. 144 – 146 of the neighboring subunit forms the (3_{10}) helix. The 3_{10} helix and two chains (106 – 110 and C-terminus) form the antiparallel layer [6]. The loop connecting the fourth and the fifth motifs is the longest one and is stabilized by a disulfide bridge located between Cys318 and Cys337; it also has the conservative ion pair Asp330-Arg364 and the Ca^{2+} binding site [1].

GLYCOSYLATION

Carbohydrate chains are attached to Asn residues located in the different regions of the NA's head. In particular, glycans attached to asparagines 86 and 234 are headed towards the lipid membrane close to the stem; those attached to Asn146 – are headed from the membrane and are located in close proximity to the active site; finally, glycosylation Asn200 is located on the side surface in the region of the subunits contact. Short oligomannose type chains were found at residues Asn86 and Asn200. Carbohydrate chains of a complex type are attached to Asn146 and Asn234. The glycosylation site at Asn146 is conservative for all NAs, and this carbohydrate chain differs from all other carbohydrates found in all influenza virus glycoproteins: it carries the O-4 sulfated N-acetylgalactosamine [1]. Asn146 glycosylation seems to have a regulatory function, because it is known that the lack of this glycosylation site determines the influenza virus A/WSN/33 (H1N1) neurovirulence. It has been shown that the carbohydrate chain at Asn146 affects NA enzymatic activity, causing a 20-fold decrease in activity [12]. Deletion of the glycosylation site at a.a. 144 of N8 NA (A/duck/

Ukraine/1/63) causes changes in its substrate specificity profile NA [13], and absence of glycosylation sites at a.a. 83 and 398 causes incorrect molecule folding.

DISULFIDE BONDS

There are eight conservative disulfide bonds in the NA structure, and one additional bond in the N2, N8, and N9 subtypes. The invariance of disulfide bonds confirms their importance in the formation of a stable NA structure. It is assumed that, because of its proximity to the symmetry axis of the tetramer, the uncoupled Cys161 of N1 NA takes part in the coupling of subunits. The tetramer assembly mechanism is not universal: for instance, in influenza virus B neuraminidases disulfide bonds are formed by Cys54, whereas Cys78 takes part in polypeptide chains binding (N2 numbering) [2].

ACTIVE SITE STRUCTURE

The Neu5Ac binding site is located above the first strands of the third and the fourth motifs in a big loop on the NA surface. The active site is located at the N-terminal end of central parallel strands [2]; (Fig.1). It is a cavity 16Å in diameter and 8 to 10Å in depth, located 32Å from the tetragonal axis. This site is surrounded by twelve flexible loops, which go upwards from that axis [6].

The enzyme active site consists of functional amino acid residues Arg118, Asp151, Arg152, Arg224, Glu276, Arg292, Arg371, and Tyr406, and structural amino acid residues Glu119, Arg156, Trp178, Ser179, Asp (or Asn in N7 and N9) 198, Ile222, Glu227, Glu277, Asp293, and Glu425.

Functional a.a. are in direct contact with sialic acid, the product of the enzymatic reaction, and they all form polar contacts with it, excluding Arg224, whose aliphatic part forms a nonpolar contact with the glycerol fragment of the Neu5Ac residue [9] (Fig.1).

Recent X-ray studies of neuraminidases from the first phylogenic group have shown that, in comparison with neuraminidases from the second phylogenic group, they have a slightly different structure of the polypeptide chain around the enzyme active centre. In particular, there is a cavity in close proximity to the active site, which is formed by a change in the dimensional orientation of "loop 150." These structural differences allow the launch of the development of influenza virus NA inhibitors, which would specifically interact only with NAs of the first phylogenic group, in particular with the NA of influenza viruses of the H5N1 subtype [3].

REACTION MECHANISM

The NA's reaction mechanism (Scheme 1) was proposed based on the results of structural studies of the crystallized protein [7].

Formation of the oxocarbonium ion at the C2 atom of Neu5Ac is the key step in the hydrolysis of the oligosaccharide substrate. After the introduction of the Neu5Ac residue into the active centre, Neu5Ac conformation changes from chair to half-chair, i.e. the oxocarbonium ion is formed, due to strong ionic interactions between the carboxylate of the substrate and the guanidine groups of the arginines 118, 292 and 371, eventually leading to glycosidic bond cleavage. The molecule of aglycone leaves the enzyme active site with glycosidic oxygen, protonated by the solvent. Multiple contacts between the intermediate product and the a.a. of the active site (Tyr406 and Asp151 are of minor importance) stabilize the positively charged oxocarbonium ion with preservation of the planar carbon at C2. Neu5Ac2en, in which the C2 atom is in sp^2-form, mimics the intermediate reaction product in planar conformation [6]. At this stage of the reaction, the neuraminic acid residue is covalently bound to the hydroxyl group of Tyr406, which is characteristic of all exosialidases [15, 17]. Hydroxylation of the oxocarbonium ion with the solvent and product leaving the enzyme active site in the form of Neu5Ac are the limiting stages of the catalytic reaction. It is worth mentioning that there are no significant changes in the coordinates of the NA active site during the reaction [18].

The presence of invariant residues in the active site, the similarity of the structural organization, and the architecture of complexes with Neu5Ac and with Neu5Ac2en allow to assume that the mechanism of NA functioning for the A and B influenza viruses is identical [6].

NEURAMINIDASE INHIBITORS AND MECHANISM OF ANI-DRUG RESISTANCE

The structure of the neuraminidase active site is strictly conservative not only between subtypes, but also between the types of the enzyme, which points to the importance of all its components and the evolutionary stabilized functioning of this system. This observation has allowed to design an NA inhibitor for the influenza virus which mimics the transition state of the hydrolysis reaction, and Neu5Ac2en (Fig.2a), 4-guanidino-Neu5Ac2en, which is now widely used under the trade name zanamivir [14] (Fig. 2b).

The success of this drug has initiated a number of studies aimed at designing new NA inhibitors. The main structural elements of the new class of inhibitors (without the oxygen atom in the cycle) are cyclohexane and cyclopentane.

One of those structures is the (3S,4R,5R)-3-amino-4-acetamido-5-(1-ethylpropoxy)-1-cyclohexene-1-carboxylic acid (oseltamivir or Tamiflu) (Fig. 2c). The structure of this molecule is adjusted to coordinates of the amino acids, which interact with the glycerol chain of Neu5Ac2en [20]. Successful use of this drug has stimulated the development of new NA inhibitors with hydrophobic groups [21].

Besides, a NA inhibitor on the base of a cyclopentane structure has been developed; it has all the functionally important parts of zanamivir (carboxyl, acetamide, C4-hydroxyl) which fit into the NA active centre. BCX-1812 (preamivir) (Fig. 2d) retains its activity towards zanamivir-resistant influenza viruses [22, 23]. At present, preamivir analogs are at the development stage.

Zanamivir and oseltamivir are already used as drug products, whereas BCX-1812 has entered the last phase of clinical trials.

Until recently, it was considered that active uncontrolled use of zanamivir and oseltamivir would not have a significant influence on the development of resistance in influenza virus strains. That is, even if resistant strains emerge, they would not be able to replicate in the absence of the inhibitor [24]. The number of resistant viruses isolated in clinical trials accounted for less than 1%, same as their presence among seasonal influenza virus isolates worldwide.

However, in January 2008 this situation changed dramatically: some H1N1 influenza viruses developed resistance to oseltamivir due to a mutation His274Tyr in NA [25], and in the epidemic season of 2008-2009 resistance was up to 100% among viral isolates (according to http://ecdc.europa.eu); it is typical that those isolates preserved sensitivity to zanamivir. The mutation His274Tyr had been spotted in studies of resistance *in vitro* and *in vivo*, as well as in clinical isolates [26]. Nevertheless, it is still too early to stop usage of this drug, because according to the most recent data, the prepandemic influenza virus of the H1N1 subtype (A/California/11/2009), which is encountered at the moment in humans, is still susceptible to oseltamivir (according to data from the Center for Disease Control and Prevention, USA (www.cdc.gov). This leaves us with hope that the strain of the influenza virus that will cause the next pandemic might be susceptible to this NA inhibitor.

NA FUNCTIONAL ACTIVITY

There is data indicating that NA is relevant at different stages of infection. Firstly, it is considered that it helps the virus approach the target cells by cleavage of sialic acids from respiratory tract mucins [26]. Secondly, it may take part in the fusion of viral and cell membranes [27]. Thirdly, it facilitates budding of new virions by preventing their aggregation, caused by the interaction of the HA of the first virus with the sialylated glycans of the second one [27]. In addition, there is data suggesting that NA amplifies HA haemagglutinating activity by cleavage of the terminal neuraminic acid residues of the oligosaccharides surrounding the receptor-binding site of HA [28].

One of the most interesting features of the influenza virus is the coexistence of two proteins whose functions are to some extent contradictory, namely: haemagglutinin, which has a receptor-binding function; and neuraminidase, which has a receptor destroying function. Since both of these proteins recognize terminal neuraminic acid residue, this brings up the question of their cooperation or, on the contrary, their competition for receptor/substrate, and of the role of their relations in viral life cycle. Studies of the viruses resistant to NA inhibitors, artificial viral reassortants (which have HA and NA of different origins), and virus particles designed by means of reverse genetics, which lack NA or HA activity, show that the NA and HA of the influenza virus act in concert and their evolution proceeds interdependently [29-35]. Also, it raises a question as to their oligosaccharide specificity, because Neu5Ac-terminated oligosaccharide chains in viral hosts are quite diverse.

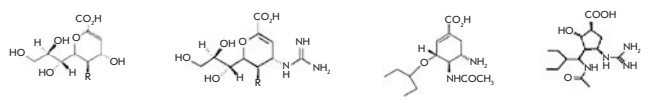

Figure 2. Structure of a) Neu5Ac2en, b) Zanamivir, c) Oseltamivir, d) BCX-1812 (preamivir), where R=NHAc

METHODS FOR DETERMINATION OF NA ACTIVITY

One of the most popular substrates for NA activity determination is MU-Neu5Ac or MU-NANA (Fig. 3a). The method based on the use of this substrate was proposed [36] first as an alternative to colorimetric or radioactive methods. After cleavage of the neuraminic acid, MU-Neu5Ac forms a fluorophore which is activated by light at a wavelength of 360 nm, and its fluorescence maximum is achieved at pH 10. The closest analog of MU-Neu5Ac is the 4-trifluoromethylumbelliferyl-α-D-N-acetylneuraminic acid, whose fluorescence maximum is located in the neutral pH range. High fluorescence intensity (10-fold higher than for MU-Neu5Ac) is useful in studies of low-activity neuraminidases [37].

The sensitivity of the chemiluminescent method of NA activity determination [38] is by a factor of 100 higher than that of MU-Neu5Ac-assay, and «NA-Star» is used as a substrate (Fig. 3b). The main disadvantage of this method is the short lifetime of the product of chemiluminescent hydrolysis, which has to be recorded within 5 minutes.

The other group of methods is based on cleavage of the neuraminic acid from high molecular weight substrates, such as fetuin, the α_1-acid glycoprotein or whole erythrocytes. The amount of free neuraminic acid is usually determined after cleavage [39]; the most convenient procedure for assay of Neu5Ac allows for conducting measurements in the presence of the sialylated substrate [40].

An alternative procedure is based on assay of the second product of the hydrolysis, the desialylated glycoprotein, with the help of lectin (for example, *Peanut agglutinin)*, which is specific for the unmasked terminal galactose [41, 42]. Carrying on with this analytical procedure requires great accuracy in control preparation, as every glycoprotein originally has terminal β-Gal residues.

METHODS FOR DETERMINATION OF NA SUBSTRATE SPECIFICITY

The substrate specificity of NA is its ability to discriminate between sialic acids (for example, Neu5Ac and Neu5Gc) and linkage type with the next residue (2-3, 2-6 or 2-8), as well as the ability to identify internal regions of the oligosaccharide chain. In particular, the following structures have been used for the determination of NA substrate specificity:

- free trisaccharides (3` SiaLac or 6`SiaLac) [43 - 45];
- glycoproteins containing only 2-3, or only 2-6-linked neuraminic acid [45, 46];
- glycoproteins or erythrocytes oversialylated with the aid of 2-3- or 2-6- sialyltransferases [47].

Methods based on the use of those substrates achieve only one of the listed goals; in particular, they allow to study specificity at the level of Sia2-3Gal or Sia2-6Gal. More broad specificity can be studied with the use of an analytical procedure which employs a number of synthetic substrates. In [42], a panel of three oligosaccharides was used: 3'SiaLac, 6'SiaLac and 6'SiaLacNAc, in the form of polyacrylamide conjugates; and neuraminidase activity was measured by lectin, specific for galactose residues, which appear as the result of NA action (see above). A new simple and sensitive method for NA specificity determination has been developed recently [48]. It is based on the use of BODIPY-labeled sialyloligosaccarides.

The fluorescent label is covalently bound to the oligosaccharide (3`SiaLac, 3`SiaLacNAc, SiaLe^c, SiaLe^a, SiaLe^x, 6`SiaLac, 6`SiaLacNAc) via spacer, i.e. it is at some distance from the cleavage site. Stability, relative hydrophility, electroneutrality, small size, and ability to use standard fluorescent filter for detection are the advantages of this label. The method is based on a quantitative separation of the electroneutral product of the reaction and the negatively charged substrate; separation is performed either on a microcartrige with an anion-exchange sorbent or microplates, the semipermeable bottom of which consists of an anion-exchange material. For greater reliability one may quantify the amount of the reaction substrate, along with the quantity of the reaction product. The high sensitivity of the method makes it possible to work with low substrate concentrations (10^{-11} mol), as well as with low virus concentrations. High accuracy (more than 95%) and good reproducibility (98%) of the new method allow to study the kinetics of enzyme-substrate interactions. Studies of desialylation kinetics, in particular the reaction velocity and its dependence on substrate and enzyme concentration, is important for understanding the reaction mechanism, as well as for the choice of the correct concentration range. In turn, the correct range allows to study desialylation specificity in cases when the NA quantity in the test sample is unknown [49]. It is worth mentioning that only this approach allows to study many aspects of NA substrate specificity (see above), namely to study the influence of the sialic acid type, the type of linkage between the sialic acid and the next sugar, and the influence of the inner glycan sugars.

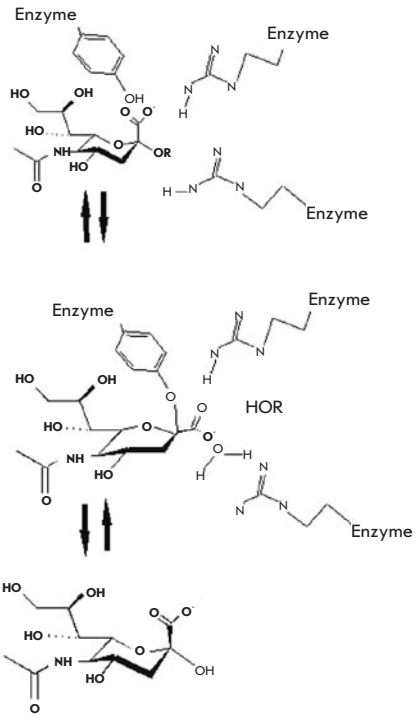

Scheme 1. Mechanism of substrate desialylation by influenza virus neuraminidase (according to [7], [15], and [16].)

FUNCTIONAL FEATURES OF SOME INFLUENZA VIRUS NEURAMINIDASES

As already mentioned above, high molecular weight substrates, along with low molecular weight substrates, can be used for studying NA activity and specificity. Low molecular weight substrates allow to study the reaction mechanism and desialylation kinetics without the complications of multivalent interactions (NA is a tetramer) and the possible influence of HA, which interacts with multivalent conjugate 3 – 5 orders of magnitude better than with the monomeric one [50]. High molecular weight substrates appear to be a more accurate model for studying natural interactions; that is when there is a necessity to account the NA tetrameric organization, the clustering of NA molecules on the cell surface, and the involvement of the second surface glycoprotein, HA, which is present on the viral surface in larger amount.

Investigation of the evolution of the influenza virus NA substrate specificity for viruses isolated from humans, and its comparison with the substrate specificity of influenza virus NAs isolated from different hosts, such as ducks and pigs, is of great importance. The first undertaking could shed light on the question of the unique character of pandemic strains, while the second could help detect in advance the properties of the enzyme which facilitate the crossing of the interspecies barrier.

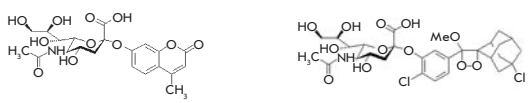

Figure 3. Structure of MU-Neu5Ac (a) and NA-Star (b)

The specificity of N2 subtype NA of human influenza viruses has gradually changed from 3'SiaLac (H2N2 strains isolated in 1957) to dual specificity, 3`SiaLac/6`SiaLac (strains from 1972 to 1987). Hydrolytic activity towards 6'SiaLac was identified only for viruses isolated in 1967 and further, and starting from 1972 isolates an increase of activity towards this substrate was registered [46].

It has been shown recently that N2 influenza viruses are highly active towards 3'SiaLac, while their activity towards 6'SiaLac varies from extremely low (avian and early human isolates) to high (swine and latter human isolates). It has been shown that NA activity towards 6'SiaLac depends also on the host type and, for human viruses, on the year of isolation [45].

For N1 strains isolated in the 70-80s [43, 44], it was shown that their neuraminidase equally recognizes 3'SiaLac and 6'SiaLac.

Data on the substrate specificity of N1 and the N2 NAs of several duck, swine and human influenza virus isolates were obtained with the use of BODIPY-labeled synthetic oligosaccharides [48 - 51]. All of the studied NAs desialylated α2-3-substrates better then α2-6 ones. In the case of viruses with N1 neuraminidase, α2-3/α2-6 activity factor was ~60 for duck viruses, ~20 for swine viruses, and ~4 for human viruses. In case of H9N2 influenza viruses, similar α2-3/α2-6 relations were found for the duck virus, whereas this relation for viruses isolated from poultry is in a range from 30 to 15, and for swine virus ~6, finally, for human iso-

late ~10. For all the studied NA, it has been shown that they discriminate the fine structure of α2-3-substrates, that is they discriminate between the structures of the inner parts of oligosaccharides.

With the use of the polyacrylamide conjugates of 3`SiaLac, 6`SiaLac and 6`SiaLacNAc, it has been shown that most of the viruses (H1N1 and H3N2 subtypes) propagated on embryonated chicken eggs and MDCK cells, preferably hydrolyze 3'SiaLac, whereas VERO-isolates of the same viruses preferably hydrolyze 6'SiaLacNAc. In summary, the nature of the host cell line used for virus accumulation influences NA substrate specificity [42]. The reason for this effect remains unknown.

It is difficult to compare the results of substrate specificity studies conducted by different authors due to the use of both different influenza virus strains and different substrates in varying concentrations. For example, the Kobasa [45] group has shown that maximum NA activity towards 6'SiaLac does not exceed the activity towards 3'SiaLac, whereas in the work of Baum & Paulson [46], this activity was much higher for the same viruses. It is also worth mentioning that studies of the influenza virus with the simultaneous use of high- and low-molecular weight substrates of a defined structure have yet to be conducted.

Despite the limited amount of data published to date, it is already possible to discuss some features. Firstly, the NA substrate specificity of human isolates differs from that of avian isolates. Secondly, the oligosaccharide specificity of the NA of viruses which circulate in different hosts (birds, pigs, humans) notably differs, at least for the characteristic "ratio of the hydrolysis velocity of 2-3 oligosaccharides towards 2-6 oligosaccharides." Thirdly, the substrate specificity of influenza virus neuraminidases propagated on different cell lines may be different.

Data on NA functioning would be incomplete without taking into account another surface protein of the influenza virus, haemagglutinin. There is only a limited number of publications describing the simultaneous study of HA and NA substrate specificity, and there is virtually no research where the dependence of HA and NA oligosaccharide specificity on one hand and virus infectivity on another hand have been studied. The state-of-the-art analytical procedures for NA introduced in the current review are now up to par with the more advanced analytical methods of HA analysis, which always developed faster; therefore, it is quite easy to predict that one of the main trends in influenza virus studies in the future would be joint studies of HA and NA specificity. ●

This review was supported by RFBR grant 04-04-49669 and RAS Presidium Program 'Molecular and Cell Biology'.

REFERENCES

1. Varghese J.N., Colman P.M. Three-dimensional structure of the neuraminidase of influenza virus A/Tokyo/3/67 at 2.2 Å resolution. // *J. Mol. Biol.* 221: 473-486 (1991).
2. Colman P.M. NA enzyme and antigen. // In The influenza viruses (R. M. Krug, ed.). Plenum Publishing Corporation, New York: 175-218 (1989).
3. Russell R.J., Haire L.F., Stevens D.J., Collins P.J., Lin Y.P., Blackburn G.M., Hay A.J., Gamblin S.J., Skehel J.J. The structure of H5N1 avian influenza neuraminidase suggests new opportunities for drug design. // *Nature* 44: 45-49 (2006).
4. Harris A., Cardone G., Winkler D.C., Heymann J.B., Brecher M., White J.M., Steven A.C. Influenza virus pleiomorphy characterized by cryoelectron tomography. // *PNAS* 103:19123-19127 (2006).
5. Varghese J.N., Colman P.M., van Donkelaar A., Blick T.J., Sharasrabudhi A., McKimm-Breschkin J.L. Structural evidence for a second sialic acid binding site in avian influenza virus neuraminidases. // *Biochemistry*. 94: 11808-11812 (1997).
6. Bossart-Whitaker P., Carson M., Babu Y.S., Smith C.D., Laver W.G., Air G.M. Three-dimensional structure of influenza A N9 neuraminidase and its complex with the inhibitor 2-deoxy-2,3-dehydro-N-acetyl neuraminic acid. // *J. Mol. Biol.* 232: 1069-1083 (1993).
7. Janakiraman M.N., White C.L., Laver W.G., Air G.M., Luo M. Structure of influenza virus neuraminidase B/Lee/40 complexed vith sialitic acid and dehydro analog at 1.8-Å resolution: implications for the catalytic mechanism. // *Biochemistry*. 33: 8172-8179 (1994).
8. Takahashi T., Suzuki T., Hidari K.I-P.J., Miyamoto D., Suzuki Y. A molecular mechanism for the low-pH stability of sialidase activity of influenza A virus N2 neuraminidases. // *FEBS Lett*. 543: 71-75 (2003).
9. Colman P.M., Hoyne P.A., Lawrence M.C. Sequence and structure alignment of paramyxovirus hemagglutinin-neuraminidase with influenza virus neuraminidase. // *J. Virol*. 67: 2972-2980 (1993).
10. Varghese J.N., Colman P.M., van Donkelaar A., Blick T.J., Sharasrabudhi A., McKimm-Breschkin J.L. Structural evidence for a second sialic acid binding site in avian influenza virus neuraminidases. // *Biochemistry*. 94: 11808-11812 (1997).
11. Matrosovich M.N., Krauss S., Webster R.G. H9N2 influenza A viruses from poultry in Asia have human virus-like receptor specificity. // *Virol*. 281: 56-162 (2001).
12. Li S., Schulman J., Itamura S., Palese P. Glycosylation of neuraminidase determines the neurovirulence of influenza A/WSN/33 virus. // *J. Virol*. 67: 6667-6673 (1993).
13. Saito T., Kawano K. Loss of glycosylation at Asn144 alters the substrate preference of the N8 influenza A virus neuraminidase. // *J. Vet. Med. Sci*. 59: 923-926 (1997).
14. von Itzstein M., Wu W.-Y., Kok G.B., Pegg M.S., Dyason J.C., Jin B., Phan T.V., Smythe M.L., White H.F., Oliver S.W., Colman P.M., Varghese J.N., Ryan D.M., Woods J.M., Bethel R.C., Hotham V.J., Cameron J.M., Penn C.R. Rational design of potent sialidase-based inhibitors of influenza virus replication. // *Nature* 363: 418-423 (1993).
15. Watts A.G., Oppezzo P., Withers S.G., Alzari P.M., Buschiazzo A. Structural and kinetic analysis of two covalent sialosyl-enzymeintermediates on Trypanosoma rangeli sialidase // *J. Biol. Chem*. 281: 4149-4155 (2006).
16. von Itzstein M. The war against influenza: discovery and development of sialidase inhibitors. // *Nat Rev Drug Discov*. 6: 967-74 (2007).
17. Watts A.G., Withers S.G. The synthesis of some mechanistic probes for sialic acid processing enzymes and the labeling of a sialidase from Trypanosoma rangeli. // *Can. J. Chem*. 82: 1581-1588 (2004).
18. Colman P.M., Smith B.J. The trypanosomal trans-sialidase: two catalytic functions associated with one catalytic site. // *Structure* 10: 1466-1468 (2002).
19. Oxford J.S., Bossuyt S., Eswarasaran R., Lambkin R. Drugs to combat the epidemic and pandemic faces of influenza. // In Influenza (C.W. Potter ed.) Elsevier: 201-234 (2002).
20. Hanessian S., Wang J., Montgomery D., Stoll V., Stewart K.D., Kati W., Maring C., Kempf D., Hutchins C., Laver W.G. Design, synthesis, and neuraminidase inhibitory activity of GS-4071 analogues that utilize a novel hydrophobic paradigm. // *Bioorg. Med. Chem. Lett*. 12: 3425-3429 (2002).
21. Babu Y.S., Chad P., Bantia S., Kotian P., Dehgani A., El-Kattan Y., Lin T.-H., Hutchson T.L., Elliot A., Parker C., Ananth S., Horn LaSun L., Laver G., Montgomery J. BCX-1812 (RWJ-270201): discovery of a novel highly potent, orally active, and selective influenza neuraminidase inhibitor through structure-based drug design. // *J. Med. Chem*. 43: 3482-3486 (2000).
22. Bianco A., Brufani M., Dri D.A., Melchioni C., Filocamo L. Design and synthesis of a new furanosic sialylmimetic as a potential influenza neuraminidase inhibitor. // *Letters in Organic Chemistry* 2: 83-88 (2005).
23. Blick T.J., Sahasrabudhe A., McDonald M., Owens I.J., Morley P.J., Fenton R.J., McKimm-Breschkin J.L. The interaction of hemagglutinin and neuraminidase mutations in influenza virus in resistance to 4-guanidino-Neu5Ac2en. // *Virol*. 246: 95-103 (1998).
24. Lackenby A., Hungnes O., Dudman S.G., Meijer A., Paget W.J., Hay A.J., Zambon M.C. Emergence of resistance to oseltamivir among influenza A (H1N1) viruses in Europe // *EUROSURVEILLANCE* 13: – 2 (2008).
25. Hui-Ling Yen, Ilyushina N.A., Salomon R., Hoffmann E., Webster R.G., Govorkova E.A. Neuraminidase inhibitor-resistant recombinant A/Vietnam/1203/04 (H5N1) influenza viruses retain their replication efficiency and pathogenicity in vitro and in vivo // *J. of Virol*. 81: 12418 – 12426 (2007).
26. Matrosovich M., Matrosovich T.,Gray T., Roberts N.A., Klenk H.-D., Neuraminidase is important for the initiation of influenza virus infection in human airway epitelium.// *J.Virol*. 78: 12665-12667 (2004).
27. Wagner R., Wolf T., Herwig A., Pleschka S., Klenk H.-D. Interdependence of hemagglutinin glycosylation and neuraminidase as regulators of influenza growth: a study by reverse genetics. // *J. Virol*. 74: 6316-6323 (2000).
28. Ohuchi M., Feldmann A., Ohuchi R., Klenk H.-D. Neuraminidase is essential for fowl

plague virus hemagglutinin to show hemagglutinating activity. Virology. 10;212(1):77-83 (1995).
29. Rudneva I.A., Kovaleva V.P., Varich N.L., Farashyan V.R., Gubareva L V., Yamnikova S.S., Popova I.A., Presnova V.P., Kaverin N.V. Influenza A virus reassortants with surface glycoprotein genes of avian parent viruses: effects of HA and NA gene combinations on virus aggregation. // *Arch. Virol.* 133: 437-450 (1993).
30. Rudneva I.A., Sklyanskaya E.I., Barulina O.S., Yamnikova S.S., Kovaleva V.P., Tsvetkova I.V., Kaverin N.V.. Phenotypic expression of HA - NA combinftions in human – avian influenza A virus reassortants. // *Arch. Virol.* 141: 1091-1099 (1996).
31. Kaverin N.V., Gambaryan A.S., Bovin N.V., Rudneva I.A., Shilov A.A., Khodova O.M., Varich N.L., Sinitsin B.V., Makarova N.V., Kropotkina E.A. Postreassortment changes in influenza A virus hemagglutinin restoring HA – NA functional match. // *Virol.* 244: 315-321 (1998).
32. Castrucci M.R., Kawaoka Y. Biologic importance of neuraminidase stalk length in influenza A virus. // *J. Virol.* 67: 759-764 (1993).
33. Mitnaul J., Matrosovich M.N, Castrucci M.R., Tuzikov A.B., Bovin N.V., Kobasa D., Kawaoka Y. Balanced hemagglutinin and neuraminidase activities are critical for efficient replication of influenza A viruses. // *J. Virol.* 74: 6015-6020 (2000).
34. Wagner R., Wolf T., Herwig A., Pleschka S., Klenk H.-D. Interdependence of hemagglutinin glycosylation and neuraminidase as regulators of influenza growth: a study by reverse genetics. // *J. Virol.* 74: 6316-6323 (2000).
35. Hughes M., Matrosovich M., Rodges M., McGregor M., Kawaoka Y. Influenza A viruses lacking sialidase activity can undergo multiple cycles of replication in cell culture, eggs, or mice. // *J. Virol.* 74: 5206-5212 (2000).
36. Potier M., Mameli L., Belisle M., Dallaire L., Melancon S.B. Fluorometric assay with a sodium (4-methylumbelliferyl-α-D-N-acetylneuraminate) substrate. // *Anal. Biochem.* 94: 287-296 (1979).
37. Engstler M., Talhouk J.W., Smith R.E., Schauer R. Chemical synthesis of 4-trifluoro methylumbelliferyl-α-D-N-acetylneuraminic acid glycoside and its use for the fluorometric detection of poorly expressed natural and recombinant sialidases. // *Anal. Biochem.* 250: 176-180 (1997).
38. Buxton R.C., Edwards B., Juo R.R., Voyta J.C., Tisdale M., Bethell R.C. Development of a sensitive chemiluminescent neuraminidase assay for the determination of influenza virus susceptibility to zanamivir. // *Anal. Biochem.* 280: 291-300 (2000).
39. Jourdian G.W., Dean L., Roselman S. A periodate-resortinol method for the quantitive estimation of five sialic acids and their glycosides. // *J. Biol.Chem.* 25: 430-435 (1971).
40. Warren L. The thiobarbituric acid assay of sialic acids. // *J. Biol. Chem.* 234: 1971-1975 (1959).
41. Lambre C.R., Terzidis H., Greffard A., Webster R.G. Measurement of anti-influenza neuraminidase antibody using a peroxidase-linked lectin and microtitre plates coated with natural substrates. // *J. Immunol. Meth.* 135: 49-57 (1990).
42. Katinger D., Mochalova L., Chinarev A., Bovin N., Romanova J. Specificity of neuraminidase activity from influenza viruses isolated in different hosts tested with novel substrates. // *Arch. Virol.* 149: 2131-2140 (2004).
43. Rudneva I.A., Kovaleva V.P., Varich N.L., Farashyan V.R., Gubareva L. V., Yamnikova S.S., Popova I.A., Presnova V.P., Kaverin N.V. Influenza A virus reassortants with surface glycoprotein genes of avian parent viruses: effects of HA and NA gene combinations on virus aggregation. // *Arch. Virol.* 133: 437-450 (1993).
44. Couceiro J.N.S.S. Baum L.J. Characterization of the hemagglutinin receptor specificity and neuraminidase substrate specificity of clinical isolates of human influenza A viruses. // *Mem. Inst. Oswaldo Cruz Rio de Janeiro* 89: 587-591 (1994).
45. Kobasa D., Kodihalli S., Luo M., Castrucci M.R., Donatelli I., Suzuki Y., Suzuki T., Kawaoka Y. Amino acid resides contributing to the substrate specificity of the influenza A virus neuraminidase. // *J. Virol* 73: 6743-6751 (1999).
46. Baum L.G., Paulson J.C. The N2 neuraminidase of human influenza virus has acquired a substrate specificity complementary to the hemagglutinin receptor specificity. // *Virol.* 180: 10-15 (1991).
47. Paulson J.C., Weinstein J., Dorland L., van Halbeek H., Viegenthart J.F.J. Newcastle disease virus contains a linkage-specific glycoprotein sialidase. // *J. Biol. Chem.* 257: 12734-12738 (1982).
48. Mochalova, L.V., Korchagina E.Y., Kurova V.S., Shtyrya Y.A., Gambaryan A.S., Bovin N.V. Fluorescent assay for studying the substrate specificity of neuraminidase. //*Anal. Biochem*, 341, 190-193 (2005).
49. Mochalova L., Kurova V., Shtyrya Y., Korchagina E., Gambaryan A., Belyanchikov I., Bovin N. Oligosaccharide specificity of influenza H1N1 virus neuraminidases. //*Arch. Virol.*, 152, 2047-2057 (2007).
50. Gambaryan A.S., Matrosovich M.N. A solid-phase enzyme-linked assay for influenza virus receptor-binding activity. //*Journal of Virological Method's* 39, 111-123(1992).
51. Shtyrya Y.A., Mochalova L.V., Gambaryan A.S., Korchagina E.Y., Xu X., Klimov A.I., Bovin N.V. Neuraminidases of H9N2 influenza viruses isolated from different hosts display various substrate specificity. //*Proceedings of international conference on options for the control of influenza VI. Canada, June 17-23, 2007. (M. Katz ed.), International Medical Press:* 64-65 (2008).

Computer Modeling of the Structure and Spectra of Fluorescent Proteins

A.V. Nemukhin*[a,b], B.L. Grigorenko[a], A.P. Savitsky[a,c]
[a] Department of Chemistry, M.V. Lomonosov Moscow State University
[b] N.M. Emanuel Institute of Biochemical Physics, Russian Academy of Sciences
[c] A.N. Bach Institute of Biochemisty, Russian Academy of Sciences
*E-mail: anemukhin@yahoo.com

ABSTRACT Fluorescent proteins from the family of green fluorescent proteins are intensively used as biomarkers in living systems. The chromophore group based on the hydroxybenzylidene-imidazoline molecule, which is formed in nature from three amino-acid residues inside the protein globule and well shielded from external media, is responsible for light absorption and fluorescence. Along with the intense experimental studies of the properties of fluorescent proteins and their chromophores by biochemical, X-ray, and spectroscopic tools, in recent years, computer modeling has been used to characterize their properties and spectra. We present in this review the most interesting results of the molecular modeling of the structural parameters and optical and vibrational spectra of the chromophore-containing domains of fluorescent proteins by methods of quantum chemistry, molecular dynamics, and combined quantum-mechanical–molecular-mechanical approaches. The main emphasis is on the correlation of theoretical and experimental data and on the predictive power of modeling, which may be useful for creating new, efficient biomarkers.
Keywords: green fluorescent protein, molecular modeling, molecular dynamics, molecular mechanics
Abbreviations: QM/MM - combined methods of quantum and molecular mechanics, MD - molecular dynamics, TD-DFT - the method of density functional theory depending on time

INTRODUCTION

The discovery and use of colored proteins from the family of the green fluorescent protein [1–7] stimulated an avalanche-like growth of interest in these amazing species. Their practical value is explained by their ability to label cell clones with colored proteins and then literally trace the inner cell events. Biotechnology perspectives are promising because of multicolor labeling, in particular, the ability to observe interprotein interactions in living systems. These proteins are well characterized in crystallography studies. The β-sheets form the walls of the can (Fig.1) which efficiently shield the chromophore from the external media. The latter is represented by the hydroxybenzylidene-imidazoline molecule (Fig.2), which is formed in nature from three amino-acid residues inside the protein globule. The photophysical properties of fluorescent proteins are explained by transformations occurring with this chromophore group inside the macromolecule upon light illumination at certain wavelengths.

Researchers from different fields concentrate on studies of all the aspects of the structure and mechanism of fluorescent proteins. In this review, we primarily analyze works on the computer modeling of the structure and spectra of these species. Using modern tools of molecular modeling [8] may provide considerable support to experimental studies, allowing one to save time and resources for a comprehensive examination of the processes occurring in such complex molecular systems. Obviously, a description of the transitions between the electronic states of chromophore molecules responsible for light absorption and emission requires the use of the quantum theory; correspondingly, quantum chemistry is an appropriate modeling tool. The conformational states of the protein macromolecule and the structure of the chromophore-containing domain are also important for the properties of fluorescent proteins, thus requesting the application of molecular mechanics and molecular dynamics methods. To employ all these approaches, substantial computer resources, as well as efficient numerical algorithms and computer programs, are necessary.

Quantum chemistry models are based on a nuclear-electron picture of a molecular system that requires a numerical solution of the Schroedinger equation by using approximations of different accuracy levels. Presently, a developed hierarchy of quantum chemistry approaches is known, each of which is oriented toward performing certain tasks. In particular, for calculating structural parameters, i.e., geometrical configurations corresponding to the minimum energy points on the ground electronic state potential energy surface for a given model molecular system, as well as to calculate vibrational spectra, electronic density functional theory approaches are often operative. Multiconfigurational wavefunction approximations are preferable (e.g., [9]) if excited state parameters are requested, which includes calculations of transition energies for estimates of band positions in the optical spectra or the location of the conical intersection points. Software packages of quantum chemistry, including GAUSSIAN, GAMESS, MOLPRO, NWCHEM, TURBOMOLE, are used in practical applications.

The potential energy surfaces which are supposed to be directly calculated in quantum chemistry models are approximated by analytical functions in the methods of molecular mechanics and molecular dynamics. These analytical functions include chemical bond stretches, valence angles and torsional angles deformations, interactions of chemically unbound atoms, electrostatic contributions, and, sometimes, other terms. Each contribution of such kind is represented by an expression with parameters (the so-called force

fields), the adjustment of which is the goal of numerous research groups. The most popular force field parameters suitable for modeling protein systems are included in the AMBER, CHARMM, OPLSAA, and GROMOS libraries, as well as others.

A certain breakthrough in the molecular modeling properties of biomolecular systems is accounted for by the development of the combined methods of quantum- and molecular mechanics (QM/MM). According to the main idea of this approach [10], the smaller fraction of the protein macromolecule, in which electronic redistributions or transitions between electronic states are assumed to be important, is included into the quantum subsystem. The energies and forces in the latter are computed by using different approaches of the quantum theory. The vast majority of the protein atoms surrounding such a selected central part are assigned to the molecular mechanical subsystem described by the force field parameters.

In QM/MM approaches, the energy of each point on the potential surface is computed as a sum of the energy of the quantum part immersed in the field of the MM subsystem and the molecular-mechanical energy itself. An analysis of such composed potential energy surfaces allows us to investigate the photophysical properties of the chromophore inside the protein.

Below, we consider the most interesting results of a molecular modeling of structural parameters, the optical and vibrational spectra of the chromophore containing domains of fluorescent proteins by methods of quantum chemistry, and molecular dynamics and combined quantum- and molecular-mechanical approaches. The main emphasis is on the correlation of theoretical and experimental data and on the predictive power of modeling, which may be useful for the creation of new efficient biomarkers.

MODELING THE STRUCTURE AND DYNAMICS OF FLUORESCENT PROTEINS USING CLASSICAL FORCE FIELDS

The macromolecules of the fluorescent proteins contain aminoacids for which the force field parameters are well presented in most conventional libraries of molecular mechanics and molecular dynamics (MD). However, for the chromophore itself formed upon the cyclization of aminoacides in the presence of molecular oxygen, nonconventional types of atoms occur.

Reuter *et al.* [11] reported the parameters compatible with the CHARMM force fields for the molecule 4'-hydroxybenzylidene-2,3-dimethylimidazolinone representing the GFP chromophore that were adjusted by the results of quantum chemical calculation. The first works [11, 12] on molecular

Fig. 1. Structure of GFP (PDB ID: 1EMA). The chromophore group is emphasized

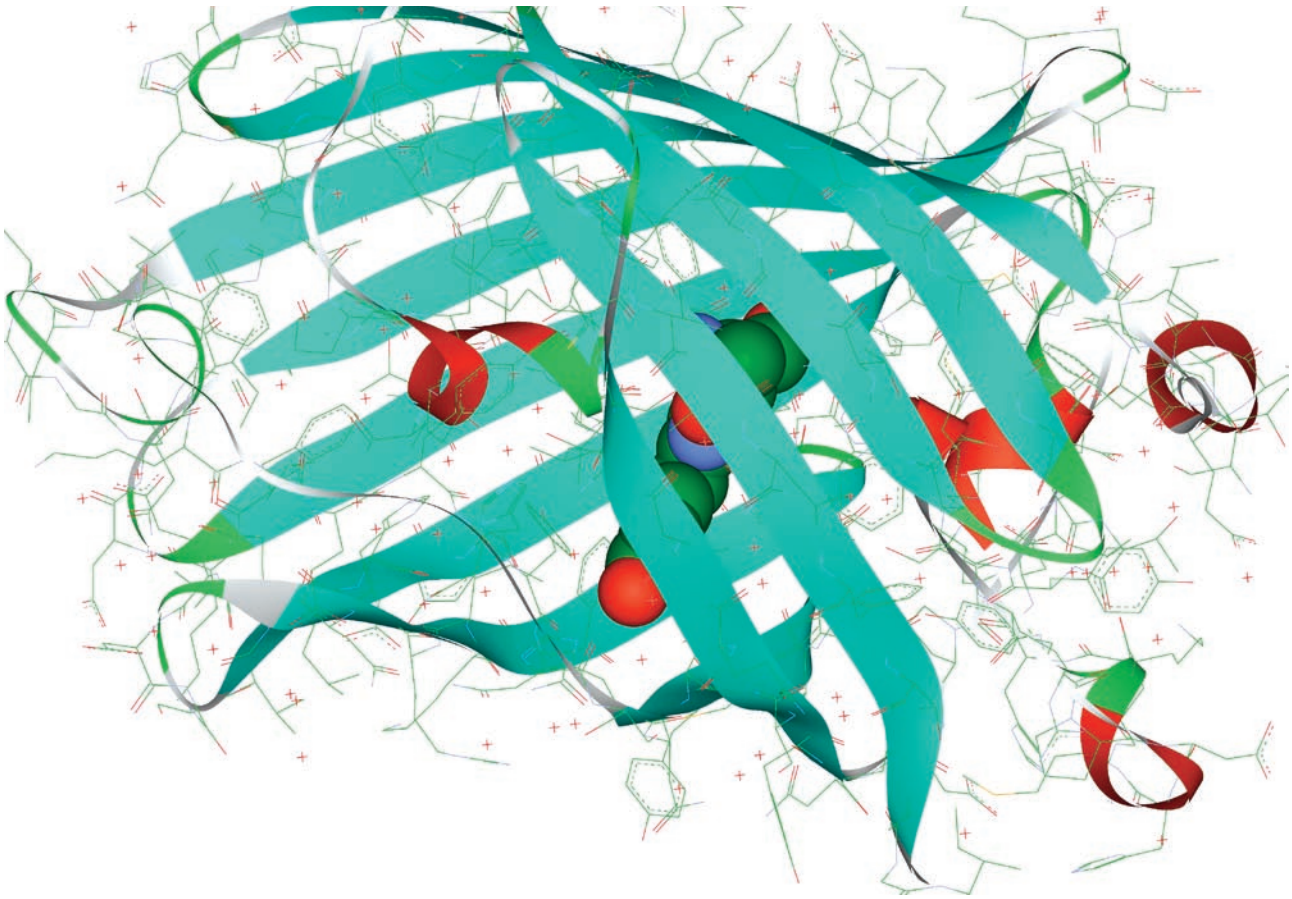

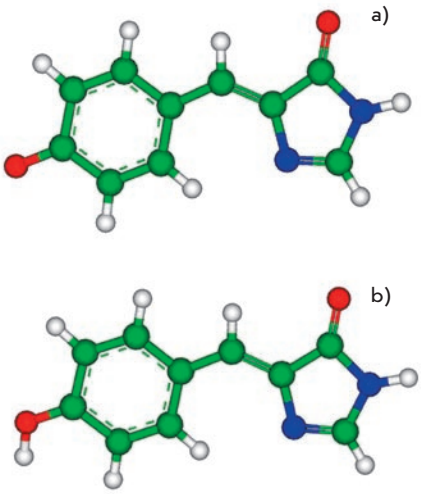

Fig.2. The chromophore molecule of GFP. Top (a): the anionic form; bottom (b): the neutral form. Here and below, carbon atoms are distinguished by green, oxygen atoms by red, and nitrogen atoms by blue

dynamical simulations with relatively short classical MD trajectories for the wild type and mutated variants of GFP were carried out using the heavy atom coordinates of crystal structures 1EMA and 1EMB from the Protein Data Bank [13]. It is worth commenting that the atomic coordinates that are deposited in this database following the results of X-ray or NMR experimental studies often are preliminarily refined by computer calculations by molecular-mechanics-based software. Simulations allow one to add missing hydrogen atoms in the model structures of protein macromolecules, although the known uncertainties appear, first and foremost, for the histidine, glutamate, and aspartate. In [11, 12], the rigidity of the protein globule was demonstrated. Also, the hydrogen bond networks near the chromophore both in the neutral and the anionic forms were reported. To emphasize the value of these data, we show in Fig. 3 the hydrogen bond network near the GFP chromophore obtained in our own calculations.

The known optical properties of GFP [14] exhibit two main absorption bands at 400 nm and 480 nm for the wild type of the protein. These bands are associated with the chromophore either in the neutral state (form B in Fig. 2b) with a shorter wavelength or in the ionized form (form A in Fig. 2a) with a longer wavelength. Since the hydrogen-bond network should provide routes for proton transfers connecting these two forms (presumably through the intermediate form I), its modeling has attracted much attention since the very first works. In this section, we mention only those theoretical papers which describe the applications of classical models.

In particular, the role of rotation of the Thr203 side chain (Fig. 3), which presumably facilitates the transition between the forms A and B, has been analyzed with the molecular dynamics simulations [15]. The papers [16, 17] describe possible proton transfer routes between various forms of the chromophore, taking into consideration water molecules and the nearest amino-acid side chains following detailed molecular dynamics simulations. Papers [18, 19] discuss the consequences of quite extended proton migration over the hydrogen bond networks (up to the exit to the protein surface) for an interpretation of the photophysical properties of GFP.

Another important transformation in fluorescent proteins, namely, the cis-trans conversion of the chromophore (Fig. 4), was analyzed by molecular mechanics [20–22] and molecular dynamics [23–25] methods. Such cis-trans isomerization may be of great value for the so-called blinking colored proteins, in which fluorescent states appearing for finite time intervals alternate with dark states, depending on external factors. The principal working hypothesis to explain the mechanism of such behavior is based on the suggestion of the cis-trans chromophore isomerization inside the protein until the fluorescent state is reached and quenched. In the forthcoming sections of our paper devoted to the results of quantum-based calculations, this hypothesis is also discussed.

One very interesting result in modeling the cis-trans chromophore isomerization inside the protein environment that also illustrates the modern achievements of classical molecular dynamics simulations was reported in a recent paper [25]. The authors computed free energy profiles as the profiles of mean force for the GFP chromophore along the internal rotation angle φ (Fig. 4) at a temperature of 300 K inside the protein matrix of the Ser65Thr mutant. All protein atoms and almost 9,000 solvent water molecules were included into the model system. By using the results of quantum chemical calculations, the authors modified the parameters of the AMBER force field in such a manner that they might be assigned to the excited electronic state. The biased MD simulations were applied to drive the φ rotation in order to remove the system from the regime of small oscillations around the minimum energy point and to scan the extended regions of the configuration space. The calculation shows that ~8 kcal/mol is required to overcome the energy barrier and provoke the cis-trans chromophore isomerization along the coordinate φ.

Paper [23] describes the results of classical MD simulations for the trans-cis isomerization of the chromophore in another colored protein asCP (or asFP595) [26], for which kindling

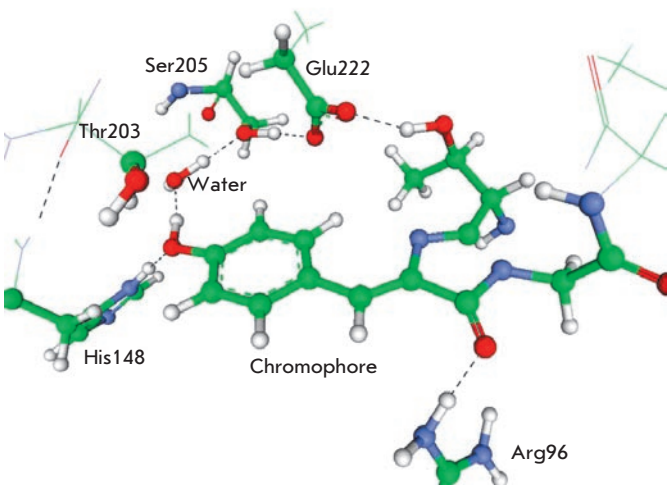

Fig.3. Hydrogen bond network (black dashed) near the GFP chromophore. Labeling amino acid residues corresponds to the structure PDB ID: 1EMA

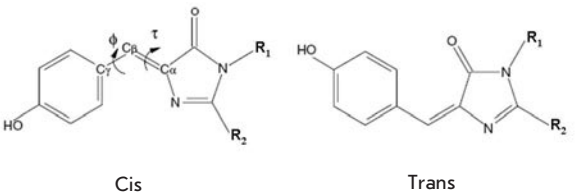

Fig. 4. Cis-trans isomerization of the GFP chromophore

fluorescence is observed. This phenomenon means that the initially nonfluorescent protein form may be transformed into a form with red emission by intense green light illumination. Presumably, the photoinduced trans-cis chromophore isomerization is responsible for such behavior. Trajectory calculations [23, 27] that have been performed with OPLSAA force field parameters allow one to visualize the possible movements of the chromophore and the nearest amino-acid residues upon speculating processes.

Methods of classical MD were used in [28] to study the possible cis-trans chromophore isomerization in the ground electronic state of the protein Dronpa [29], for which the light-induced switch from the fluorescent state to the dark state was observed. As in the case of other photoswitchable color proteins, the hypothesis that the chromophore isomerization was responsible for the adjustment of the photophysical properties of the protein was verified. The authors of [28] used the AMBER force field modified by new parameters for the chromophore molecule by the results of quantum chemical calculations. It was shown that the chromophore group resided in the cis conformation; however, point mutations on the positions of the nearest amino-acid residues might enhance the flexibility of the protein macromolecule.

Not long ago, a research group from the bioengineering and bioinformatics department of Moscow State University used classical MD simulations to model the structural features of the monomeric red fluorescent protein mRFP1 upon point mutations on position Glu66.

At the end of this section, we note the important role of molecular mechanics and molecular dynamics methods in modeling the conformational states of proteins. Estimates of equilibrium atomic coordinates and an analysis of the time evolution of geometric parameters in protein macromolecules containing several thousand atoms can be practically performed only within classical mechanics by using empirical or semiempirical force fields. Since the conventional force-field parameters from the AMBER and CHARMM libraries are well calibrated to describe hydrogen bonds, an apparent achievement of such modeling for the fluorescent proteins is the picture of the hydrogen bond network in the chromophore-containing domain. On the contrary, the computed energy parameters, such as the internal rotation energy barriers upon cis-trans chromophore isomerization in the ground state and, especially, in the excited state, should be considered with caution, taking into account the high sensitivity of the results to the ambiguously defined force-field parameters for these properties. The qualitative conclusions that can be drawn from the results of MD simulations, i.e., the time evolution of the hydrogen bond network, crude estimates of energy barriers upon conformational changes accompanied by the movements of peptide groups, or the chromophore provide valuable information. However, for more accurate estimates, which may include proton transfers over hydrogen bond networks, as well as for an analysis of potential energy surfaces in the ground and excited states, the quantum calculations should be addressed.

QUANTUM CHEMISTRY OF CHROMOPHORES IN THE GAS PHASE AND IN SOLUTIONS

The very first quantum chemical calculations of the electronic structure of the model chromophore molecule of GFP [31–34] allowed one to assign the light-induced electronic excitation (photoabsorption) to the transition between singlet states $S_0 \rightarrow S_1$. In terms of orbitals, this transition corresponds to the electron transfer from the highest occupied molecular orbital (HOMO) of the π–type to the lowest unoccupied molecular orbital (LUMO) of the π^*–type. Figure 5 illustrates images of these orbitals for the anionic form of the molecule 4'-hydroxybenzylidene-imidazolinone (see also Fig. 4) calculated in [35]. According to these results, the electronic excitation affects the local properties of the electronic density in the bridging region connecting the phenyl and imidazolinone rings of the chromophore molecule. As a consequence, the parameters of the initially single (C-CH) and double (-CH=C) chemical bonds (in the ground state) become more alike, thus facilitating internal rotation over the angle τ (Fig. 4) around the initially double bond.

The choice of a strategy to provide accurate calculations of the most important quantitative properties of the chromophore groups of the colored proteins from the GFP family is constantly under discussion among specialists in computational quantum chemistry. These properties include the energy differences upon excitation ($S_0 \rightarrow S_1$) and descent ($S_1 \rightarrow S_0$), which are associated with the band maxima in the excitation and fluorescent spectra and the corresponding band intensities, as well as the sections of the ground and excited state potential energy surfaces needed for interpreting the phototransformations of the chromophore groups. The first review of earlier calculations is most likely due to Helms [36]; one of the most recent discussions of the achievements of quantum chemistry for the chromophores *in vacuo* is presented [37]. The methodology aspects of quantum chemical approximations suitable for modeling photochemical processes with organic molecules are clearly presented in the review articles [9, 38, 39]. To avoid getting mired into quantum chemistry terminology and the details of different approximations used presently for computer calculations of the properties of organic chromophores in the ground and excited states, we limit ourselves to a superficial description of the most common approaches. Several commonly used abbreviations will be used below.

Currently, it is accurate to state that the calculations of equilibrium geometry parameters in the ground electronic state for molecules composed of up to a hundred atoms are not problematic. By using the methods of the density functional theory (DFT), a large community of chemists can calculate the three-dimensional structure of the chromophore

molecule and visualize its details on the screen of a monitor with suitable software.

The difficulties of modeling optical spectra are due to the necessity of maintaining a similar accuracy level when calculating the ground state electronic properties with a leading electronic configuration $...\pi^2$ and those of the excited state with a leading electronic configuration $...\pi^1\pi^{*1}$ (three dots ahead of the π-type HOMO refer to the entire set of preceding orbitals doubly occupied by electrons). It would be beneficial to take into account the superposition of electronic configurations for the ground electronic states as well. The reasons for such a description are clear, e.g., when considering the resonance structures for the anionic form of the GFP chromophore (Fig. 6). Correspondingly, the quantum chemical approaches with the multiconfigurational wavefunctions seem suitable for calculations. The complete active space self-consistent field (CASSCF) method is one approach often met in papers devoted to the photochemistry of organic molecules.

The calculations with multiconfigurational approaches require practical skills, access to powerful computational resources, and patience in waiting for the results; therefore, the temptation arises to resort to shortcuts. In the first papers devoted to the calculation of the absorption spectra of the chromophores from the fluorescent proteins [31–33, 40, 41], as well as in recent papers [27, 42, 43], fairly good results for the band maxima in the optical spectra and band intensities are often obtained with simple semiempirical methods like ZINDO [44]. In this method, considerable simplifications of the electronic structure theory are balanced by the successful adjustment of parameters using suitable reference experimental data. As always happens with semiempirical methods, it is unclear a priori when their application may be successful and when they will lead to large errors.

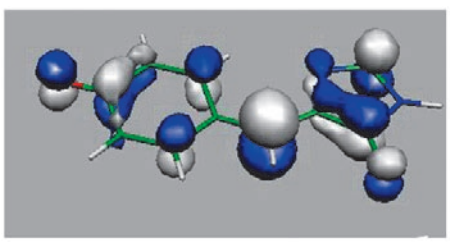

HOMO

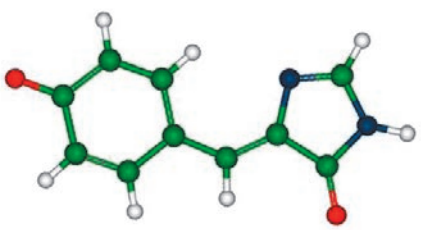

hydroxybenzylidene-imidazoline

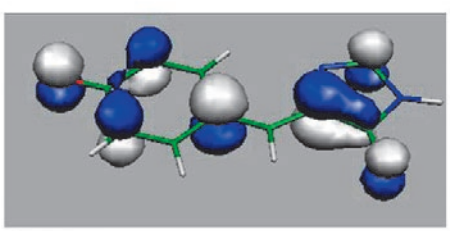

LUMO

Fig.5. Middle: the hydroxybenzylidene-imidazoline molecule in the cis-anionic form representing the GFP chromophore; bottom: the highest occupied molecular orbital (HOMO); top: the lowest unoccupied molecular orbital (LUMO)

The current state of things regarding another modern calculation method of the energy differences between the ground and excited electronic states which is becoming more and more popular among quantum chemists due to its simplicity – the time-dependent density functional theory (TD-DFT) – is even more complicated. In many applications, TD-DFT leads to excellent agreement with the experimental data for the positions of band maxima in the optical spectra of organic chromophores, but in other applications the results are considerably less ambitious (see, e.g., [35]). There are fundamental reasons for this failure [45] that are due to errors in describing the charge-transfer states that are common for such molecules.

We can compare the achievements of these two "user friendly" calculation methods of band parameters in the absorption spectra of the chromophores of colored proteins, ZINDO, and TD-DFT. According to the first paper [41] devoted to studies of the red fluorescent protein DsRed [46] (in particular to modeling properties of its chromophore), the results of ZINDO are closer to experimental findings than those of TD-DFT. In a recent paper [42], the authors compared the computed spectral parameters of the anionic forms of the chromophores from GFP and DsRed with those measured by using photodestruction spectroscopy in the gas phase [47–49]. The experimental value for the absorption band of the anionic GFP chromophore is 479 nm, while calculations with ZINDO result in 477–481 nm and the position of the intense absorption band calculated with TD-DFT (390 or 405 nm, depending on computational details) deviates considerably from the experimental value. For the anionic form of the model chromophore synthesized by the motives of the DsRed chromophore, the position of the experimental absorption band is 521 nm [49], and calculation results are 533 nm (ZINDO) and 449 nm (TD-DFT). A similar conclusion follows in [43], which is devoted to studies of the anionic GFP chromophore: the ZINDO method allows one to obtain a position of the absorption band that practically coincides with the experimental value, while the TD-DFT method overestimates the vertical excitation energy, giving rise to a blue shift from the experimental estimate (479 nm) by 50–90 nm. Nevertheless, we stress again that the predictions of the semiempirical ZINDO method should be taken with caution. It is unclear how to systematically improve ZINDO, unlike the TD-DFT approach, for which sooner or later more reliable representations of the electronic density functional will be found. Meanwhile, new publications appear that report the results of excitation energy calculations for the chromophore molecules from different-colored proteins in different versions of the TD-DFT approach [27, 35, 37, 50–55].

Let us turn to methods on the grounds of multiconfigurational approaches, which are more creditable in the quantum theory – but less "user-unfriendly" – and the use of which requires substantial computer resources and experience in quantum chemical calculations. Potentially, these methods

are necessary for solving a wider range of problems than calculations of the absorption bands of the chromophores. Namely, the multiconfigurational approaches are used to compute sections of the potential energy surfaces of the excited electronic states with the proper localization of the minimum energy points needed to estimate fluorescence spectra. Also, they are used to locate the points of conical intersections of the ground and excited states where quenching of photoexcitation occurs.

Using the less developed [34] and more sophisticated [37, 55, 56] versions of the so-called configuration interaction methods – in which superposition of electronic configurations takes place for calculations of energy differences between the ground and excited states of the chromophore molecules in the gas phase – allows one to achieve, in favorable cases, estimates for the optical band positions with errors not exceeding 20–50 nm. Additional efforts (see, for instance, [9, 38, 39] for details) are spent on optimizing the orbitals entering the multiconfigurational wavefunctions to make these orbitals suitable "on average" for the ground and excited electronic states and for the optimal choice of the number of orbitals occupied by electrons in the ground and excited state. Thus, we arrive to the CASSCF method with state-averaging, SA-CASSCF, which seems to be the most basic one for calculating the excited state potential surfaces of organic chromophores. For better accuracy, the SA-CASSCF energies are corrected by adding the perturbation energy contributions. After such corrections, the errors upon estimating the band maxima in the optical spectra of the gas phase chromophores are reduced to 15–20 nm. Examples of these state-of-the-art calculations are presented in [37, 57, 58] for the GFP chromophore and in [59] for the asFP595 chromophore. Papers [58, 59] include results for different protonation states of the chromophore molecule.

Figure 7 illustrates possible transformations of the chromophore molecule upon photoexcitation, taking the GFP case as an example. Upon transition from the ground state S_0 minimum energy point to the potential energy surface of the excited state S_1, the system relaxes to the energy minimum responsible for fluorescence. The drift on the excited state potential energy surface can lead to the conical intersection point S_1/S_0 with a distinct geometry configuration through which descent to the ground state occurs.

This picture, which provides important information on the photophysical processes with chromophore molecules, can be reliably obtained with quantum chemistry methods on the basis of the SA-CASSCF approach. The first such study for the anionic form of the GFPchromophore *in vacuo* was reported in [57]. Later, the calculations for the gas phase anionic chromophores in both cis- and trans-conformations from the green (GFP) and red (DsRed, asFP595) proteins were described [60–62], which helped rationalize the chromophore photoisomerization processes.

Beyond calculations of excited states, quantum chemistry methods have been used for computations of structural parameters, vibrational spectra, and for analyzing possible re-arrangements in the ground electronic state in model systems composed of the chromophore with the nearest molecular groups by motives of the protein structure. The first such calculations for a fairly large molecular cluster mimicking the chromophore containing domain of GFP are described in [63]. By using the cluster model, the authors of [64] also calculated the proton transfer pathways along the hydrogen bond network (see Fig. 3) for the chromophore containing the domain of GFP in the ground electronic state, concluding that the activation barriers for these transitions should not be large.

The vibrational spectra of the GFP chromophore in various protonation states were computed in [65] by using the Car-Parrinello molecular dynamics, which presents a quite popular methodology based on estimates of the forces acting on a nuclei by solving quantum equations in the density functional theory. In [66], the authors considered a larger model for the chromophore-containing domain of GFP. A direct comparison was performed for the Raman spectra calculated for the chromophore molecule and those measured experimentally for GFP. By using the same methodology, the bands in the Raman spectra of the DsRed chromophore were computed in [67]. The results of calculations of the vibrational spectra of the GFP chromophore molecule in different protonation states are reported in [68]. Despite a certain practical use for the calculation results of the vibrational spectra of a small model system composed of the gas-phase chromophore molecule and several of the nearest peptide groups, the disadvantages of such an approach are also evident. These disadvantages are related to the insufficient inclusion of the protein environment. In this respect, the results of approaches in which solvent effects are taken into account, as in [69, 70], seem to be more interesting.

Modeling chromophore molecules in solutions by quantum chemistry tools presents an important step in studying the effects of the condensed phase environment on chromophore properties. These studies are usually performed either within the continuum model, treating the solvent as a media with a specific value of the dielectric constant in whose cavity a solute species is inserted, or within the discrete model with an explicit consideration of the solvent molecules in the model system.

Fig.6. Resonance structures of the anionic form of the GFP chromophore

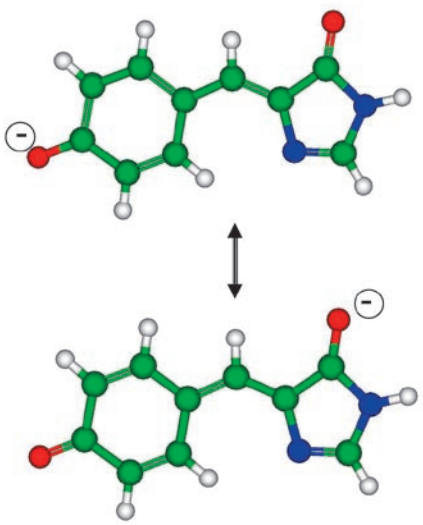

The continuum solvation model is used in paper [71], along with the semiempirical calculation method of excited state energies [31] for estimates of the solvent-induced shifts in ethanol in the optical spectra of the GFP chromophore in different protonation states. A qualitative correlation between the theoretical and experimental data was obtained.

Important results were obtained in paper [72], in which the diagram illustrating the photo-induced transformations with the neutral form of the GFP chromophore (see Fig. 7) was calculated for a model system composed of a chromophore surrounded by water molecules. In this work, the sections of potential energy surfaces for the ground and excited states were computed and the coordinates of minimum energy points and conical intersection points were located. The semiempirical quantum chemistry method AM1 with parameters specially adjusted for this project was used to perform such complex calculations. The main conclusion of this paper, which is widely cited in the literature devoted to studies of fluorescent proteins, is that the solvent reduces the lifetime of the excited electronic state of the chromophore over the gas phase by an order of magnitude. Unlike in the gas phase conditions, the internal rotation of the chromophore over the bridging double bond (Fig. 4) is facilitated inside the shell of solvent molecules. In [73], the molecular dynamics of the neutral form of the GFP chromophore surrounded by water molecules was studied using the *ab initio* quantum chemistry approach SA-CASSCF for potential surfaces. It was concluded that the solutions have increased quenching efficiency compared to the gas phase process.

Papers [70, 71] describe calculations of the vibration spectra and of energy profiles for the quenching of the photoexcitation of various protonation forms of the GFP chromophore in aqueous solution. The continuum solvation models, i.e., the polarized continuum model (PCM) was used, and the *ab initio* computation quantum chemistry methods on the basis of CASSCF for the potential surfaces were applied. The increased efficiency of internal conversion in solvent was also confirmed.

Another approach to the model properties of the modified GFP chromophore in the cis- and trans-conformations in various protonation forms in an aqueous solution was demonstrated in [52]. The distribution of particles in the model system composed of the chromophore and the solvent shell of 857 water molecules were simulated by the Monte Carlo method for the NPT ensemble. The excited state energies of the chromophore were computed in the TD-DFT and CASSCF approaches, the latter being recognized as the better choice. The solvent shifts in the absorption spectra and the cis-trans isomerization options of the chromophore in solution were analyzed. Similar methodology was later used for studies of the DsRed chromophore [74].

The authors of [55] calculated the absorption spectral band maxima for a series of the GFP-type chromophores with changes inside the chromophore molecule itself by using the continuum PCM model and different versions for estimates of the excitation energies. It was concluded that there is fairly poor agreement between theoretical and experimental data, although qualitative correlations could be established. Synthetic molecules on the basis of the GFP chromophore were also studied experimentally in aqueous solution in [75], accompanied by theoretical estimates for the optical spectra by the TD-DFT method and contributions from the solvent within the PCM approach.

The optical spectra of the chromophore 2-acetyl-4-(p-hydroxybenzylidene)-1-methyl-5-imidazolone from the protein asFP595 were studied experimentally in several solvents at different pH values. In aqueous solution, the band at 418 nm was assigned to the neutral form, and the band at 520 nm was assigned to the anionic form of the chromophore. Band positions in ethanol, propanol, and dimethylformamide were found to be considerably shifted with respect to water, and no correlation was observed with the corresponding values of the solvent dielectric constant. Simulations of these spectra were carried out for different protonation states of the chromophore in the cis- and trans-conformations in water, ethanol, acetonitrile, and dimethylsulfoxide (DMSO) [35]. The PCM continuum model and the TD-TDF approach for calculations of excitation energies were applied. The data collected in Table 1 illustrate the relationship between the experimental and theoretical results. The qualitative correlation is evident – both investigations establish a weak dependence band position on the solvent. The assignment of the shorter absorption band to the neutral form and the assignment of the longer absorption band to the anionic form are also apparent, although the quantitative disagreements are fairly large (up to 50 nm). The experimentally observed spectra cannot be definitely assigned either to the trans- or the cis-conformation of the chromophore in solution. The energy calculations for both conformations *in vacuo* and in the solution clearly predict that the energy of the cis-form is lower by about 1.5

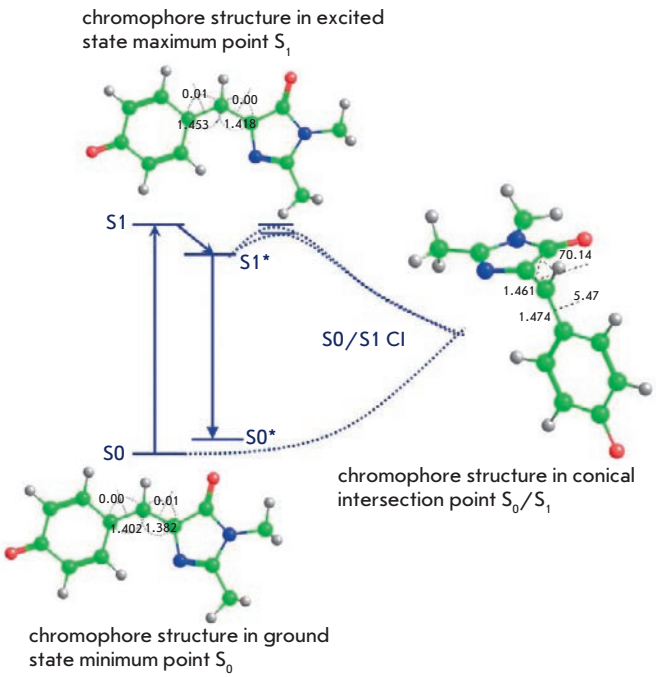

Fig.7. Possible transformations of the GFP chromophore in the cis-anionic form upon photoexcitation

kcal/mol than that of the trans-form. These calculations do not confirm the hypothesis formulated in [76] that the weak fluorescence of the chromophore observed in dimethylformamide is evidence of the similarity between the optical properties of this solvent and those of the protein asFP595.

The question of whether or not the cis-trans isomerization of chromophores from the colored proteins in solutions is possible has been debated for a long time [77]. The experiments described in paper [78] show that the GFP chromophore, e.g., in the anionic form, can be transformed from one conformation to another with an activation barrier of about 13 kcal/mol. The latter was estimated by kinetic measurements using the Arrhenius equation. On the other hand, earlier quantum chemical calculations [33] resulted in barriers greater than 50 kcal/mol. This discrepancy was resolved only recently. In [79], the energy profile for the cis-trans isomerization of the anionic GFP chromophore in water was calculated to be 10–11 kcal/mol, correspondingly, which is very close to the experimental estimates. This theoretical result was obtained within new versions of the continuum solvation models and within the discrete model with an explicit treatment of water molecules in the first salvation shell. Figure 8 shows the structure of the model system in the conformation on the top of the activation barriers upon transition from the cis-isomer to the trans-isomer. Paper [79] underlines the necessity of using multiconfigurational approaches of quantum chemistry to adequately describe the isomerization energy profile.

Finally, we mention one more important application for the computer modeling properties of chromophores from fluorescent proteins in solutions, namely, calculations of pKa's. This information is of value for an analysis of the chromophore properties in protein matrices since it helps estimate the chromophore's protonation states and on-the-proton transfer pathways over hydrogen-bond networks. The pKa values are computed using the thermodynamics cycle components, which include the free energies of deprotonation on specific atoms in the gas phase and free energies of solvation of the protonated molecule, the anion, and free energy of proton solvation. A series of quantum chemical calculations should be carried out to obtain the parameters of the particles, including equilibrium geometry parameters and vibrational frequencies in the gas phase and in solution (in the latter case, with the continuum solvation models). Such a procedure and the corresponding results for the oxygen and nitrogen centers of the GFP chromophores are described in [80–82]. In [81], the pKa's for the excited state were estimated as well. The computed pKa's for the chromophores of colored proteins asFP595 and zFP538 in the trans- and cis-conformations are presented in [82].

To conclude this section, we stress the necessity of quantum chemical calculations for modeling the properties of the chromophores from the fluorescent proteins, despite their high cost. Upon improving the computational methods of quantum chemistry, the latter will become more and more user-friendly. The routine of calculating geometric structures (equilibrium geometry parameters in the ground electronic state) for molecules with a number of atoms up to 100 serves as an illustrative example – the user can obtain fairly reliable results on personal computers even without clear knowledge of the algorithms. So far, such a service is not available for modeling the entire process of photoexcitation; however, the situation may change with time.

MODELING THE PROPERTIES OF THE FLUORESCENCE PROTEINS USING THE QM/MM METHOD

Modeling properties of the chromophores inside the protein matrix should be carried out using a combination of the quantum-mechanics and molecular-mechanics (QM/MM) methods. Apparently, the chromophore molecule itself should be assigned to the quantum subsystem by placing the boundary between the QM and MM parts in such a manner that all the conjugated bonds responsible for light absorption and emission are described by quantum equations. It should also be reasonable to include the side chains of amino-acids nearest to the chromophore molecule in the QM part, because they can be involved in the proton transfer process with the chromophore.

For practical purposes, the size of the quantum subsystem may amount to up to a hundred atoms. Figure 9 illustrates the possible choice of the QM subsystem for the QM/MM calculations of the protein properties of the GFP family. The chromophore group (here it originates from the protein asFP595) is represented in the QM part almost as a whole. The side chains of Glu, His, and Ser, as well as the water molecule, may participate in proton transfers. The positively charged side chain of Arg may considerably affect the quantum subsystem.

With such a selected model, calculations of the structures and energies for the chromophore-containing domains from

Table 1. Comparison of calculated [35] and measured [76] (bold, in parentheses) wavelengths for the absorption band maxima of the chromophore asFP595. The asterisk distinguishes the wavelengths measured in DMF (ε =38.3)

Solvent	Neutral form	Anionic form	Zwitterionic form
Cis-conformation			
Vacuo (ε =1)	430	484	521
Ethanol (ε =24,3)	453 (**425**)	504 (**542**)	538
Acetonitrile (ε =36,3)	453 (**422***)	502 (**572***)	537
DMSO (ε =47,2)	458 (**422***)	511 (**572***)	545
Water (ε =80)	453 (**418**)	502 (**520**)	537
Trans-conformation			
Ethanol (ε =24,3)	438 (**425**)	476 (**542**)	504
Water (ε =80)	437 (**418**)	474 (**520**)	538

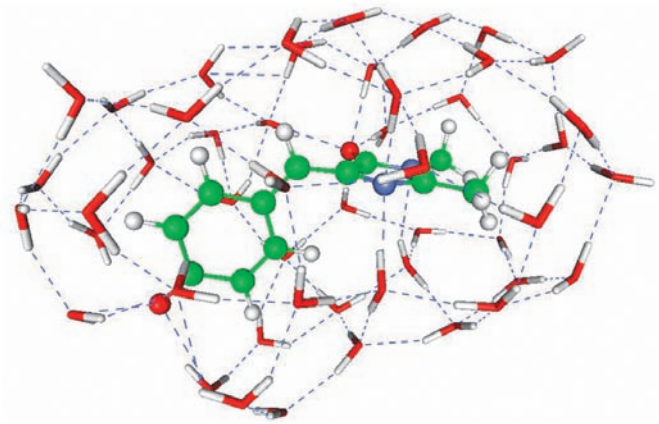

Fig.8. Structure of the transition state of the anionic GFP chromophore on the way from the cis-isomer to the trans-isomer inside the shell of water molecules

the asFP595 protein by considering both the trans- and cis-conformations of the chromophore were performed in [83, 84]. The largest part of the protein macromolecule including more than 2,000 atoms surrounding the quantum subsystem was assigned to the MM subsystem. The initial coordinates of heavy atoms were taken from the crystal structure of the dark form of the protein PDBID:1XMZ [85] with the chromophore in the trans-conformation. After the hydrogen atoms (or protons) were added, the equilibrium geometry configuration of the model protein system was calculated with the flexible effective fragment QM/MM method [86, 87] using the Hartree-Fock approximation in the quantum subsystem and the AMBER force field for the molecular mechanic part. The obtained atomic coordinates were consistent with the crystal structure [83, 84]. Then, a model system was prepared in which the cis-conformation of the chromophore inside the protein matrix and the coordinates were re-optimized with the QM/MM method. One of the most important results of this study was the conclusion that the energy of the system with the trans anionic chromophore was lower than that with the cis-conformations. *In vacuo*, the ordering of conformations is reversed and the cis-isomer of the isolated chromophore should be lower than the trans-isomer. Therefore, the protein matrix provides greater stabilization for the trans-isomer of the chromophore, which is in agreement with X-ray studies [23, 85, 88]. Estimates of the vertical excitation energies in the quantum subsystem using the TD-DFT method were performed for the structures optimized with the QM/MM method. It was found that the structure with the cis-conformation should correspond to the transition S_0-S_1, with a longer wavelength in the optical spectra. This result is also qualitatively consistent with experimental observations and with the working hypothesis [23, 26, 89, 90] according to which asFP595 absorbs green light in the state with trans-conformation of the chromophore and emits red light in the state with cis-conformation of the chromophore.

Attempts to theoretically describe the mechanism of kindling in asFP595 were undertaken in [27, 91] using other versions of the QM/MM method. The common TD-DFT and SA-CASSCF approaches were applied to calculate the points on the potential energy surfaces of the ground and excited states within a relatively small quantum subsystem. In [91], forces computed "on the fly" were used for trajectory calculations, and transitions between potential surfaces were allowed upon photoisomerization of the chromophore inside the protein. The main result of this modeling is a conclusion about the coupling of the trans-cis isomerization of the chromophore in the protein asFP595 with the protonation state of the chromophore. Similar technical approaches assuming trajectory calculations with forces estimated "on the fly" by quantum equations were used for an analysis of GFP photodynamics [73]. In a series of papers [92–96], the results of molecular dynamics simulations of proton transfers over hydrogen bond networks in the vicinity of the chromophore in GFP were presented using various presentations of the potential surfaces, including those by the quantum calculations.

In the very first applications of the QM/MM method for calculating the properties of fluorescent proteins [50, 51], an essentially simpler – but less reliable – methodology was applied. According to it, the structural parameters of the protein molecule were obtained with the semiempirical quantum chemistry approach AM1 and the excitation energies were estimated in the TD-DFT approximation. By using this methodology, the bands in the optical spectra of GFP [50] (as well as those of the blue fluorescent protein BFP [51], in which the GFP chromophore was modified) were estimated.

In the actively cited paper [97], the positions of bands in optical spectra of GFP corresponding to the transitions $S_0 \rightarrow S_1$ and $S_1 \rightarrow S_0$ were computed in the QM/MM approach using the ab initio CASSCF method in the quantum subsystem and the force field CHARMM in the MM subsystem. The computed band positions are consistent with the experimental results, giving rise to discrepancies of about 20–30 nm. By considering a series of models with gradually increasing quantum subsystems, the authors studied the effect of the charged amino acid residue Arg located near the chromophore (Fig. 9) on the calculated spectrum.

The optical spectra of GFP and several mutated variants with different protonation states of chromophore groups were computed in [98]. To calculate the energy differences of the ground and excited states, the authors used a specific version of the configuration interaction method as in previous studies of the gas phase chromophores [56], but they accounted for the effect of the protein matrix within the QM/MM approach. Good agreement between the calculated and experimental transition energies both for excitation and emission was reported.

The use of one of the so-called multi-level quantum chemistry approaches for treating extended systems – the fragment molecular orbital (FMO) method – to calculate the optical spectra of the red fluorescent proteins DsRed and mFruits was described in [99, 100]. The results were obtained within various versions of the configuration interaction approximation for estimates of the energy differences between the ground and excited states. The FMO method is potentially interesting due to the possibility of avoiding the use of the empirical force fields, avoiding the combined QM/MM ap-

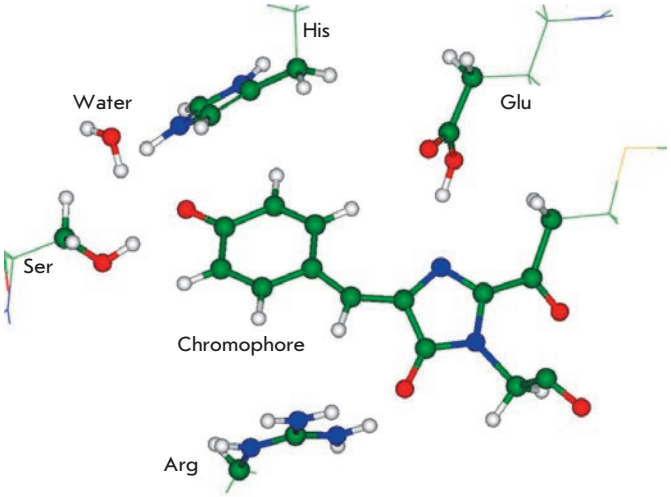

Fig.9. One possible choice of the quantum subsystem (balls and sticks) for modeling the properties of fluorescent proteins from the GFP family by using the QM/MM method

proach in calculations of protein properties, and applying only quantum chemical approximations to the model system.

CONCLUSIONS

Over the ten years since the publication of the first papers [12, 31, 33] devoted to the computer modeling properties of fluorescent proteins and their chromophores, a large amount of results have been obtained, most of which were discussed in this review. Apparently, the greatest interest is in answering the question as to what the experimenters can learn from the results of computer modeling that is particularly useful. Let us turn to one of the recent review papers written by experts in the studies of fluorescent proteins, Tonge and Meech [7]. They draw attention to several computational papers that they selected, which are mentioned below. An analysis of the electronic structure of the chromophore molecule, hydroxybenzylidene-imidazoline, in the ground and excited electronic states performed in the first calculations using the semiempirical methods of quantum chemistry [32, 33] allowed to relate the photophysical properties of GFP with the local properties of the bridging fragment of the molecule (Fig. 2). In particular, increasing the bond order of the methylene's double bond upon electronic excitation should lead to the internal rotation barrier decreasing and facilitate internal conversion and benefit the trans-cis chromophore isomerization. The importance of calculating the sections of the potential energy surfaces, the minimum energy pathways along the angular coordinates near the bridging fragment, and the conical intersection points for the chromophore molecule in the isolated state and in solution upon the gradually increasing complexity of the quantum chemistry approaches [57, 60, 61, 69, 72, 91, 101] is underlined. Since such calculations with an explicit consideration of the role of the protein matrix on the photophysical properties of the chromophore are too complicated, several modeling results [21, 22] obtained with molecular mechanics methods are distinguished (in particular, those that formulated the role of sterical hindrance for the internal conversion of the chromophore). As is shown in QM/MM calculations [97], the charged amino acid residue may considerably affect the photoexcitation dynamics. Molecular dynamics simulations (sometimes in conjunction with quantum chemistry calculations) [16, 28, 64, 92-96, 102, 103] allow one to visualize the proton transfer pathways along oriented hydrogen bond networks in proteins or transformations with the chromophore groups. The latter observations seem to be important for a prognosis of perspective point mutations, which may either enhance or diminish these pathways.

Therefore, the entire range of modern tools of computer molecular modeling, including molecular mechanics, molecular dynamics, quantum chemistry, and combined-quantum mechanics and molecular-mechanics (QM/MM) methods – all of which were used for modeling the structure and spectra of fluorescent proteins –described in this review are considered in [7] as useful support in experimental studies that are, in turn, oriented toward the practically important tasks of designing new and efficient biomarkers in living systems by the directed modification of natural objects [104].

We consider modeling with the QM/MM method the most prospective, but the most time-consuming tool for simulations of chemical and photophysical phenomena in proteins. Future success in this direction depends on how progress in the construction of supercomputers goes; on the development of efficient algorithms to solve the equation of quantum mechanics; and, even to a larger extent, on the existence of qualified specialists capable of understanding a wide range of subjects from biology to computational mathematics. These efforts will be granted if reliable predictions of perspective variants of protein macromolecules can be provided quickly to biotechnologists at least as efficiently as computer modeling turned out to be useful in drug design [105]. ●

When preparing this article, works supported by the Russian Foundation of Basic Research (project # 07-03-00059) and the Program of the Russian Academy of Sciences on molecular and cell biology and the Federal Science and Innovation Agency (project 02.522.11.2002) were used.

REFERENCES

1. Tsien R. Y. // *Ann. Rev. Biochem.* 1998. V. 67. P. 509--544
2. Zimmer M. // *Chem. Rev.* 2002. V. 102. P. 759--781
3. Labas Yu. A., Gordeeva A.V., Fradkov A.F. // *Priroda* (Russian). 2003. #3. P. 33--43
4. Schmid J. A., Neumeier H. // *ChemBioChem.* 2005. V. 6. P. 1–9
5. Remington S. J. // *Curr. Opin. Struct. Biol.* 2006. V. 16. P. 714–721
6. Wachter R. M. // *Photochem. Photobiol.* 2006. V. 82. P. 339–344
7. Tonge P. J., Meech, S. R. // *J. Photochem. Photobiol. A: Chemistry.* 2009, V.205. P. 1-11.
8. Nemukhin A. V. //*Soros Educational J.* (Russian). 1998. #. P. 48--52
9. Robb M. A., Garavelli M., Olivucci M., Bernardi F. // in *Rev. Comput. Chem.*, Eds. Lipkowitz K. B., Boyd. D. B. Wiley-VCH Publishers. New York. 2000. V. 15. P. 87--146
10. Warshel A., Levitt M. // *J. Mol. Biol.* 1976. V. 109. P. 227--249
11. Reuter N., Lin H., Thiel W. // *J. Phys. Chem.* B. 2002. V. 106. P. 6310--6321
12. Helms V., Straatsma T. P., McCammon J. A. // *J. Phys. Chem.* B. 1999. V. 103.

P. 3263--3269
13. Berman H. M., Westbrook J., Feng Z., Gilliland G., Bhat T. N., Weissig H., Shindyalov I. N., Bourne P. E. // *Nucl. Acids Res.* 2000. V. 28. P. 235--242
14. Chattoraj M., King B. A., Bublitz G. U., Boxer S. G. // *Proc. Natl. Acad. Sci.* USA. 1996. V. 93. P. 8362–8367
15. Warren A., Zimmer M. //*J. Molec. Graphics Model.* 2001. V. 19. P. 297-303
16. Lill M. A., Helms V. // *Proc. Natl. Acad. Sci.* USA. 2002. V. 99. P. 2778–2781
17. Patnaik S. S., Trohalaki S., Pachter R. // *Biopolymers.* 2004. V. 75. P. 441–452
18. Agmon N. // *Biophys. J.* 2005. V. 88. P. 2452–2461
19. Leiderman P., Huppert D., Agmon N. // *Biophys. J.* 2006. V. 90. P. 1009–1018
20. Baffour-Awuah N. Y. A., Zimmer M. // *Chem. Phys.* 2004. V. 303. P. 7–11
21. Maddalo S. L., Zimmer M. // *Photochem. Photobiol.* 2006. V. 82. P. 367–372
22. Megley C. M., Dickson L. A., Maddalo S. L., Chandler G. J., Zimmer M. // *J. Phys. Chem. B.* 2009. V. 113. P. 302–308
23. Andresen M., Wahl M. C., Stiel A. C., Grater F., Schäfer L. V., Trowitzsch S., Weber G., Eggeling C., Grubmüller H., Hell S. W., Jakobs S. // *Proc. Natl. Acad. Sci.* USA. 2005. V. 102. P. 13070–13074
24 Nifosì R., Tozzini V. // *Chem. Phys.* 2006. V. 323. P. 358–368
25. Vallverdu G., Demachy I., Ridard J., Lévy B. // J. *Molec. Struct. THEOCHEM.* 2009. V. 898. P. 73–81
26. Lukyanov K. A., Fradkov A. F., Gurskaya N. G., Matz M. V., Labas Y. A., Savitsky A. P., Markelov M. L., Zaraisky A. G., Zhao X. N., Fang Y., Tan W. Y., Lukyanov S. A. // *J. Biol. Chem.* 2000. V. 275. P. 25879--25882
27. Schäfer L.V., Groenhof G., Klingen A. R., Ullmann G. M., Boggio-Pasqua M., Robb M. A., Grubmüller H. // *Angew. Chemie Int. Ed.* 2007. V. 46: P. 530–536
28. Moors S. L. C., Michielssens S., Flors C., Dedecker P., Hofkens J., Ceulemans A. // *J. Chem. Theory Comput.* 2008**.** V. 4. P. 1012–1020
29. Habuchi S., Ando R., Dedecker P., Verheijen W., Mizuno H., Miyawaki A., Hofkens J. // *Proc. Natl. Acad. Sci.* USA. 2005. V. 102. P. 9511–9516
30. Khrameeva E. E., Drutsa V. L., Vrzheshch E. P., Dmitrienko D. V., Vrzheshch P. V. // *Biochemistry (Mosc).* 2008. V. 73. P. 1085-95
31. Voityuk A. A., Michel-Beyerle M. E., Rösch N. //*Chem. Phys. Lett.* 1997. V. 272. P. 162–167
32. Voityuk A. A., Michel-Beyerle M. E., Rösch N. //*Chem. Phys.* 1998. V. 231. P. 13–25
33. Weber W., Helms V., McCammon J. A., Langhoff P. W. // *Proc. Natl. Acad. Sci.* USA. 1999. V. 96. P. 6177–6182
34. Helms V., Winstead C., Langhoff P. W. //J. *Molec. Struct. THEOCHEM.* 2000. V. 506. P. 179-189
35. Nemukhin A. V., Topol I. A., Burt S. K. // *J. Chem. Theor. Comput.* 2006. V.2. P. 292-299
36. Helms V. // *Curr. Opin. Struct. Biol.* 2002. V. 12. P. 169-175
37. Epifanovsky E., Polyakov I., Grigorenko B., Nemukhin A., Krylov A. I. // *J. Chem. Theor. Comput.* 2009. V. 5. P. 1895–1906
38. Sinicropi A., Andruniow T., De Vico L., Ferré N., Olivucci M. // *Pure Appl. Chem.* 2005. V. 77. P. 977–993
39. Wanko M., Hoffmann M., Frauenheim T., Elstner M. // *J. Comput. Aided Mol. Des.* 2006. V. 20. P. 511–518
40. Voityuk A. A., Michel-Beyerle M. E., Rösch N. //*Chem. Phys. Lett.* 1998. V. 296. P. 269–276
41. Gross L. A., Baird G. S., Hoffman R. C., Baldridge K. K., Tsien R. Y. // *Proc. Natl. Acad. Sci.* USA. 2000. V. 97. P. 11990–11995
42. Wan S., Liu S., Zhao G., Chen M., Han K., Sun M. //*Biophys. Chem.* 2007. V. 129. P. 218-223
43. Collins J. R., Topol I. A., Nemukhin A. V., Savitsky A. P. //*Proc. SPIE.* 2009. V. 7191. P.71912
44. Zerner M. C. //*Rev. Comput. Chem.* Ed. Lipkowitz K.B. and Boyd D.B. 1991. Vol.2 (VCH Publishing, New York), P. 313-366
45. Dreuw A., Head-Gordon M. // *J. Am. Chem. Soc.* 2004. V. 126. P. 4007-4016
46. Matz M. V., Fradkov A. F., Labas Y. A., Savitsky A. P., Zaraisky A. G., Markelov M. L., Lukyanov S. A. // *Nature Biotechnol.* 1999. V. 17. P. 969–973
47. Nielsen S. B., Lapierre A., Andersen J. U., Pedersen U. V., Tomita S., Andersen L. H. // *Phys. Rev. Lett.* 2001. V.87. P. 228102
48. Andersen L. H., Lapierre A., Nielsen S. B., Nielsen I. B., Pedersen S. U., Pedersen U. V., Tomita S. // *Eur. Phys. J. D.* 2002**.** V. 20. P. 597-600
49. Boyé S., Nielsen S. B., Krogh H., Nielsen I. B., Pedersen U. V., Bell A. F., He X., Tonge P. J., Andersen L. H. // *Phys. Chem. Chem. Phys.* 2003. V. 5. P. 3021–3026
50. Marques M. A. L., Lopez X., Varsano D., Castro A., Rubio, A. // *Phys. ReV. Lett.* 2003, V. 90. P. 258101
51. Lopez X., Marques M. A. L., Castro A., Rubio A. // *J. Am. Chem. Soc.* 2005. V. 127. P. 12329-12337
52. Xie D., Zeng X. // *J. Comp. Chem.* 2005. V. 26. P. 1487-1496
53. Sun M. // *Int. J. Quant. Chem.* 2006. V. 106. P. 1020–1026
54. Amat P., Granucci G., Buda F., Persico M., Tozzini V. // *J. Phys. Chem. B***.** 2006**.** V.110. P. 9348-9353
55. Timerghazin Q. K., Carlson H. J., Liang C., Campbell R. E., Brown A. // *J. Phys. Chem. B.* 2008. V. 112. P. 2533-2541
56. Das A. K., Hasegawa J.-Y., Miyahara T., Ehara M., Nakatsuji H. // *J. Comput. Chem.* 2003. V. 24. P. 1421–1431
57. Martin M. E., Negri F., Olivucci M. // *J. Am. Chem. Soc.* 2004. V. 126. P. 5452–5464
58. Bravaya K. B., Bochenkova A. V., Granovsky A. A., Nemukhin A. V. // *Russ. J. Phys. Chem. B.* 2008. V. 2. P. 671-675
59. Bravaya K. B., Bochenkova A. V., Granovsky A. A., Savitsky A. P., Nemukhin A. V. // *J. Phys. Chem. A.* 2008. V. 112. P. 8804–8810
60. Olsen S., Smith S. C. //*J. Am. Chem. Soc.* 2007. V. 129. P. 2054–2065
61. Olsen S., Smith S. C. //*J. Am. Chem. Soc.* 2008. V. 130. P. 8677–8689
62. Olsen S., McKenzie R. H. //*J. Chem. Phys.* 2009. V.130. P. 184302
63. Laino T., Nifosì R., Tozzini V. // *Chem. Phys.* 2004. V. 298. P. 17–28
64. Zhang R. B., Nguyen M. T., Ceulemans A. // *Chem. Phys. Lett.* 2005. V. 404. P. 250–256
65. Tozzini V., Nifosí R. // *J. Phys. Chem. B.* 2001. V. 105. P. 5797-5803
66. Tozzini V., Bizarri A. R., Pellegrini V. , Nifosí R., Giannozzi P., Iuliano A., Cannistraro S., Beltram F. // *Chem. Phys.* 2003. V. 287. P. 33–42
67. Tozzini V., Giannozzi P. // *ChemPhysChem.* 2005. V. 6. P. 1–4
68. Yoo H.-Y., Boatz J. A., Helms V. J., Andrew McCammon J. A., Langhoff P. W. // *J. Phys. Chem. B.* 2001. V. 105. P. 2850-2857
69. Altoe P., Bernardi F., Garavelli M., Orlandi G., Negri F. //*J. Am. Chem. Soc.* 2005. V. 127. P. 3952–3963
70. Altoè P., Bernardi F., Conti I., Garavelli M., Negri F., Orlandi G. // *Theor. Chem. Acc.* 2007. V. 117. P. 1041–1059
71. Voityuk A. A., Kummer A. D., Michel-Beyerle M. E., Rösch N. // *Chem. Phys.* 2001. V. 269. P. 83-91
72. Toniolo A., Olsen S., Manohar L., Martinez T. J. // *Faraday Discus.* 2004. V. 127. P. 149–163
73. Virshup A. M., Punwong C., Pogorelov T. V., Lindquist B. E., Ko C., Martínez T. D. // *J. Phys. Chem. B.* 2009. V. 113. P. 3280–3291
74. Yan W., Zhang L., Xie D., Zeng J. // *J. Phys. Chem. B.* 2007. V. 111. P.14055-14063
75. Voliani V., Bizzarri R., Nifosi R., Abbruzzetti S., Grandi E., Viappiani C., Beltram F. // *J. Phys. Chem. B.* 2008. V. 112. P.10714–10722
76. Yampolsky I. V., Remington S. J., Martynov V. I., Potapov V. K., Lukyanov S., Lukyanov K. A. // *Biochem.* 2005. V. 44. P. 5788-5793
77. Dong J., Abulwerdi F., Baldridge A., Kowalik J., Solntsev K. M., Tolbert L. M. // *J. Am. Chem. Soc.* 2008. V. 130. P. 14096-14098
78. He X., Bell A. F., Tonge P. J. // *FEBS Lett.* 2003. V. 549. P. 35-38
79. Polyakov I., Epifanovsky E., Grigorenko B., Krylov A. I., Nemukhin A. // *J. Chem. Theor. Comput.* 2009. V. 5. P. 1907–1914
80. El Yazal J., Prendergast F. G., Shaw D. A., Pang Y.-P. // *J. Am. Chem. Soc.* 2000. V. 122. P. 11411--11415
81. Scharnagl C., Raupp-Kossmann R. A. // *J. Phys. Chem. B.* 2004. V. 108. P. 477--489
82. Nemukhin A. V., Topol I. A., Grigorenko B. L., Savitsky A. P., Collins J. R. // *J. Mol. Struct. THEOCHEM.* 2008. V. 863. P. 39–43
83. Grigorenko B., Savitsky A., Topol I., Burt S., Nemukhin A. // *Chem. Phys. Lett.* 2006. V. 424. P. 184–188
84. Grigorenko B., Savitsky A., Topol I., Burt S., Nemukhin A. // *J. Phys. Chem. B.* 2006. V. 110. P. 18635--18640
85. Quillin M. L., Anstrom D. M., Shu X., O'Leary S., Kallio K., Chudakov D. M., Remington S. J. // *Biochem.* 2005. V. 44. P. 5774--5787
86. Grigorenko B. L., Nemukhin A. V., Topol I. A., Burt S. K. // *J. Phys. Chem. A.* 2002. V. 106. P. 10663--10672
87. Nemukhin A. V., Grigorenko B. L., Topol I. A., Burt S. K. // *J. Comput. Chem.* 2003**.** V. 24. P. 1410--1420
88. Wilmann P. G., Petersen J., Devenish R. J., Prescott M., Rossjohn J. // *J. Biol. Chem.* 2005. V. 280. P. 2401-2404
89. Chudakov D. M., Feofanov A. V., Mudrik N. N., Lukyanov S., Lukyanov K. // *J. Biol. Chem.* 2003. V. 278. P. 7215–7219
90. Schüttrigkeit T. A., von Feilitzsch T., Kompa C. K., Lukyanov K. A., Savitsky A. P., Voityuk A. A., Michel-Beyerle M. E. // *Chem. Phys.* 2006. V. 323. P. 149–160
91. Schäfer L. V., Groenhof G., Boggio-Pasqua M., Robb M. A., Grubm ller H. //*PLoS Comput. Biol.* 2008. V. 4. P. e1000034
92. Vendrell O., Gelabert R., Moreno M., Lluch J. M. // *Chem. Phys. Lett.* 2004. V. 396. P. 202–207
93. Vendrell O., Gelabert R., Moreno M., Lluch J. M. // *J. Am. Chem. Soc.* 2006. V. 128. P. 3564–3574
94. Vendrell O., Gelabert R., Moreno M., Lluch J. M. *// J. Chem. Theor. Comput.* 2008. V. 4. P. 1138–1150
95. Vendrell O., Gelabert R., Moreno M., Lluch J. M. // *J. Phys. Chem. B.* 2008. V. 112. P. 13443–13452
96. Vendrell O., Gelabert R., Moreno M., Lluch J. M. // *J. Phys. Chem. B.* 2008. V. 112. P. 5500–5511
97. Sinicropi A., Andruniow T., Ferre N., Basosi R., Olivucci M. *// J. Am. Chem. Soc.* 2005. V. 127. P. 11534–11535
98. Hasegawa J., Fujimoto K., Swerts B., Miyahara T., Nakatsuji H. //*J. Comput. Chem.* 2007. V. 28. P. 2443–2452
99. Mochizuki Y., Nakano T., Amari S., Ishikawa T. // *Chem. Phys. Lett.* 2007. V. 433. P. 360–367
100. Taguchi N., Mochizuki Y., Nakano T., Amari S., Fukuzawa K., Ishikawa T., Sakurai M., Tanaka S. *//J. Phys. Chem. B.* 2009. V. 113. P. 1153–1161
101. Olsen S., Manohar L., Martinez T. J. //*Biophys. J.* 2002. V. 82. P. 359A–459A
102. Wang S. F., Smith S. C. //*Phys. Chem. Chem. Phys.* 2007. V. 9. P. 452–458
103. Zhang H., Smith S. C. // *J. Theor. Comput. Chem.* 2007. V. 6 P. 789–802
104. Lukyanov K. A., Chudakov D. M., Lukyanov S., Verkhusha V. V. // *Nat. Rev. Mol. Cell Biol.* 2005. V. 6. P. 885—891
105. Baskin I. I., Palyulin V. A., Zefirov N. S. // *Russ. Chem. Rev.* 2009. V. 78. P. 539--557.

New Approaches for Cancer Treatment: Antitumor Drugs Based on Gene-Targeted Nucleic Acids

O.A. Patutina, N.L. Mironova, V.V. Vlassov, M.A. Zenkova*
Institute of Chemical Biology and Fundamental Medicine, Siberian Branch, Russian Academy of Sciences, Novosibirsk
*E-mail: marzen@niboch.nsc.ru

ABSTRACT Currently, the main way to fight cancer is still chemotherapy. This method of treatment is at the height of its capacity, so, setting aside the need for further improvements in traditional treatments for neoplasia, it is vital to develop now approaches toward treating malignant tumors.
This paper reviews innovational experimental approaches to treating malignant malformations based on the use of gene-targeted drugs, such as antisense oligonucleotides (asON), small interfering RNA (siRNA), ribozymes, and DNAzymes, which can all inhibit oncogene expression. The target genes for these drugs are thoroughly characterized, and the main results from pre-clinical and first-step clinical trials of these drugs are presented. It is shown that the gene-targeted oligonucleotides show considerable variations in their effect on tumor tissue, depending on the target gene in question. The effects range from slowing and stopping the proliferation of tumor cells to suppressing their invasive capabilities. Despite their similarity, not all the antisense drugs targeting the same region of the mRNA of the target-gene were equally effective. The result is determined by the combination of the drug type used and the region of the target-gene mRNA that it complements.
Keywords: cancer therapy, antisense oligonucleotides, ribozymes, DNAzymes, small interfering RNA
Abbreviations: antisense oligonucleotides (asON), small interfering RNA (siRNA), RNA interference (RNAi)

INTRODUCTION

At the current stage of modern medicine, one of the most important projects is to increase the effectiveness of cancer treatment by searching for and developing new therapies and improving traditional therapeutic approaches. A combination of surgery, radio- and chemotherapy is still the golden standard for cancer treatment, and these approaches have led to an 8-fold increase in patient survival over the last 30 years. The negative features of surgery-only treatment are recurrent tumors, the spread of metastases, and the formation of unresectable malignant malformations. This forces doctors to use radio- and chemotherapy. Alas, even this combination of powerful cancer therapies often doesn't bring positive results. Therefore, despite the undeniable achievements of modern oncology, increasing the effectiveness of cancer treatment is of utmost importance.

During the last several decades, complex chemotherapy has become the main approach for treating cancer patients. Its use however is limited, despite the fact that it increases survival rates by 30% to 90%, depending on the type of malformation. The main hindrances are systemic toxicity, nonselective action (the effect is not specifically targeted towards tumor tissue), and the emergence of drug-resistant tumor cell clones.

Recent discoveries have provided scientists with detailed knowledge of the molecular processes underlying carcinogenesis, tumor invasiveness, angiogenesis, and metastasis, as well as other processes, such as tumor suppression, growth control, apoptosis, and immune response. These data have led to the development of a new generation of chemotherapeutic drugs, such as Gleevec (aka Glivec or Imatinib mesylate), Mabthera (aka Rituximab), etc., which have a highly selective effect on their cellular target. It is well known that creating a new drug takes about 10–20 years of research, and improving its selectiveness increases its cost manifold. Currently, chemotherapy as a high-dose active attack aimed at tumor cells is at the limit of its ability. Despite the achieved level of patient survival (for certain cancer types it has made a 10-fold increase in the last 20 years), there is still a 10% to 70% proportion of patients who, for a number of reasons, do not react to treatment. Therefore, the creation of new methods of therapy is a relevant problem at this time. Among the drugs which are currently being developed, gene-targeted drugs are of considerable interest. The possibility of inhibiting a gene's expression was first discovered in the ground-breaking research of N.I. Grineva and her colleages [1–3] and was studied further in order to regulate the expression of genes involved in carcinogenesis using antisense [4] and gene-targeted oligonucleotides [5]. Currently, the main lines of inquiry into gene-targeted cancer therapy are strategies to suppress oncogene overexpression, restore the expression of tumor suppressing genes, boost the activity of the immune system, suppress angiogenesis and metastasis, and initiate tumor self-destruction.

This paper reviews the new experimental approaches to cancer treatment based on gene-targeted oligonucleotides,

which are currently being used in experiments on cell cultures and laboratory animals. Some of these drugs are also in various stages of clinical trial.

HOW GENE-TARGETED NUCLEIC ACIDS WORK

Antitumor drugs based on nucleic acids are highly specific tools which allow the gene expression to be regulated, and they have been attracting the attention of scientists as possible regulators of carcinogenesis at the molecular level. The suppression of several genes whose anomalously high expression is associated with neoplastic transformation can be achieved by nucleic acid-based drugs, such as antisense oligonucleotides (asON), small interfering RNAs (siRNA), ribozymes, and DNAzymes. Generally speaking, the mechanism of gene suppression by these drugs is the complementary binding of oligonucleotides to their mRNA target, which causes the target mRNA molecule to be destroyed or blocks its translation.

AsON are synthetic single-strand DNA, 15–20 nucleotides long, and they can form a complementary complex with the target mRNA sequence [6]. Protein synthesis is suppressed by asON due to the fact that the mRNA target is degraded by the intracellular RNase H, which identifies the hybrid DNA/RNA complex (Fig. 1a), or due to a block of translation, since the formation of a hybrid complex hampers the ribosome's movement on the mRNA strand (Fig. 1b) [7]. Recently discovered asON can block the transfer of spliced mRNA from the nucleus to the cytoplasm; other asON can block a splicing site in pre-mRNA and thus cause the expression of an alternate protein product. [8, 9].

The ability of asON to selectively suppress the production of a protein was demonstrated by Zamechnik and Stephenson in 1978 [4]. They showed that a 13-base oligonucleotide complementary to the 3'-terminal sequence of the RNA of the Rouse sarcoma virus inhibits viral replication *in vitro*. This study led to the research of asON as a potential therapeutic method in cancer and viral infection treatment, as well as treatments for inflammatory processes, blood diseases, and cardio-vascular conditions [10–14].

Since it is known that naturally occurring oligodeoxyribonucleotides are rapidly degraded by nucleases *in vivo* and in cell cultures, several chemical modifications are incorporated into the asON structure to increase their stability [11]. These modifications increase not only asON stability against nucleases, but also their biological effectiveness, hybridization efficiency, and cellular uptake. Among the most notable antisense oligonucleotide derivates are thiophosphate oligonucleotides, in which one of the oxygen atoms not incorporated in the phosphodiester bond is substituted for a sulphur atom [11,15]. Thiophosphate asON are resistant to nucleases, highly soluble, effective in hydridization, and form a heteroduplex with mRNA, which is targeted by RNase H [11]. One drawback of thiophosphate asON is their high affinity to a range of proteins [16, 17]. Second-generation asON carried an alkyl residue in the ribose 2'-position: 2'-*O*-methyl and 2'-*O*-methoxyethyl oligoribonucleotides were effective in blocking mRNA translation, but they did not activate the degradation of the mRNA/asON heteroduplex by RNase H. [18]. Later Nielsen and co-authors substituted the sugar-phosphate backbone of the nucleic acid to an N-(2'-aminoethyl)-glycine polyamide structure [19], which gave rise to polyamide nucleic acids (PNA). PNA are biologically stable and hybridize effectively, although they do not activate RNase H. Also, PNA are neutral molecules, which poses difficulties for solubilization and cellular uptake [20, 21]. Aside from PNA, third-generation asON are N3'-N5'–phosphoramidates (NP), in which the 2'-deoxyribose 3'-hydroxyl group is substituted for a 3'-aminogrop [22], and morpholino-oligonucleotides (MF), whose backbone is based on morpholine and a dimethylamidephosphate linker [23]. On the molecu-

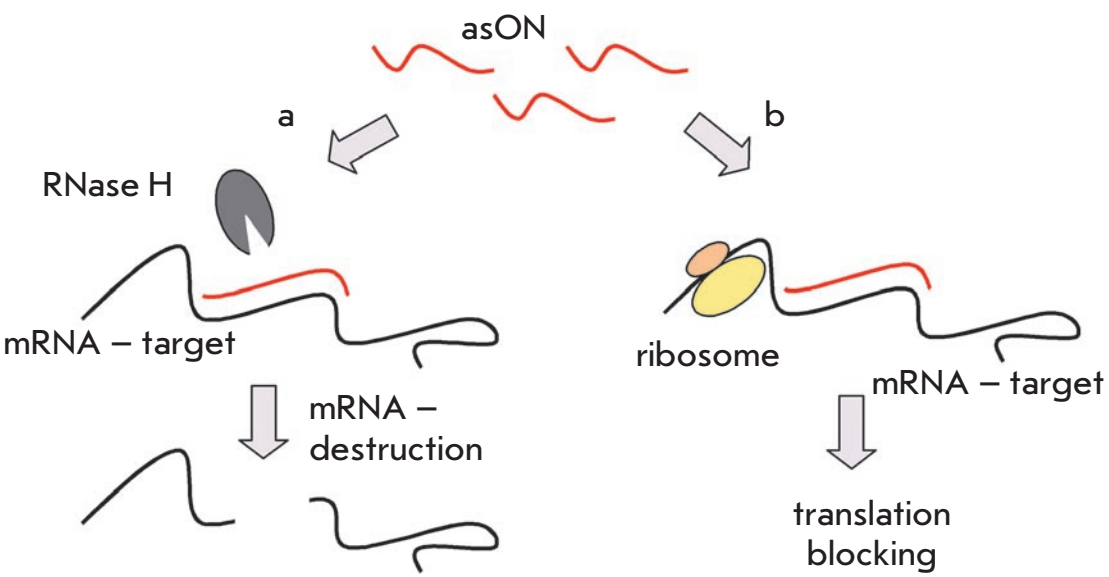

Fig. 1. How antisense oligonucleotides (asON) work. (a) RNA is cleaved as a part of a heteroduplex with the asON by RNase H. (b) Blockage of translation caused by binding of the oligonucleotide onto the mRNA

lar level, these oligonucleotides block translation by way of the asON binding to the target mRNA and/or by modulating splicing. [23]. NP and MF oligonucleotides are used primarily for developmental biology studies on zebra fish (*Danio rerio*) embryos [24].

Some of the more promising chemically modified oligonucleotides are LNAs (Locked Nucleic Acids). These are oligonucleotides with an additional structural element, a 2'-O,4'-C-methylene linker, which fixes the sugar residue in the C3'-endo-conformation [25,26]. LNA are resistant to degradation by nucleases and have a very high affinity towards nucleic acids. The promise of LNA use *in vivo* is supported by their extremely low toxicity when injected intravenously or microinjected directly into the brains of animals. [27].

RNA interference (RNAi) was first discovered on the nematode *Caenorhabditis elegans* (*C. elegans*) as a biological response to the introduction of foreign double-stranded RNA (dsRNA). This response brought on the specific suppression of the respective genes' expression (gene silencing) [28]. RNAi is an evolutionarily conserved mechanism which allows the organism to defend itself against an invasion of foreign RNA such as viruses [29, 30]. After entering the cell, exogenous dsRNA is processed into small interfering RNA (siRNA) by an intracellular ribonuclease called Dicer [31]. These siRNAs are about 21–22 nucleotides long and are incorporated into the multiprotein RISC complex (RNA-induced silencing complex). siRNA that are part of the RISC complex specifically bind to the complementary mRNA sequence, which is then degraded by the ribonuclease Argonaute 2, which is also a member of the RISC complex (Fig. 2) [30, 32]. After that, the siRNA molecules are used repeatedly to destroy more molecules of the complementary mRNA, which leads to very efficient gene silencing [32]. The specific abrogation of gene expression can be achieved by using synthetic siRNA, or siRNA enzymatically constructed *in vitro*, as well as by using short hairpin RNA (shRNA), which are expressed in the cell from DNA templates obtained by PCR or included into DNA vectors [33].

During the 1980s, catalytic RNA molecules were discovered. These molecules could cleave RNA and are called ribozymes [34]. Naturally occurring catalytic RNA are divided into large and small ribozymes. Large ribozymes include RNA which is encoded by introns of groups I and II and also the RNA subunits of RNase P. Small ribozymes are hammer-head-like ribozymes, hairpin ribozymes, hepatitis D virus ribozymes, and Varkud Satellite RNA ribozymes [35, 36]. RNA degradation by ribozymes is a 3-step process. First the ribozyme binds to a complementary sequence by forming classical Watson-Crick base pairs; then it cleaves the RNA substrate at a specific site; and, finally, it releases the degradation products (Fig. 3a) [36].

Almost all the ribozyme types are being tested as therapeutic drugs, but the hammer-head-like ribozymes are being used more, because they have been studied more extensively [35]. This ribozyme cleaves the target RNA primarily at the NUH triplet (N is any nucleotide and H is any nucleotide except guanosine), with AUC and GUC sequences being the most effective processing sites [37]. Another ri-

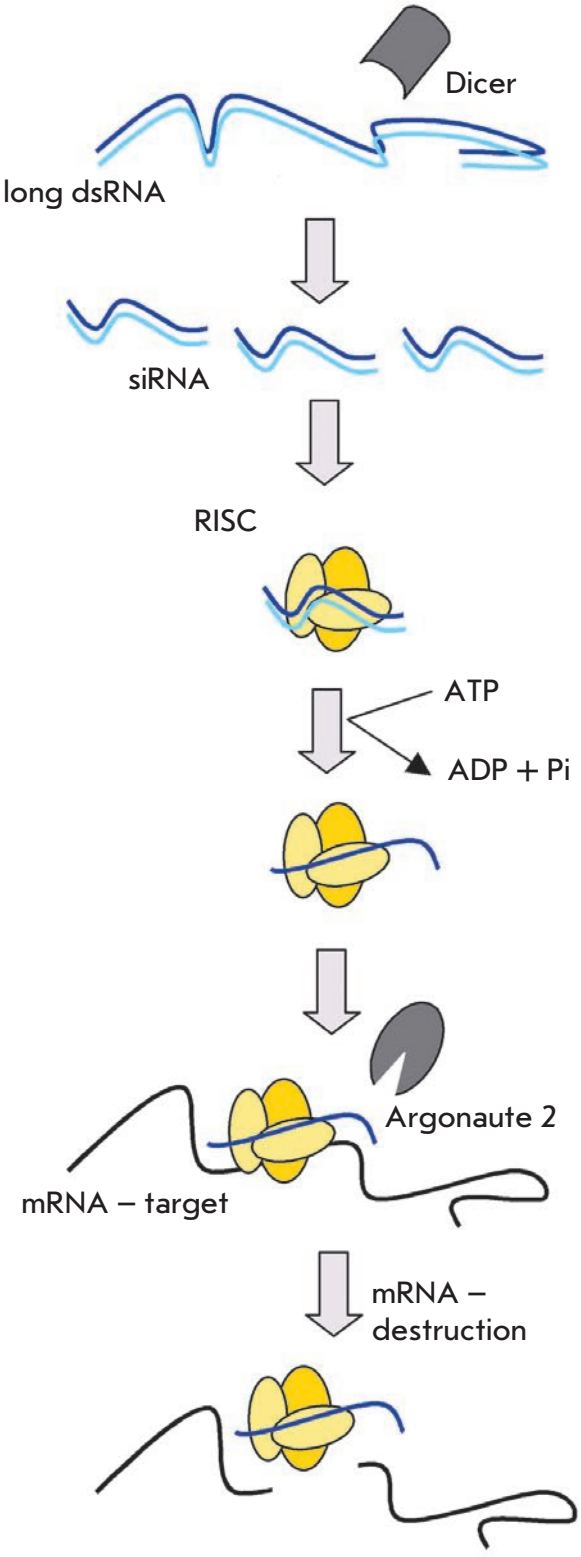

Fig. 2. How RNA interference happens

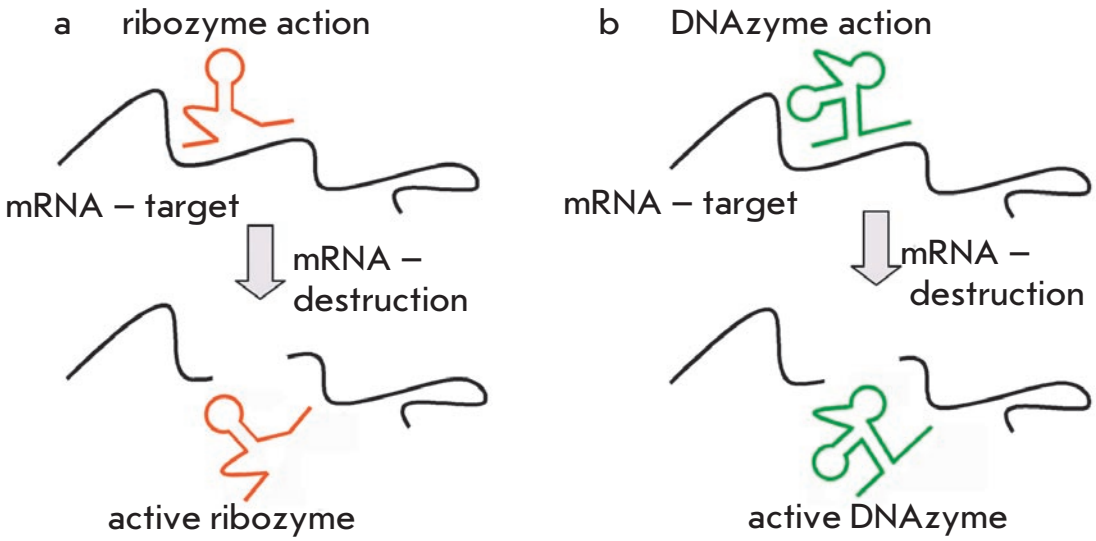

Fig. 3. Processes of ribozyme action (**a**) and DNAzyme action (**b**)

bozyme often used in therapeutic studies is the hairpin ribozyme [38]. The hairpin ribozyme cleaves the target RNA at the N*GUC sequence (N is any nucleotide).

DNA molecules which exhibit catalytic activity have yet to be discovered in nature. In 1997 Santoro and Joyce, using the SELEX *in vitro* selection procedure, obtained oligodeoxyribnucleotides that could catalyze RNA cleavage. These molecules were named deoxyribozymes or «10-23» DNAzymes [39]. «10-23» DNAzymes are single-stranded DNA molecules which have a conserved catalytic core of 15 nucleotides flanked by two variable oligonucleotide sequences. These flanking sequences facilitate the formation of a complementary complex with the target RNA. (Fig. 3b) [39]. RNA molecules are cleaved between the unpaired purine and the paired pyrimidine in the presence of magnesium ions. The most effective cleavage is achieved at the AU and GU sites.

TARGET GENES FOR DRUGS BASED ON GENE-TARGETED NUCLEIC ACIDS

A key role in carcinogenesis is played by the change in the expression levels of certain genes whose anomalous expression leads to the defective regulation of cell proliferation, apoptosis, differentiation, and invasion. [40]. At the molecular level, malignant transformation is a complicated cascade of reactions; therefore, the effects of oncogenes are often multifunctional and tightly interconnected [40]. Since oncogenes are transcription factors and components of the signal transduction machinery of the cell, they are involved in many regulatory pathways, such as cell proliferation, the inhibition of apoptosis, invasion, etc. The main target genes for gene-targeted therapy are listed in Table 1.

Firstly, malignant cell growth is based on the autonomous and unlimited proliferation of the cell clone. That is why researchers are most interested in genes which control proliferation and cell cycle progression such as *c-myc*, *ras*, genes encoding PKC-α (protein kinase C-α) and IGF-1R (insulin growth factor-1 receptor). Another effective approach would be to target the programmed cell death system by inhibiting the expression of antiapoptotic genes such as *bcl-2*, survivin, etc.

Proteins of the Ras family (K-ras, H-ras, and N-ras) are among the best studied molecules involved in transducing signals from tyrosine kinase receptors to the nucleus [41]. Overexpression or a point mutation of the *ras* gene found in certain types of oncological diseases causes the Ras protein to lose its ability to dephosphorylate; therefore, it stays constantly activated, imitating and transducing signals that stimulate proliferation and promote tumor-cell survival [42]. Genes of the Ras family are good targets for gene-targeted inhibition therapy. Notably, ribozymes have a characteristic way of inhibiting the activity of the *ras* oncogene which involves an increase in the degree of tumor cells' differentiation [43–47]. But the leader among the gene-targeted drugs which suppress *ras* oncogene expression is asON ISIS 2503. The results of phase II clinical trials for the combined use of asON ISIS 2503 and gemcitabine were announced in 2004 [48].

The important role of the *c-myc* oncogene in cell proliferation and malignant transformation was discovered in the late 1970s by Bishop [49], and this protein was among the first that were tested as a target for antisense therapy. The premier drug which regulates *c-myc* expression is a morpholine oligonucleotide asON AVI-4126, which blocks the production of the protein by steric inhibition of translation, as opposed to RNase H activation [50]. This drug has successfully passed preclinical trials and has been shown to be well tolerated by patients. It is now in the second phase of clinical trials [51, 52].

The protein kinase C gene family is a group of serine-threonine kinases which are involved in regulating vital cel-

Table 1. A list of target genes for drugs based on gene-targeted nucleic acids

Carcinogenic events	Target gene	Function	Drugs used to suppress function
Proliferation	*Ras oncogenes* (*K-ras*, *H-ras* и *N-ras*)	Part of the cellular signal transduction system and regulates a wide range of processes, such as proliferation, differentiation, and survival [42]	asON, ribozymes, siRNA
	c-myc	Activates the proliferation of tumor cells (regulates the cell cycle and telomerase activity) [49, 160]	asON, siRNA, DNAzymes
	PKC-α	Is involved in the cellular signal transduction and controls proliferation and cell survival [53, 54]	asON, ribozymes, DNAzymes
	Clusterin	Is involved in lipid transport, cell division, and apoptosis; supports cell survival in response to therapy; and increases tumor drug resistance [57, 58]	asON
	IGF-1R	Activates the MAPK and PI-3K signal pathways, which stimulate proliferation and mitogenesis and inhibit apoptosis [61–63]	asON
Blocking of apoptosis	bcl-2	Negativly regulates apoptosis by blocking the excretion of cytochrome c from the mitochondria into the cytoplasm [67]	asON, siRNA, ribozymes
	Survivin	Regulates cell division (interacts with microtubules in the mitotic spindle and promotes mitotic entry through G_2/M checkpoint) and suppresses apoptosis (inhibits the inner caspase-9-dependant apoptosis pathway) [73, 74]	asON, ribozymes
	bcr-abl	Stimulates a mitogenic and antiapoptotic signal mediated by Ras-regulated signal pathways [81, 82]	Ribozymes, DNAzymes, siRNA
	c-raf	Activates the MAPK/ERK cascade and negative regulation of apoptosis by inactivating the proapoptotic Bad protein [88, 90]	asON
Drug resistance	MDR1	Forms transmemrane channels for ATP-dependant expulsion of drugs out of the cell, which endows tumors with drug resistance [95–97]	asON, siRNA, ribozymes
	γ – glutamylcysteine syntetase (glutathione system)	Intracellular detoxication of anticancer drugs [95]	Ribozymes
Dysfunction of tumor suppressor genes	DNMT1	Hypermethylation and inactivation of tumor suppressor genes [102, 103]	asON
Increase of tumor cell lifespan	hTERT	Hyperactivation of the telomere repeat elongation machinery and, as a result, an increase in the malignancy and the lifespan of transformed cells [109]	asON, ribozymes
DNA synthesis arrest	*RRR2* or *RRM2*	Controls the amount of deoxyribonucleotides needed for DNA synthesis via regulating the conversion of ribonucleotides into deoxy ribonucleotides [113]	asON, siRNA
Tumor angiogenesis	*Flt-1* (VEGFR)	Active neovascularization and suppression of the anti-tumor immune response [119, 120]	asON, ribozymes, DNAzymes, siRNA
	neu (HER2 or ErbB2, EGFR family)	Activation of signal transduction pathways, which lead to the stimulation of tumor progression events such as proliferation, invasion, and apoptosis inhibition [127,128]	asON, ribozymes
	eIF4E	Increases the translation of growth factors such as VEGF, C-myc, surviving, etc. [133 - 135]	asON
	PTN	Is a growth factor, promotes active tumor growth and vascularization [137 - 139]	Ribozymes
	ALK	Is a tyrosine kinase PTN receptor, facilitates its function, thus promoting tumor vascularization [141]	Ribozymes
Tumor invasion	MMP9	Elimination of components of the extracellular matrix and basal membrane and promotes tumor invasion [144 – 146]	Ribozymes, siRNA
	FGF-BP	Activation of FGF-2, which induces tumor cell proliferation and increases the invasive and angiogenic potential [148]	Ribozymes
	Egr-1	Activates proliferation and tumor invasion and is involved in establishment of the MDR phenotype [154,155]	DNAzymes
	FAK	Regulates adhesion and invasion into the extracellular matrix [158]	siRNA
	CXCR4	Stimulates metastatic processes [159]	siRNA

lular functions such as differentiation, cell-cell interactions, secretion, cytoskeleton functions, gene transcription, proliferation, and apoptosis [53]. Among a dozen of isoforms of this protein, only PKC-α is shown to be involved in cell survival, proliferation and apoptosis [54]; it is also actively involved in neoplastic transformation of the cell. The best candidate for selective suppression of the tumor-specific PKC-α isoform turned out to be the thiophosphate asON ISIS 3521 (Affinitak™, USA), which selectively binds the *PKC-α* mRNA and does not interact with the other, non-oncogenic members of the PKC family [55]. This drug has been approved for clinical trials.

Clusterin was first described in 1983 as a secretory glycoprotein [56] associated with a wide variety of physiological and pathological processes, such as lipid transport, tissue transformation, cell membrane defense, apoptosis, and the complement system function [57]. Later research showed that clusterin is a chaperone-like protein which increases cell survival in response to stress [58]. The inactivation of this gene by gene-directed drugs could compromise the DNA repair-system response to external hazards, such as chemotherapy. This turned out to be true; for instance, asON OXG-011 increases the toxic effect of paclitaxel on tumor cells in mice [59] and is on the clinical path in combination with chemotherapeutic drugs [60].

IGF-1R (insulin growth factor-1 receptor) is a transmembrane protein kinase which promotes independent cell growth [61]. Anomaly in *IGF-1R* expression is well known to be connected with carcinogenesis [61]. It was demonstrated that *IGF-1R* overexpression promotes the development of P-glycoprotein- and Bcl-2-mediated multiple drug resistance (MDR) [61,63]. Suppressing the *IGF-1R* gene with a gene-targeted antisense oligonucleotide prevents tumor formation in mice in *ex vivo*[1] experiments [64], which confirms the idea that asON are promising drugs to counteract the cancer cell defense system.

The Bcl-2 protein is the major representative of a family of pro- (Bax, Bak, Bad) and anti- (Bcl-xl, Mcl-1) apoptotic factors and was first discovered in B-cell lymphoma cells in 1985 [65]. *Bcl-2* gene expression is associated with aggressive tumor behavior in response to chemo- and radiotherapy [66]. Excess Bcl-2 protein promotes the inhibition of mitochondrial membrane depolymerization, thus blocking apoptotic mechanisms which are triggered by the therapy [67]. Suppressing *bcl-2* expression with gene-targeted oligonucleotides facilitated apoptosis induction in tumor cells and increased cell sensitivity to apoptosis-inducing chemotherapeutic drugs [68, 69]. AsON G3139 showed a considerable therapeutic effect and is currently in phase III clinical trials [70–72].

Survivin is a member of the apoptosis-inhibiting protein family (IAP). Despite the fact that its precise function in the cell is yet unclear, it was shown that this protein is involved in regulating cell division and apoptosis [73]. Survivin selectively inhibits the inner caspase-9-dependant apoptotic pathway [74], and it also bypasses apoptosis mechanisms by interacting with the microtubules of the mitotic spindle, which promotes mitotic entry through the G_2/M checkpoint [75] and in turn stimulates anomalous cell cycle progression. Suppressing the survivin encoding gene with asON led straight to apoptosis induction and tumor cell death [76, 77]. The inhibitory effect of a ribozyme on the activity of the gene in the absence of additional apoptosis inducers did not affect the viability of cells [78–80]. There have been no *in vivo* studies of survivin as a target gene so far.

The chromosome translocation t(9;22) combines two independent genes – *bcr*, which is located on the human chromosome 22, and *abl*, located on chromosome 9 – and thus forms a hybrid oncogene [81]. Like the original *abl* gene, the chimeric *bcr-abl* gene shows increased kinase activity. By phosphorylating certain cell factors, BCR-ABL facilitates malignant transformation and blocks apoptosis [82]. Specifically, the appearance of *bcr-abl* can lead to myeloid or lymphoid leukemia [83]. The hybrid nature of this protein presented several difficulties in trying to affect its production. In some cases, the gene-targeting drugs suppressed not only the chimeric gene expression, but also that of the original *abl* [84]. It turned out that Maxizyme, a double ribozyme which could cleave the target mRNA at two sites, was an effective tool for circumventing this non-specificity [85]. The drug Imatinib, which specifically inhibits tyrosine kinase, was developed for preventing chronic myeloleukemia and can be used to effectively control leukemia progression [86]. However, there are known cases of the disease where the tumor is resistant to Imatinib because of point mutations in the gene or for other reasons. In such cases, RNAi methods can be helpful. Experiments using siRNA have shown that BCR-ABL+ cells can be sensitized to Imanitib by RNAi [87].

Proteins of the Raf family are serine-threonine kinases which transduce signals from a wide variety of membrane growth factor receptors to apoptosis regulators. It was determined that the functionally active Raf-1 kinase activates the MAPK/ERK pathway (mitogen-activated protein kinases/extracellular signal-regulated kinases) [88], takes part in the signaling pathways of proliferation and cell survival via NF-κB [89], and inhibits the proapoptotic Bad protein [90]. Thus, Raf-1 is at the center of a network of vital signalling pathways; thus, mutations or defective expression of the *raf-1* gene play a considerable carcinogenic role in cell transformation. In addition, Raf-1 is an effector of the protein product of the *ras* oncogene [91], which is often found to be mutated in malignantly transformed cells; this is why therapy directed at suppressing *raf-1* can prove to be effective against ras-mediated neoplasias. The most promising results of specific *c-raf* gene suppression and the corresponding antitumor effect were obtained using asON. Investigators reported the results of phase II clinical trials in 2002 using a drug based on a thiophosphate asON [92-94].

In general, about 30% of the patients who receive traditional chemotherapy develop multi-drug resistance related to the *MDR1* gene [95–97], which encodes the P-glycoprotein. P-glycoprotein is a member of the ABC-transporter protein superfamily, which uses ATP-hydrolysis to expel chemotherapeutic drugs from the cell. P-glycoprotein hy-

[1] *Here and further in the text, an ex vivo experiment is defined as tumor material being removed from the organism, treated by a gene-targeting drug in vitro, and introduced back into the organism.*

peractivity endows tumor cells with resistance to a wide variety of chemotherapeutic drugs. Because of this, inactivating the *MDR1* gene can facilitate chemotherapeutic drug retention in cells and cause their death. *MDR1* is a fairly common target for gene-targeted oligonucleotide drugs. Among these, ribozymes and siRNA are currently considered the most effective. These drugs almost entirely blocked tumor growth in mice [98, 99].

One of the most important cytostatic drug neutralizing systems of the cell is the glutathione system. Glutathione is a nonprotein thiol which has a sulfhydryl group that can interact with the reactive group of a drug and, as a result, form a conjugate of glutamine with the drug [95]. These conjugates are less reactive, more soluble, and are expelled from the cell by transporter proteins [95]. Thus, the activation of the glutathione system genes can cause tumor drug resistance [100]. To circumvent MDR caused by the glutathione system, a ribozyme that effectively restored tumor cell sensitivity to chemotherapeutic drugs was constructed [101].

Many studies have shown anomalous methylation at certain sites in the genome in tumor cells [102]. The enzyme DNMT1 (DNA methyltransferase 1) catalyses the transfer of a methyl residue from S-adenosinemethionine to the 5th position of the cytosine residues in CpG islets, affecting the expression of certain genes [103]. It was shown both that tumor cells have elevated DNA methyltransferase activity [104] and that the initiated hyperactivity of this enzyme leads to malignant transformation [105]. Furthermore, it is alleged that anomalies in methylation processes are a key factor in determining the tumors' response to chemotherapy [106]. Antisense inhibition of *DNMT1* gene expression led to the restoration of the function of tumor suppressor genes and increased tumor cell death [107]. The artificial antisense oligonucleotide MG98 is currently in phase II clinical trials [108].

The telomerase reverse transcriptase restores the telomere length by adding tandem repeats (TTAGGG) and is needed to fully replicate the ends of chromosomes [109]. It was demonstrated that the hyperactivation of *hTERT* (human telomerase reverse transcriptase) and carcinogenesis are highly correlated [110]. In order to suppress the gene's activity, several differently modified asON were constructed, including a 2'-O-methyl asON, PNA [111] and a 2'5'-oligoadenilate oligonucleotide [112]. The 2'-O-methyl asON suppressed *hTERT* expression in a cell culture by 97% [111], and the 2'5'-oligoadenilate oligonucleotide caused a 50% regression of tumors [112].

Ribonucleotidereductase catalyzes the synthesis of 2'-deoxyribonucleotides from the corresponding ribonucleoside 5'-diphosphates. This is the limiting step in the formation of 2'-deoxyribonucleoside-5'-triphosphates, precursors in DNA synthesis [113]. The R2 subunit of ribonucleotidereductase (RRR2) is synthesized in the late G_1 phase and the early S phase and is a key factor in determining the rate of DNA replication [113]. Also, it is well known that RRR2 plays a significant role in determining the malignant potential of cells by acting synergistically with certain oncogenes and being connected with the membrane protein Raf-1 and the mitogen-associated protein kinase 2 (MAPK2) [114, 115]. For this reason, the specific suppression of the *RRR2* mRNA can cause a whole array of antineoplastic effects via a wide variety of mechanisms. AsON GTI-2040, which suppressed *RRR2* expression, caused a 98% regression of renal carcinoma transplanted into mice [116]. Clinical trials showed that this drug was well-tolerated by patients [117].

In the early 70s Folkman proposed that the growth of solid tumors and metastasis are critically dependant on angiogenesis – the formation of new blood vessels from the surrounding vascular network [118]. The pathological growth of new vessels promotes solid tumor progression and metastasis. Over the last few decades, the main mediators of angiogenesis have been identified and characterized, providing researchers with novel targets for cancer therapy. Among the numerous neoangiogenic factors, the most prominent is VEGF (vascular endothelial growth factor) [119]. By activating receptors VEGFR-1 and VEGFR-2, VEGF induces the activity of intracellular signaling tyrosine kinases, which play a central role in stimulating the proliferation of endothelium cells [120]. At least 5 VEGF isoforms are generated by alternative splicing: $VEGF_{206}$, $VEGF_{189}$, $VEGF_{165}$, $VEGF_{145}$, $VEGF_{121}$ [121, 122]. It has been shown that increased angiogenesis and tumor progression are associated with the overexpression of isoform $VEGF_{165}$ [123]. Specific oligonucleotides and siRNA were developed in order to suppress the expression of the VEGF-encoding gene [124, 125]. An interesting approach towards inhibiting VEGF activity was the construction of ribozymes, and later DNAzymes, targeted at inhibiting the expression of *Flt-1*, which encodes the VEGF receptor VEGFR-1, and the *KDR* gene, encoding VEGFR-2 [126]. Among all the proposed strategies of VEGF inhibition, this approach proved to be the most effective, and the ribozyme-based drug Angiozyme, targeting the *Flt-1* gene, is currently in phase II clinical trial [35].

The protooncogene *neu*, also known as *HER-2/erbB-2* or *NGL*, encodes a transmembrane receptor that exhibits tyrosine kinase activity, which is important for intracellular signal transduction [127]. Normally, the HER-2 protein is not produced in most human tissues, and in neoplasias this receptor exhibits tyrosine kinase activity even when there is no ligand to activate it [128]. The overexpression of HER-2 in carcinogenesis is often attributed to the amplification of the corresponding gene [129]. The recently developed drugs Herceptin and Rituxanar are based on monoclonal antibodies that bind the HER-2 receptor, but clinical trials showed some negative side-effects, the worst being cardiotoxicity [130, 131]. This is why the gene-targeted therapy of HER-2-mediated neoplasias looks so promising. Of all the drugs based on nucleic acids and used to suppress HER-2 activity, the drug Herzyme, based on a hammer head ribozyme, is currently in clinical trials. Phase I clinical trials showed that the drug is well tolerated by patients [132].

The eukaryotic translation initiation factor 4E (eIF4E) binds to the capped 5' terminus of cellular mRNAs and delivers them into the eIF4E translation initiation complex. This complex reads the mRNA sequence in the 5'-3' direction and unwinds the secondary mRNA structure in the 5'-untranslated region, thus uncovering the translation start codon and promoting ribosome binding [133, 134]. In normal

conditions, eIF4E activity is down-regulated by a specific eIF4E- binding protein 4E-BP (4E-binding protein). Malignant transformation is often accompanied by eIF4E overexpression or by the phosphorylation of 4E-BP. This leads to the release of an active eIF4E which forms the eIF4E translation complex [135]. Notably, many researchers have shown that hyperactive eIF4E in tumors mostly enhances the translation of proteins which are involved in tumor progression such as Bcl-2, survivin, cyclin D1, C-myc, and VEGF [133, 134]. Because of this, the specific suppression of eIF4E activity can turn out to be very useful in inhibiting tumor progression. An asON complementary to eIF4E showed good results. When injected into tumor-bearing mice, it caused a 10-fold regression of the tumor and had no noticeable side effects [136].

Pleiotropin (PTN) is a secreted growth factor which is produced in large quantities during the development of the nervous system and "turned off" in adults [137], except in some cancer patients [138]. PTN is an active mitogen for fibroblasts and epithelial cells [137, 138]. Also, it can induce the release of active proteolytic enzymes from endothelial cells [139]. These data point to the potentially crucial role of PTN in angiogenesis. In order to suppress the expression of *PTN* in tumor cells, a ribozyme complementary to the *PTN* mRNA was constructed. It showed considerable antitumor and antimetastatic activity [140]. Moreover, it was recently discovered that the inhibition of the expression of anaplastic lymphoma kinase (APK), which causes the development of anaplastic lymphoma [141] and functions as a pleiotropin receptor [142], did not only cause tumor regression, but also caused a two-fold increase in mean survival time in mice [143].

Tumor progression is accompanied by the tumor's ability to spread beyond the boundary of its own tissue and to continue to grow into nonrelated tissues. Modulating the expression of genes which are involved in stimulating migration and invasion by means of gene-targeted drugs is a strategy that is often used by researchers. Matrix metalloproteinase-9 (MMP9) can initiate the degradation of certain components of the extracellular matrix and the basal membrane (collagens IV and V, elastin, entactin, casein, and galectin) [144, 145], which promotes the epithelial-mesenchymal transition of tumor cells and stimulates metastasis [146]. The suppression of metalloproteinases by ribozymes partially abrogates metastasis and increases the mean survival time of tumor-bearing mice, but it does not cause tumor regression [147].

The fibroblast growth factor (FGF) is interesting to researchers because it is a powerful mitogen which induces differentiation and angiogenesis during development and also stimulates tumor cell invasion [148]. Normally, adults produce only a small quantity of FGF, but during certain oncological diseases, FGF production is elevated [149]. Secreted FGF binds tightly to heparan sulphate proteoglycans in the extracellular matrix, thus blocking FGF activity [150]. One of the mechanisms of FGF release is binding to FGF-BP (FGF-binding protein), which mobilizes and activates FGF [150]. Studies have shown that FGF-BP is expressed in certain carcinomas [151] and also promotes the conversion of nononcogenic FGF-expressing cell line SW-13 to oncogenic and angiogenic phynotype [150]. A ribozyme designed to suppress the FGF-BP gene expression effectively abrogated tumors in mice [152].

The early growth response factor-1 (EGR-1) is a typical representative of a family of transcription factors which possess a "zinc-finger" structural domain [153]. EGR-1 activity is induced by a number of external and intracellular stimuli such as growth factors, cytokines, ultraviolet light, ionizing radiation, etc [153]. It has been shown that EGR-1 is involved in multiple regulatory pathways in tumor cells. Its activity is involved in the development of malignant transformation [154], in the regulation of *MDR1* gene transcription [155], and in the negative response to estrogen in mammary gland carcinoma [156]. In order to suppress EGR-1 gene expression, a DNAzyme, which caused a 3-fold decrease in tumor size in mice, was designed [157].

The focal adhesion kinase (FAK) is a non-receptor tyrosine kinase, located in integrin clusters, through which the cytoskeleton interacts with proteins of the extracellular matrix (focal adhesion sites). FAK receives signals from growth factors and adhesion factors and transmits them into the cell. FAK is an important mediator of signal transduction pathways, regulating proliferation, migration and cell viability and it is often overexpressed in tumor cells. siRNA effectively suppresses FAK activity and tumor growth in mice [158].

In mammary gland tumors, the transformed cells express the chemokine receptor CXC (CXCR4), which causes metastasis into organs containing a lot of CXCR4 ligands. The inhibition of CXCR4 expression with siRNA suppresses the adhesive and invasive properties of tumor cells [159].

APPLICATION GENE-TARGETED NUCLEIC ACID DRUGS IN TISSUE CULTURES, EXPERIMENTAL ANIMAL MODELS AND CLINICS

Drugs based on nucleic acids have attracted the attention of researchers for a long time, being potentially useful for gene-targeted cancer therapy due to their ability to interact with the key pathways of carcinogenesis. Table 2 sums up the main results of *in vitro* studies in this area and Table 3 combines the data of preclinic *in vivo* tests and clinical trials. In this section, we describe the development of drugs based on gene-targeted oligonucleotides which specifically inhibit the functions of target genes involved in carcinogenesis.

Ras

In vitro. The established location of point mutations in the *ras* oncogene mRNA allows the development of oligonucleotides specifically targeted at the mutated sites in the mRNA target. Such drugs efficiently switch off oncogene expression. The first drug developed for *ras* oncogene suppression was a thiophosphate olignucleotide asON (now known as ISIS 2503) targeted at the initiation codon of *H-ras* mRNA [161]. ISIS 2503 treatment of cervical carcinoma HeLa cells transfected with a plasmid encoding a gene for *ras*-luciferase fusion protein led to 98% suppression of the reporter gene. In a study by Chinese researchers, treatment of human hepatoma cells by a thiophosphate asON for 5 days caused an 87.8% inhibition of tumor cell growth [162]. Additionally, a blockage of H-ras-dependant entry of tumor cells into the S-phase of the cell cycle was observed, and

DNA fragmentation detected in the treated cells indicated the initiation of apoptosis [162].

The antitumor potential of ribozymes targeted at Ras family genes is being actively investigated. In the melanoma, throat carcinoma and bladder tumor cell models, several research groups have demonstrated that H-ras ribozymes induced apoptosis, inhibited the proliferation of tumor cells, and helped reestablish cell differentiation [44–47].

An alternative approach to the suppression of Ras-family gene expression uses RNAi technology. Retrovirus-mediated expression of siRNA targeted at *H-ras* and *K-ras* mRNA effectively suppressed the synthesis of these proteins in ovarian and pancreatic carcinoma cells [163, 164]. The tumor proliferation activity decreased as the cells accumulated in the G_0/G_1 phase of the cell cycle, their proportion reaching 66.2% [163] and the number of apoptotic cells increasing from 4% to 21% [163]. Zhang and coauthors used an adenoviral system of K-ras-siRNA delivery into cells and obtained an 80% decrease in the amount of K-ras protein in lung tumor cells, along with the suppression of tumor-cell proliferation [165].

In vivo. The transfection of hepatocellular carcinoma cells by *H-ras* asON produced a decrease in the average tumor weight in mice [162, 166] and inhibited metastasis [166]. The antitumor efficiency of asON ISIS 2503 in mice with prostate tumors increased upon the addition of LNA nucleotides into the oligonucleotide sequence [167]. AsON ISIS 2503 was approved for clinical trials. In a phase I trial, the patients received 10 mg per kg asON ISIS 2503 injections for 14 days [168]. After a one week recess, the injection course was repeated. AsON ISIS 2503 did not display any marked toxicity and prevented the further progression of the disease. The results of phase II trials, performed on patients suffering from pancreatic adenocarcinoma have established that combined treatment by asON ISIS 2503 and Gemcytabine is well tolerated and demonstrated a positive response to treatment in 10.4% of patients [48].

The use of anti-H-ras ribozymes *in vivo* led to a significant retardation of tumor growth in mice and to a decrease in their invasive potential, as well as a two-fold increase in mouse lifespan [43–45]. Kijima and coauthors developed a ribozyme targeted at codon 12 of the mutant K-ras gene (GGT triplet substituted for GTT) and obtained a recombinant adenovirus expressing this ribozyme [169]. An intratumor injection of this drug into athymic mice with a transplanted pancreatic carcinoma caused tumor regression in 68% of mice [169].

In vitro treatment of tumor cells with a retroviral vector containing siRNA targeted at *K-ras и H-ras* mRNA caused a complete inhibition of pancreatic carcinoma growth and 80% inhibition of ovary tumors in mice [163, 164]. A one-time intratumor injection of adenoviral siRNA targeted at *K-ras* caused a 45% inhibition of lung tumor development, and multiple injections completely stopped tumor growth in 8 out of 10 mice. In these experiments, the apoptotic activity of tumor cells showed a 2.8-fold increase [165].

C-myc

In vitro. The first drug developed for specific suppression of the *c-myc* protooncogene was a phosphodiester, asON, which caused a 50% decrease in the protein level in leukemia cells and inhibited their proliferation by 50% after 5-day incubation with the olignucleotide [170]. Watson *et al.* developed a thiophosphate asON which demonstrated a more prolonged (up to 9 days) and effective (75%) inhibition of breast cancer cells proliferation and caused a 95% inhibition of estrogene-induced overexpression of *c-myc* gene [171]. The next step involved the substitution of the thiophosphate backbone for a morpholino-phosphorodiamidate one. Such an anti-*c-myc*-asON not only caused a decrease in the protein level, but also a complete G_0/G_1 cell cycle blockage [172].

A "hammer head" type ribozyme was developed in order to suppress *c-myc* activity. Transfection by a retroviral vector encoding the ribozyme led to a 1.7-fold decrease of the protein level in hepatoma cells and a 1.85-fold decrease in the proliferation potential of the cell [173].

The ability to suppress C-myc protein hyperactivity was evaluated for gene-targeted siRNA drugs. It was shown that siRNA caused a 60–92% decrease in the mRNA level and a 55–83% decrease in C-myc protein synthesis [174, 175]. The partial abrogation of *c-myc* expression was associated with a 2.5-fold suppression of cell growth in human epidermoid carcinoma KB-3-1 and with a complete proliferation blockage in SK-N-MC neuroblastoma [175]. In order to improve the stability and facilitate intracellular delivery, a special poly-DNP-RNA (poly-2-O-(2,4-dinitrophenyl)-oligoribonucleotide) was designed. This drug lowered the *c-myc* mRNA level to 15% in mammary and lung adenocarcinoma tumor cells [176].

In vivo. *In vivo* experiments showed that AVI-4126 (AVIBioPharma, United States), a morpholino-oligonucleotide developed for inhibiting *c-myc* expression, causes an 80% decrease in prostate tumor growth in athymic mice [50]. This drug is currently in phase II clinical trials [52]. Phase I trials showed that AVI-4126 had no serious side effects for healthy people who received a single intravenous injection of AVI-4126 with a dosage of 90 mg [51]. Also, AVI-4126 was assessed for accumulation in the prostate and mammary tumor tissues of patients who were injected with 90 mg of the drug (the test was performed 24 hours after the injection using surgically removed tumors) [51].

The inhibition of *c-myc* expression by RNAi looks promising in preclinical trials. Breast cancer cells transfected with a plasmid encoding anti-c-myc-siPHK did not give rise to tumors when transplanted into mice [177]. In transgenic mice with developing lymphoma, real-time RT-PCR detected a 15%–20% decrease in *c-myc* mRNA in the plasma of mice treated by poly-DNP-RNA [176].

PKC-α

In vitro. In order to inhibit the expression of the *PKC-α* gene, Dean *et al.* performed a thorough study of the efficiency of 20 thiophosphate asON and their 2'-O-methyl analogs [55]. The most effective oligonucleotide (known under the commercial name ISIS 3521) caused a 90–95% decrease in the level of *PKC-α* mRNA, but its 2'-O-methyl derivative did not affect the expression of the *PKC-α* gene, which indicates that RNAse H activity is required [55].

In the glioblastoma model, the inhibitory potential of an anti-PKC-α ribozyme was evaluated. A 73% decrease

Table 2. Results of nucleic acid-based drugs testing *in vitro*

Target-genes	Drug	Tumor type	Effect
H-ras/K-ras	asON	Cervical carcinoma [161], hepatoma [162]	A decrease in H-ras-luciferase-mRNA level by 98% [161]; inhibition of cellular growth by 87.8%, block of the entry into the S-pahse of the cell cycle, apoptosis induction [162]
	Ribozyme	Melanoma, throat carcinoma, bladder cancer	Decrease in *H-ras* expression; retardation of proliferation and an increase in the level of differentiation of tumor cells [43–47]
	siRNA	Ovarian, pancreatic [163], lung [165] carcinoma	80% decrease in the protein level [165], suppression of proliferation [163,164], changes in the cell-cycle schedule, and increased number of apoptotic cells [163]
c-myc	asON	Leukemia [170], breast cancer [171]	50%–95% decrease in *c-myc* expression [170, 171]; complete cell cycle arrest in the G_0/G_1 phase [172]
	Ribozyme	Hepatoma	1.7-fold decrease of the protein level and 1.85-fold drop in proliferative activity [173]
	siRNA	Epidermoid carcinoma, neuroblastoma [175], breast cancer and lung adenocarcinoma [176]	60–92% decrease in mRNA level and 55–85% inhibition of protein synthesis [175,176]; slowing and blockage of cell division [175]
PKC-α	asON	Lung carcinoma	90–95% decrease in *PKC-α* mRNA level [55]
	Ribozyme	Glioblastoma [178], prostate carcinoma [179]	Decreases protein level by 73% and proliferative activity below 90% [178]; restores sensitivity to cisplatin [179]
Clusterin	asON OGX-001	Renal carcinoma	Decreases clusterin mRNA level by 64% and increases cell sensitivity to paclitaxel by 80% [59]
IGF-1R	asON	Bladder cancer	Decrease of mRNA level by 74% and protein level by 61.3% [207]
bcl-2	asON G3139 (Genasense™, USA)	Lymphoma [183], leukemia [68, 69]	Decrease of *bcl-2* mRNA level and Bcl-2 protein level by 60–80% and 80–95%, respectively, hence increasing cell death rate by 76–90%; as a result of apoptosis induction, increases doxorubicin senstivity [68, 69, 183]
	Ribozyme	Lymphoma	5-fold decrease in mRNA level, 3-fold decrease in protein level, and 2-fold increase in apoptosis rate [184]
	siRNA	Cervical [185] and pancreatic [189] carcinoma	Suppresses Bcl-2 protein synthesis by 90%, induces apoptosis in 50% of cells [185]; increases proportion of apoptotic cells by 37% [189]
Survivin	asON	Malignant lung mesothelioma, glioma, breast cancer, lung adenocarcinoma [76], thyroid cancer [77]	7-8- fold increase in caspase-3 activity, induction of apoptotic cell death in 42.5% of cells [76]; decrease of the mRNA level by 75% and protein level by 73%, inhibits cell proliferation by 53%, 11-fold increase in the proportion of apoptotic cells [77]
	Ribozyme	Melanoma [78, 79], breast cancer [80]	Decreases mRNA and protein levels by 75% and 74% respectively, increases tumor cell sensitivity to chemo- and radio-therapy, no effect without an additional apoptose inducing stimulus [78 - 80]
bcr-abl	asON	Chronic myeloid leukemia	Complete inhibition of cell growth, apoptosis induction [208]
	Maxizyme	Chronic myeloid leukemia	95% decrease in the chimeric gene mRNA, apoptosis induction, tumor cell growth retardation [85]
	siRNA	Chronic myeloid leukemia	Suppression of BCR-ABL-associated cell growth, 4-fold increase in tumor cell sensitivity to imanitib [87]
	DNAzyme	Chronic myeloid leukemia	Suppresses protein production by 40-75% [208]
c-raf	asON	Lung, colon, prostate[190, 191], ovary [192, 193] cancer	100% suppression of C-raf protein, 80% inhibition of cell proliferation [190 - 192]; growth suppression in various ovary carcinoma lines by 10% to 90% [193]
	siRNA	Bladder cancer	Decrease of protein level by 37.5% [194]
MDR1, mdr1a/ mdr1b	asON	Colon adenocarcinoma [211], epidermoid carcinoma [212]	Complete MDR phenotype reversal, increases accumulation of doxorubicin in cells 6.4-fold, promotes cell death [211, 212]
	siRNA	Human epidermoid carcinoma [215], ovary cancer cells" на "human pancreatic cancer and gastric carcinoma [217], ovarian cancer cells, ovary cancer cells [218], murine lymphosarcoma [219]	*MDR1* mRNA level is down by 91% and the P-glycoprotein by 72%-83%, increases cell sensitivity to vinblastin [99, 215], duanorubicin [217] and paclitaxel [218]
	Ribozyme	Liver cancer	Reverses MDR phenotype, increases cell sensitivity to vincristin [214]
Glutathine	Ribozyme	Colon cancer	Increases tumor cell sensitivity to chemotherapeutic drugs [101]
DNMT1	asON MG98	Lung and bladder cancer	Restores *p16* function, promotes accumulation of hypomethylated form of retinoblastoma protein, inhibits proliferation [107]
hTERT	asON	Bladder cancer [111, 112]	Decreases the protein level by 97%, increases cytostatic drug sensitivty, causes 3-fold increase of proportion of apoptotic cells, activates caspase-3 [111, 112]
	Ribozyme	Breast cancer	Reduces the length of the telomere tandem repeat region from 5.5 kbp to 3.5 kbp and reduces cell growth rate [224]
RRR2	asON GTI-2040 (Genasense™, USA)	Lung, bladder carcinoma, fibrosarcoma	Results in total disappearance of R2 subunit mRNA
	siRNA	Pancreatic adenocarcinoma	Increases tumor cell sensitivity to gemcytabin [198]
VEGF, *Flt-1* (VEGFR1), *KDR* (VEGFR2)	asON	Breast and bladder cancer	Decreases VEGF level by 45–83% and lowers cell survival [124]
	siRNA	Ovarian, cervical cancer, osteosarcoma	Reduces *VEGF* expression by 33–53% [125]
	Ribozyme Angizyme, Sirna Ther., USA	Lung and colon carcinomas, breast cancer	Causes specific cleavage of RNA-substrate and effectively decreases mRNA level in cell culture [199]
	DNAzyme	Breast cancer	Decreases VEGFR-2 level by 90% and cell survival by 34–65% via inducing apoptosis [200]
neu (HER-2/ erbB2)	asON	Ovarian and breast cancer	Additive inhibition of tumor cell proliferation in combination with doxorubicin [205]
	Ribozyme Herzyme	Ovarian and breast cancer	Lowers *neu* mRNA levels by 40–60%, thus inhibiting cell growth [131]
eIF4E	asON LY2275796	Non-Hodgkin lymphoma, lung, bladder, colon, prostate and breast cancer	Decreases eIF4E protein level by 80%; lowers protein levels of Bcl-2, survivin, cyclin D1, C-myc and VEGF; and induces apoptosis [136]
PTN и *ALK*	Ribozyme (anti-PTN)	Melanoma	Decreases *PTN* mRNA level by 75% [140]
	Ribozyme (anti-ALK)	Glioblastoma	Decreases PTN activity [143]
MMP9	Ribozyme	Prostate cancer	Causes complete degradation of *MMP9* mRNA [220]
	siRNA	Juvenile osteosarcoma	50% decrease in cell migration [221]
FGF-BP	Ribozyme	Prostate and colon carcinoma [152, 222]	80% suppression of FGF-BP protein synthesis; slowing down of tumor cell proliferation [152, 222]
EGR-1	DNAzyme	Breast cancer	6-fold decrease of protein level, blocking of proliferation, and 3-fold drop in tumor cell invasion activity [157]
FAK	siRNA	Prostate and breast cancer	Inhibits tumor cell adhesion, migration, and proliferation [158]
CXCR4	siRNA	Breast cancer	Inhibits cell migration and invasion by more than 70% [225]

in the protein level after ribozyme treatment was demonstrated, and proliferative activity of the tumor cells was down by 90% as compared to 50% after treatment with a control ribozyme [178]. In another study, a PKC-α-targeted ribozyme re-established prostate carcinoma cells' sensitivity to cisplatin-induced apoptosis, increasing its rate 2.6–3.2-fold [179].

In vivo. Intravenous injections of ISIS 3521 to mice with three different heterotransplants (lung carcinoma, bladder, and colon cancer) caused complete tumor growth suppression in mice at a comparatively low dosage of 0.06–0.6 mg/kg [55]. In phase I clinical trials of asON ISIS 3521, several different treatment schedules were investigated. The main cause of toxicity was thrombocytopenia and fatigue [180]. In phase II trials with a recommended treatment schedule of 2 mg/kg/day for 3 weeks, an objective treatment response was documented for one patient with ovarian carcinoma, and 2 patients with ovarian carcinoma displayed tumor regression [181]. However, the treatment of patients with metastatic colon carcinoma did not produce any statistically significant responses [182].

CLUSTERIN

In vitro. In the inhibition of clusterin expression, thiophosphate asON affected a 64% decrease in gene expression and an 80% increase in paclitaxel sensitivity in renal carcinoma [59].

In vivo. 2'-methoxyethyl-modified thiophosphate asON OXG-011 combined with paclitaxel caused a two-fold drop in the volume of renal carcinoma in mice [59]. Phase I of the clinical trials of asON OXG-011 at the dose of 640 mg reduced clusterin levels in human tumor tissue [60]. Currently, the therapeutic potential of asON OXG-011 combined with chemotherapy is being investigated in phase II clinical trials.

Bcl-2

In vitro. Anti-mRNA drugs targeted at the antiapoptotic Bcl-2 protein emerged as undisputed leaders among the gene-targeted oligonucleotides used for cancer treatment. An 18-bp phosphodiester asON, complementary to the first 6 codons of the open reading frame of *bcl-2* mRNA, was developed by Kitada and coauthors. This oligonucleotide almost completely blocked Bcl-2 protein synthesis in lymphoma cells [183]. Reed *et al.* compared the inhibitory effects of phosphodiester and thiophosphate oligonucleotides complementary to *bcl*-2 mRNA on the growth of *bcl-2*-expressing leukemia cells [68]. It turned out that a detectable inhibitory effect of the phosphodiester asON could be observed in about half the time needed to develop a comparable effect of the thiophosphate analog. However, the latter was more effective in suppressing the growth of tumor cells. The thiophosphate asON had the same effect as the phosphodiester asON at about a 5- to 10-time lower concentration [68]. It was shown that an 80–95% reduction in Bcl-2 protein synthesis after thiophosphate asON treatment elevates the apoptosis rate and increases doxorubicin sensitivity [69].

Luzi and coauthors [184] developed a chemically modified ribozyme targeted at *bcl-2* mRNA. The lipotransfection of this drug into human Raji lymphoma cells led to a 5-fold drop in the *bcl-2* mRNA level and to a 3-fold drop in the protein level, which was associated with a significant increase in the proportion of apoptotic cells [184].

Fu *et al.* used *bcl-2* siRNA to suppress Bcl-2 synthesis by 90% in cervical tumor cells HelaB2 and BGC-823, which led to apoptosis induction [185].

In vivo. The decrease of the Bcl-2 protein level after treatment with G3139 asON, which was targeted at the respective gene's mRNA, was associated with the suppression of the oncogenic potential of lymphoma cells and a complete blockage of tumor growth in mice [186]. The use of G3139 in combination with cisplatin increased the anticancer chemotherapeutic effect by 70% [187].

Recently, Morris *et al.* [188] reported the results of phase I clinical trials of an 18-bp thiophosphate asON G3139 (Genasense™, United States), which were complementary to the first six codons of the *bcl-2* open reading frame. Its was shown that, after seven days of daily intravenous infusions at a dose of 6.9 mg/kg, patients with non-Hodgkin lymphoma registered minor side effects, such as fatigue and a reversible increase of transglutaminases in the blood serum. Subcutaneous injection of the drug turned the cancer process onto a stable, non-progressive mode in 9 out of 21 patients with non-Hodgkin lymphoma, and improved the quality of life in 3 patients (a total objective response in 57% of patients). In September 2000, the phase III trial of asON G3139 was launched on patients with chronic lymphatic leukemia and acute myeloid leukemia [70]. The clinical trials of this drug's combinations with various chemotherapies for melanoma and prostate carcinoma in patients resistant to hormone therapy are now in progress [71, 72]. In February 2001, in 65 oncological clinics in the United States, Canada, and Great Britain, a phase III clinical trial of asON G3139 was also launched for patients with multiple myeloma.

Tumor-bearing mice, which recieved *bcl*-2 siRNA treatment, displayed a retardation of liver tumor growth by 66.5% [185]. Mice with heterotransplants of pancreatic tumors registered a 56% decrease in tumor volume [189].

Raf-1

In vitro. The 20-bp thiophosphate asON ISIS 5132 oligonucleotide is targeted at the 3′-nontranslated region of *c-raf* mRNA. This oligonucleotide effectively inhibited *c-raf* mRNA accumulation and decreased the protein level in lung carcinoma and colon and prostate tumor cells [190]. The addition of 2'-methoxyethyl modifications into the oligonucleotide asON ISIS 13650 designed for *c-raf* suppression did not lead to a significant increase of the inhibitory potential [191]. In ovarian carcinoma cells, ISIS 5132 and ISIS 13650 induced 100% Raf-1 suppression and an 80% drop in cell proliferation [192]. Also, anti-*c-raf* asON ISIS 5132 and ISIS 13650 were tested on 15 ovarian carcinoma cells lines. The proliferation suppression efficacy varied from 10% to 90%. Growth inhibition was associated with apoptosis and the accumulation of cells in the G_2/M and S phases of the cell cycle [193].

The comparison of *c-raf* suppression efficiency of asON and siRNA, which targeted the same region of mRNA, has established that 125 nM of oligonucleotide caused a 52.4% decrease in the Raf-1 protein level, while the siRNA caused only a 37.5% drop [194].

In vivo. Oligon ucleotide ISIS 5132 demonstrated a pronounced antitumor effect in mice with ovarian carcinoma heterotransplants [192]. The results obtained in *in vitro* and *in vivo* experiments helped advance the studies of ISIS 5132 anticancer activity to clinical trials. A phase I trial demonstrated that the drug was tolerated well by patients and caused only a short period of thrombocytopenia in a few cases [195]. A low toxicity treatment schedule was devised which featured the slow intravenous infusion of the drug at a daily dose of 2mg/kg in 21-day courses with a one week break in between [195]. In the phase II clinical trial, the use of this treatment scheme for patients with prostate cancer [92], ovarian cancer [93], and colon adenocarcinoma [94] demonstrated the stabilization of the cancer process in approximately 25% of the cases.

DNMT1

In vitro. The specific inhibition of the DNA-methyltransferase DNMT1 in cancer cells was achieved by the use of a 2'-O-methyl thiophosphate asON MG98. The suppression of DNMT1 by an asON results in the demethylation of the *p16* gene promoter, the reestablishment of its activity, the accumulation of cells with a hypomethylated retinoblastoma gene, and the inhibition of cancer cell proliferation [107].

In vivo. *In vivo* experiments with asON MG98 demonstrated a significant growth retardation and regression of intestine carcinoma and non-small cell lung cancer heterotransplants. Successful preclinical studies insured the use of MG98 in clinical trials [196]. The phase I clinical trial was focused on evaluating the toxicity and establishing a pharmacological profile of asON MG98. Intravenous administration of the drug at a daily dose of 80 mg/m^2 to patients with various solid tumors for 21 days every 4 weeks proved to be relatively safe [196]. However, no significant antitumor effect was observed. Higher doses of the drug administered according to the above-mentioned scheme were not tolerated well by patients [196, 197]. In the phase II clinical trial, an improved treatment scheme was tested on patients with metastatic renal carcinoma. The dosage of 360 mg/m^2 was administered twice a week for three weeks [108]. However, this treatment schedule did not yield any positive response. The authors argued that the clinical failure was due to inappropriate choice of tumor type [108].

RRR2

In vitro. The study of the asON GTI-2040 targeted at RRR2 mRNA demonstrated a complete abrogation of RRR2 mRNA accumulation in human lung carcinoma and significantly decreased its amount in human bladder and murine fibrosarcoma tumors [116].

Duxbury *et al.* studied the ability of RRR2 siRNA to increase the gemcytabine sensitivity of human pancreatic adenocarcinoma cells implanted into mice via suppressing the RRR2 subunit synthesis. Specific siRNA molecules targeted at RRR2 mRNA significantly increased gemcytabine-induced cytotoxicity [198].

In vivo. *In vivo* experiments demonstrated that anti-RRR2 siRNA, in combination with gemcytabine, yield a synergistic antitumor antimethastatic effect [198].

The inhibitory potential of GTI-2040 was evaluated in animal experiments. GTI-2040 suppressed tumor growth in all experimental models, and the maximal effect was observed in the renal carcinoma model, where a 95–98% regression in the tumor was demonstrated [116]. A study of asON GTI-2040 in phase I clinical trials yielded a recommended treatment schedule with the daily administration of 185 mg/m^2/day for 21 days repeated every 4 weeks. Monotherapy according to this schedule did not cause any serious side effects [117].

VEGF

In vitro. *In vitro* experiments demonstrate that a thiophosphate asON targeting *VEGF* mRNA can reduce VEGF synthesis by 45–83% in breast and bladder cancer cell lines [124].

An RNAi approach was also assessed for the efficacy of *VEGF* expression inhibition. Vector delivery of siRNA into tumor cells caused the prolonged suppression of VEGF synthesis by 33–53% [125].

In order to therapeutically interfere with pathological angiogenesis, as an alternative strategy it was proposed to target the VEGFR-1 and VEGFR-2 receptors, but not VEGF itself. With this in mind, ribozymes complementary to regions of *Flt-1*(VEGFR-1) and *KDR* (VEGFR-2) were designed [199]. It was shown that these ribozymes specifically cleave RNA substrates *in vitro* and efficiently decrease the mRNA level in cell cultures. Currently, studies of the effect of DNAzymes on VEGFR-2 function are being published. Zhang and coauthors demonstrate a 90% decrease of VEGFR-2 protein level along with a 34–65% drop in the viability of breast cancer cells due to apoptosis induction [200].

In vivo. Experiments *in vivo* demonstrated that VEGF inhibition by thiophosphate asON led to a 5-fold growth retardation of renal carcinoma in mice [201].

In order to prolong the action and improve the drug permeability into the tumor cells, VEGF- targeted modified siRNA were designed. An intratumor injection of cholesterol oligoarginine-siRNA conjugate provided a 10-fold decrease in the growth rate of colon adenocarcinoma [202], and injecting an siRNA complex with a water-soluble lipopolymer led to a 1.5-fold growth retardation of prostate adenocarcinoma [203]. In these experiments, a notable decrease in tumor vascularization and reduction of VEGF expression were also observed.

In preclinical trials, the *Flt-1*-targeted ribozyme exerted antitumor, antiangiogenic and antimetastatic effects in a metastatic lung cancer model [199]. Mice with grafted Lewis lung carcinoma were surgically implanted with mini pumps infusing the ribozyme at a rate of 12-100mg/kg daily. After 19 days, the mini pumps were removed and new ones installed. After treatment, a 92% tumor regression and a 70–80% reduction of lung metastasis were observed [199]. In mice with grafted intestinal carcinoma, the number of metastases after treatment with anti-Flt-1 ribozyme decreased 3-fold [199]. This ribozyme was named Angiozyme (Ribozyme Pharmaceuticals, United States) and is now being evaluated in phase I and II clinical trials in patients with various cancer types. Phase I trials were concluded in June

2001 and demonstrated good tolerance and disease stabilization in 25% of patients [204]. Phase II trials in patients with malignant forms of colon and breast cancer were aimed at evaluating Angiozyme monotherapy and combinations with traditional chemotherapeutic agents [35]. It was shown that Angiozyme decreased the levels of soluble VEGFR-1 in serum, but no significant clinical response was demonstrated. These data underscore the importance of combining gene-targeted and conventional chemotherapy. Promising results were obtained in studies involving patients suffering from colon tumors and featuring the simultaneous use of Angiozyme with the Saltz therapeutic protocol (a combination of bolus 5-fluoruracil, leucovorin, and irinotecan). This approach led to disease progression in only 12.5% of the cases, as opposed to 25% in chemotherapy-only patients [35].

Interesting results were obtained *in vivo* with a DNAzyme complementary to *KDR* (VEGFR-2) mRNA. After four injections of anti-VEGFR2 DNAzyme, a 75% regression of breast cancer was observed [200]. The antiangiogenic action of the DNAzyme reduced the vascularization of the tumor tissue and therefore promoted cell death in the tumor periphery.

neu/HER-2 (ErbB-2)

In vitro. An asON complementary to HER-2/*neu* oncogene was created and studied with respect to the antisense-mediated suppression of the gene in order to increase the efficiency of conventional chemotherapy. In combination with doxorubicin, the asON additively suppressed tumor cell proliferation [205].

The plasmid-encoded ribozyme complementary to *neu* mRNA efficiently cleaved the RNA substrate *in vitro*. The transfection of ovarian carcinoma cells by such a construct caused a 50% reduction of the gene expression and a 39–42% decrease in HER-2 protein level [131].

In vivo. AsON targeting *neu* mRNA combined with doxorubicin induced a synergistic anticancer effect [205].

The efficacy of HER-2 inhibition was assessed *in vivo* using injections of a recombinant adenovirus encoding a HER-2 specific rybozyme [206]. Three days after an intra-tumor injection into subcutaneously grafted mammary cell carcinoma, a 59% decrease of HER-2/*neu* mRNA was observged in tumor tissue. Treating such grafted mice with five weekly injections resulted in 89% tumor regression [206]. Preliminary results of phase I trials of a HER-2/*neu*-targeted ribozyme called Herzyme (Ribozyme Pharmaceuticals, United States) in therapy-resistant mammary tumor patients demonstrated disease stabilization but did not yield any cases of a partial or complete positive response [132].

OTHER TARGET GENES

Another asON was designed to inhibit IGF-1R activity. It caused the mytocin-induced death of bladder carcinoma cells *in vitro* [207], and the preincubation of melanoma cells with this oligonucleotide prior to injection completely blocked tumor graft development in mice [64].

The treatment of tumor cells with asON targeted against survivin helped increase the proportion of apoptotic cells [76, 77], and the use of anti-survivin ribozymes increased the sensitivity of tumor cells to radio- and chemotherapy [79–80].

In *in vitro* experiments, the efficacy of drugs based on asON, siRNA, ribozymes and DNAzymes specifically for suppressing BCR-ABL was demonstrated [84, 85, 87, 208, 209]. *In vivo* a thiophosphate asON, complementary to BCR-ABL mRNA, proved to be most successful. The intravenous injection of this drug prolonged the survival of mice with developing leukemia [210].

To suppress the expression of the *MDR1* gene and sensitize the cells to cytostatics, the respective asON [211, 212], conjugate of asON with doxorubicin [213], ribozyme [214], and siRNAs targeted at different regions of the mRNA were designed [215–218]. It was discovered that these drugs greatly increased or reestablished *in vitro* tumor cell sensitivity to doxorubicin [211, 213], vinblastin [215], vincristin [214], daunorubicin [217], and paclitaxel [218]. *In vivo*, the mice, which received subcutaneous grafts of colon cancer cells expressing the anti-MDR1 ribozyme and were later treated by doxorubicin, showed an almost complete regression of hetereotransplant growth [98]. Our experiments show that anti-mdr1b siRNA is effective in supressing *mdr1b* expression in the cells of highly chemotherapy-resistant RLS_{40} lymphosarcoma [219] and, when combined with chemotherapy, specifically stimulates cell death *in vitro*. If cyclophosphamide and anti-mdr1b siRNA are used in combination *in vivo*, they cause the complete regression of RLS_{40} lymphosarcoma in mice and increase the efficiency of cyclophosphamide therapy more than 3-fold when compared to cyclophosphamide monotherapy [99].

In order to circumvent MDR caused by the glutathione system, a ribozyme targeted at the γ-glutamylcystein synthetase was constructed. This drug increased the sensitivity of colon tumor cells to cisplatin, doxorubicin, and etoposide 1.8-, 4.9- and 1.5-fold, respectively [101].

To overcome hTERT-mediated tumor cell immortality, specific hTERT-targeted asON were developed, such as PNA, 2'-O-methyl asON, (2-5A) asON, which has a 2'5'-oligoadenilate group [111, 112]. 2'-O-methyl asON and (2-5A) asON proved to be the most successful and caused the death of 90% of the tumor cells *in vitro* [111, 112]. Daily intratumoral injections of (2-5A) asON for 14 days caused a more than 50% regression of a subcutaneous grafted glioma [112].

Cells transfected by eIF4E-targeted asON decreased not only the level of the factor itself, but also that of other cancer-associated proteins, such as Bcl-2, survivin, cyclin D1, C-myc, and VEGF [136]. The intravenous infusion of anti-eIF4E asON to tumor-bearing mice caused a 10-fold regression of the tumor and did not have any toxic effect on the animals' healthy tissues and organs [136].

In order to suppress anomalous PTN expression, a ribozyme-based approach was suggested. *In vivo* experiments showed that anti-PTN ribozymes caused a more than 65% retardation of melanoma growth in mice and inhibited angiogenesis by 70–85% [140]. Moreover, non-direct inhibition of the PTN signaling pathway by ribozymes targeted at ALK gene mRNA (which encodes a tyrosine kinase receptor for PTN) caused a 50–95% retardation of tumor growth and a two-fold increase in the mean survival time for mice with grafted glioblastoma [143].

Suppressing metalloproteinases by ribozymes did not cause the complete cell death of tumors, but it retarded tu-

Table 3. Results of nucleic acid-based drugs testing *in vivo*

RNA-target	Drug	Tumor type	Effect	Trial stage
H-ras/K-ras	asON ISIS 2503	Hepatocellular carcinoma [162, 166]	Decreased tumor weight in mice and suppressed metastatic processes [162, 166]. Low toxicity, optimized therapy schedule [48, 168], positive response in combination with gemcytabine in 10% of patients; one complete response, 4 partial [48]	Phase II
	Ribozyme	Throat, pancreatic and bladder carcinoma, melanoma	Suppresses mouse tumor growth as a result of an increased proportion of apoptotic tumor cells, decreases the invasive potential of the tumor, and increases animal survival time [43–45, 169]	*In vivo*
	siRNA	pancreatic and ovarian carcinoma [163, 164], lung cancer [165]	Inhibition of tumor growth [163–165]	*In vivo*
c-myc	asON AVI-4126 (AVIBioPharma, USA)	Prostate and breast cancer [50, 51]	Suppresses tumor growth by 80% in mice [50]. Moderate toxicity, accumulation of the drug in tumor tissue [51]	Phase II
	siRNA	breast cancer [177], lymphoma [176]	Opposes tumor progression [177]; decreases *c-myc* mRNA level in serum down to 15–20% [176]	*In vivo*
PKC-α	asON ISIS 3521 (Affinitak™, USA)	Bladder carcinoma, lung and colon cancer [55], ovarian cancer [181], colon carcinoma [182]	Completely suppresses tumor growth in mice at a dosage of ISIS 3521 of 0.06–0.6 mg/kg [55]. Moderate toxicity in clinical trial [180]; 3 objective responses to therapy [181]; no response to therapy [182]	Phase II
Clusterin	asON OGX-001	Renal carcinoma [59], prostate cancer [60]	Caused a 2-fold decrease in tumor volume in mice when used in combination with paclitaxel [62]. Decreased clusterin levels in the patients' pathological tissues [60]	Phase I/II
IGF-1R	asON	Melanoma	Completely blocked tumor development from cells transfected with the asON [64]	*Ex vivo*
bcl-2	asON G3139 (Genasense™, USA)	Lymphomas, lymphatic leukemia, myeloleukemia [186, 187], melanoma [71], lymphoma [188], lympholeucosis [70], prostate carcinoma [72]	Decreased tumor volume in mice [186], additive antitumor effect of asON G3139 and cisplatin [187]. Moderate toxicity in clinical trial, stabilized the tumor process, improved life quality [188]	Phase III
	siRNA	Murine liver H22 tumor [185], pancreatic cancer [189]	Slowed liver tumor growth in mice by 66.5% [185]; decreased pancreatic cancer heterotransplant volume by 56% [189]	*In vivo*
bcr-abl	asON	Chronic myeloleukemia	2-fold increase of mice mean survival time [210]	*In vivo*
c-raf	asON ISIS 5132 (Neopharm, USA)	Ovarian [93, 192] prostate cancer [92], colon adenocarcinoma [94]	Suppressed tumor growth in mice [192]. Moderate toxicity in clinic [195], stabilization of the disease in more than 25% of cases [92, 93]	Phase II
MDR1, mdr1a/mdr1b	Ribozyme	Colon adenocarcinoma	A virtually complete regression of mouse tumors in an *ex vivo* experiment, in combination with doxorubicin [98]	*Ex vivo*
	siRNA	Murine lymphosarcoma [99, 219]	A virtually complete regression of mouse tumors in an in vivo experiment, in combination with cyclophosphamide [102]	*In vivo*
DNMT1	asON MG98	Non-small cell lung cancer, colon carcinoma, metastatic renal carcinoma and other solid tumors [108, 196, 197]	Regression of tumors in nude mice [196]. No serious side effects, no clinical response from patients [108,196, 197]	Phase II
hTERT	asON	Glioma	A more than 50% regression of tumor [112]	*In vivo*
RRR2	asON GTI-2040 (Genasense™, USA)	Solid tumors	Inhibited tumor growth in all the experimental models studied, maximal effect in renal carcinoma. 95–98% regression [116]. No serious side effects, optimized treatment schedule [117]	Phase II
	siRNA	Pancreatic adenocarcinoma	Synergistic siRNA and hemcytabine cytotoxicity [198]	*In vivo*
VEGF, *Flt-1* (VEGFR1), *KDR* (VEGFR2)	asON	Renal carcinoma	Fivefold tumor regression [201]	*In vivo*
	siRNA	Colon and prostate adenocarcinoma [202, 203]	Tenfold retardation of colon adenocarcinoma growth [202] and 1.5-fold inhibition for prostate carcinoma [203], suppresses tumor vascularization [202, 203]	*In vivo*
	Ribozyme Angiozyme, Sirna Ther., USA	Lung carcinoma [199], colon cancer [35, 204], breast cancer [35]	Growth regression of Lewis lung carcinoma in mice by 92% and 70–80% decrease in metastasis in the lungs [199]. Well-tolerated by patients, decreases VEGFR-1 protein level in tumor cells, stabilizes the disease in 25% of patients [35, 204]	Phase II
	DNAzyme	Breast cancer	Causes tumor regression by 75% in mice, reduces vasularization in tumors, and causes cell death in the tumor's peripherial tissue [200]	*In vivo*
neu (HER-2/erbB2)	asON	Ovarian and breast cancer	Synergistic anticancer effect with doxyrubicin [205]	*In vivo*
	Ribozyme Herzyme	Breast carcinoma	Regression of tumors in mice by 89% [206]. Well-tolerated by patients, stabilizes the disease [132]	Phase I
eIF4E	asON LY2275796	Prostate carcinoma	Tenfold regression of the tumor; has no toxic effect on healthy organs or tissues in mice [136]	
PTN и ALK	Ribozyme (anti-PTN)	Melanoma	Reduces tumor size by 65%, inhibits vascularization by 70–85%, and induces apoptosis [140]	*In vivo*
	Ribozyme (anti-ALK)	Glioblastoma	Delays tumor growth, increases tumor-bearing mice survival time 2-fold [143]	*In vivo*
MMP9	Ribozyme	Metastatic fibrobalsts [220], prostate cancer[147]	Causes an 8-fold decrease in metastasis, a 1/3 increase in mean mouse survival time, and has no effect on primary tumor development [147, 220]	*Ex vivo*
FGF-BP	Ribozyme	Prostate carcinoma	Suppresses tumor development [152]	*Ex vivo*
EGR-1	DNAzyme	Breast carcinoma	Suppresses tumor growth 3-fold [157]	*In vivo*
FAK	siRNA	Prostate and breast carcinoma	Tumor regression [158]	*In vivo*
CXCR4	siRNA	Breast carcinoma	Virtually completely inhibits metastasis, decreases *CXCR4* mRNA level to 10% [159], and causes tumor regression [223]	*In vivo*

mor growth, limited its volume increase, and suppressed angiogenesis and metastasis [147, 220, 221].

A ribozyme targeted at FGF-BP causes an 80% suppression of the proteins synthesis which inhibited cell proliferation in prostate and colon carcinomas [152, 222]. Tumors transfected by an anti-FGF-BP ribozyme and later subcutaneously grafted into mice did not show any signs of progressive development [152].

In order to suppress EGR-1, a DNAzyme was constructed. It targeted the mRNA of the transcription factor EGR-1. Intratumoral injections of this drug caused a 3-fold decrease in the tumor's size [157].

Specific siRNA was developed to suppress FAK hyper function in the cells of prostate and mammary glands. Cells transfected by this siRNA demonstrated the inhibition of cell adhesion, migration, and proliferation *in vitro* and tumor growth suppression *in vivo* in mice [158].

In vivo experiments showed that intravenous injections of anti-CXCR4 siRNA not only decreased the *CXCR4* mRNA level to 10% of the control level, but also virtually blocked metastasis into the lungs [159] and suppressed the primary tumor growth [223].

Using drugs based on nucleic acids to fight cancer is one of the most promising and rapidly developing areas of modern molecular oncology. Gene-targeted oligonucleotides make it possible to inhibit key links in the malignant growth process. These drugs can not only help regulate proliferation, apoptosis, and drug resistance, but they also affect the cell–cell interactions that promote malignant progression in the entire organism. However, it is worth noting that, although gene-directed oligonucleotides share the mechanism of action (which involves switching off the target gene), the efficiency of drugs directed at suppressing the same gene, even through the same region in the mRNA target, can vary significantly.

Some companies have already undertaken the development and marketing of anticancer drugs based on gene-targeted oligonucleotides, such as asON and ribozymes, which are well recognized as forerunners of the gene-targeted therapeutic approach. As is evident from Table 3, the genes most sensitive to asON turned out to be involved in proliferation and apoptosis blockage in tumor cells. Also, genes like *Flt-1* (VEGFR) and *neu* (HER-2) turned out to be very susceptible to the effect of ribozymes. AsON targeted at suppressing *H-ras*, *c-myc*, *PKC-α*, clusterin, *bcl-2*, *c-raf*, and ribozymes, which cleave the *Flt-1* and *neu* mRNA, are currently being evaluated in clinical trials. Certain types of gene-targeted nucleic acid drugs such as DNAzymes and siRNA have only recently started to be seen as promising therapeutic tools; however, the amount of successful clinical trials is rapidly catching up with asON and ribozymes. Drugs for curing age-related retinal degeneration based on siRNA are currently being tested in clinical trials. However, siRNA for treating cancer have not been introduced into clinical trials yet.

Despite the undoubted achievements of modern oncology, the problem of raising the efficiency of malignant neoplasia treatment is still very pressing. Notably, one of the main objectives of gene-targeted therapy is to provide the delivery of drugs to the target cells, which presumes the transport into a specific organ or tissue, traversing the cellular membrane, and arriving at specific cell compartments. It is clear that oligonucleotides cannot do this by themselves. Therefore, the development of vehicle systems which could increase the efficiency of these drugs is of utmost importance. The problem of transporting a specific RNA or DNA sequence into a tumor cell is still unsolved.

As was noted above, changes in the expression of certain genes play a key role in oncogenesis. The dysfunction of these genes can affect the correct regulation of the signaling pathways that control transitions between the phases of the cell cycle, proliferation, apoptosis, genetic stability, differentiation, and morphogenetic reactions of the cell. These processes in the cell are tightly connected and are often interchangeable. In many cases, drugs based on nucleic acids affect a specific mechanism, which leads to the abrogation of a whole chain of malignant growth regulation. However, it is important to bear in mind that one of the most crucial properties of tumor cells is the ability to exploit cell survival pathways, which allows these cells to escape gene-targeted molecular control. This consideration, however, does not undermine the importance of cancer therapy using nucleic acid-based drugs directed at a specific regulatory link. Nevertheless, the flexibility and plasticity of the biochemical profile, as well as the robustness of the regulation of functions vital for the survival of tumor cells, require that gene-targeted cancer therapy be optimized as much as possible. ●

REFERENCES
1. Belikova A.M., Zarytova V.F., Grineva N.I. // Tetrahedron Letters. 1967. № 37. P. 3557–3562.
2. Гринёва Н.И., Карпова Г.Г. // Молекулярная биология. 1974. Т. 8. С. 832–844.
3. Гринёва Н.И., Карпова Г.Г., Кузнецова Л.М. и др. // Молекулярная биология. 1976. Т. 10. С. 1260–1271.
4. Zamecnik P.C., Stephenson M.L. // Proc. Natl. Acad. Sci. USA. 1978. V. 75. № 1. P. 280–284.
5. Falvey A.K., Kantor J.A., Robert-Guroff M.G. et al. // J. Biol. Chem. 1974. V. 249. № 22. P. 7049–7056.
6. Lee L.K., Roth C.M. // Curr. Opin. Biotechnol. 2003. V. 14. № 5. P. 505–511.
7. Helene C., Toulme J.J. // Biochim. Biophys. Acta. 1990. V. 1049. № 2. P. 99–125.
8. Boiziau C., Tarrago-Litvak L., Sinha N.D. et al. // Antisense Nucleic Acid Drug Dev. 1996. V. 6. № 2. P. 103–109.
9. Zelphati O., Imbach J. L., Signoret N. et al. // Nucleic Acids Res. 1994. V. 22. № 20. P. 4307–4314.
10. Jason T.L., Koropatnick J., Berg R.W. // Toxicol. Appl. Pharmacol. 2004. V. 201. № 1. P. 66–83.
11. Kurreck J. // Eur. J. Biochem. 2003. V. 270. № 8. P. 1628–1644.
12. Pirollo K.F., Rait A., Sleer L.S., Chang E.H. // Pharmacol. Ther. 2003. V. 99. № 1. P. 55–77.
13. Stahel R.A., Zangemeister-Wittke U. // Lung Cancer. 2003. V. 41. P. 81–88.
14. Tafech A., Bassett T., Sparanese D. et al. // Curr. Med. Chem. 2006. V. 13. № 8. P. 863–881.
15. Matsukura M., Shinozuka K., Zon G. et al. // Proc. Natl. Acad. Sci. USA. 1987. V. 84. № 21. P. 7706–7710.
16. Brown D.A., Kang S.H., Gryaznov S.M. et al. // J. Biol. Chem. 1994. V. 269. № 43. P. 26801–26805.
17. Guvakova M.A., Yakubov L.A., Vlodavsky I. et al. // J. Biol. Chem. 1995. V. 270. № 6. P. 2620–2627.
18. Zamaratski E., Pradeepkumar P.I., Chattopadhyaya J. // J. Biochem. Biophys. Methods. 2001. V. 48. № 3. P. 189–208.
19. Nielsen P.E., Egholm M., Berg R.H. et al. // Science. 1991. V. 254. № 5037. P. 1497–100.
20. Larsen H.J., Bentin T., Nielsen P.E. // Biochim. Biophys. Acta. 1999. V. 1489. № 1. P. 159–166.
21. Elayadi A.N., Corey D.R. // Curr. Opin. Investig. Drugs. 2001. V. 2. № 4. P. 558–561.
22. Gryznov S.M., Lloyd D.H., Chen J.K. et al. // Proc. Natl. Acad. Sci. USA. 1995. V. 92. № 13. P. 5798–5802.
23. Heasman J. // Dev. Biol. 2002. V. 243. № 2. P. 209–214.
24. Nasevicius A., Ekker S.C. // Nat. Genet. 2000. V. 26. № 2. P. 216–220.
25. Koshkin A.A., Wengel J. // J. Org. Chem. 1998. V. 63. № 8. P. 2778–2781.
26. Obika S., Morio K., Hari Y. et al. // Bioorg. Med. Chem. Lett. 1999. V. 9. № 4. P. 515–518.
27. Wahkestedt C., Salmi P., Good L. et al. // Proc. Natl. Acad. Sci. USA. 2000. V. 97. № 10. P. 5633–5638.
28. Fire A., Xu S., Montgomery M K. et al. // Nature. 1998. V. 391. № 6669. P. 806–811.
29. Downward J. // Brit. Med. J. 2004. V. 328. № 7450. P. 1245–1248.
30. Lingel A., Izaurralde E. // RNA. 2004. V. 10. № 11. P. 1675–1679.
31. Leung R.K., Whittaker P.A. // Pharmacol. Ther. 2005. V. 107. № 2. P. 222–239.
32. Rand T.A., Ginalski K., Grishin N.V. et al. // Proc. Natl. Acad. Sci. USA. 2004. V. 101. № 40. P. 14385–14389.
33. Hannon G.J., Rossi J.J. // Nature. 2004. V. 431. № 7006. P. 371–378.
34. Kruger K., Grabowski P.J., Zaug A.J. et al. // Cell. 1982. V. 31. № 1. P. 147–157.
35. Bagheri S., Kashani-Sabet M. // Curr. Mol. Med. 2004. V. 4. № 5. P. 489–506.
36. Schubert S., Kurreck J. // Curr. Drug Targets. 2004. V. 5. № 8. P. 667–681.
37. Kore A.R., Vaish N.K., Kutzke U. et al. // Nucleic Acids Res. 1998. V. 26. № 18. P. 4116–4120.
38. Ferré-D'Amaré A.R. // Biopolymers. 2004. V. 73. № 1. P. 71–78.
39. Santoro S.W., Joyce G.F. // Proc. Natl. Acad. Sci. USA. 1997. V. 94. № 9. P. 4262–4266.
40. Копнин Б.П. // Биохиия. 2000. Т. 65. № 1. С. 5–33.
41. Barbacid M. // Annu. Rev. Biochem. 1987. V. 56. P. 779–827.
42. Campbell S.L., Khosravi-Far R., Rossman K.L. et al. // Oncogene. 1998. V. 17. № 11. P. 1395–1413.
43. Wang C.H., Tsai L.J., Tsao Y.P. et al. // Biochem. Biophys. Res. Commun. 2002. V. 298. № 5. P. 805–814.
44. Tone T., Kashani-Sabet M., Funato T. et al. // *In Vivo*. 1993. V. 7. № 6A. P. 471–476.
45. Kashani-Sabet M., Funato T., Tone T. et al. // Antisense Res. Dev. 1992. V. 2. № 1. P. 3–15.
46. Ohta Y., Kijima H., Ohkawa T. et al. // Nucleic Acids Res. 1996. V. 24. № 5. P. 938–942.
47. Ohta Y., Kijima H., Kashani-Sabet M., Scanlon K.J. // J. Invest. Dermatol. 1996. V. 106. № 2. P. 275–280.
48. Alberts S.R., Schroeder M., Erlichman C. et al. // J. Clin. Oncol. 2004. V. 22. № 24. P. 4944–4950.
49. Bishop J.M. // Adv. Cancer Res. 1982. № 37. P. 1–32.
50. Iversen P.L., Arora V., Acker A.J. et al. // Clin. Cancer Res. 2003. V. 9. P. 2510–2519.
51. Devi G.R., Beer T.M., Corless C.L. et al. // Clin. Cancer Res. 2005. V. 11. № 10. P. 3930–3938.
52. Kipshidze N., Iversen P., Overlie P. et al. // Cardiovasc. Revasc. Med. 2007. V. 8. № 4. P. 230–235.
53. Jaken S. // Curr. Opin. Cell Biol. 1996. V. 8. № 2. P. 168–173.
54. Deacon E.M., Pongracz J., Griffiths G., Lord J.M. // Mol. Pathol. 1997. V. 50. № 3. P. 124–131.
55. Dean N.M., McKay R., Condon T.P., Bennett C.F. // J. Biol. Chem. 1994. V. 269. № 23. P. 16416–16424.
56. Blaschuk O., Burdzy K., Fritz I.B. // J. Biol. Chem. 1983. V. 258. № 12. P. 7714–7720.
57. Rosenberg M.E., Silkensen J. // Int. J. Biochem. Cell Biol. 1995. V. 27. № 7. P. 633–645.
58. Humphreys D.T., Carver J.A., Easterbrook-Smith S.B., Wilson M.R. // J. Biol. Chem. 1999. V. 274. № 11. P. 6875–6881.
59. Zellweger T., Miyake H., July L.V. et al. // Neoplasia. 2001. V. 3. № 4. P. 360–367.
60. Chi K.N., Siu L.L., Hirte H. et al. // Clin. Cancer Res. 2008. V. 14. № 3. P. 833–839.
61. Blakesley V.A., Stannard B.S., Kalebic T. et al. // J. Endocrinol. 1997. V. 152. № 3. P. 339–344.
62. Guo Y.S., Jin G.F., Houston C.W. et al. // J. Cell Physiol. 1998. V. 175. № 2. P. 141–148.
63. Singleton J.R., Dixit V.M., Feldman E.L. // J. Biol. Chem. 1996. V. 271. № 50. P. 31791–31794.
64. Resnicoff M., Coppola D., Sell C. et al. // Cancer Res. 1994. V. 54. № 18. P. 4848–4850.
65. Tsujimoto Y., Cossman J., Jaffe E., Croce C.M. // Science. 1985. V. 228. № 4706. P. 1440–1443.
66. Dive C. // J. Intern. Med. 1997. № 740. P. 139–145.
67. Decaudin D., Geley S., Hirsch T. et al. // Cancer Res. 1997. V 57. № 1. P. 62–67.
68. Reed J.C., Stein C., Subasinghe C. et al. // Cancer Res. 1990. V. 50. № 20. P. 6565–6570.
69. Chi K.C., Wallis A.E., Lee C.H. et al. // Breast Cancer Res. Treat. 2000. V. 63. № 3. P. 199–212.
70. O'Brien S., Moore J.O., Boyd T.E. et al. // Appl. Immunohistochem. Mol. Morphol. 2005. V. 13. № 1. P. 6–13.
71. Bedikian A.Y., Millward M., Pehamberger H. et al. // J. Clin. Oncol. 2006. V. 24. № 29. P. 4738–4745.
72. Tolcher A.W., Chi K., Kuhn J. et al. // Clin. Cancer Res. 2005. V. 11. № 10. P. 3854–3861.
73. Altieri D.C. // Trends Mol. Med. 2001. V. 7. № 12. P. 542–547.
74. Altieri D.C., Marchisio P.C. // Lab. Invest. 1999. V. 79. № 11. P. 1327–1333.
75. Li F., Ambrosini G., Chu E.Y. et al. // Nature. 1998. V. 396. № 6711. P. 580–584.
76. Xia C., Xu Z., Yuan X. et al. // Mol. Cancer Ther. 2002. V. 1. № 9. P. 687–694.
77. Du Z.X., Zhang H.Y., Gao da X. et al. // Exp. Mol. Med. 2006. V. 38. № 3. P. 230–240.
78. Pennati M., Colella G., Folini M. et al. // J. Clin. Invest. 2002. V. 109. № 2. P. 285–286.
79. Pennati M., Binda M., Colella G. et al. // J. Invest. Dermatol. 2003. V. 120. № 4. P. 648–654.
80. Choi K.S., Lee T.H., Jung M.H. // Cancer Gene Ther. 2003. V. 10. № 2. P. 87–95.
81. Rowley J.D. // Nature. 1973. V. 243. № 5405. P. 290–293.
82. Lugo T.G., Pendergast A.M., Muller A.J., Witte O.N. // Science. 1990. V. 247. № 4946. P. 1079–1082.
83. Dobrovic A., Morley A.A., Seshadri R., Januszewicz E.H. // Leukemia. 1991. V. 5. № 3. P. 187–190.
84. Kuwabara T., Warashina M., Tanabe T. et al. // Nucleic Acids Res. 1997. V. 25. № 15. P. 3074–3081.
85. Kuwabara T., Warashina M., Tanabe T. et al. // Mol. Cell. 1998. V. 2. № 5. P. 617–627.
86. Druker B.J., Talpaz M., Resta D.J. et al. // N. Engl. J. Med. 2001. V. 344. № 14. P. 1031–1037.
87. Wohlbold L., van der Kuip H., Miething C. et al. // Blood. 2003. V. 102. № 6. P. 2236–2239.
88. Daum G., Eisenmann-Tappe I., Fries H.W. et al. // Trends Biochem. Sci. 1994. V. 19. № 11. P. 474–480.
89. Mayo M.W., Baldwin A.S. // Biochim. Biophys. Acta. 2000. V. 1470. № 2. P. M55–62.
90. Downward J. // Nat. Cell Biol. 1999. V. 1. № 2. P. E33–35.
91. Bos J.L. // Cancer Res. 1989. V. 49. № 17. P. 4682–4689.
92. Tolcher A.W., Reyno L., Venner P.M. et al. // Clin. Cancer Res. 2002. V. 8. № 8. P. 2530–2535.
93. Oza A.M., Elit L., Swenerton K. et al. // Gynecol. Oncol. 2003. V. 89. № 1. P. 129–133.
94. Cripps M.C., Figueredo A.T., Oza A.M. et al. // Clin. Cancer Res. 2002. V. 8. № 7. P. 2188–2192.
95. Ставровская А. // Биохимия. 2000. Т. 65. № 1. P. 95–106.
96. Gottesman M.M., Fojo T., Bates S.E. // Nat. Rev. Cancer. 2002. V. 2. № 1. P. 48–58.
97. Ambudkar S.V., Kimchi-Sarfaty C., Sauna Z.E. // Oncogene. 2003. V. 22. № 47. P. 7468–7485.
98. Gao Z., Gao Z., Fields J.Z., Boman B.M. // Int. J. Cancer. 1999. V. 82. № 3. P. 346–352.
99. Шкляева О.А. Дисс. канд. биол. Наук. ИХБФМ СО РАН. Новосибирск. 2009.
100. Tew K.D. // Cancer Res. 1994. V. 54. № 16. P. 4313–4320.
101. Nagata J., Kijima H., Hatanaka H. et al. // Biochem. Biophys. Res. Commun. 2001. V. 286. № 2. P. 406–413.
102. Szyf M. // Drug Resist. Updat. 2003. V. 6. № 6. P. 341–353.
103. Adams R.L., McKay E.L., Craig L.M., Burdon R.H. // Biochim. Biophys. Acta. 1979. V. 563. № 1. P. 72–81.
104. Kautiainen T.L., Jones P.A. // J. Biol. Chem. 1986. V. 261. № 4. P. 1594–1598.
105. Wu J., Issa J.P., Herman J. et al. // Proc. Natl. Acad. Sci. USA. 1993. V. 90. № 19. P. 8891–8895.
106. Strathdee G., MacKean M.J., Illand M., Brown R. // Oncogene. 1999. V. 18. № 14. P. 2335–2341.
107. Fournel M., Sapieha P., Beaulieu N. et al. // J. Biol. Chem. 1999. V. 274. № 34. P. 24250–24256.
108. Winquist E., Knox J., Ayoub J.P. et al. // Invest. New Drugs. 2006. V. 24. № 2. P. 159–167.
109. Bryan T.M., Cech T.R. // Curr. Opin. Cell Biol. 1999. V. 11. № 3. P. 318–324.
110. Artandi S.E., DePinho R.A. // Curr. Opin. Genet. Dev. 2000. V. 10. № 1. P. 39–46.
111. Pitts A.E., Corey D.R. // Proc. Natl. Acad. Sci. USA. 1998. V. 95. № 20. P. 11549–11554.
112. Kondo S., Kondo Y., Li G. et al. // Oncogene. 1998. V. 16. № 25. P. 3323–3330.
113. Engström Y., Eriksson S., Jildevik I. et al. // J. Biol. Chem. 1985. V. 260. № 16. P. 9114–9116.
114. Fan H., Villegas C., Huang A., Wright J.A. // Cancer Res. 1998. V. 58. № 8. P. 1650–1653.
115. Fan H., Villegas C., Wright J.A. // Proc. Natl. Acad. Sci. USA. 1996. V. 93. № 24. P. 14036–14040.
116. Lee Y., Vassilakos A., Feng N. et al. // Cancer Res. 2003. V. 63. № 11. P. 2802–2811.

117. Desai A.A., Schilsky R.L., Young A. et al. // Ann. Oncol. 2005. V. 16. P. 958–965.
118. Folkman J. // N. Engl. J. Med. 1971. V. 285. № 21. P. 1182–1186.
119. Dvorak H.F., Brown L.F., Detmar M., Dvorak A.M. // Am. J. Pathol. 1995. V. 146. № 5. P. 1029–1039.
120. Zachary I., Gliki G. // Cardiovasc. Res. 2001. V. 49. № 3. P. 568–581.
121. Houck K.A., Ferrara N., Winer J. et al. // Mol. Endocrinol. 1991. V. 5. № 12. P. 1806–1814.
122. Poltorak Z., Cohen T., Sivan R. et al. // J. Biol. Chem. 1997. V. 272. № 11. P. 7151–7158.
123. Petrova T.V., Makinen T., Alitalo K. // Exp. Cell Res. 1999. V. 253. № 1. P. 117–130.
124. Förster Y., Meye A., Krause S., Schwenzer B. // Cancer Lett. 2004. V. 212. № 1. P. 95–103.
125. Zhang L., Yang N., Mohamed-Hadley A. et al. // Biochem. Biophys. Res. Commun. 2003. V. 303. № 4. P. 1169–1178.
126. Ferrara N., Heinsohn H., Walder C.E. et al. // Ann. NY. Acad. Sci. 1995. V. 752. № 246–256.
127. Stern D.F., Heffernan P.A., Weinberg R.A. // Mol. Cell Biol. 1986. V. 6. № 5. P. 1729–1740.
128. Di Fiore P.P., Pierce J.H., Fleming T.P. et al. // Cell. 1987. V. 51. № 6. P. 1063–1070.
129. Gusterson B.A. // Eur. J. Cancer. 1992. V. 28. № 1. P. 263–267.
130. Baselga J., Norton L., Albanell J. et al. // Cancer Res. 1998. V. 58. № 13. P. 2825–2831.
131. Lui V.W., He Y., Huang L. // Mol. Ther. 2001. V. 3. № 2. P. 169–177.
132. Tafech A., Bassett T., Sparanese D., Lee C.H. // Curr. Med. Chem. 2006. V. 13. № 8. P. 863–881.
133. De Benedetti A., Graff J.R. // Oncogene. 2004. V. 23. № 18. P. 3189–3199.
134. Mamane Y., Petroulakis E., Rong L. et al. // Oncogene. 2004. V. 23. № 18. P. 3172–3179.
135. Gingras A.C., Kennedy S.G., O'Leary M.A. et al. // Genes Dev. 1998. V. 12. № 4. P. 502–513.
136. Graff J.R., Konicek B.W., Vincent T.M. et al. // J. Clin. Invest. 2007. V. 117. № 9. P. 638–2648.
137. Li Y.S., Milner P.G., Chauhan A.K. et al. // Science. 1990. V. 250. № 4988. P. 1690–1694.
138. Wellstein A., Fang W.J., Khatri A. et al. // J. Biol. Chem. 1992. V. 267. № 4. P. 2582–2587.
139. Kojima S., Inui T., Muramatsu H. // Biochem. Biophys. Res. Commun. 1995. V. 216. № 2. P. 574–581.
140. Czubayko F., Schulte A.M., Berchem G.J., Wellstein A. // Proc. Natl. Acad. Sci. USA. 1996. V. 93. № 25. P. 14753–14758.
141. Morris S.W., Kirstein M.N., Valentine M.B. et al. // Science. 1994. V. 263. № 5151. P. 1281–1284.
142. Stoica G.E., Kuo A., Aigner A. et al. // J. Biol. Chem. 2001. V. 276. № 20. P. 16772–16779.
143. Powers C., Aigner A., Stoica G.E. et al. // J. Biol. Chem. 2002. V. 277. № 16. P. 14153–14158.
144. Ochieng J., Fridman R., Nangia-Makker P. et al. // Biochemistry. 1994. V. 33. № 47. P. 14109–14114.
145. Sires U.I., Griffin G.L., Broekelmann T.J. et al. // J. Biol. Chem. 1993. V. 268. № 3. P. 2069–2074.
146. Bernhard E.J., Muschel R.J., Hughes E.N. // Cancer Res. 1990. V. 50. № 13. P. 3872–3877.
147. Sehgal G., Hua J., Bernhard E.J. et al. // Am. J. Pathol. 1998. V. 152. № 2. P. 591–596.
148. Gospodarowicz D., Ferrara N., Schweigerer L. et al. // Endocr. Rev. 1987. V. 8. № 2. P. 95–114.
149. Yan G., Fukabori Y., McBride G. et al. // Mol. Cell Biol. 1993. V. 13. № 8. P. 4513–4522.
150. Czubayko F., Smith R.V., Chung H.C., Wellstein A. // J. Biol. Chem. 1994. V. 269. № 45. P. 28243–28248.
151. Okamoto T., Tanaka Y., Kan M. et al. // *In Vitro* Cell Dev. Biol. Anim. 1996. V. 32. № 2. P. 69–71.
152. Aigner A., Renneberg H., Bojunga J. et al. // Oncogene. 2002. V. 21. № 37. P. 5733–5742.
153. Khachigian L.M., Collins T. // J. Mol. Med. 1998. V. 76. № 9. P. 613–616.
154. Huang R.P., Fan Y., de Belle I. et al. // Int. J. Cancer. 1997. V. 72. № 1. P. 102–109.
155. Gill P.K., Gescher A., Gant T.W. // Eur. J. Biochem. 2001. V. 268. № 15. P. 4151–4157.
156. Gu Z., Lee R.Y., Skaar T.C. et al. // Cancer Res. 2002. V. 62. № 12. P. 3428–3437.
157. Mitchell A., Dass C.R., Sun L.Q. et al. // Nucleic Acids Res. 2004. V. 32. № 10. P. 3065–3069.
158. Tsutsumi K., Kasaoka T., Park H.M. et al. // Int. J. Oncol. 2008. V. 33. № 1. P. 215–224.
159. Liang Z., Yoon Y., Votaw J. et al. // Cancer Res. 2005. V. 65. № 3. P. 967–971.
160. Bouchard C., Staller P., Eilers M. // Trends Cell Biol. 1998. V. 8. № 5. P. 202–206.
161. Monia B.P., Johnston J.F., Ecker D.J. et al. // J. Biol. Chem.1992. V. 267. № 28. P. 19954–19962.
162. Liao Y., Tang Z.Y., Liu K.D. et al. // J. Cancer Res. Clin. Oncol. 1997. V. 123. № 1. P. 25–33.
163. Yang G., Thompson J.A., Fang B., Liu J. // Oncogene. 2003. V. 22. № 36. P. 5694–5701.
164. Brummelkamp T.R., Bernards R., Agami R. // Cancer Cell. 2002. V. 2. № 3. P. 243–247.
165. Zhang Z., Jiang G., Yang F., Wang J. // Cancer Biol. Ther. 2006. V. 5. № 11. P. 1481–1486.
166. Liao Y., Tang Z.Y., Ye S.L. et al. // Hepatogastroenterology. 2000. V. 47. № 32. P. 365–370.
167. Fluiter K., Frieden M., Vreijling J. et al. // Chembiochem. 2005. V. 6. № 6. P. 1104–1109.
168. Adjei A.A., Dy G.K., Erlichman C. et al. // Clin. Cancer Res. 2003. V. 9. № 1. P. 115–123.
169. Kijima H., Yamazaki H., Nakamura M. et al. // Int. J. Oncol. 2004. V. 24. № 3. P. 559–564.
170. Wickstrom E.L., Bacon T.A., Gonzalez A. et al. // Proc. Natl. Acad. Sci. USA. 1988. V. 85. № 4. P. 1028–1032.
171. Watson P.H., Pon R.T., Shiu R.P. // Cancer Res. 1991. V. 51. № 15. P. 3996–4000.
172. Hudziak R.M., Summerton J., Weller D.D., Iversen P.L. // Antisense Nucleic Acid Drug Dev. 2000. V. 10. № 3. P. 163–176.
173. Cheng J., Luo J., Zhang X. et al. // Cancer Gene Ther. 2000. V. 7. № 3. P. 407–412.
174. Kabilova T.O., Chernolovskaya E.L., Vladimirova A.V., Vlassov V.V. // Nucleosides Nucleotides Nucleic Acids. 2004. V. 23. № 6-7. P. 867–872.
175. Kabilova T.O., Chernolovskaya E.L., Vladimirova A.V., Vlassov V.V. // Oligonucleotides. 2006. V. 16. № 1. P. 15–25.
176. Shen L., Zhang C., Ambrus J.L. et al. // Oligonucleotides. 2005. V. 15. № 1. P. 23–35.
177. Wang Y.H., Liu S., Zhang G. et al. // Breast Cancer Res. 2005. V. 7. № 2. P. 220–228.
178. Leirdal M., Sioud M. // Br J Cancer. 1999. V. 80. № 10. P. 1558–1564.
179. Orlandi L., Binda M., Folini M. et al. // Prostate. 2003. V. 54. № 2. P. 133–143.
180. Nemunaitis J., Holmlund J.T., Kraynak M. et al. // J. Clin. Oncol. 1999. V. 17. № 11. P. 3586–3595.
181. Yuen A.R., Halsey J., Fisher G.A. et al. // Clin. Cancer Res. 1999. V. 5. № 11. P. 3357–3363.
182. Marshall J.L., Eisenberg S.G., Johnson M.D. et al. // Clin. Colorectal Cancer. 2004. V. 4. № 4. P. 268–74
183. Kitada S., Miyashita T., Tanaka S., Reed J.C. // Antisense Res. Dev. 1993. V. 3. № 2. P. 157–169.
184. Luzi E., Papucci L., Schiavone N. et al. // Cancer Gene Ther. 2003. V. 10. № 3. P. 201–208.
185. Fu G.F., Lin X.H., Han Q.W. et al. // Cancer Biol. Ther. 2005. V. 4. № 8. P. 822–829.
186. Cotter F.E., Johnson P., Hall P. et al. // Oncogene. 1994. V. 9. № 10. P. 3049–3055.
187. Wacheck V., Heere-Ress E., Halaschek-Wiener J. et al. // J. Mol. Med. 2001. V. 79. № 10. P. 587–593.
188. Morris M.J., Tong W.P., Cordon-Cardo C. et al. // Clin. Cancer Res. 2002. V. 8. № 3. P. 679–683.
189. Ocker M., Neureiter D., Lueders M. et al. // Gut. 2005. V. 54. № 9. P. 1298–1308.
190. Monia B.P., Johnston J.F., Geiger T. et al. // Nat. Med. 1996. V. 2. № 6. P. 668–675.
191. Monia B.P. // Anticancer Drug Des. 1997. V. 12. № 5. P. 327–339.
192. McPhillips F., Mullen P., Monia B.P. et al. // Br. J. Cancer. 2001. V. 85. № 11. P. 1753–1758.
193. Mullen P., McPhillips F., MacLeod K. et al. // Clin. Cancer Res. 2004. V. 10. № 6. P. 2100–2108.
194. Lou T.F., Gray C.W., Gray D.M. // Oligonucleotides. 2003. V. 13. № 5. P. 313–324.
195. Cunningham C.C., Holmlund J.T., Schiller J.H. et al. // Clin. Cancer Res. 2000. V. 6. № 5. P. 1626–1631.
196. Davis A.J., Gelmon K.A., Siu L.L. et al. // Invest. New Drugs. 2003. V. 21. № 1. P. 85–97.
197. Stewart D.J., Donehower R.C., Eisenhauer E.A. et al. // Ann. Oncol. 2003. V. 14. P. 766–774.
198. Duxbury M.S., Ito H., Zinner M.J. et al. // Oncogene. 2004. V. 23. № 8. P. 1539–1548.
199. Pavco P.A., Bouhana K.S., Gallegos A.M. et al. // Clin. Cancer Res. 2000. V. 6. № 5. P. 2094–2103.
200. Zhang L., Gasper W.J., Stass S.A. et al. // Cancer Res. 2002. V. 62. № 19. P. 5463–5469.
201. Shi W., Siemann D.W. // Anticancer Res. 2004. V. 24. № 1. P. 213–218.
202. Kim W.J., Christensen L.V., Jo S. et al. // Mol. Ther. 2006. V. 14. № 3. P. 343–350.
203. Kim W.J., Chang C.W., Lee M., Kim S.W. // J. Control. Release. 2007. V. 118. № 3. P. 357–363.
204. Weng D.E., Masci P.A., Radka S.F. et al. // Mol. Cancer Ther. 2005. V. 4. № 6. P. 948–955.
205. Roh H., Hirose C.B., Boswell C.B. et al. // Surgery. 1999. V. 126. № 2. P. 413–421.
206. Suzuki T., Anderegg B., Ohkawa T. et al. // Gene Ther. 2000. V. 7. № 3. P. 241–248.
207. Sun H.Z., Wu S.F., Tu Z.H. // Cell Res. 2001. V. 11. № 2. P. 107–115.
208. Smetsers T.F., Skorski T., van de Locht L.T. et al. // Leukemia. 1994. V. 8. № 1. P. 129–140.
209. Takamori K., Kubo T., Zhelev Z. et al. // Nucleic Acids Symp. Ser. (Oxf). 2005. V. 49. P. 333–334.
210. Skorski T., Nieborowska-Skorska M., Nicolaides N.C. et al. // Proc. Natl. Acad. Sci. USA. 1994. V. 91. № 10. P. 4504–4508.
211. Bertram J., Palfner K., Killian M. et al. // Anticancer Drugs. 1995. V. 6. № 1. P. 124–134.
212. Kostenko E.V., Laktionov P.P., Vlassov V.V., Zenkova M.A. // Biochim. Biophys. Acta. 2002. V. 1576. № 1–2. P. 143–147.
213. Ren Y., Zhan X., Wei D., Liu J. // Biomed. Pharmacother. 2004. V. 58. № 9. P. 520–526.
214. Wang H., Chen X.P., Qiu F.Z. // World J. Gastroenterol. 2003. V. 9. № 7. P. 1444–1449.
215. Логашенко Е.Б., Черноловская Е.Л., Владимирова А.В. и др. // ДАН. 2002. № 386. С. 296–297.
216. Logashenko E.B., Vladimirova A.V., Repkova M.N. et al. // Nucleosides Nucleotides Nucleic Acids. 2004. V. 23. № 6–7. P. 861–866.
217. Nieth C., Priebsch A., Stege A., Lage H. // FEBS Lett. 2003. V. 545. № 2–3. P. 144–150.
218. Duan Z., Brakora K.A., Seiden M.V. // Mol. Cancer Ther. 2004. V. 3. № 7. P. 833–838.
219. Mironova N., Shklyaeva O., Andreeva E. et al. // Ann. NY. Acad. Sci. 2006. V. 91. P. 490–500.
220. Hua J., Muschel R.J. // Cancer Res. 1996. V. 56. № 22. P. 5279–5284.
221. Sanceau J., Truchet S., Bauvois B. // J. Biol. Chem. 2003. V. 278. № 38. P. 36537–36546.
222. Czubayko F., Liaudet-Coopman E.D., Aigner A. et al. // Nat. Med. 1997. V. 3. № 10. P. 1137–1140.
223. Lapteva N., Yang A.G., Sanders D.E. et al. // Cancer Gene Ther. 2005. V. 12. № 1. P. 84–89.
224. Yeo M., Rha S.Y., Jeung H.C. et al. // Int. J. Cancer. 2005. V. 114. № 3. P. 484–489.
225. Chen Y., Stamatoyannopoulos G., Song C.Z. // Cancer Res. 2003. V. 63. № 16. P. 4801–4804.

Self-Renewal of Stem Cells

V.V. Terskikh*, Ye. A. Vorotelyak, A.V. Vasiliev
N.K. Koltsov Institute of Developmental Biology, Russian Academy of Sciences
*E-mail: terskikh@bk.ru

ABSTRACT Asymmetric division is one of the most fundamental characteristics of adult stem cells , which ensures one daughter cell maintains stem cell status and the other daughter cell becomes committed to differentiation. New data emerged recently that allow us to conclude that asymmetric division has another important aspect: it enables self-maintenance of stem cells.
Keywords: asymmetric division, stem cells, aging of stem cells, self-renewal of stem cells, aggresomes, *Drosophila* neuroblasts.
Abbreviations: Hemopoietic stem cells (HSC), mutant protein huntingtin Htt, tumor suppressor Lgl (lethal giant larvae), stem cells (SC), tumor suppressor Discs-large (Dlg), Partitioning defective protein (Par)

INTRODUCTION

The central aspect of stem cell biology is asymmetric division. Earlier it was suggested that with the help of asymmetric division two problems could be solved at the same time: one daughter cell preserves the qualities of the stem cell and continues to self- renew, whereas the other acquires the ability to differentiate [1. 2, 3, 4]. Stem cell niches create an asymmetric microenvironment and control local processes of proliferation and differentiation of stem cells through the integration of signals from neighbor cells, from the organism, and from the external environment [5]. Niches create a system of signals directed toward the maintenance of stem cells. That has been studied in detail on germline stem cells in *Drosophila*. For example, it was shown on the germinal stem cells in the *Drosophila* ovary how the signal from the stromal cells (Dpp) regulates the self-renewal of the stem cells and influences the fate of the daughter cells [6]. In the process of ontogenesis and during the neoplastic transformation, stem cells may divide both symmetrically and asymmetrically, depending on the circumstances under which they reside [2].

Asymmetric division and cell–cell interactions are universal mechanisms of the formation of cell diversity and are of primary importance in development of multicellular organisms. Diversity of cell types may be created in two major ways [7]. One way is when a great number of identical cells are initially formed which later acquire various ways of differentiation due to cell–cell interaction. In another case, daughter cells become different from their time of birth when, in the process of mitosis of polarized mother cell, cell fate determinants segregate only in one of the daughter cells. This distribution of determinants provides for specialization of one daughter cell in a certain way, which differs from the specialization of the sister cell.

In order for the asymmetric division to proceed successfully, it is necessary that several key processes take place: (1) the cell undergoing the division should be initially polarized. Polarization may include differences in the structure of certain parts of the cell membrane and uneven distribution of determinants in the cortex and in the cytoplasm of the cell. (2) Mitotic spindle is oriented parallel to the cell polarization axis. (3) The forming mitotic spindle is also asymmetric. This results in the fact that the two centrosomes that form the spindle are different (4). As a result of the division, the cell fate determinants are distributed asymmetrically between the daughter cells.

Both ways of cell differentiation and the strategy of development can be seen in closely related nematodes [8]. Early development starts from asymmetric mitoses in *Caenorhabditis elegans* and *Acrobeloides nanus*, and the formed cells have strictly determined fate: out of the 949 mitoses that appear during *C. elegans* development, 807 are asymmetric. In *Enoplus brevis* nematode, identical blastomeres are formed first which differentiate during the further development as a result of asymmetric divisions. Asymmetric division is a conservative mechanism that provides the possibility of daughter cells development in different directions, which is why the problem of asymmetric division is of fundamental importance to developmental biology and, in particular, to the biology of stem cells [9, 7, 10]. Asymmetric division has been identified in different groups of organisms: in bacteria [11, 12], yeasts [7], *Volvox* [13], nematodes [14], *Drosophila* [15], vertebrates [16, 17], and plants. Several subjects have been thoroughly studied and are considered classical: dividing *Drosophila* neuroblasts [15] and division of first blastomeres in *Caenorhabditis elegans* [14, 18]. A prerequisite for asymmetric cell division apparently exists in all organisms, but whether or not it happens depends on the particular situation. It is possible to state now that two programs are written in a cell: for symmetric and asymmetric division. In development and during tumor transformation, stem cells may divide both symmetrically and asymmetrically, depending on their microenvironment [2]. For example, during the embryonic development of mouse, asymmetric division is directed toward regulating the number of neural stem cells. During the 12–16 d of gestation in the ventricular brain zone, a lot of apoptotic cells are found and, at the same time, ceramide expression increases. It was shown [19]

that, at that time, the neural progenitor cells divide in such a way that asymmetric distribution of the nestin and prostate apoptosis response 4 (PAR-4) occurs. As a result of such division, one daughter cell is PAR-4$^+$ nestin$^-$, in which the increased contents of ceramide incite apoptosis, and another cell not expressing PAR-4 is nestin-positive and not subjected to apoptosis. Besides, the asymmetric division is functionally connected with the apoptosis, because some genes involved in the regulation of the asymmetric division control signal pathways responsible for apoptosis [20]. Transition of daughter cells to apoptosis, as well as to the differentiated state, may be used in the organism for maintaining the cell homeostasis. In *Drosophila*, mutations in some genes in the homozygous state cause the disturbance of the apical-basal cell polarity and disorganization of the epithelium structure; this is why these genes were termed cell polarity genes . Formation and maintenance of the apical-basal cell polarity is of great importance for their functioning and for undergoing asymmetric mitosis. Polarization of cells is controlled by the complex interaction of a great number of genes [21, 22]. The loss of cell polarity and the succeeded alteration of asymmetric mitosis may result in the loss of proliferation control and that, in turn, may induce the chain of events leading to the malignant growth. It was shown in *Drosophila* neuroblasts that genes controlling asymmetric mitosis may be tumor suppressors, and mutations of those genes induce neoplastic growth [23, 24].

THE ASYMMETRIC DIVISION OF DROSOPHILA NEUROBLASTS

One of the most studied models of asymmetric division is neural progenitor cells (neuroblasts) of *Drosophila* that produce the majority of the central nervous system cells. Neuroblast undergoes asymmetric division and produces two daughter cells of different sizes. The bigger cell maintains the qualities of the neuroblast and may divide several times asymmetrically, whereas the smaller daughter cell, which is called the mother ganglion cell, is committed to differentiation and divides only once, producing two neurons or two glia cells. A large number of protein complexes take part in cell polarization [25, 26]. Apical-basal polarization of the neuroblast takes place in the late G2, when the set of proteins called Par complex localizes in the apical part of the cell. For the successful proceeding of mitosis, correct localization of the protein complexes in the apical cortex of neuroblast is needed [24]. Segregation of baso-lateral and apical protein complexes is based on their antagonism that brings about their polar distribution in the cell.

In *Drosophila* neuroblast, the apically localized proteins form two complexes interconnected by the adaptor Inscuteable protein. The evolutionally conserved Par complex includes Bazooka/Par3, aPKC, and Par6 and is the first complex of proteins that localizes in the cell cortex of the neuroblast and is initially involved in the displacement of the proteins from the apical cortex, the proteins that localize in the basal part of the cell. This protein complex regulates the activity of the tumor suppressor Lgl (lethal giant larvae), which is also necessary for the correct targeting of basal protein complexes. Lgl is directly associated with Par6 and, in this complex, it seems that aPKC inactivates Lgl through its phosphorylation. Due to the activity of the non-phosphorylated Lgl, Miranda protein is recruited in the basal cortex.

The second apical protein complex contains proteins bound to the signaling way of the heterotrimeric G-protein and includes Gαi, Partner of Inscuteable (Pins), and Locomotion defects (Loco). The Gαi–Pins–Loco complex intercedes the mitotic spindle formation, as well as its correct position (in a way parallel to the apical basal axis), toward the plane of the neuroblast division.

The mitotic spindle of the neuroblast is asymmetric, its length is longer in the apical part, and, as a result, it is shifted to the side of the basal cortex. That is why, as was mentioned earlier, two cells of different sizes are formed. Centrosomes in the *Drosophila* neuroblast, which are under division, appear to be non-equivalent; the mother centrosome, which is bigger, is surrounded by more extensive astral microtubules and remains in the neuroblast in later divisions.

Due to tumor suppressors Discs large(Dlg) and Lethal (2) giant larvae (Lgl) localized in the cortex, the apical Par complex provides the basal localization of the RNA-binding Staufen protein, the transcription Prospero (Pros) factor, the Numb protein which associates with plasma membrane, and the adaptor proteins Miranda (Mira) and Partner of Numb (Pon) [27,28]. Tumor suppressor Lgl, which is the cytoskeletal protein and which directly binds with non muscular myosin II (Zipper), suppresses its activity and prevents binding with the apical complex. Lgl is evenly distributed through the entire cell cortex. However, in the area of the apical cortex, the aPKC phosphorylates and inactivates Lgl, releasing myosin II. Activated myosin II may form filaments and displace the Miranda protein. On the contrary, Lgl is active in the basal cortex because of aPKC absence and it suppresses the activity of myosin II, which allows the Miranda to locate in the basal cortex [29]. In contrast to myosin II, which displaces the determinants from the apical cortex, myosin VI (Jaguar) provides basal localization and segregation of Mira/Pros by means of vesicular transport [30].

The Pins protein may associate with the protein Mud (mushroom body defective) of the mitotic apparatus, which is associated with the centrosome and apical cortex that is necessary for the correct orientation of the spindle. Dlg and the Khc-73 (Kinesin-73) protein situated on the plus ends of the astral microtubules are also necessary for correct positioning of the spindle. Actinomyosin cytoskeleton plays an important part in the assembling of these apical and basal protein complexes. It seems that actin filaments, not the microtubules, take part in the binding of proteins with the cortex. *Drosophila* myosins II and VI are present in mutually exclusive complexes with Miranda and are necessary for the correct localization of the determinants that determine the fate of the cell. Asymmetric Numb localization is regulated by the phosphorylation cascade that triggers the activated Aurora-A. This kinase phosphorylates Par-6, the regulatory aPKC subunit, which triggers the activation of aPKC. This in turn leads to the phosphorylation of Lgl, which binds and suppresses aPKC activity in the interphase. Phosphorylated Lgl becomes free from aPKC and allows for Bazooka to take its place in the protein complex. As a result, the specificity of the substrate changes and aPKC is able

to phosphorylate Numb. Phosphorylated Numb is localized asymmetrically as a crescent in the basal part of the cell [31]. Proteins of the basal part of the neuroblast form two complexes. One of these complexes contains Miranda adaptor protein that is associated with transcription repressor Brat (Brain tumor) and assists in its asymmetric localization, the homeodomain transcription factor Prospero, and the protein Staufen, which binds the two-stranded RNA and which can itself bind *prospero* transcripts. The second complex contains Numb, the Notch protein antagonist, and binding it protein Pon (Partner of Numb). After segregation into the mother ganglion cell, Miranda degrades, which allows Prospero translocation into the nucleus and activation of genes involved in the differentiation and repression of genes involved in proliferation processes. Mitotic spindle plays an active part in the process of asymmetric division. It has been shown on several objects that it is created by structurally and functionally different centrosomes. Mitotic spindle also appears to be asymmetric, because it is formed by structurally and functionally different centrosomes. For the yeasts *S. cerevisiae* [32, 33], "c o m p a s model" was proposed which suggests that mitotic spindle, like the magnetic needle of a compass, localizes in the cell not passively but reacts to the signals from the cortical layer of the cytoplasm. During daughter cell budding, the Kar9 protein, which is necessary for correct spindle orientation, is located at the pole that is oriented to the side of the daughter cell. Then, Kar9 moves from the pole to the microtubules, which are directed to the specific parts of the cortical layer of cytoplasm in the daughter cell. This type of model suggests that spindle asymmetry is necessary for reaction to the cortex signals and for correct orientation in a dividing cell. In *Drosophila* neuroblasts [34] and in embryonic cortex of murine brain [35], the asymmetric cell division is accompanied by the active movement of mitotic spindle. However, in *Drosophila* germinal stem cells, the centrosomes take their final place in the interphase, and asymmetric division proceed with the permanent spindle position [36].

THE ASYMMETRIC DIVISION OF HIGHER ORGANISMS

Asymmetric division in higher organisms has yet to be studied sufficiently. Sporadic findings show that such divisions take place. In many epithelial tissues, both symmetric and asymmetric cell divisions are detected. For example, during symmetric mitoses, both cells are morphologically identical and situated on the basal membrane; during asymmetric mitosis, the daughter cells are morphologically different, whereas one of them transits immediately to the epithelial suprabasal layer. It is possible to suggest that during the asymmetric and symmetric divisions different mechanisms of cell migration to the suprabasal layer can exist. In the basal cells of the human esophagus, epithelium asymmetric division has been described [37], during which mitotic spindle is oriented perpendicularly to the basal membrane, which is why one daughter cell retains contact with the basal membrane and another moves into the suprabasal layer. The authors suggest that this is how stem cells divide. In a mouse epidermis on the 12.5 d of embryonic development, the large part of epidermis consists of one layer and the overwhelming number of cell divisions take place in the epithelium plane (i.e. they are symmetric); however, some cells divide perpendicularly to the basal membrane. While multilayered epithelium appears after 15.5 d of gestation, more than 70% of the cells have vertically aligned spindle. Evidently, stratification of epidermis resulted from asymmetric mitotes [38]. In mouse tail epidermis, about 30% of the basal layer cells may undergo asymmetric division [39]. Lamprecht [40] showed that, in the basal cells of rat cornea epithelium, both symmetric and asymmetric mitoses occur.

Single progenitor haematopoietic cells isolated from the human fetal liver undergo asymmetric divisions *in vitro* [41]. It was found that approximately 30% of $CD34^+$ cells gave birth to two daughter cells with different behaviors. One cell remained quiescent for 8 d, whereas the other started to proliferate exponentially with a doubling time of 12 h. Even more often (circa 40% of cases) asymmetric division was found in $CD34^+CD38^-$ cells. Asymmetric division in mammalian stem cells still remains insufficiently studied, but some indirect findings suggest such a possibility. Mammalian tissues comprise small fractions of stem cells, about one percent or several percents, and, in many cases, they are very hard to identify *in situ*. The role of asymmetric segregation of the determinants in the cells of vertebrates has practically not been studied: however, homologues of some genes that provide the origin of *Drosophila* asymmetric mitosis were discovered. The evolutionally conservative *numb* gene was discovered in many vertebrates [44, 45]. Asymmetric divisions take place in the cells of the ferret cerebral cortex [42] and in the stem cells of the mouse cerebral cortex and neuroblasts [43]. And in all cases accomplishment of asymmetric division, just like in *Drosophila* neuroblasts, it is necessary to have an asymmetrically distributed Numb factor. Asymmetric Numb localization has been found in dividing satellite cells of mouse [46]. In *Drosophila,* Numb function is to suppress Notch signaling during neurogenesis. In vertebrates, Numb fulfills the same functions as in *Drosophila* neuroblasts and takes part in the regulation of the asymmetric division of mammalian cells [45, 47, 48]. Two Pins homologues [49] were found in vertebrates. In rats, the AGS-3 corresponds to the Pins protein, which is expressed only in some tissues. Another Pins homolog, LGN, is expressed in many human tissues. During the interphase, this protein is in the cytoplasm, and it is associated with the poles of the spindle during mitosis. Suppression of the LGN expression destroys the spindle organization and prevents chromosomes from normal disjunction [50]. Insc functioning is necessary for the correct orientation of asymmetric mitosis in the progenitor cells of rat retina [51]. Also, homologues for Par-3, Par-6, and aPKC have been found.

AGING STEM CELLS

The question of age-related changes in stem cells in the course of aging of the organism and its tissues where stem cells are localized is of crucial importance for stem cell biology [52]. In quickly renewing tissues (such as blood, epidermis, and the intestinal epithelium), stem cells make up a remarkable component and have a big proliferative potential. Mouse hematopoietic stem cells function throughout the lifetime of the animal, and serial transplantations have shown that the life expectancy of stem cells may significantly exceed the life ex-

pectancy of the organism. It was shown in many experiments that aging, as well as younger bone-marrow cells are able to restore hematopoiesis in recipients after repeated transplantations [53, 54, 55]. After several rounds of transplantation, the ability of stem cells to rescue lethally irradiated animals is lower: however, it is worth noticing that, at the same time, the proliferative potential of stem cells may not be exhausted, but unfavorable effects may be connected with the technique of isolation and transplantation of stem cells, as well as the radiation treatment of recipient niches [56, 57}. This makes it possible to suggest that, with the organism aging, no essential lowering of the proliferative potential occurs in stem cells. Naturally, then, the question arises as to whether stem cells age or not. This question cannot be unambiguously solved right now. Stem cells aging can be of a replicative character (as a result of the accumulation of errors during the repeated proliferative cycles) and of a chronological character, connected with different aspects of stem cell behavior. Though the hemopoietic stem cells (HSC) of younger and older mice were similar in their ability to restore hematopoiesis, older animals had five times more HSC than the younger ones: however, they were worse at finding niches and engrafting the bone marrow of irradiated recipirnts. HSCs of young animals were predominantly quiescent, whereas in older animals they were more often in the proliferative cycle [58, 59]. Clonal analysis of the repopulating HSCs showed that aging animals have a diminished number of lymphoid-biased HSCs, while the number of the long-term HSCs of the myeloid series rises. Myeloid HSCs of the younger and older animals behave in the same way in all aspects. This leads us to suggest that aging does not influence the qualities of individual SC, but it affects the clonal composition of the HSC. Evidently, the reduction in the level of lymphocytes in the blood may be an indicator of HSC aging [60]. Rossi *et al*. [61] showed that in aging animals endogenous DNA errors accumulate in stem cells; that may be the cause of cell aging and can be reflected in the SC functioning and maintenance of the tissue homeostasis during stress. Behavior of HSCs as the organism ages may also depend on the genetic factors manifested in different lines of mice. The number of HSCs in DBA line barely changes with the age of animals, and the number of young HSCs even falls, whereas both factors in older animals significantly increase in C57BL/6 line.

There are grounds to believe that age-related changes in stem cells are reversible, because in skeletal muscle satellite cells of mouse, it was shown [63] that a rejuvenation of the satellite cells of older animals takes place during heterochronic parabiosis. Age-related changes in the HSCs of mice may also be reversible [64]. As for germinal SC, significant aging of niches where they are located was demonstrated [65]. Embryonic SCs cultivated *in vitro* apparently do not age [66]. During the lifetime of a mouse, no pronounced aging or lowering of the physiological functions of epidermal SCs was discovered [67], which may be connected with the special biological significance of the barrier function of epidermis in the life of animals. These findings make it possible to speculate about age-specific reversible (epigenetic) changes in the SCs and about long-term retaining of their proliferative potential. On the whole, it is possible to conclude that the number of tissue SCs and their functioning may change as the organism ages. However, the stem cells retain their ability to self-renew. One of the processes connected with cell aging is the formation of intracellular protein inclusions. Correct folding of the nascent proteins in the cell requires the participation of different protein cofactors known as molecular chaperones. Those molecules recognize and bind growing chains of polypeptids and partly folded proteins in order to provide them with the native conformation and prevent misfolding and subsequent aggregation. There are several chaperone families, including heat shock proteins. Throughout the cell cycle, permanent synthesis and degradation of proteins take place. Misfolded proteins or the proteins damaged due to oxidative stress or heat shock are destroyed in the cell because of proteolysis; however, the cells appear to be unable to degrade the misfolded and damaged proteins in some situations [68], and they may form microaggregates. In higher eucariots, those microaggregates accumulate in the aggresomes which are formed as a result of direct transportation of microaggregates from the cell periphery to centrosomes or microtubules organization centers, where they are surrounded by intermediate microfilaments [69]. Formation of aggresomes is the generalized cell answer to the clustering of the aggregated nondegraded proteins. After inclusion in aggresomes, proteins are not able to undergo degradation by proteasomes. Aggregation of a large number of aggresomes ("biological garbage") is considered one of the important factors of cell aging and dying [70, 71]. Formation of aggresomes may be the reason for the dysfunction and death of postmitotic cells such as neurons and cardiomyocytes. Many neurodegenerative diseases, including Alzheimer's, Parkinson's, and Huntington's diseases, are characterized by the selective death of neurons due to aggresomes formation resulting from abnormal processing of the mutant, misfolded or damaged proteins by the ubiquitin-proteasome system [72]. For example, the mutant protein Huntingtin (Htt), which characterizes for Huntington's disease, contains a polyglutamine fragment which assists aggresome formation. Arrasate *et al.* [73] showed that, when there is an increase in the quantity of diffused Htt in cells, the death of particular neurons occurs. Microaggresomes accumulation, along with the formation of inclusion bodies, increases the vitality of neurons and protects them from the toxic effect of Htt. In a similar way, aging cells accumulate oxidized proteins, e.g., carbolinylated proteins which form high-molecular aggregates that are not subjected to degradation [74]. To a certain degree, aggresomes formation near centrosomes does not influence the correct organization of the spindle and mitosis flowing: however, when there is a great excess of aggresomes, mitosis and cell functions are disturbed [75]. The functional inequality of the centrosomes in the cell causes asymmetric orientation of the spindle. This was shown for *Drosophila* neuroblasts [76], germinal stem cells of *Drosophila* [77], and budding yeasts cells [32]. The centrosomes asymmetry is expressed particularly in that aggresomes are accumulated only around one of them [75]. Because the mechanism of asymmetric division in *Drosophila* neuroblasts is well studied and the neuroblasts themselves are frequently used for modeling the stem cells behavior, they were chosen for an examination of the mutant proteins behavior in the asymmetric mitosis [75]. A recombinant *Drosophila* was created in which the N-end fragment of the human Htt protein was ex-

pressed; this human protein contained 128 glutamine repeats (Htt-Q128). It was shown in the culture of the isolated neuroblasts that the aggregated Htt-Q128 protein usually formed a protein inclusion associated with only one pole of the spindle. As a result of the asymmetric division, the inclusion moved to the newly formed neuroblasts and mother ganglion cells were free from damaged proteins. These findings made it possible to suggest that the mechanism of aggresomes segregation in the process of symmetric mitosis may fulfill the same function in mammalian SCs. In *Drosophila* cells on the blastoderm stage, asymmetric divisions take place and, at the same time, the proteins predestined for degradation are distributed asymmetrically [78]. There is an indication that, in the stem cells of the crypt of small intestines of patients with type-3 spinocerebellar ataxy (ScA-3), an asymmetric distribution of the mutant protein ataxin-3 takes place [75]. This protein does not form inclusions in normal patients, but patients with ScA-3 manifest the aggresomes in committed and differentiated cells; however, they are not formed in the SCs situated at the crypt bottom near the Paneth cells. Judging by the microscopic inclusions that can be seen with an electron microscope, ataxin-3 is expressed in the crypt SCs as well; however, they are freed from the aggresomes after asymmetric mitosis. These findings make it possible to suggest that another exclusively important function of the asymmetric division is the self-renewal of the adult stem-cell line. In this case, one of the two daughter cells breaks free from the damaged non-degraded protein molecules and maintains its biological age, whereas the other daughter cell, which inherits the damaged molecules, either dies as a result of apoptosis or differentiates. Continuous proliferation is a necessary factor of self-renewal of adult SCs, because in nonproliferating cells damaged proteins accumulate and chronological aging of the cells takes place. ●

REFERENCES

1. Watt F M., Hogan B.L. // Science. 2000. V. 287. P. 1427–1430.
2. Morrison S.J., Kimble J. // Nature. 2006. V. 441. P. 1068 –1074.
3. Fuchs E. // J. Cell Biol. 2008. V. 180. P. 273–284.
4. Lin H. // J. Cell Biol. 2008. V. 180. P. 257–260.
5. Fuchs E., Tumbar T., Guasch G. // Cell. 2004. V. 116. P. 769–778.
6. Chen D, McKearin D. // Curr. Biol. 2003. V. 13. P. 1786–1791.
7. Horvitz H.R., Herskowitz H. // Cell. 1992. V. 68. P. 237–255.
8. Schierenberg E. // BioEssays. 2001. V. 23. P. 841–847.
9. Wolpert L. // J. Cell Sci. 1988. Suppl. 10. P. 1–9.
10. Knoblich J.A. // Nature Rev. Mol. Cell Biol. 2001. V. 2. P. 11–20.
11. Newton A., Ohta N. // Ann. Rev. Microbiol. 1990. V. 44. P. 689–719.
12. Lawler M.L., Brun Y.V. // Cell. 2006. V. 124. P. 891–893.
13. Kirk D., Kaufman M., Keeling R., Stamer K. // Development. 1991. V. 1 (Suppl.). P. 67–82.
14. Strome S. // Int. Rev. Cytol. 1989. V. 114. P. 81–123.
15. Lin H., Schagat T. // Trends in Genet. 1997. V. 13. P. 33–39.
16. Shen Q., Zhong W., Jan Y.N., Temple S. // Development. 2002. V. 129. P. 4843–4853.
17. Roegiers F., Jan Y.N. // Curr. Opin. Cell Biol. 2004. V. 16. P. 195–205.
18. Guo S., Kempus K.J. // Curr. Opin. Genet. Develop. 1996. V. 6. P. 408–415.
19. Bieberich E., MacKinnon S., Silva J., Noggle S., Condie B.G. // J. Cell Biol. 2003. V. 162. P. 469–479.
20. Hatzold J. , Conradt B. // PloS Biol. 2008. V. 6. Issue 4 | e84.
21. Bilder D., Li M., Perriman N. // Science. 2000. V. 289. P. 113–116.
22. Johnson K., Wodarz A. // Nature Cell Biol. 2003. V.5. P. 12–14.
23. Caussinus, E., Gonzalez C. // Nature Genet. 2005. V. 37. P. 1125–1129.
24. Chia W., Somers W.G., Wang H. // J. Cell Biol. 2008. V. 180. P. 267–272.
25. Margolis B., Borg J-P. // J. Cell Sci. 2005. V. 118. P. 5157–5159.
26. Assémat E., Bazellières E., Pallesi-Pocachard E. et al. // Biochim. Biophys. Acta. 2008. V. 1778. P. 614–30.
27. Ohshiro T., Yagami T., Zhang C., Matsuzaki F. // Nature. 2000. V. 408. P. 593–596.
28. Betschinger, J., Mechtler K., Knoblich J.A. // Nature. 2003. V. 422. P. 326–330.
29. Barres B.A., Siderovski D.P. Knoblich J.A. // Neuron. 2005. V. 48. P. 539–545.
30. Petritsch, C., Tavosanis, G., Turck, C.W. et al. // Dev. Cell. 2003. V. 4. P. 273–281.
31. Wirtz-Peitz F., Nishimura T., Knoblich J.A. // Cell. 2008. V. 135. P. 161–173.
32. Kusch J., Liakopoulos D., Barral Y. // Trends Cell Biol. 2003. V. 13. P. 562–568.
33. Liakopoulos D., Kusch J., Grava S., et al. // Cell. 2003. V. 112. P. 561–574.
34. Kaltschmidt J.A., Davidson C.M., Brown N.H., Brand A.H. // Nature Cell Biol. 2000. V. 2. P. 7–12.
35. Haydar T.F., Ang E. Jr., Rakic P. // Proc. Natl. Acad. Sci. USA. 2003. V. 100. P. 2890–2895.
36. Yamashita Y.M., Jones D.L., Fuller M.T. // Science 2003. V. 301. P. 1547–1550.
37. Seery J.P., Watt F.M. // Curr. Biol. 2000. V. 10. P. 1447–1450.
38. Lechler T., Fuchs E. // Nature. 2005. V. 437. P. 275–280.
39. Clayton E., Doupe D.P., Klein A.M. et al. // Nature. 2007. V. 446. P. 185–189.
40. Lamprecht J. // Cell Tissue Kinet. 1990. V. 23. P. 203–216.
41. Huang S., Law P., Francis K. et al. // Blood. 1999. V. 94. P. 2595–2604.
42. Chenn A., McConnell S.K. // Cell. 1995. V. 82. P. 631–641.
43. Shen Q., Zhong W., Jan Y.N., Temple S. // Development. 2002. V. 129. P. 4843–4853.
44. Petersen P.H., Zou K., Hwang J.K. et al. // Nature. 2002. V. 419. P. 929–934.
45. Cayouette M., Raff M., Koster R.W., Fraser S.E. // Nature Neurosci. 2002. V. 5. P. 1265–1269.
46. Shinin V., Gayraud-Morel B., Gomés D., Tajbakhash S. // Nature Cell Biol. 2006. V. 8. P. 677–687.
47. Wakamatsu Y., Maynard T.M., Jones S.U., Weston J.A. // Neuron 1999. V. 23. P. 71–81.
48. Verdi J.M., Bashirullah A., Goldhawk D.E. et al. // Proc. Natl. Acad. Sci. USA. 1999. V. 96. P. 10472–10476.
49. Yu F., Morin X., Kaushik R. et al. // J. Cell Sci. 2003. V. 116. P. 887–896.
50. Du Q., Stukenberg P.T., Macara I.G. // Nat. Cell Biol. 2001. V. 12. P. 1069–1075.
51. Žigman M., Cayouette M., Charalambous C. et al.// Neuron. 2005. V. 48. P. 539–545.
52. Rando T.A. // Nature. 2006. V. 441. P. 1080–1086.
53. Harrison D.E. // Proc. Natl. Acad. Sci. USA. 1973. V. 70. P. 3184–3188.
54. Ogden D.A., Micklem H.S. // Transplantation. 1976. 22:287–293.
55. Harrison D.E. // J. Exp. Med. 1983. V. 157. P. 1496–1504.
56. Ross E.A., Anderson N., Micklem H.S. // J. Exp. Med. 1982. V. 155. P. 432–444.
57. Iscove N.N., Nawa K. // Curr. Biol. 1997. V. 7. P. 805–808.
58. Morrison S.J., Wandycz A.M.K. Akashi A. et al. // Nat. Med. 1996. V. 2. P. 1011–1016.
59. Liang Y., Van Zant G., Szilvassy S.J. // Blood. 2005. V. 106. P. 1479–1487.
60. Cho R.H., Sieburg H.B., Muller-Sieburg C.E. // Blood. 2008. V. 111. P. 5553–5561.
61. Rossi D.J., Bryder D., Seita J. et al. // Nature. 2007. V. 447. P. 725–729.
62. Geiger H., True J.M., de Haan G., Van Zant G. // Blood. 2001. V. 98. P. 2966–2972 .
63. Conboy I.M., Conboy M.J., Wagers A.J. et al. // Nature. 2005. V. 433. P. 760–764.
64. Van Zant G., Scott-Micus K., Thompson B.P. et al. // Exp. Hematol. 1992. V. 20. P. 470–475.
65. Jones D.L. // Stem. Cell Rev. 2007. V. 3. P. 192–200.
66. Zeng X. // Stem. Cell Rev. 2007. V. 3. P. 270–279.
67. Stern M.M., Bickenbach J.R. // Aging Cell. 2007. V. 64. P. 439–452.
68. Kopito R.R. // Trends Cell Biol. 2000. V. 10. P. 524–530.
69. Johnston J.A., Ward C.W., Kopito R.R. // J. Cell Biol. 1998. V. 143. P. 1883–1898.
70. Terman A. // Redox Rep. 2001. V. 6. P. 15–26.
71. Bucciantini M., Giannoni E., Chiti F. et al. // Nature. 2002. V. 416. P. 507–511.
72. Moore D.J., Dawson V.L., Dawson T.M. // Molecular Med. 2003. V. 4. P. 95–108.
73. Arrasate M., Mitra S., Schweitzer E.S. et al. // Nature. 2004. V. 431. P. 805–810.
74. Nystrom T. // EMBO J. 2005. V. 24. P. 1311–1317.
75. Rujano M.A., Bosveld F., Salomons F.A. et al. // PloS Biol . 2006. V. 4. Issue12: e417.
76. Rebollo E., Sampaio P., Januschke J. et al. // Developmental Cell. 2007. V. 12. P. 467–474.
77. Yamashita Y.M., Jones D.L., Fuller M.T. // Science. 2003. V. 301. P. 1547–1550.
78. Fuentealba L.C., Eivers E., Geissert D. et al. // Proc. Nat. Acad. Sci. USA. 2008. V. 105. P. 7732–7737.

Covalent Binding Antibodies Suppress Advanced Glycation: On the Innate Tier of Adaptive Immunity

T. Shcheglova[b], S. P. Makker[a], and A. Tramontano[a]*
[a]Department of Pediatrics, University of California, Davis – School of Medicine Davis, California USA
[b]Institute of Cytology and Genetics, Siberian Branch of the Russian Academy of Sciences, Lavrentiev Av. 10, Novosibirsk 630090, Russia
*E-mail: tramontano@ucdavis.edu

ABSTRACT Non-enzymatic protein glycation is a source of metabolic stress that contributes to cytotoxicity and tissue damage. Hyperglycemia has been linked to elevation of advanced glycation endproducts, which mediate much of the vascular pathology leading to diabetic complications. Enhanced glycation of immunoglobulins and their accelerated vascular clearance is proposed as a natural mechanism to intercept alternative advanced glycation endproducts, thereby mitigating microvascular disease. We reported that antibodies against the glycoprotein KLH have elevated reactivity for glycopeptides from diabetic serum. These reactions are mediated by covalent binding between antibody light chains and carbonyl groups of glycated peptides. Diabetic animals that were immunized to induce reactive antibodies had attenuated diabetic nephropathy, which correlated with reduced levels of circulating and kidney-bound glycation products. Molecular analysis of antibody glycation revealed the preferential modification of light chains bearing germline-encoded lambda V regions. We previously noted that antibody fragments carrying V regions in the germline configuration are selected from a human Fv library by covalent binding to a reactive organophosphorus ester. These Fv fragments were specifically modified at light chain V region residues, which map to the combining site at the interface between light and heavy chains. These findings suggest that covalent binding is an innate property of antibodies, which may be encoded in the genome for specific physiological purposes. This hypothesis is discussed in context with current knowledge of the natural antibodies that recognize altered self molecules and the catalytic autoantibodies found in autoimmune disease.

Keywords: Natural autoantibodies, covalent binding, reactive antibody, advanced glycation, carbonyl group, diabetic complications, hydrolytic abzymes

Abbreviations: NAbs, Natural antibodies; KLH, Keyhole limpet hemocyanin; VL, light chain variable region; VH, heavy chain variable region; CDR, complementarity determining region; LDL, low-density lipoprotein; AGEs, advanced glycation endproducts; RAGE, receptor of AGE; OP, organophosphorus ester; scFv, single-chain variable fragment; FR, framework region; PC, phosphorylcholine; PAMPs, pathogen-associated molecular patterns; TLR, toll-like receptor.

INTRODUCTION

The generation of an enormous diversity of antibodies in response to the multitude of possible antigens is a signature of instructive or adaptive immunity. The structural basis for adaptive immunity is expressed in the variability of the antigen binding sites displayed on antibodies and B cell receptors. Thus, antibodies are conventionally associated with the genetic recombination and accumulated mutations in their variable (V) regions that incrementally improve the complementarity between the antibody combining site and groups on the antigen. In contrast to affinity that matures gradually over time through multiple weak interactions, binding through strong forces such as a covalent bond could enable a more rapid and efficient way to capture certain antigens. Is there any case where antibodies use this form of binding and what purpose could such a binding mechanism serve?

Antibodies that bind ligands covalently have been sought in approaches to generate enzyme-like catalytic antibodies (1). Covalent binding is used by enzymes to stabilize reactive intermediates in catalysis of many types of reactions. Reactive immunization was conceived as a strategy to elicit antibodies that bind their ligands through a covalent complex (2). Such antibody complexes might mimic enzyme intermediates to catalyze the transformation of the bound substrate. The premise assumes that this form of binding could be evoked through the conventional affinity maturation process for antibody induction. Implicitly, such antibodies would have experimentally conferred, and therefore artificial, activity. In the prototypical example, immunization against synthetic antigens containing a reactive dicarbonyl group provided antibodies that bind through Schiff base - enamine adducts. The covalently reactive clones were shown to possess remarkable aldolase activity (2). As predicted, the covalent binding function arises from the somatically mutated V region genes, positioning one or more nucleophilic lysine residues in the combining site (3).

COVALENT BINDING ANTIBODIES IN GLYCATION AND PATHOLOGY

In an alternative framework one could postulate that covalent binding antibodies might also occur naturally if this activity were advantageous to the host. We proposed that binding through a single strong interaction to an antibody would be an appropriate mechanism for the sequestration and clearance of chemically damaged proteins and cells. Such a function is increasingly recognized in studies of naturally occurring antibodies that have inherent affinity for altered structures on self (4). For example, certain IgM antibodies that compete with macrophage receptors for binding of oxidized LDL particles rely on the recognition of distinct chemical moieties such as the phosphorylcholine headgroup on oxidized phospholipids. These natural autoantibodies (nAbs) are encoded in the germline and typically lack somatic mutations (5). Armed with this "innate-like" reactivity, nAbs are believed to constitute a disposal system for continuous surveil-

lance and elimination of altered self, or "neoantigens" shed from apoptotic cells and damaged tissues (6). The same nAbs also bind to phosphorylcholine groups on bacterial cell wall polysaccharides, thus providing a first line of defense against infections (7). This dual purpose could explain the conservation of this function in the germline repertoire. The molecular basis for the interaction of V regions of nAbs with oxidized phospholipids remains under investigation.

Another kind of cytotoxic metabolic waste is generated through glycation or glycoxidation as sugars and carbohydrates are constantly bathing proteins and cells and modifying them through nonspecific reactions of their exposed carbonyl groups. Glycation is a slow and continuous process that occurs in normal aging. However, it is significantly elevated in diabetes due to recurring hyperglycemia or poor glycemic control. The role of this pathway in leading to vascular complication of diabetes is now firmly established (8-10). A bewildering array of advanced glycation endproducts (AGEs) constitutes a class of altered self, which has only been superficially characterized. AGEs initiate pathologies of vascular tissues by two major mechanisms: alteration of the extracellular matrix through protein crosslinks, and the modulation of cellular functions by interacting with specific receptors. Diverse routes of cytotoxicity are suggested by the variety of receptors implicated in AGE uptake, including the receptor of AGE (RAGE), macrophage scavenger receptor, galectin-3 and megalin (11-15). The resulting cellular responses, including plaque formation and tissue restructuring, contribute to the progression of cardiovascular, renal, and microvascular diseases (**Figure 1**). A number of approaches to therapy of AGE-related pathogenesis are under investigation, including pharmacological inhibition of AGE formation (16) and biopharmaceutical blockade of AGE receptors (17). In principle, a natural homeostatic mechanism to deplete cytotoxic AGEs from circulation could mitigate pathology from ongoing or excessive glycation. Such a mechanism would likely include regulation to boost protection in a stress response. Is there a molecular basis for antibodies to fulfill such a housekeeping function? While AGEs can be highly heterogeneous, the chemical intermediates leading to their formation often bear carbonyl groups derived from the reducing sugars as a distinct chemical signature (18). Initially, carbonyls are introduced through the Amadori reaction and may be retained in various protein adducts generated in the subsequent Maillard reaction. Further degradation of these adducts produces low molecular weight aldehydes, dialdehydes, and glycated peptides, which can react again to modify other proteins (**Figure 2**). Thus, the concept of "carbonyl stress" has come to denote the chronic pathologies resulting from glycation and oxidation. An obvious mechanism to mitigate cytotoxic AGE formation is to reduce the carbonyl load. A reducing environment within cells allows one level of protection. However, extracellular scavengers might also be expected to protect targets in circulation, on cell surfaces, and in the interstitial space. The efficacy of certain carbonyl-reactive pharmaceutical agents (19) and of monoclonal anti-Amadori albumin antibodies (20, 21) in therapy of diabetic complications provides a further rationale to implicate natural carbonyl scavenging. Covalent binding by antibodies would have distinct advantages in this capacity, which conventional antibody binding could not match. In the hypothetical immune process, a common antibody would recognize diverse modified antigens by strong covalent binding to the carbonyl residue, rather than requiring many antibodies to bind a multitude of conventional epitopes on all the possible glycation products.

A favorable chemical reaction of antibodies with glycation products is suggested by the enhanced glycation of normal immunoglobulins (22-24). Glycated peptides from diabetic animals were shown to react *in vitro* with normal IgG to modify their L chains (25). Furthermore, glycated L chain is one of three major serum proteins isolated from diabetic subjects (26). Most proteins can undergo glycation to a varying degree, with some proteins more reactive than others. Hence, the modification of immunoglobulin is not surprising in itself, but the selectivity for L chain suggested that highly reactive sites must be available on these polypeptides. The chemical reactivity of L chains could be attributed to their unique sequences found in either the constant or variable domain. The preferential glycation of Fab and Fv (22, 24) and impaired antigen binding of glycated antibodies (23) support the idea that reactive residues are located in the variable sequences. Accordingly, reactivity might also be modulated by somatic diversification of V region sequences of the L chains.

INDUCTION OF COVALENT BINDING ANTIBODIES

In order to test this hypothesis we sought to demonstrate that covalent binding antibodies could be elevated in an immune response and that these could attenuate a glycation stress by reducing the carbonyl load. Reactive immunization suggested a feasible approach. Previously, we showed that antibodies induced to a pyruvate-containing hapten-KLH conjugate could bind to antigen by recognizing only the carbonyl group in the hapten (27). However, to our surprise the anti-KLH antibodies accounted in large part for this reactivity. Antibodies to KLH bound to the reactive pyruvate in the same way as established by differential binding to the pyruvate/glycolate hapten pair (**Figure 3**). Covalent Schiff base formation between antibody and the pyruvate carbonyl was the most plausible explanation for this focused binding. To test whether these antibodies could also neutralize carbonyl groups on glycation products, we compared anti-KLH antibody and normal IgG in the reaction with glycated peptides from sera of diabetic rats. In fact, this assay showed that L chains of anti-KLH antibody were more reactive than L chains of normal IgG (28). The chemically reduced glycated peptides failed to form covalent adducts, indicating that carbonyl groups were necessary for the reaction (**Figure 4**). Proteomic analysis of the modified L chains by tandem mass spectrometry showed V region peptides derived from only two lambda L chains, even though kappa L chains comprise more than 90% of rat IgG. Remarkably, these lambda L chain peptides revealed sequences identical to the germline-encoded VL (28). However, these results also suggested that L chain reactivity was enhanced by immunization. Although mass analysis detected only peptides of unmutated germline VL, modified peptides with mutated residues might not have been identified by proteomic analysis. Alternatively, L chains with innate reactivity might be recruited in combination with somatically diversified VH domains, which provide specificity for KLH and cross-reactivity for glycated peptides.

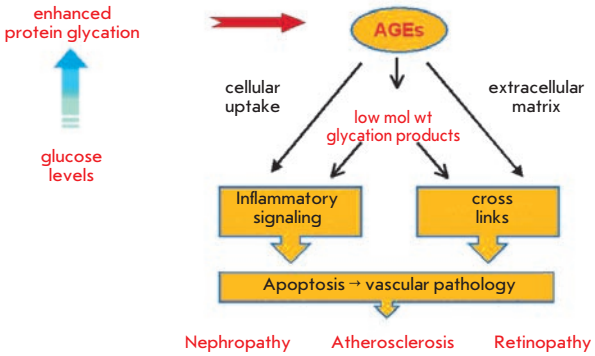

Fig. 1. Advanced Glycation Endproducts in Pathology. Protein glycation due to hyperglycemia or normal aging are further modified in the body to advanced glycation endproducts. These AGE may be further broken down to glycated peptides and low molecular weight AGEs. Both high and low molecular weight AGEs could be taken up by vascular tissues by cellular receptors and by cross-linking of the extracellular matrix. These modifications account for cytotoxicity and tissue necrosis and ultimately lead to vascular pathologies as is seen in diabetic complications

REACTIVE ANTIBODIES AMELIORATE GLYCATION-ASSOCIATED PATHOLOGY

The streptozotocin-induced diabetic rat, serving as a suitable model for diabetic nephropathy, was used to demonstrate the potential of the reactive immune response to mitigate AGE formation *in vivo*. Compared to diabetic animals immunized with adjuvant alone, KLH-immunized diabetic rats had significantly diminished AGE levels, which correlated with attenuated nephropathy (28). Improved renal function, as determined by glomerular morphology and proteinuria levels, was accompanied by reduced AGE staining in the renal extracellular matrix. We hypothesized that the therapeutic benefit derived from improved capture of glycation products in circulation by the reactive antibodies. This mechanism presumes that AGEs formed from antibody molecules are less cytotoxic than the alternative protein AGEs. Formation of glycated IgG in diabetic subjects and, in particular, the identification of glycated L chain in the diabetic serum (26) indicated that these molecules might play a role in AGE pathogenesis. Although modified L chains accumulated in the reaction with glycated peptides *in vitro*, these products were not significantly elevated in the serum of diabetic animals. Glycated IgG is cleared from circulation and taken up by kidney more efficiently than unmodified IgG (29). Furthermore, the filtration properties of low mass glycated proteins favor their selective excretion (30). Thus, native and modified L chains are found in the urine of both healthy and diabetic subjects (31, 32). Taken together, these observations are consistent with the hypothesis of enhanced clearance of selectively glycated antibodies.

These studies provide evidence that a natural covalent reactivity of antibodies is augmented by adaptive immunity. However, the predominance of unmutated V region sequences in the reaction products suggested that reactivity is inherent to the germline encoded VL (28). How could reactivity be enhanced by affinity maturation, yet conserved in an unmutated germline configuration? Glycosylated residues of KLH are believed to account for the cross-reactivity of anti-KLH antibodies for carbohydrate epitopes of microbial antigens (33). Similarly, anti-KLH antibodies may also cross-react against glycosylated epitopes of tumor antigens, as suggested by the therapeutic benefits of KLH in bladder carcinoma (34). Thus, a carbohydrate-specific response could account for the specificity of KLH antibodies for glycated peptides. This specificity could be imprinted in the H chain, which when paired with a nonspecific, reactive L chain would enhance reactivity of the latter against the bound substrate. The structures of reactive Ig V regions and the adaptive mechanisms guiding their reactivity remain subjects for further investigation.

COVALENT BINDING ANTIBODIES FROM REACTIVE SELECTION AND REACTIVE IMMUNIZATION

In an alternative approach, we used synthetic reactive substrates as antigens to probe for antibodies capable of covalent binding. This idea followed the original concept that antibodies selected for nucleophilic reactivity could also express enzymatic activity through covalent catalysis. Irreversible covalent binding to a small organophosphorus (OP) ester was used to chemically select single-chain VH-VL fragments (scFv) from a phage display library (35). All of the selected chemically reactive scFv molecules were modified on the VL polypeptide and could be described by two canonical sequences. The more reactive clone A.17 used the DPL-5 germline VL product, which was phosphonylated at Tyr37 within the framework region FR-L2. By contrast, six other reactive clones used the DPL-3 germline VL, which reacted at Tyr32 in CDR-L1. These nucleophilic Tyr residues are conserved in the VL germline and three-dimensional models of the scFv

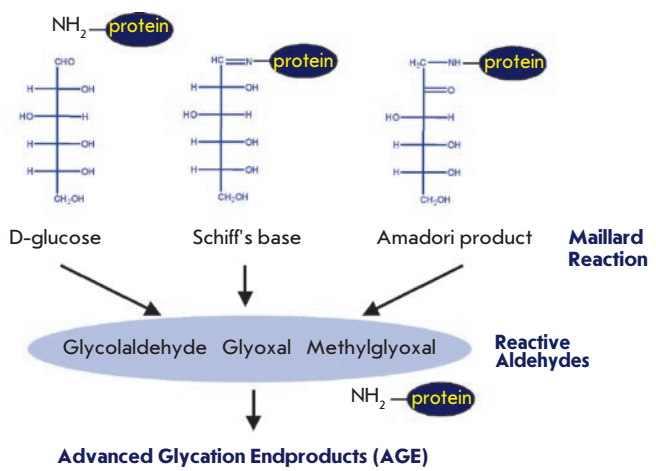

Fig. 2. Reactive carbonyls and aldehydes are intermediates in the formation of cytotoxic AGEs. Early glycation products are primarily the result of Amadori reaction of proteins with reducing sugars. Further non-enzymatic fragmentation of these products generate additional reactive aldehydes, which participate in the further protein modifications and cross-linkages know as the Maillard reaction to produce AGEs

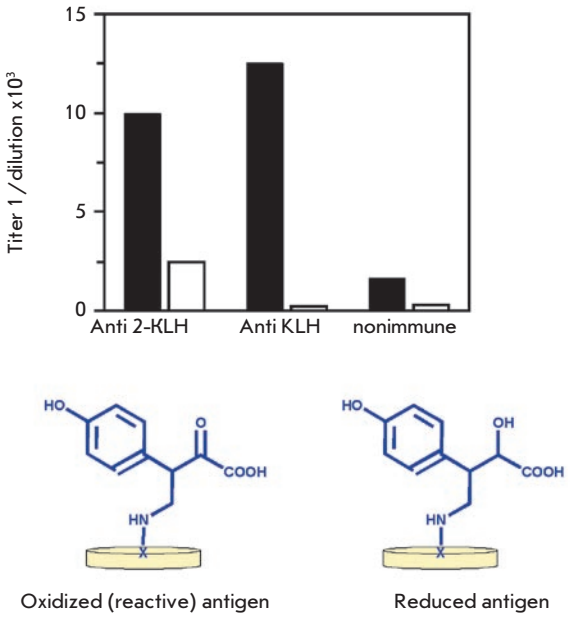

Fig. 3. Covalent-binding ELISA. Antibodies induced against a pyruvate-KLH conjugate (anti-2 KLH) or against unmodified KLH reacted specifically by ELISA with the pyruvate (2) coupled to BSA (filled bars). Binding to chemically reduced glycolate-BSA (open bars) could be observed with anti-2 KLH antibodies but not with anti-KLH antibodies. Normal, non-immune IgG bound poorly to either molecule. We hypothesized that this binding is mediated by a reaction resulting in covalent binding of the pyruvate carbonyl group with anti-KLH antibodies

suggest that either residue can be oriented toward the combining site. However, the models also indicate that the Tyr37 is buried at the interface between VL and VH domains in A.17, where it could be sterically inaccessible to ligand contact without large conformational motions (**Figure 5**). Since the library was constructed by shuffling of germline VL and VH gene segments, we did not expect natural pairs in the scFv (36). Nevertheless, the VH chains of reactive clones were represented primarily by highly homologous sequences belonging to the VH4 family. These results strongly suggested that the VH chain plays an important part in enhancing the chemical reaction at residues on the VL region. The scFv could also bind other structurally unrelated OP compounds indicating a lack of fine specificity for ligand structure (35). The A.17 scFv was also shown to have modest hydrolytic activity for peptide amides and simple carboxylic ester substrates. These Ig V regions could thus serve as primitive covalent catalysts. Most intriguing is the notion that the reactivity emerges from certain germline-encoded VL-VH pairs. Additional studies of these monoclonal Fv fragments will be of interest for understanding the origins and biochemical functions of chemically reactive Ig molecules.

Chemical selections *in vitro* might represent the first step in adaptive immunity for acquisition of reactivity. However, the contribution of irreversible covalent binding to clonal selection *in vivo* remains speculative. Using a reactive OP ester-protein conjugate as immunogen, we examined the potential for the immune response to elicit reactive antibodies that are modified by the antigen. Antisera against the OP conjugate included reactive antibodies, which could be detected by their covalent modification with biotin-tagged OP reagent (27). Remarkably, these polyclonal antibodies were also modified predominantly on their L chains. Thus, it appeared that the reactivity was enhanced by affinity maturation. However, it is not clear whether the covalent binding contributed to clonal selection or whether it is merely incidental to the affinity matured antibodies. Considered as an enzyme system, the rate of modification (antigen capture) should increase as the non-covalent binding, expressed by the K_d of the Michaelis-like Ab*OP complex, increases. While affinity maturation does not require it, an increasing chemical rate (k_s) of irreversible covalent modification (Ab-X) might provide kinetic selection for clonal expansion of B cells (Scheme I). Ultimately, the question is whether covalent capture of antigen is adopted in a natural function for immunity or for host survival.

Scheme I

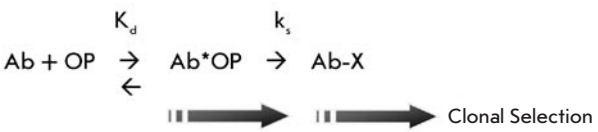

CARBONYL CHEMISTRY OF OXIDATION-DERIVED EPITOPES FOR NATURAL ANTIBODIES

IgM nAbs are predominantly produced by a population of long-lived, self-replenishing B-cells, including the B-1 and B-1a subsets. It is believed that this B cell repertoire is conserved in evolution for its contribution to host defense (5). The germline-encoded nAbs are best known for their capacity to bind conserved determinants on pathogens, referred to as pathogen-associated molecular patterns (PAMPs). More

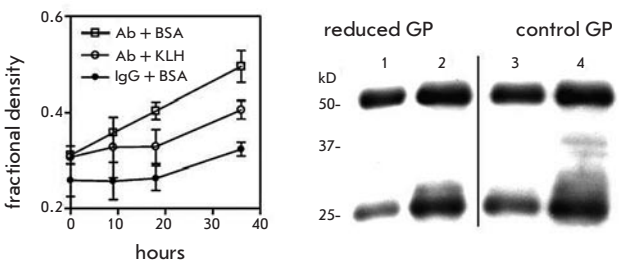

Fig. 4. Reaction of anti-KLH antibodies with glycated peptides from diabetic serum. (Right panel) The density of the bands for products at 30 – 34 kDa detected by SDS-PAGE and immunoblot analysis is plotted as a fraction of the total L chain density. Formation of L chains of higher mass was observed in the reaction of antibodies from normal and KLH-immunized rats. The rate of the latter was inhibited in the presence of KLH. (Left panel) The reaction of L chains with glycopeptides from diabetic rat serum at 0 h (lanes 1 and 3) and 24 h (lanes 2 and 4). Glycopeptides that were reduced by sodium borohydride failed to react in this time (lanes 1 and 2), while the untreated glycopeptides showed enhanced formation of L chain adducts at 30 – 34 kDa (lanes 3 and 4)

recently it was shown that nAbs also bind to altered epitopes on apoptotic cell and self proteins (37). These findings support the concept of a homeostatic function of nAbs for clearance of debris from cell death and protein decay (6, 38). Chemical structures generated by oxidation and glycoxidation of membrane phospholipids are thus the natural targets for nAb binding, presenting a case where carbonyl chemistry intersects with immune recognition. The phosphorylcholine (PC) headgroup of oxidized phospholipids and PC residues on the bacterial cell wall polysaccharides provide a common molecular determinant for the immune and homeostatic functions of nAbs (7). As a molecular receptor of PAMPs, the nAb V region can be regarded as akin to the evolutionarily conserved Toll-like receptors (TLR) of innate immunity (39). This emerging paradigm has far-reaching implications for the linkage between innate and adaptive immunity.

Oxidized phospholipids, which accumulate in atherosclerotic lesions, are targets of both innate and adaptive immunity (40). The role of reactive oxygen chemistry in defining epitopes for nAbs or for somatically diversified antibody is a subject of continuing investigation. Oxidation in the syn-2 unsaturated fatty acid chain of the phospholipids introduces reactive species, including aldehyde functional groups, into the lipid moieties. One hypothesis suggests that the carbonyl group serves as the reactive anchor for modification of self by the phospholipid moieties. Small aldehydes that are by-products of lipid peroxidation, such as 4-hydroxynonenal and 4-hydroxyhexenal, are also implicated in protein damage and cytotoxicity and may play a role in autoimmune responses (41). Moreover, malondialdehyde, glycolaldehyde, and other reactive aldehydes generated from early glycation also contribute to LDL modification and to the production of autoantibodies in pathologic conditions (42). The reaction of small aldehydes with residues on the protein surface, including lysine and histidine side chains, might define the neoepitopes of autoantibodies emanating from the nAb population. For example, it has been reported that antibodies induced to histidine adducts of lipid oxidation-derived aldehydes also bind to DNA (43). Structural mimicry between these adducts and 2-deoxyribonucleosides was suggested to explain this DNA binding. These antibodies have high sequence homology to natural anti-DNA autoantibodies and are related to the polyreactive nAbs. Thus, the role of carbonyl residues in promoting immune responses to modified self may have several dimensions. In an expanded context, proteins modified by two or three carbon aldehydes or other reactive small molecules often define ligands for innate immune receptors such as macrophage scavenger receptor and RAGE (44). Although covalent binding of aldehyde-modified proteins to scavenger receptors through Schiff base or carbinolamine adducts was contemplated the early investigations, such interactions between modified self and innate immune receptors, and antibody paratopes in particular, remain to be demonstrated.

CHEMICAL REACTIVITY, CATALYSIS AND THE BASIS FOR POLYREACTIVE ANTIBODIES

Polyreactivity of nAbs is defined as the promiscuous avidity of multivalent IgM molecules to disparate molecules, including intracellular proteins and nucleic acids (45). This binding capacity, which can also be manifested as autoreactivity to self, remains poorly understood in structural terms. Enhanced avidity by the recognition of repetitive structures on self molecules or membranes provides a plausible molecular mechanism for polyreactivity. Within this conceptual framework, the repetitive structures suggest another form of molecular pattern identifying the damaged cells and tissues. Thus, the

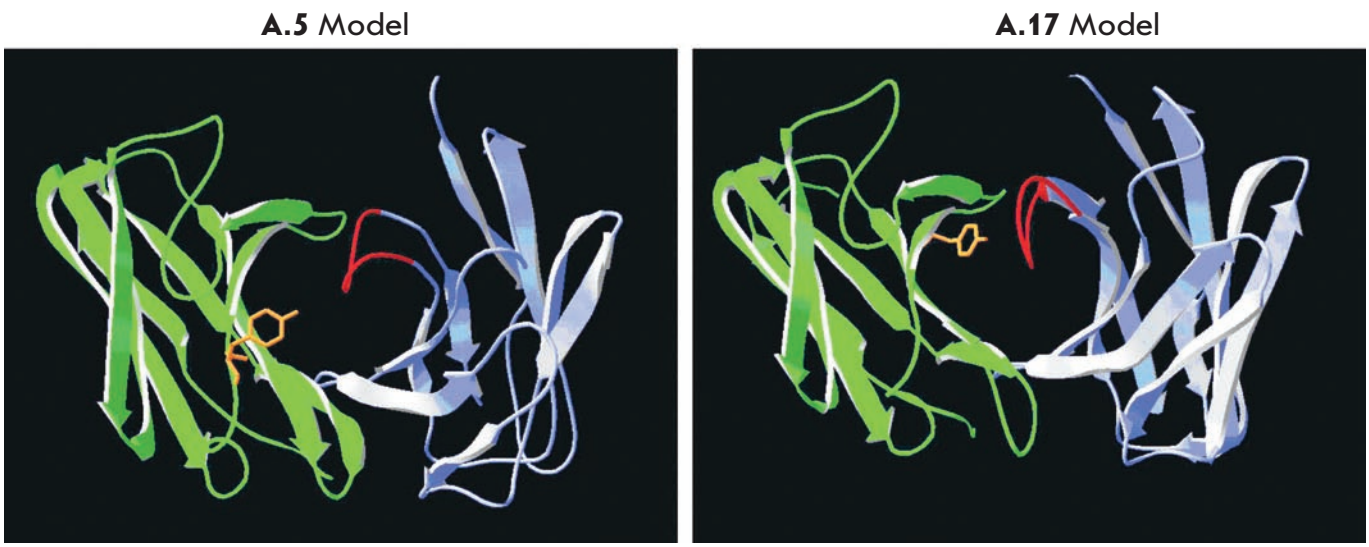

Fig. 5. Molecular models of the variable regions of covalent binding antibody Fv fragments. The yellow side wire model indicates the side chain Tyr residues participating in nucleophilic attack on the organophosphorus reagent. The Tyr at VL32 in A.5 is part of CDR1 that is oriented near the surface of the Fv domain, whereas Tyr at VL37 in A.17 is in FR1 at the interface between VL and VH. This model implicates a conserved active site in a deep cleft on A.17

high density of PC groups on oxidized phospholipids and on cell wall polysaccharides offers a common feature for nAb binding. Similarly, phosphate linkages or nucleotide sequences on DNA strands could represent the molecular pattern for DNA antibodies to recognize surface features of apoptotic cells (46, 47).

Reports showing that DNA autoantibodies found in lupus or other autoimmune diseases have phosphodiesterase activity suggests a further case where molecular recognition in the Ig V domains is manifested as chemical reactivity (48). These antibodies utilize their binding site residues to promote the cleavage of DNA ligands. A remarkable feature of the DNA-hydrolytic autoantibodies is their dependence on metal ions, reminiscent of the natural DNAse enzymes (49, 50). However, these enzyme-like antibodies show little DNA sequence specificity, hydrolyzing single-stranded and double-stranded substrates promiscuously (49, 51). Structural studies proposed that a catalytic site for DNA-hydrolysis could be encoded in a VL domain having a near-germline configuration (51). In a more recent example, it was suggested that mutations in VH or VL that enhance DNA binding could also contribute to hydrolytic activities (49). It is well established that anti-DNA IgG autoantibodies are significantly diversified by antigen-driven adaptive immunity (52, 53). For example, positively charged lysine and arginine residues in the combining sites improve binding for anionic DNA. Yet, these residues could also arise from biased VH or VL germline gene usage (54, 55). X-ray crystallographic structure studies reveal that DNA-binding autoantibodies interact with DNA through the conventional combining site comprised of CDR loops (56, 57). Mutations in both VL and VH contribute residues for direct antigen contact or for conformational changes that indirectly improve complementarity. Nevertheless, the ontogeny of DNA autoantibodies could also reflect the inherent DNA binding activity of nAbs. DNA binding can evolve directly from the PC recognition function by a single mutation in the murine monoclonal nAb T15 (58). Earlier reports also showed that DNA autoantibodies have restricted VH family usage (59) and can be encoded entirely by germline V genes without any somatic change (60-62). Reactivity of the germline-encoded V region has also been proposed to account for proteolytic activity of natural autoantibodies (63). Collectively, these findings strengthen the hypothesis that catalytic activities of Ig V regions exist as an innate immune function. The focus on polypeptide or oligonucleotide substrates for catalytic autoantibodies obscures the distinction between innate and adaptive immunity, as these substrates can engage in extended interactions with the conventional antigen combining sites. Specificity for extended features of autoantigens implies the work of adaptive immunity. However, broad reactivity without regard for the substrate structures flanking the cleavage site suggests promiscuity of a primitive active site. In depth biochemical and structural investigation of the inherent reactive or catalytic sites of natural antibodies will further illuminate the biological significance of the chemical function.

CONCLUSIONS

Covalent-binding antibodies obtained by immunization or reactive selection and catalytic antibodies found in autoimmune pathologies appear to have features in common with nAbs. These features include VH and VL domains in germline or near-germline configurations and the recognition of molecules presenting uncommon chemical functionality, such as reactive carbonyls and phosphorus esters. Such features may be fundamentally related in that the chemical or enzymatic function is presumably highly evolved and therefore conserved in the genome. Whereas nAbs are IgMs that rely on weak multivalent binding to molecular patterns on antigens for high avidity, chemically reactive or catalytic antibodies are also expressed as IgG that can bind antigens with high affinity. However, the latter may also react with diverse substrates through weak, noncovalent pre-reaction complexes. According to the transition state theory of catalysis the strongest binding is expressed between an enzyme and the transition state. In the covalent complex, binding is dominated by the chemical bond between a residue of the active site and a group on the ligand. The focus of the weak binding by nAbs on small, minimally altered epitopes is consistent with the recognition of substrate functionality for reactivity. Thus, chemical reactivity could provide a mechanism to translate weak non-covalent binding to strong binding or to catalytic activity. The physiological purpose of chemically reactive and catalytic antibodies must also be addressed, even as the role of nAbs in protective immunity and homeostasis is only beginning to emerge. Participation of nAbs as response elements in oxidative stress and apoptotic cell clearance suggests a housekeeping function that predates the evolution of adaptive immunity. Similar considerations may apply to the rationale for covalent-binding antibodies acting as buffers against glycation stress. The preservation of covalent reactivity or catalytic functions in adaptive responses and in autoimmunity could be attributed to biological design or to defects in immune regulation. Inducibility through adaptive immunity might offer an appropriate mechanism to invoke beneficial responses to oxidative or glycoxidative stress. On the other hand, the role or contribution of natural catalytic autoantibodies in autoimmune pathology remains obscure, and their existence could simply reflect a failure in the V gene repertoire shift on induction of IgG autoantibodies (64, 65). Designed catalytic antibodies can also be educed from the adaptive immune response by affinity maturation that is appropriate for substrate reactivity or transition state binding. To what extent do designer catalytic antibodies co-opt the functions of natural autoantibody catalysts? An important clue was provided in an earlier report indicating a high frequency of antibodies with hydrolytic activity among hybridomas sampling an autoimmune repertoire (66). Continuing studies of antibody chemical reactivity induced by immunization or discovered in the germline repertoire should provide further insights into its role in immunity or pathology and could enable technological applications of this unconventional antibody function in the future. ●

This work was supported by the American Diabetes Association grant 1-05-RA-136, NIH grant CA90564, and the UC Davis, Medical School - Children's Miracle Network.

REFERENCES
1. Lerner R.A., Benkovic S.J., Schultz P.G. // At the crossroads of chemistry and immunology: catalytic antibodies. Science. 1991. 252. 659–667.
2. Wagner J., Lerner R.A., Barbas C.F., 3rd. Efficient aldolase catalytic antibodies that use the enamine mechanism of natural enzymes.// Science. 1995. 270. 1797–1800.
3. Zhu X., Tanaka F., Hu Y., Heine A., Fuller R., Zhong G., Olson A.J., Lerner R.A., Barbas C.F., 3rd, Wilson I.A.// The origin of enantioselectivity in aldolase antibodies: crystal structure, site-directed mutagenesis, and computational analysis. J Mol Biol. 2004. 343. 1269–1280.
4. Chou M.Y., Fogelstrand L., Hartvigsen K., Hansen L.F., Woelkers D., Shaw P.X., Choi J., Perkmann T., Backhed F., Miller Y.I., et al.// Oxidation-specific epitopes are dominant targets of innate natural antibodies in mice and humans. J Clin Invest. 2009. 119. 1335–1349.
5. Kearney J.F.// Innate-like B cells. Springer Semin Immunopathol. 2005. 26. 377–383.
6. Lutz H.U., Binder C.J., Kaveri S.// Naturally occurring auto-antibodies in homeostasis and disease. Trends Immunol. 2009. 30.43–51.
7. Briles D.E., Forman C., Hudak S., Claflin J.L.// Anti-phosphorylcholine antibodies of the T15 idiotype are optimally protective against Streptococcus pneumoniae. J Exp Med. 1982. 156.1177–1185.
8. Vlassara H., Palace M.R.// Diabetes and advanced glycation endproducts. J Intern Med. 2002. 251.87–101.
9. Brownlee M.// Glycation products and the pathogenesis of diabetic complications. Diabetes Care. 1992. 15. 1835–1843.
10. Cerami A., Vlassara H., Brownlee M.// Role of advanced glycosylation products in complications of diabetes. Diabetes Care. 1988. 11 Suppl 1. 73–79.
11. Saito A., Nagai R., Tanuma A., Hama H., Cho K., Takeda T., Yoshida Y., Toda T., Shimizu F., Horiuchi S., et al.// Role of megalin in endocytosis of advanced glycation end products: implications for a novel protein binding to both megalin and advanced glycation end products. J Am Soc Nephrol. 2003. 14. 1123–1131.
12. Zhu W., Sano H., Nagai R., Fukuhara K., Miyazaki A., Horiuchi S.// The role of galectin-3 in endocytosis of advanced glycation end products and modified low density lipoproteins. Biochem Biophys Res Commun. 2001. 280. 1183–1188.
13. Vlassara H.// The AGE-receptor in the pathogenesis of diabetic complications. Diabetes Metab Res Rev. 2001. 17. 436–443.
14. Pricci F., Leto G., Amadio L., Iacobini C., Romeo G., Cordone S., Gradini R., Barsotti P., Liu F.T., Di Mario U., et al.// Role of galectin-3 as a receptor for advanced glycosylation end products. Kidney Int Suppl. 2000. 77. S31–39.
15. Smedsrod B., Melkko J., Araki N., Sano H., Horiuchi S.// Advanced glycation end products are eliminated by scavenger-receptor-mediated endocytosis in hepatic sinusoidal Kupffer and endothelial cells. Biochem J. 1997. 322 (Pt 2). 567–573.
16. Vasan S., Foiles P.G., Founds H.W.// Therapeutic potential of AGE inhibitors and breakers of AGE protein cross-links. Expert Opin Investig Drugs. 2001. 10. 1977–1987.
17. Bucciarelli L.G., Wendt T., Qu W., Lu Y., Lalla E., Rong L.L., Goova M.T., Moser B., Kislinger T., Lee D.C., et al.// RAGE blockade stabilizes established atherosclerosis in diabetic apolipoprotein E-null mice. Circulation. 202. 106. 2827–2835.
18. Liggins J., Furth A.J.// Role of protein-bound carbonyl groups in the formation of advanced glycation endproducts. Biochim Biophys. 1997. Acta. 1361. 123–130.
19. Soulis-Liparota T., Cooper M., Papazoglou D., Clarke B., Jerums G.// Retardation by aminoguanidine of development of albuminuria, mesangial expansion, and tissue fluorescence in streptozocin-induced diabetic rat. Diabetes. 1991. 40. 1328–1334.
20. Cohen M.P., Sharma K., Jin Y., Hud E., Wu V.Y., Tomaszewski J., Ziyadeh F.N.// Prevention of diabetic nephropathy in db/db mice with glycated albumin antagonists. A novel treatment strategy. J Clin Invest. 1995. 95. 2338–2345.
21. Cohen M.P., Hud E., Wu V.Y.// Amelioration of diabetic nephropathy by treatment with monoclonal antibodies against glycated albumin. Kidney Int. 1994. 45. 1673–1679.
22. Lapolla A., Tonani R., Fedele D., Garbeglio M., Senesi A., Seraglia R., Favretto D., Traldi, P.// Non-enzymatic glycation of IgG: an in vivo study. Horm Metab Res. 2002. 34. 260–264.
23. Kennedy D.M., Skillen A.W., Self, C.H.// Glycation of monoclonal antibodies impairs their ability to bind antigen. Clin Exp Immunol. 1994. 98. 245–251.
24. Danze P.M., Tarjoman A., Rousseaux J., Fossati P., Dautrevaux M.// Evidence for an increased glycation of IgG in diabetic patients. Clin Chim Acta. 1987. 166. 143–153.
25. Gugliucci A., Menini T.// Circulating advanced glycation peptides in streptozotocin-induced diabetic rats: evidence for preferential modification of IgG light chains. Life Sci. 1998. 62. 2141–2150.
26. Mitsuhashi T., Li Y.M., Fishbane S., Vlassara H.// Depletion of reactive advanced glycation endproducts from diabetic uremic sera using a lysozyme-linked matrix. J Clin Invest. 1997. 100. 847–854.
27. Armentano F., Knight T., Makker S., Tramontano A.// Induction of covalent binding antibodies. Immunol Lett. 2006. 103. 51–57.
28. Shcheglova T., Makker S., Tramontano A.// Reactive immunization suppresses advanced glycation and mitigates diabetic nephropathy. J Am Soc Nephrol. 2009. 20. 1012–1019.
29. Kennedy D.M., Skillen A.W., Self C.H.// Glycation increases the vascular clearance rate of IgG in mice. Clin Exp Immunol. 1993. 94. 447–451.
30. Kowluru A., Kowluru R.A.// Preferential excretion of glycated albumin in C57BL-Ks-J mice: effects of diabetes. Experientia. 1992. 48. 486–488.
31. Groop L., Makipernaa A., Stenman S., DeFronzo R.A., Teppo A.M.// Urinary excretion of κ light chains in patients with diabetes mellitus. Kidney Int. 1990. 37. 1120–1125.
32. Hutchison C.A., Harding S., Hewins P., Mead G.P., Townsend J., Bradwell A.R., Cockwell P.// Quantitative assessment of serum and urinary polyclonal free light chains in patients with chronic kidney disease. Clin J Am Soc Nephrol. 2008. 3. 1684–1690.
33. May R.J., Beenhouwer D.O., Scharff M.D.// Antibodies to keyhole limpet hemocyanin cross-react with an epitope on the polysaccharide capsule of Cryptococcus neoformans and other carbohydrates: implications for vaccine development. J Immunol. 2003. 171. 4905–4912.
34. Harris J.R., Markl J.// Keyhole limpet hemocyanin (KLH): a biomedical review. Micron. 1999. 30. 597–623.
35. Reshetnyak A.V., Armentano M.F., Ponomarenko N.A., Vizzuso D., Durova O.M., Ziganshin R., Serebryakova M., Govorun V., Gololobov G., Morse H.C., 3rd, et al. // Routes to covalent catalysis by reactive selection for nascent protein nucleophiles. J Am Chem Soc. 2007. 129. 16175–16182.
36. Griffiths A.D., Williams S.C., Hartley O., Tomlinson I.M., Waterhouse P., Crosby W.L., Kontermann R.E., Jones P.T., Low N.M., Allison T.J., et al.// Isolation of high affinity human antibodies directly from large synthetic repertoires. Embo J. 1994. 13. 3245–3260.
37. Shaw P.X., Goodyear C.S., Chang M.K., Witztum J.L., Silverman G.J.// The autoreactivity of anti-phosphorylcholine antibodies for atherosclerosis-associated neo-antigens and apoptotic cells. J Immunol. 2003. 170. 6151–6157.
38. Quartier P., Potter P.K., Ehrenstein M.R., Walport M.J., Botto M.// Predominant role of IgM-dependent activation of the classical pathway in the clearance of dying cells by murine bone marrow-derived macrophages in vitro. Eur J Immunol. 2005. 35. 252–260.
39. Pasare C., Medzhitov R.// Toll-like receptors: linking innate and adaptive immunity. Adv Exp Med Biol. 2005. 560. 11–18.
40. Binder C.J., Shaw P.X., Chang M.K., Boullier A., Hartvigsen K., Horkko S., Miller Y.I., Woelkers D.A., Corr M., Witztum J.L.// The role of natural antibodies in atherogenesis. J Lipid Res. 2005. 46. 1353–1363.
41. Toyoda K., Nagae R., Akagawa M., Ishino K., Shibata T., Ito S., Shibata N., Yamamoto T., Kobayashi M., Takasaki Y., et al.// Protein-bound 4-hydroxy-2-nonenal: an endogenous triggering antigen of antI-DNA response. J Biol Chem. 2007. 282. 25769–25778.
42. Younis N., Sharma R., Soran H., Charlton-Menys V., Elseweidy M., Durrington P.N. // Glycation as an atherogenic modification of LDL. Curr Opin Lipidol. 2008. 19. 378–384.
43. Akagawa M., Ito S., Toyoda K., Ishii Y., Tatsuda E., Shibata T., Yamaguchi S., Kawai Y., Ishino K., Kishi Y., et al.// Bispecific abs against modified protein and DNA with oxidized lipids. Proc Natl Acad Sci U S A. 2006. 103. 6160–6165.
44. Horiuchi S., Murakami M., Takata K., Morino Y.// Scavenger receptor for aldehyde-modified proteins. J. Biol. Chem. 1986. 261. 4962–4966.
45. Zhou Z.H., Tzioufas A.G., Notkins A.L.// Properties and function of polyreactive antibodies and polyreactive antigen-binding B cells. J Autoimmun. 2007. 29. 219–228.
46. Kawarada Y., Miura N., Sugiyama T.// Antibody against single-stranded DNA useful for detecting apoptotic cells recognizes hexadeoxynucleotides with various base sequences. J Biochem. 1998. 123. 492–498.
47. Frankfurt O.S., Robb J.A., Sugarbaker E.V., Villa L.// Monoclonal antibody to single-stranded DNA is a specific and sensitive cellular marker of apoptosis. Exp Cell Res. 1996. 226. 387–397.
48. Shuster A.M., Gololobov G.V., Kvashuk O.A., Bogomolova A.E., Smirnov I.V., Gabibov A.G.// DNA hydrolyzing autoantibodies. Science. 1992. 256. 665–667.
49. Kim Y.R., Kim J.S., Lee S.H., Lee W.R., Sohn J.N., Chung Y.C., Shim H.K., Lee,S.C., Kwon M.H., Kim Y.S.// Heavy and light chain variable single domains of an anti-DNA binding antibody hydrolyze both double- and single-stranded DNAs without sequence specificity. J Biol Chem. 2006. 281. 15287–15295.
50. Gololobov G.V., Chernova E.A., Schourov D.V., Smirnov I.V., Kudelina I.A., Gabibov A.G.// Cleavage of supercoiled plasmid DNA by autoantibody Fab fragment: application of the flow linear dichroism technique. Proc Natl Acad Sci U S A. 1995. 92. 254–257.
51. Gololobov G.V., Rumbley C.A., Rumbley J.N., Schourov D.V., Makarevich O.I., Gabibov A.G., Voss E.W., Jr., Rodkey L.S.// DNA hydrolysis by monoclonal anti-ssDNA autoantibody BV 04-01: origins of catalytic activity. Mol Immunol. 1997. 34. 1083–1093.
52. Wellmann U., Letz M., Herrmann M., Angermuller S., Kalden J.R., Winkler T.H. //The evolution of human anti-double-stranded DNA autoantibodies. Proc Natl Acad Sci U S A. 2005. 102. 9258–9263.
53. Demaison C., Chastagner P., Theze J., Zouali M.// Somatic diversification in the heavy chain variable region genes expressed by human autoantibodies bearing a lupus-associated nephritogenic anti-DNA idiotype. Proc Natl Acad Sci U S A. 1994. 91. 514–518.
54. Harada T., Suzuki N., Mizushima Y., Sakane T.// Usage of a novel class of germ-line Ig variable region gene for cationic anti-DNA autoantibodies in human lupus nephritis and its role for the development of the disease. J Immunol. 1994. 153. 4806–4815.
55. O'Keefe T.L., Datta S.K., Imanishi-Kari T.// Cationic residues in pathogenic anti-DNA autoantibodies arise by mutations of a germ-line gene that belongs to a large VH gene subfamily. Eur J Immunol. 1992. 22. 619–624.
56. Tanner J.J., Komissarov A.A., Deutscher S.L.// Crystal structure of an antigen-binding fragment bound to single-stranded DNA. J Mol Biol. 2001. 314. 807–822.
57. Herron J.N., He X.M., Ballard D.W., Blier P.R., Pace P.E., Bothwell A.L., Voss E.W., Jr., Edmundson A.B.// An autoantibody to single-stranded DNA: comparison of the three-dimensional structures of the unliganded Fab and a deoxynucleotide-Fab complex. Proteins. 1991. 11. 159–175.
58. Giusti A.M., Chien N.C., Zack D.J., Shin S.U., Scharff M.D.// Somatic diversification of S107 from an antiphosphocholine to an anti-DNA autoantibody is due to a single base change in its heavy chain variable region. Proc Natl Acad Sci U S A. 1987. 84. 2926–2930.
59. Kieber-Emmons T., von Feldt J.M., Godillot A.P., McCallus D., Srikantan V., Weiner D.B., Williams W.V.// Isolated VH4 heavy chain variable regions bind DNA characterization of a recombinant antibody heavy chain library derived from patient(s) with active SLE. Lupus. 1994. 3. 379–392.
60. Siminovitch K.A., Chen P.P.// The biologic significance of human natural autoimmune responses: relationship to the germline, early immune and malignant B cell variable gene repertoire. Int Rev Immunol. 1990. 5. 265–277.
61. Siminovitch K.A., Misener V., Kwong P.C., Song Q.L., Chen P.P.// A natural autoantibody is encoded by germline heavy and lambda light chain variable region genes without somatic mutation. J Clin Invest. 1989. 84. 1675–1678.
62. Sanz I., Dang H., Takei M., Talal N., Capra J.D.// VH sequence of a human anti-Sm autoantibody. Evidence that autoantibodies can be unmutated copies of germline genes. J Immunol. 1989. 142. 883–887.
63. Planque S., Bangale Y., Song X.T., Karle S., Taguchi H., Poindexter B., Bick R., Edmundson A., Nishiyama Y., Paul S.// Ontogeny of proteolytic immunity: IgM serine proteases. J Biol Chem. 2004. 279. 14024–14032.
64. Matejuk A., Beardall M., Xu Y., Tian Q., Phillips D., Alabyev B., Mannoor K., Chen C.// Exclusion of natural autoantibody-producing B cells from IgG memory B cell compartment during T cell-dependent immune responses. J Immunol. 2009. 182. 7634–7643.
65. Brown M., Schumacher M.A., Wiens G.D., Brennan R.G., Rittenberg M.B.// The structural basis of repertoire shift in an immune response to phosphocholine. J Exp Med. 2000. 191. 2101–2112.
66. Tawfik D.S., Chap R., Green B.S., Sela M., Eshhar Z.// Unexpectedly high occurrence of catalytic antibodies in MRL/lpr and SJL mice immunized with a transition-state analog: is there a linkage to autoimmunity? Proc Natl Acad Sci U S A. 1995. 92. 2145–2149.

M. tuberculosis Gene Expression during Transition to the "Non-Culturable" State

E.G. Salina[1], H.J. Mollenkopf[2]*, S.H.E. Kaufmann[2], A.S. Kaprelyants[1]
[1]A.N. Bach Institute of Biochemistry, RAS, 119071, Moscow, Leninsky pr., 33, fax (495) 954-27-32, elenasalina@mail.ru
[2]Max Planck Institute for Infection Biology, 10117, Berlin, Chariteplatz 1, fax 49-30-284 605 01,
*E-mail: mollenkopf@mpiib-berlin.mpg.de

ABSTRACT We analyzed the gene expression profile under specific conditions during reversible transition of *M. tuberculosis* cells to the "non-culturable" (NC) state in a prolonged stationary phase. More than 500 genes were differentially regulated, while 238 genes were upregulated over all time points during NC cell formation. Approximately a quarter of these upregulated genes belong to insertion and phage sequences indicating a possible high intensity of genome modification processes taking place under transition to the NC state. Besides the high proportion of hypothetical/conserved hypothetical genes in the cohort of upregulated genes, there was a significant number of genes belonging to intermediary metabolism, respiration, information pathways, cell wall and cell processes, and genes encoding regulatory proteins. We conclude that NC cell formation is an active process involved in the regulation of many genes of different pathways. A more detailed analysis of the experimental data will help to understand the precise molecular mechanisms of dormancy/latency/persistence of *M. tuberculosis* in the future. The list of upregulated genes obtained in this study includes many genes found to be upregulated in other models of *M. tuberculosis* persistence. Thirteen upregulated genes, which are common for different models, can be considered as potential targets for the development of new anti-tuberculosis drugs directed mainly against latent tuberculosis.
Keywords: *M. tuberculosis*, latent tuberculosis, "non-culturable" cells, global gene expression profile

INTRODUCTION

Mycobacterium tuberculosis – the causative agent of tuberculosis – can persist in the human host for decades after infection. Such a latent *M. tuberculosis* state is traditionally connected with its transition to the dormant state, accompanied by loss of culturability [1]. This makes it practically impossible to reveal latent infection by traditional biochemical and microbiological means and attempt to cure it by antibiotic therapy. To study latent infection in live organisms, several modifications of the experimental model of dormancy during hypoxia *in vitro* are used [2, 3]. However, none of them imitates such an important state of bacteria as their "non-culturability" in the dormant state. We have established an experimental model where dormant *M. tuberculosis* cells are "non-culturable" (NC) and can reactivate under special conditions [4].

To reveal the biochemical processes accompanying the transition of bacteria to the NC state and to understand the mechanisms of this phenomenon, we analyzed *M. tuberculosis* gene expression profile during the formation of NC cells.

METHODS

M. tuberculosis total RNA samples were extracted from cells in the late logarithmic phase (5 days of cultivation) and during the transition of cells to the NC state under incubation in the stationary phase at different time points (21, 30, 41 and 62 days of cultivation) as described previously [5]. cDNA was generated from 1μg RNA using random hexamers and reverse transcriptase (Superscript III, Invitrogen, Karlsruhe, Germany) according to the manufacturer's instructions. Reverse transcribed samples were purified with the QIAquick PCR purification kit (Qiagen, Hilden, Germany) and labeled with Cy3- and Cy5-ULS according the suppliers' recommendations (Kreatech Diagnostics, Amsterdam, The Netherlands). Finally, labeled samples were purified with KREApure spin columns. Microarray experiments were performed as dual-color hybridizations. In order to compensate for the specific effects of the dyes and to ensure statistically relevant data, a color-swap dye-reversal analysis was performed. Cy3-labeled cDNA (250ng) corresponding to cells from different time points in the stationary phase was competitively hybridized with the same amount of Cy5-labeled cDNA of the control sample as color-swap technical replicates onto self-printed microarrays comprising a collection of 4,325 M. *tuberculosis*-specific "Array-Ready" 70mer DNA oligonucleotide capture probes and 25 control sequences (Operon Biotechnologies, Koeln, Germany) at 42°C for 20 h. Arrays were washed 3 times using a SSC wash protocol followed by scanning at 10 μm (Microarray Scanner BA, Agilent, Technologies, Waldbronn, Germany). Image analysis was carried out with Agilent's feature extraction software version (Agilent, Technologies, Waldbronn, Germany). The extracted MAGE-ML files were further analyzed with the Rosetta Resolver Biosoftware, Build 7.1 (Rosetta Biosoftware, Seattle, USA). Ratio profiles comprising color-swap hybridizations were combined in an error-weighted fashion to create ratio experiments. Anticorrelation of dye-reversals was determined by the compare function of Resolver. Next we applied a Student's t-test. Finally, by combining a 1.5-fold change cutoff to ratio experiments and the anticorrelation criterion together with the signatures from the Student's t-test, all valid data points had a P-value < 0.01, rendering the analysis highly robust and reproducible.

RESULTS AND DISCUSSION

We found earlier that *M. tuberculosis* cultivation in the modified Sauton medium without K^+ supplemented by dextrose, BSA, and sodium chloride led to a decrease in colony forming units (CFU) on the solid medium in the stationary phase [4]. After 60 days of cultivation, the CFU count dropped to 10^5 per ml **(Fig. 1),** which meant a transition of 99.9% of cells to the NC state. During further cultivation of cells, spontaneous recovery of NC cells was observed. It is important that the NC state was reversible, and that cells with a minimum CFU count could be reactivated after regrowing them in fresh medium.

Comparison of the gene expression profile at different time points from the stationary to the logarithmic phase (5-day cultivation) revealed a different expression (at least 1.5-fold) for a significant number of genes (566), which corresponds to 14% of the *M. tuberculosis* genome. Some 238 genes are upregulated and 237 downregulated over all time points during the entire culture period. **Table 1** shows the functional category of differentially regulated genes during the transition of cells to the NC state.

Besides the significant amount of conserved hypotheticals/unknown genes, many genes involved in the intermediary metabolism and respiration, virulence, detoxification and adaptation, lipid metabolism, information pathways, cell wall and cell processes were downregulated.

A considerable amount of genes coding hypothetical proteins were also found to be upregulated in the NC state: remarkably, genes encoding insertion sequences and phages represented about a quarter of the genes upregulated in the NC state, whereas their proportion in the genome was smaller – only 3.7%. This fact is a possible illustration of the high intensity of genome modification processes during the transition of cells to the NC state.

A significant proportion of upregulated genes belonged to the intermediary metabolism and respiration category, in particular, *gcvB* and *ald,* coding, respectively, glycine dehydrogenase and L-alanine dehydrogenase, proteases *pepR* and *clpC2*. *icl1* – one of the genes coding isocitrate lyase, anaplerotic enzyme, existing in the *M. tuberculosis* cells in two isoforms icl 1 and icl 2 – was found upregulated. Isocitrate lyase is the key enzyme of the glyoxylate cycle – a metabolic pathway, which is an alternative for the tricarboxylic acid cycle and allows the synthesis of carbohydrates from simple precursors. In particular, it plays an important role in seed germination, where fatty acids are used as the main storage of carbon and energy. The induction of some genes involved in lipid degradation, such as *fadD9*, *fadE24*, *fadE26*, and fatty acid degradation, *scoA*, is indicative of the active role of the glyoxylate cycle in NC cells already found for the Wayne persistence model [2].

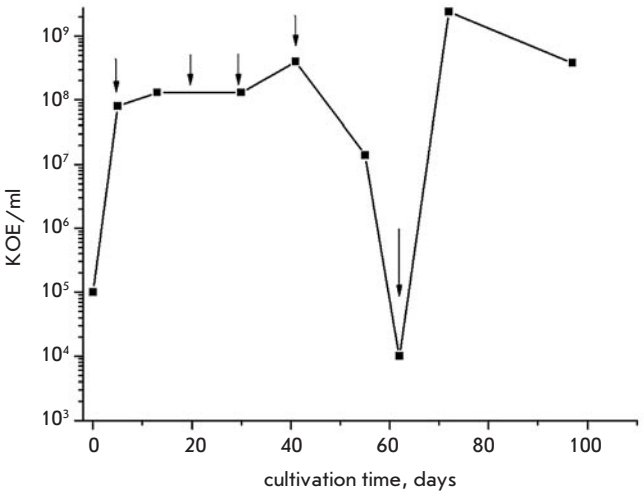

Fig. 1. Formation of NC *M. tuberculosis* cells in the stationary phase. Time points where RNA was isolated are marked by arrows

Table 1. Functional categories of *M. tuberculosis* genes with changed expression level during transition to the NC state

Functional categories	Genes induced during transition to the NC state		Genes repressed during transition to the NC state		Percent (%) in the genome
	Number of genes	%	Number of genes	%	
Virulence, detoxification, adaptation	5	2.1	7	2.9	2.6
Lipid metabolism	6	2.5	20	8.4	5.9
Information pathways	13	5.5	23	9.7	5.8
Cell wall and cell processes	24	10.1	59	24.8	18.8
Insertion sequences and phages	58	24.4	1	0.4	3.7
PE/PPE	7	2.9	11	4.6	4.2
Intermediary metabolism and respiration	42	17.7	50	21.1	22.4
Regulatory proteins	16	6.7	4	1.7	4.8
Unknown/hypothetical	67	28.1	63	26.5	31.9
Total number of genes	238	–	237	–	3924/100

Table 2. Significantly upregulated genes during transition to the NC state in the stationary phase

ORF	Gene	Gene product	Change of gene expression level				
			5 days	21 days	30 days	41 days	62 days
Rv0186	*bglS*	Beta-glucosidase	1	4.20459	8.33686	6.51867	5.24295
Rv0840c	*pip*	Proline iminopeptidase	1	6.33559	11.0004	4.58881	3.86572
Rv0841c		Transmembrane protein	1	31.11093	52.56174	13.79488	11.85425
Rv0989c	*grcC2*	Polyprenil-diphosphate synthase	1	7.60797	6.29748	7.58723	3.94285
Rv0990c		Hypothetical protein	1	7.12899	6.60915	6.652	3.57343
Rv0991c		Conserved hypothetical protein	1	3.31598	3.87521	5.44297	3.70462
Rv1369c		Transposase	1	3.17178	3.9213	4.22925	3.86883
Rv1394c	*cyp132*	Cytochrome P450 132	1	8.89047	7.50161	3.72981	3.12534
Rv1395		Transcriptional regulatory protein	1	3.22394	11.65875	7.03908	4.27327
Rv1397c		Conserved hypothetical protein	1	6.95276	11.79184	5.97336	5.77752
Rv1460		Transcriptional regulatory protein	1	3.87617	5.50637	6.90405	3.78332
Rv1575		phiRV1 phage protein	1	17.29509	37.08693	51.7473	20.53329
Rv1576c		phiRV1 phage protein	1	28.17817	33.97652	10.11378	12.88182
Rv1577c		phiRV1 phage protein	1	26.27261	39.87495	19.41512	11.49041
Rv1584c		phiRV1 phage protein	1	3.27674	5.68552	3.3055	3.02886
Rv1831		Hypothetical protein	1	3.1468	5.74692	5.14019	4.04747
Rv1991c		Conserved hypothetical protein	1	4.04696	4.12618	4.06786	4.65579
Rv1992c	*ctpG*	Metal cation transporter ATPase	1	5.2883	7.31348	4.7442	4.22806
Rv2106		Transposase	1	3.01418	5.61324	4.77882	5.09925
Rv2254c		Integral membrane protein	1	7.09534	6.53956	3.33899	4.63885
Rv2278		Transposase	1	3.28663	6.78129	6.28036	4.13102
Rv2354		Transposase	1	3.1594	6.15299	5.21098	3.13151
Rv2497c	*pdhA*	Pyruvate dehydrogenase alpha subunit	1	3.73133	4.52197	5.04976	4.00306
Rv2642		ArsR family transcriptional regulator	1	3.76985	5.16757	4.39006	3.93426
Rv2644c		Hypothetical protein	1	3.36059	7.58921	5.36796	3.51825
Rv2645		Hypothetical protein	1	3.45006	8.21393	6.70101	3.25709
Rv2646		Integrase	1	5.04391	12.16535	7.82435	9.96087
Rv2647		Hypothetical protein	1	5.32983	13.40623	9.43796	7.2163
Rv2649		Transposase IS6110	1	3.2505	5.3557	5.59089	3.74714
Rv2650c		phiRv2 prophage protein	1	21.46669	29.74372	16.65359	20.66349
Rv2651c		phiRv2 prophage protease	1	20.04086	34.29153	20.61728	13.41666
Rv2660c		Hypothetical protein	1	13.43717	41.25793	67.29882	19.6699
Rv2661c		Hypothetical protein	1	9.23174	28.30861	52.34967	11.04351
Rv2662		Hypothetical protein	1	20.62942	18.83647	14.72059	12.88898
Rv2663		Hypothetical protein	1	7.61461	9.43216	8.19525	7.3034
Rv2664		Hypothetical protein	1	6.24636	8.49102	7.10191	5.60291
Rv2666		Truncated transposase IS1081	1	6.91867	13.89339	7.89331	5.86579
Rv2667	*clpC2*	ATP-dependent protease	1	9.44815	17.89662	9.64508	6.46149
Rv2707		Conserved transmembrane protein	1	3.35002	5.09024	14.83903	4.53239
Rv2711	*ideR*	Transcriptional regulatory protein	1	3.48877	4.30099	6.06795	3.83858
Rv2713	*sthA*	Soluble pyridine nucleotide transhydrogenase	1	4.43327	6.35516	6.80833	3.83838
Rv2780	*ald*	Secreted L-alanine dehydrogenase ALD	1	5.2891	4.65988	4.52694	4.92656
Rv2814c		Transposase	1	3.3279	5.52338	4.86873	4.60102
Rv2815c		Transposase	1	3.13667	6.24306	5.87423	4.84337
Rv3185		Transposase	1	3.58899	6.43621	5.67335	5.82686
Rv3186		Transposase	1	3.2903	6.21375	6.14822	5.77427
Rv3290c	*lat*	L-lysine aminotransferase	1	4.32023	5.06387	3.54801	3.9704
Rv3474		Transposase IS6110	1	3.04947	6.19754	6.19869	3.22266
Rv3475		Transposase IS6110	1	3.73966	5.79892	5.63617	6.23465
Rv3580c	*cysS*	Cysteinyl-tRNA synthetase	1	3.87797	6.67899	3.14124	3.40852
Rv3582c	*ispD*	2-C-methyl-D-erythritol 4-phosphate cytidylyltransferase	1	3.50012	4.07861	3.78626	3.51221

During transition to the NC state, some genes used as markers of stress conditions were induced: the heat-shock protein *hsp*, the chaperones Rv0440 and Rv3417c, as well as sigma-factors: *sigG* – regulating genes which are necessary for survival inside the macrophages and *sigB*, which can control stationary phase regulons and general resistance to stress. Induction of *ccsA*, whose product takes part in the cytochrome biosynthesis at the step of heme attachment, and *cyp132*, coding one of the cytochrome's P450 oxidizing different xenobiotics, could evidently reflect accumulation of toxic components in cultures during transition. Enzymes of the non-mevalonate pathway of isoprenoid biosynthesis *ispF* and *ispD* were also induced in the NC cells. There are data indicating that some of the metabolites of this pathway can affect the immune response of the host [6]. A number of induced genes are involved in the information pathways and those encoding regulatory proteins; in particular, the transcriptional regulator *furA*, which acts as a global negative control element, employing Fe^{2+} as a cofactor to bind the operator of the repressed genes. It seems to regulate the transcription of *katG*, which is induced in the NC state. *katG* encodes a multifunctional enzyme, exhibiting both catalase, a broad-spectrum peroxidase and peroxynitritase activities and is believed to play a role in the intracellular survival of mycobacteria within macrophages, protecting them against the aggressive components produced by phagocytic cells. Some genes taking part in the cell wall and cell processes, in particular the transporters *ctpG* and *ctpC* encoding ATPases-transporting metal cations and the transporter Rv2688c involved in antibiotic resistance and export of antibiotics across the membrane, are activated.

To identify the genes that were significantly upregulated during transition to the NC state, we used stringent criteria: the expression level during the whole time course in the stationary phase was upregulated at least 3-fold in comparison to the expression in the logarithmic phase. Fifty-one genes met this criterion **(Table 2).**

Among the genes with a substantially high level of expression, genes encoding insertion sequences and phages – 20 genes out of the 51– are prime candidates, while 13 genes encode hypothetical proteins with unknown function. It is remarkable that the significantly upregulated genes belonged to intermediary metabolism and the respiration category. Moreover, these genes mainly encode proteins involved in degradation processes; namely *bglS* – beta-glycosidase (hydrolyzes the terminal, non-reducing beta-D-glucose residue); *pip* – proline iminopeptidase (specifically catalyses the removal of N-terminal proline residues from small peptides); *clpC2* ATP-dependent protease; and *ald* – L-alanine dehydrogenase (catalyses alanine hydrolyze – an important constituent of the peptidoglycan layer). In addition, the *pdhA* coding the alpha subunit of pyruvate dehydrogenase and taking part in the energetic metabolism and catalyzing the conversion of pyruvate to acetyl-CoA was highly expressed. Significant upregulation of *sthA*, a soluble pyridine nucleotide transhydrogenase that catalyses the conversion of NADPH generated by catabolic pathways to NADH, which is oxidized by the respiratory chain for energy generation, is a sign of the prevalence of catabolic reactions in cell metabolism in the NC state.

Analysis of the global gene expression profile has been published for several *M. tuberculosis* persistence models, in particular the Wayne model of the non-replicating state during hypoxia [5,7,8], the gradual depletion of the carbon source under decreased oxygen tension [9], the adaptation of *M. tuberculosis* within macrophages [10], and *in vivo* within artificial granulomas in mice [11]. Considering the results of these studies, the gene expression profile in our model of "non-culturability" in the stationary phase has, evidently, some overlaps with the above-mentioned models of persistence (**Table 3**).

Little in common was found between the genes induced in our model of "non-culturability" and the Wayne dormancy model during hypoxia (**Table 3**). The Wayne model is characterized by the induction of genes of the dormancy survival regulon (Dos-regulon), a group of 49 genes under the control of *devR* which codes the regulatory part of the two-component system. Upregulation of the Dos-regulon was found not only for dormant cells under hypoxia *in vitro*, but also for *M. tuberculosis* cells within macrophages [10], and in the artificial granulomas in mice [11]. In our model of *M. tuberculosis* transition to the NC state in the stationary phase, only two genes from Dos-regulon – Rv0571c and Rv2631 – were found upregulated. Dos-regulon induction was not found in the persisting cells during starvation [12], and only two genes of Dos-regulon were activated during persistence at gradual depletion of the carbon source [9].

A recently published paper [13] demonstrated that the role of Dos-regulon is apparently overestimated not only as a universal regulator of the dormant state of mycobacteria, but also as a general response on hypoxia. Genes of the Dos-regulon were shown to be activated only 2 hours after hypoxia.

Table 3. Comparison of genes upregulated during transition to the NC state in the stationary phase (at least 1.5-fold) to the genes activated in other models of persistence

Models of *M. tuberculosis* persistence	**Overlapping to 238 genes activated in the stationary phase during transition to the NC state.**	
	Number of genes	**%**
Wayne non-replicating state (Voskuil *et al.*, 2004)	23	9.7
Persistence at gradual depletion of carbon source at 50% oxygen tension (Hampshire *et al.*, 2004)	82	34.5
Persistence within macrophages (Schnappinger *et al.*, 2003)	77	32.4
Artificial granuloma in mice (Karakousis *et al.*, 2004)	32	13.4
Enduring hypoxia response (Rustad *et al.*, 2008)	40	16.8

Table 4. Shared genes of *M. tuberculosis* persistence state. Genes of EHR regulon are in bold

ORF	Gene	Non-replicating state of Wayne (Voskuil et al., 2004)	Gradual depletion of carbon source (Hampshire et al., 2004)	Persistence within macrophages (Schnappinger et al., 2003)	Artificial granuloma in mice (Karakousis et al., 2004).	NC state in the stationary phase (this study)
Rv0188		0.8	67.2	2.8	2.7	2.5
Rv0211	*pckA*	-	1.7	3.6	2.6	1.64
Rv0251c	***hsp***	**4.5**	**18.6**	**25.6**	3.9	**4.5**
Rv1894c		2.0	5.1	1.8	-	2.8
Rv1909c	***furA***	-	**5.4**	**2.2**	2.8	**2.7**
Rv2011c		**2.1**	**9.5**	**2.5**	-	**2.8**
Rv2497c	***pdhA***	**3.4**	**8.4**	**2.1**	2.0	**4.0**
Rv2660c		**1.5**	**4.3**	**2.1**	3.3	**19.7**
Rv2662		**1.5**	**1.5**	**2.0**	-	**12. 9**
Rv2710	*sigB*	-	34.6	3.8	4.7	4.6
Rv2780	*ald*	6.1	2.6	2.4	2.4	4.9
Rv3139	*fadE24*	-	2.2	2.0	5.8	2.4
Rv3290c	*lat*	3.6	25.9	7.5	5.6	4.0

Thereafter expression of at least half of these returned to the baseline [13]. The authors observed a significant induction of another 230 genes after further cultivation during hypoxia, and hereafter their expression level was stable. Thus, the authors refer to this group of genes as enduring hypoxia response (EHR) genes. Considering the gene expression profile for our model of transition to the NC state, we found significant overlap with this group of genes **(Table 3),** which was rather unexpected because the conditions for NC cell formation developed in our laboratory did not imply any oxygen limitation. Some overlap with EHR [13] was found for the persistence model of gradual depletion of the carbon source [9] and the transcriptional response to multiple stresses [14]. Therefore, it is possible to conclude that EHR genes may not only play a role as hypoxia markers, but may also be a general regulon of the dormant state of *M. tuberculosis,* independent of its induction.

Thus, the data presented here indicate that cell transition to dormant state is an active process and that numerous genes are involved in it. The future task is to investigate this process in detail in order to understand the molecular mechanisms in the cells during the transition to the dormant state.

Based on the results of the transcriptome analysis of the NC cells obtained in our model and those obtained in several models of persistence, it is possible to pinpoint some shared genes that are upregulated in these models **(Table 4**). The genes presented in **Table 4** and their products are believed to be important for further study, because some of them could represent new targets for anti-tuberculosis drug candidates directed mainly against latent tuberculosis. ●

This work was supported by the Program of the Presidium of the RAS "Molecular and Cellular Biology"

REFERENCES

1. Gangadharam P. R. J. *Tuber. Lung Dis.*, 1995, **76**, 477-479.
2. Wayne L. G. and Lin K.-Y. *Infect. Immun.*, 1982, **37**, 1042-1049.
3. Wayne L. G. and Hayes L. G. *Infect. Immun.*, 1996, **64**, 2062-2069.
4. Mukamolova G. V., Salina E. G., Kaprelyants A. C. in *National Institute of Allergy and Infectious Diseases, NIH* (Georgiev, V., ed), Humana Press, USA, 2008, **1**, 83-90.
5. Voskuil M. I., Visconti K. C., Schoolnik G. K. *Tuberculosis* (Edinb.), 2004, **84**, 218-227.
6. Shao L., Zhang W., Zhang S., Chen CY., Jiang W., Xu Y., Meng C., Weng X., Chen Z.W. *AIDS*, 2008, **22(17),** 2241-508.
7. Muttucumaru D. G., Roberts G., Hinds J., Stabler R. A., Parish, T. *Tuberculosis (Edinb.),* 2004, **84**, 239-246.
8. Bacon J., James B. W., Wernisch L., Williams A., Morley K. A., Hatch G.J., Mangan J.A., Hinds J., Stoker N.G., Butcher P.D., and Marsh P.D. *Tuberculosis (Edinb.),* 2004, **84**, 205-217.
9. Hampshire T., Soneji S., Bacon J., James B. W., Hinds J., Laing K., Stabler R. A., Marsh P. D., and Butcher P. D. *Tuberculosis (Edinb),*2004, **84**, 228-238.
10. Schnappinger D., Ehrt S., Voskuil M. I., Liu Y., Mangan J. A., Monahan I. M., Dolganov G., Efron B., Butcher P. D., Nathan C., Schoolnik G. K. *J. Exp Med.*, 2003, **198(5),** 693-704.
11. Karakousis P. C., Yoshimatsu T., Lamichhane G., Woolwine S. C., Nuermberger E.L., Grosset J., Bishai, W. R. *J. Exp. Med.*, 2004, **200**, 647-657.
12. Betts J. C., Lukey P. T., Robb L. C., McAdam R. A., and Duncan K. *Mol. Microbiol.,* 2002, **43**, 717-731.
13. Rustad T. R., Harrell M. I., Liao R, Sherman D. R.. *PLoS ONE*, 2008, **3(1)**, 1502.
14. Boshoff H. I., Myers T. G., Copp B. R., McNeil M. R., Wilson M. A., and Barry C. E., 3rd *J. Biol. Chem.*, 2004, **279,** 40174-40184.

Relative Comparison of Catalytic Characteristics of Human Foamy Virus and HIV-1 Integrases

E. S. Knyazhanskaya[1], M. A. Smolov[2], O. V. Kondrashina[2], M. B. Gottikh[3]*
[1] Chemistry Department of MSU and MSU
[2] Department of Bioengineering and Bioinformatics of MSU,
[3] A. N. Belozersky Institute of Physico-Chemical Biology, M. V. Lomonosov Moscow State University, Leninskie Gory, Moscow, 119992.
*E-mail: gottikh@libro.belozersky.msu.ru

ABSTRACT Due to their ability to integrate into the host cell's genome, retroviruses represent an optimal basis for the creation of gene therapy vectors. The integration reaction is carried out by a viral enzyme integrase: thus, a detailed research of this enzyme is required. In this work, the catalytic properties of human foamy virus integrase were studied. This virus belongs to the Retroviridae family. The dissociation constant was determined, together with the kinetics of integrase catalytic activity. The data obtained were compared to those for the human immunodeficiency virus integrase and a considerable similarity in the activity of the two enzymes was observed.
Keywords HIV – (Human immunodeficiency virus), HFV – (Human foamy virus), integrase, catalytic activity

Due to their ability to integrate into the genomes of non-dividing cells, retroviruses are widely used as a base for gene therapy vectors construction. A number of papers [1-6] report on systems employing human immunodeficiency virus type 1 integrase (HIV-1 IN) as a basis for the creation of constructs enabling integration of a certain vector into a given DNA sequence. However, directed integration vectors on the basis of HIV carry a potential danger to human health because of their high pathogenicity. In this regard, human foamy virus (HFV), which infects human cells efficiently, but is not pathogenic [7], seems attractive. HFV belongs to the *Spumaviridae* genus of the retrovirus family and carries an enzyme, integrase (HFV IN), which accomplishes the integration of the viral genome into the host cell's genome. At present, the HFV IN catalytic properties are relatively little-studied. In this paper, an attempt has been made to explore the IN HFV catalytic properties and compare them with those of HIV-1 IN, so as to evaluate the potential for using HFV integrase for site-directed integration.

One of the factors hampering the study of the catalytic properties of retroviral integrases is their low activity: to accomplish 3'-processing, a very large excess of the enzyme over DNA is required (usually > 30:1). Therefore, in our study of the HFV IN properties we first explored the dependence of the 3'-processing efficiency on the enzyme concentration in the reaction mixture. To this end, synthetic DNA duplexes imitating the terminal sequence of the U5 domain of the viral DNA's long terminal repeat were employed. Incubation of IN with such DNA-substrate resulted in dinucleotide removal from the 3'-end of the processed strand (U5B-strand). For both Ins, maximum reaction efficiency was achieved at an enzyme concentration of 100 nM (Figure 1). HIV IN's low enzymatic activity is accounted for by the single-turnover mechanism of the catalytic process, the causes for which include the formation of a strong complex between the enzyme and the DNA sequence [8]. Therefore, in the next step of our study of the HFV IN properties we explored the DNA-binding stage of the integration process.

In order to determine the dissociation constant of the HFV IN-DNA complex, we examined 2 or 10 nM DNA substrates binding at different enzyme concentrations (Figure

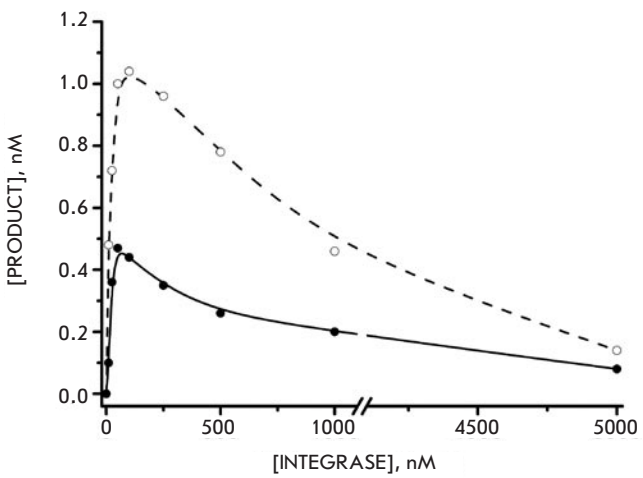

Figure 1. The influence of the HIV-1 (white spots) and HFV (black spots) integrase concentrations on the outcome of the 3'-processing reaction. The integrase solution (5nM - 5μM) was incubated with a 4 nM DNA substrate for 1h at 37 °C

2A). Application of the approach based on the simple ligand-receptor interaction theory to the system under study allowed employing equation (1)

$$[IN * DNA] = \frac{1}{2}\left([DNA]_0 + [IN]_0 + K_d' - \sqrt{\left([DNA]_0 + [IN]_0 + K_d'\right)^2 - 4 \times [DNA]_0 \times [IN]_0}\right) \quad (1)$$

to calculate the Kd value, which appeared to be 15-20 nM. This value indicates that the DNA forms a rather stronger complex with HFV IN than with HIV IN (40 nM [8]).

We also studied the DNA-binding kinetics of both enzymes by the fluorescence polarization method. The experiment was performed at 25°C, since it is known that under such conditions retroviral INs are capable of associating with their substrates without executing the substrates processing. When the IN solution was added to a fluorescently labeled DNA-duplex, an abrupt increase in the fluorescence signal's anisotropy, conditioned by a slower complex rotation, was observed (Figure 2B). The DNA-HIV IN complex formation is accomplished in 3-4 minutes, which is approximately five times longer than the time required for the DNA association with HFV IN [8]. This fact is also indicative of greater favorability of HFV IN binding to the DNA.

The results obtained accord well with the data on the time dependence of accumulation of the DNA-substrate's catalytic conversion products. Figure 3 presents the curves corresponding to accumulation of the products of the 3'-processing and strand-transfer reactions catalyzed by the two INs.

It can be seen that the lag-phase, preceding the linear growth phase of product accumulation, characteristic of HIV IN action, is entirely absent in the case of HFV IN. Instead, the process passes straight into the linear growth phase. The calculated stationary rates of product formation at this stage have similar values for both integrases (V_{linear} (HIV) = 0.011 nmole/min, V_{linear} (HFV) = 0.014 nmole/min) and are remarkably low, which is not typical for a multiple-turnover mode of the enzyme action at the concentrations concerned. It has been shown that the reason for such behavior of HIV INs isolated in the presence of zinc ions and in the absence of detergents according to the procedure in [9] is their low natural catalytic activity rather than low active protein form content in the preparations used. This leads to the inapplicability of the classical Michaelis-Menten formalism to the description of HIV IN's catalytic action. Instead, one has to employ kinetic equations which assume that the reactions catalyzed by the IN proceed under so-called "single-turnover" conditions, implicating a large excess of enzyme over the sub-

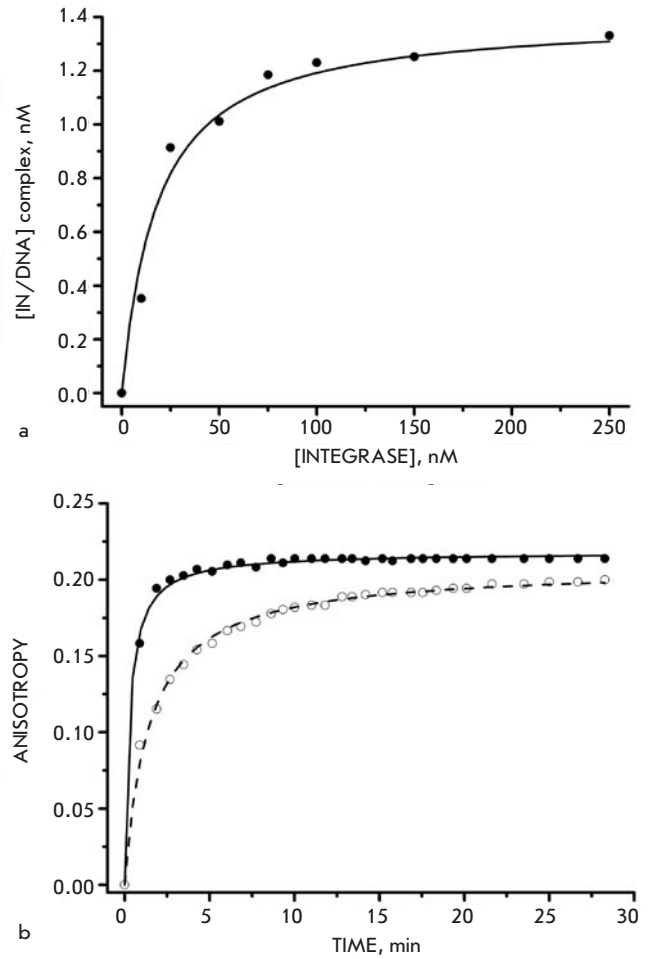

Figure 2. The binding of DNA with HIV and HFV Ins. (a). The isotherm of IN HFV binding a 2nM U5-HFV substrate. The incubation was carried out for 20 min at 25 °C in buffer solution containing 20 mM Tris (pH 7.2), 20 mM NaCl, 1 mM DTT, and a 5 mM $MgCl_2$. The DNA/protein complexes were analyzed by gel retardation assay. (b). The fluorescence polarization assay was applied for constructing the kinetics of the binding of a 4 nM DNA substrate by 100 nM HIV (white spots) and HFV (black spots) integrases at 25 °C

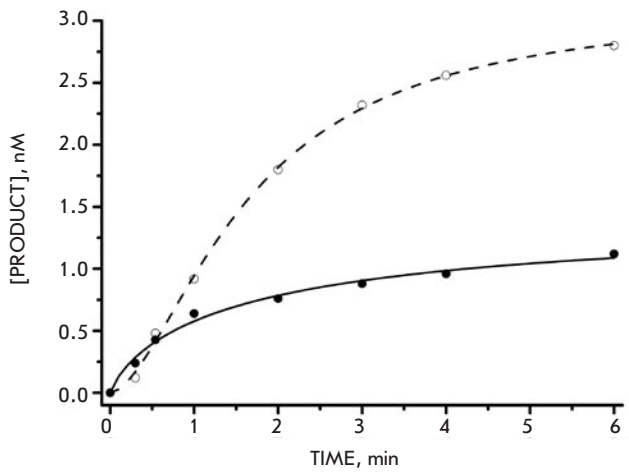

Figure 3. The kinetics of the 3'-processing reaction. The product accumulation curve of a 4 nM U5 substrate 3'-processing reaction while incubated with a 100 nM HIV (white spots) and HFV (black spots) integrases

strate [8]. The same assumption was made in case of HFV IN. The value of the catalytic constant analogue determined using the "single-turnover" approach appeared to be virtually the same for both enzymes ($k_{cat}' = 0.004 \pm 0.001$ min^{-1}), which also denotes similar properties of both integrases. Moreover, it should be noted that the value of the Michaelis constant analogue computed from kinetic data for HIV IN ($K_m = 30 \pm 5$ nM) coincides well with the value of the HIV IN-DNA complex dissociation constant ($K_d = 40$ nM). At the same time, for HFV IN such correlation is not observed. The calculated $K_m' = 60 \pm 10$ nM correlates very poorly with the determined K_d value (15-20 nM). Further we are planning to study the reasons for such a discrepancy.

In conclusion, our results demonstrate that HIV IN is similar to HIV-1 IN in its kinetic characteristics. In the nearest future, we plan to use this enzyme for creating a directed DNA integration system.

EXPERIMENTAL SECTION

Oligonucleotides

U5B-HIV (5'-GTGTGGAAAATCTCTAGCAGT-3'),
U5A-HIV (5'-ACTGCTAGAGATTTTCACAC-3'),
U5B-HFV (5'-ATACAAAATTCCATGACAAT-3'),
U5A-HFV (5'-ATTGTCATGGAATTTTGTAT-3')

were synthesized by the amidophosphite method on an automatic DNA synthesizer ABI 394 (Applied Biosystems) according to the standard procedure using commercial reagents (Glen Research) and purified by electrophoresis in 20% polyacrylamide gel containing 7M urea.

Recombinant HIV-1 integrase was expressed in Escherichia coli, isolated and purified without detergent as previously described [9]. HFV integrase was a kind gift of Dr. Mouscadet J-F. (Normal Superior School of Cachan, France).

3'-Processing was performed by incubating the corresponding 4 nM DNA-substrate, containing 5'-[P^{32}]-labeled processed strand U5B and HFV IN or HIV IN in 20 μL buffer (20 mM Hepes (pH 7.2), 1 mM DTT and 7.5 mM $MgCl_2$), at 37°C. The reaction was arrested by adding 80 μL of solution containing 10 mM Tris-HCl (pH 7.5), 0.3 M sodium acetate, 1 mM EDTA, and 0.125 μg /ml glycogen; the integrase was extracted with phenol, the reaction products were precipitated with ethanol and resuspended in 80% formamide-water solution. The products were separated by electrophoresis in 20% polyacrylamide gel under denaturating conditions (7M urea) with subsequent gel analysis on a Phosphorimager. The 3'-processing completion was determined by the appearance of a band corresponding to a 2-nucleotide truncated processed strand of the duplex on a radiograph.

Gel-retardation method. [P^{32}]-labeled DNA-substrate (2 or 10 nM) was incubated with HFV IN of different concentrations (0-300 nM) in a buffer containing 20 mM HEPES, pH 7.2, 1 mM DTT, 7.5 mM $MgCl_2$, and 5% glycerin at 25°C for 20 min. Afterwards, the mixture was analyzed by electrophoresis in 8% polyacrylamide gel in a buffer containing 20 mM Tris-CH_3COOH, pH 7.5, and 7.5 mM $MgCl_2$ at 4-8°C. Gel was analyzed using a STORM 840™ Phosphorimager (Molecular Dynamics). The effective dissociation constant was computed using equation (1).

Fluorescence polarization method. DNA-substrate (4 nM) containing a fluorescein residue in the 5'-processed strand U5B, was incubated with 100 nM HFV IN or HIV IN in 200 μL buffer containing 20 mM HEPES, pH 7.2, 1 mM dithiothreitol, and 7.5 mM $MgCl_2$ at 37°C. The fluorescence anisotropy alteration during the incubation was registered using a Cary Eclipse spectrophotometer (Varian).

Computation of the Michaelis constant and the catalytic constant analogues was done in a single-turnover mode using equation (2) according to the previously reported data [8]:

$$\ln\frac{[DNA]_0}{[DNA]_0-[DNA_P]} = k_{obs}\times t, \text{ где } k_{obs} = \frac{k_{cat}'}{\frac{K_m'}{[IN]_0}+1}. \qquad (2)$$

This work was supported by the Russian Foundation for Basic Research (grants 08-04-01252 and 09-04-93107-NCNIL).

REFERENCES

1. Goulaouic H, Chow S. A.// J. Virol. 1996 V. 70 P. 37-46.
2. Katz R. A, Merkel G, Skalka A. M. // Virology 1996 V. 217 (1) P. 178-190.
3. Bushman F. D. // Proc Natl Acad Sci U S A. V. 91 (20) P. 9233-9237.
4. Bushman F. D., Miller M. D. // J. Virol. V. 71(7) P. 458-464.
5. Tan W., Zhu K., Segal D. J., Barbas C. F. 3rd, Chow S. A. // J. Virol. 2004 V. 78(3) P. 1301-1313.
6. Tan W., Dong Z., Wilkinson T. A., Barbas C. F. 3rd, Chow S. A. // J. Virol. 2006 V. 80(4) P. 1939-1948.
7. Linial M. L. // J. Virol. V. 73 P. 1747-1755.
8. Smolov M., Gottikh M., Tashlitskii V., Korolev S., Demidyuk I., Brochon J. C., Mouscadet J. F., Deprez E. // FEBS J. 2006 V. 273 P. 1137-1151.
9. Leh, H., Brodin, P., Bischerour, J., Deprez, E., Tauc, P., Brochon, J. C., LeCam, E., Coulaud, D., Auclair, C. & Mouscadet, J.F. Biochemistry 2000, 39, 9285-9294.

Telomerase Complex from Yeast *Saccharomyces cerevisiae* Contains a Biotinylated Component

D.M. Shcherbakova, M.I. Zvereva,* and O.A. Dontsova
Department of Chemistry, Moscow State University,
Moscow, 119992 Russia,
*E-mail: zvereva@genebee.msu.su

ABSTRACT Telomerase adds telomeric repeats to single-stranded DNA at the ends of the chromosomes. This enzyme is a ribonucleoprotein complex. Telomerase from yeast *Saccharomyces cerevisiae* consists of TLC1 RNA, which serves as a template for the synthesis of telomeric repeats, telomerase reverse transcriptase Est2p, and a number of accessory proteins (Est1p, Est3p, Ku70/Ku80, and Sm-complex). We found that the yeast telomerase complex contains a biotinylated component. The telomerase fraction containing biotinylated protein is active *in vitro* and constitutes a small part of the total amount of active telomerase isolated from cells. We speculate about the nature of the biotinylated component.
Keywords: yeast telomerase, biotin, biotinylation.
Abbreviations: DEAE-fraction – telomerase isolated from yeast extract using chromatography on DEAE-cellulose

INTRODUCTION

Telomeres are located at the ends of eukaryotic chromosomes. These DNA-protein structures protect chromosomes from degradation and end-to-end fusion [1]. Telomerase is the enzyme that maintains the length of telomeres by adding telomeric DNA repeats to the 3'-ends of chromosomal DNA [2]. Telomerase is active in the cells of organisms able to unlimitedly propagate, in 85% of cancers [3], and in cells of unicellular eukariotes (ciliates and yeasts) [2, 4].

Telomerase is a ribonucleoprotein complex [5, 6]. In yeast *Saccharomyces cerevisiae*, telomerase is composed of telomerase reverse transcriptase Est2p [7]; telomerase RNA TLC1 [8], a region of which serves as a template for telomeric repeats synthesis; accessory proteins Est1p [9] and Est3p [10] (without which telomerase is inactive *in vivo*) [11]; and several other proteins (Sm-proteins [12], Ku-proteins [13], etc.). Other than subunits of the telomerase complex, there are several proteins that interact with telomerase and contribute to telomerase functioning. For example, Cdc13p, which tethers telomerase to telomere and is crucial for its activity, is not a subunit of telomerase, although it interacts with Est1p [14]. Currently, a large number of genes whose absence leads to telomere shortening are known [15]. Some proteins (e.g., chaperone Hsp82p [16]) have also been shown to interact with subunits of the telomerase complex. Such proteins are probably important for complex assembly or form a transient part of telomerase on a particular step of regulation. Therefore, the sophisticated arrangement of telomerase is related to the complex regulation of its activity. It is known that telomere elongation occurs during the late S phase of the cell cycle [17, 18], and telomerase preferentially extends the shortest telomeric ends [19–21]. Also, regulation may occur at the assembly stage of the telomerase complex and the degradation of its components. Revealing new interactions between various proteins and telomerase subunits, post-translational modifications of proteins important for telomerase activity, and the elucidation of its roles will lead us to a better understanding of how telomerase functions in a cell.

We found that an active telomerase complex contains a biotinylated compound. Such telomerase complexes comprise less than half of the total amount of telomerase isolated from cells.

MATERIALS AND METHODS

STRAINS Strain DBY-746 α (*ura3-52, leu2-3,112, trp1-289, his3-Δ1*) was used.

TELOMERASE PURIFICATION USING STREPTAVIDI-BASED AFFINITY CHROMATOGRAPHY The cell culture was grown to A_{600} = 1 in 3.2 liters of a SC – Trp medium supplemented with glucose. Cells were harvested by centrifugation (5 min, 5,000 rpm, 4°C, JA-10 rotor; Beckman, USA); washed four times with water; and, finally, washed with a "str" buffer (20 mM Tris-HCl, pH 7.5, 100 mM NaCl, 2 mM $MgCl_2$, 1 mM dithiothreitol (DTT), 0.1 mM EDTA, 10% (v/v) glycerol, 0.1% (v/v) Triton X-100). The cell pellet was mechanically disrupted in liquid nitrogen and thawed on ice with 10 ml of an ice-cold "str" buffer supplied with "Complete protease inhibitor" (Roche, Switzerland), phenylmethylsulfonyl fluoride (0.5 mM), and RNasin (40 U/ml of extract) (Helicon, Russia). The cell debris was removed by centrifugation (once at 5 min, 5,000 g and twice at 15 min, 15,000 rpm; 4°C, JA-20 rotor, Beckman, USA). An aliquot of the extract was used to measure the total protein concentration using the Compat-Able

Protein Assay Kit and BCA Protein Assay Reagent (Pierce Biotechnology, USA). During the experiment, the extract was pretreated with avidin: 10 μg of avidin per 1 mg of total protein was added, and the sample was incubated for 10 min at 4°C. Then, the yeast extract (10 mg/ml total protein) was added to a streptavidin-sepharose resin preequilibrated with a "str" buffer (200 μl of resin from GE Healthcare (USA) for 10 ml of extract). The mixture was incubated at 4°C for 1.5 h under agitation. Then, the resin was washed six times with a "str" buffer. The resin that was obtained and all other fractions were frozen in liquid nitrogen and stored at − 80°C for further analysis.

TELOMERASE PURIFICATION USING DEAE-BASED ANIONIC CHROMATOGRAPHY Yeast telomerase was prepared according to [4, 22] with a slight modification: the telomerase fraction was obtained by elution from a DEAE-cellulose column with a linear gradient concentration of sodium acetate (from 100 mM to 1 M). From 10 ml of the initial extract (10 mg/ml total protein), 1ml of the active telomerase fraction was obtained. Then it was aliquoted, frozen in liquid nitrogen, and stored at − 80°C for further analysis.

FRACTIONATION OF S100 EXTRACT AND DEAE-FRACTION IN A GLYCEROL DENSITY GRADIENT The yeast extract was prepared as described above for the isolation of telomerase using chromatography on straptavidin-sepharose, except that the YPD medium was used for cell growth and a lysis buffer (25 mM Tris-HCl (pH 7.5), 300 mM NaOAc, 2 mM $MgCl_2$, 1 mM DTT, 0,1 mM EDTA, 10% (v/v) glycerol) was used instead of a "str" buffer. Then, the S100 extract was obtained by the ultracentrifugation of the yeast extract (1h, 100,000*g*, 4°C, Ti-70 rotor; Beckman, USA). Then, it was concentrated on a Vivaspin 20 (Sartorius, Germany). The S100 extract (0.5 ml, 15 mg/ml total protein) or DEAE-fraction (0.5 ml) was loaded onto a 15−40% glycerol gradient (10.5 ml, in a lysis buffer). Ultracentrifugation was performed at the following conditions: 24h, 40,000rpm, 4°C, SW41 rotor; Beckman. Twenty-two fractions (0.5 ml each) were gathered, frozen in liquid nitrogen, and stored at − 80°C for further analysis.

IN VITRO TELOMERASE ASSAY Ten microliters of the sample (obtained after isolating the streptevidin-sepharose suspension, DEAE-fraction, or the fraction obtained by ultracentrifugation) was used in the elongation reaction. The final reaction mixture (20 μl) contained 50 mM Tris-HCl (pH 8.0), 5 mM $MgCl_2$, 1 mM DTT, 1 mM spermidine, 0.05 mM EDTA (contributed by telomerase fraction), 5% (v/v) glycerol or more for the sample obtained in ultracentrifugation (contributed by telomerase fraction), 100 μM dTTP, 20 μCi [α-32P]dGTP (3000 Ci/mmol), and 5 μM oligodeoxyribonucleotide TEL11 (5'-TGGTGTGTGGG-3'). Control reactions were pretreated with RNase A (1 μl of 10 mg/ml solution, 30 min, 30°C). The telomerase reaction was carried out for 1 h at 30°C followed by the addition of 200 μl of a "stop" buffer (20 mM Tris_HCl, pH 8.0, 20 mM EDTA, 0.2% SDS) and 3 μl proteinase K (20 mg/ml). After incubation at 30°C for 1 h, the reaction products were extracted twice with equal volumes of phenol, once with an equal volume of chloroform−isoamyl alcohol (24 : 1), and precipitated with 3 volumes of ethanol in the presence of 1/10 volume of 3 M NaOAc and 5 μg of tRNA from *E. coli* as a carrier. The pellet was washed twice with 80% ethanol, dried and dissolved in the formamide loading buffer (80% of deionized formamide, 1 × TBE buffer, 0.1% xylene cyanole, and 0.1% bromophenol blue). Reaction products, along with 5'-[^{32}P]-phosphorylated oligodeoxyribonucleotide TEL11 as a length marker, were separated electrophoretically in 15% TBE denaturing PAAG. The gel was dried and analyzed using the PhosphorImager system (Molecular Dynamics, USA).

WESTERN BLOTTING DETECTION OF BIOTINYLATED PROTEINS In the samples obtained after ultracentrifugation, the proteins were precipitated by the slow addition of 5 volumes of ice-cold acetone and incubation of the mixture for 24 h at − 20°C. The pellet was washed with ice-cold acetone, dried, dissolved in a buffer containing 8M Urea and 70 mM Tris-HCl (pH 7.5), and diluted in water. Protein mixtures were separated by electrophoresis in 15% SDS-PAGE according to Laemmli [23]. Proteins from extract and DEAE-fraction were separated in 10−12% SDS-PAGE without the precipitation step. They were transferred to nitrocellulose (GE Healthcare) or PVDF (BioRad) membranes. To detect biotinylated proteins, streptavidin-HRP conjugate [24] and ECL kit (GE Healthcare) were used.

RT-PCR ANALYSIS RNA for RT-PCR was obtained using phenol extraction, chloroform−isoamyl alcohol (24 : 1) extraction, and ethanol precipitation in the presence of 1/10 volume 3 M NaOAc and tRNA from *Escherichia coli* as a carrier (5 μg per probe). Samples containing RNA bound to the streptavidin-sepharose resin were pretreated with proteinase K as described above for telomerase assay *in vitro*. All the samples were treated with DNase I (1 U/μg nucleic acids or 1 U/100 μl fraction obtained by ultracentrifugation, 1 h at 37°C). After that, RNA was purified from proteins with the use of extraction and precipitation as described above. All the samples were diluted in an equal amount of water (usually 10 μl), and RNA concentration was measured spectrophotometrically at 260 nm. The volume of the initial extract containing 0.1−0.5 μg RNA was used for RT-PCR analysis. An equal volume of unbound fraction and corresponding volume of bound fraction corrected for TLC1 concentration in binding from the extract were taken for RT-PCR analysis. If fractions obtained by ultracentrifugation were analyzed, 1 μl of the sample was used for analysis. For RT-PCR reactions, a OneStep RT-PCR Kit (Qiagen) was used. The gene-specific primers for TLC1 were P2 (5'-GTTTATTCTAGTTTTTTCCG-3') and T8 (5'-CGAAGGCATTAGGAGAAG-3'). RT-PCR products were analyzed by electrophoresis in 2% agarose gel with a TBE buffer (89 mM Tris, 89 mM boric acid, 2 mM EDTA, pH 8.3).

RESULTS AND DISCUSSION

THE ACTIVE YEAST TELOMERASE COMPLEX CONTAINS BIOTINYLATED PROTEIN It is known that yeast telomerase activity cannot be detected directly in the yeast extract obtained by the disruption of yeast cells. This becomes possible only after the step of enriching the telomerase complex by specifically binding the complex subunits on affinity resin (Est1 [25], Est2p [26], Est3p [10]) or by enriching the whole complex using anion-exchange chromatography [4, 22]. We found that when the yeast extract was bound to streptavidin-sepharose, active telomerase could be detected on the resin (Fig. 1a). This fact indicates that active telomerase is concentrated on affinity resin because there is no activity in the initial extract. The pattern of detected activity is the same as the pattern of activity

of telomerase isolated via the anion-exchange chromatography on DEAE-cellulose and corresponds to the addition of one telomeric repeat in the *in vitro* reaction (Fig. 1a).

To test if the binding of telomerase with streptavidin-Sepharose results from the "biotin-streptavidin" interaction (dissociation constant $K_d = 10^{-14}$ M [27]), we performed the binding experiment with the pretreatment of the yeast extract with avidin. Adding avidin is a common way to prevent binding with the streptavisin-sepharose of biotinylated proteins from the yeast extract [28], because the "biotin-avidin" interaction (dissociation constant $K_d = 10^{-15}$ M [29]) completely blocks the "biotin-sreptavidin" interaction. In fact, adding avidin prevents the binding of telomerase with the affinity resin (Fig. 1b). This result indicates that the interaction is specific. Telomerase binding to the resin and the prevention of this binding by adding avidin were also shown for TLC1 RNA by RT-PCR analysis (Fig. 1c).

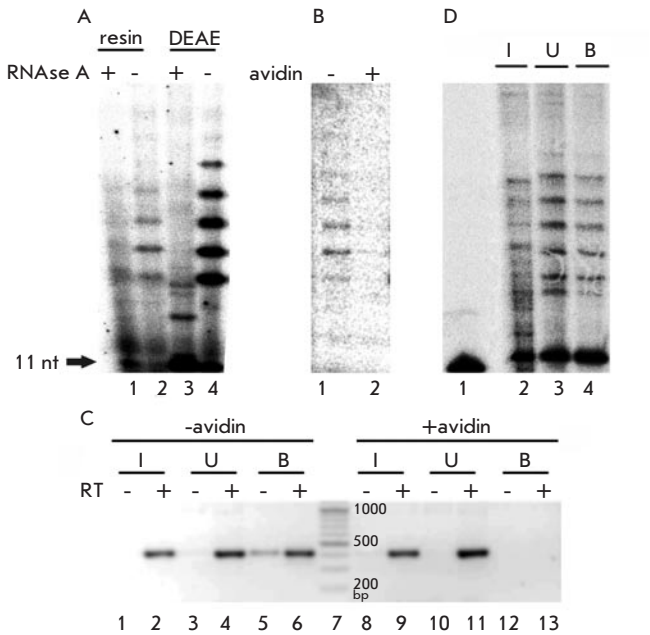

Figure 1. Isolation of yeast telomerase using chromatography on streptavidin-sepharose. (a) Activity assay (elongation of oligodeoxyribonucleotide TEL11) of telomerase isolated on streptavidin-sepharose from extract. RNase A(+) and RNase A(−) are the reactions with and without pretreatment with RNase A. (*1*, *2*) the products of TEL11 elongation by telomerase isolated on streptavidin-sepharose; (*3*, *4*) the same for telomerase isolated on DEAE-cellulose. (b) The same as in (a) with pretreatment with and without avidin. Avidin(+) and Avidin(−) are the reactions with and without pretreatment with avidin. (*1*, *2*) the same as (a; *1*, *2*). (c) RT-PCR analysis of TLC1 RNA in samples obtained by telomerase isolation on streptavidin-sepharose with and without pretreatment with avidin. RT(−) and RT(+) are RT-PCR analyses without and with reverse transcription reaction. (*1*, *2*) RT-PCR products obtained in an analysis of the initial extract (I); (*3*, *4*) the same for unbound fraction (U); (*5*, *6*) the same for bound fraction (B) without avidin pretreatment; (*7*) molecular weight marker; (*8*–*13*) the same as in (*8*–*13*) with avidin pretreatment. (*d*) Activity assay of telomerase isolated on streptavidin-sepharose from DEAE-fraction. (*1*) 5′-[^{32}P]- phosphorylated oligodeoxynucleotide TEL11; (*2*) the products of TEL11 elongation by telomerase of initial DEAE-fraction (I); (*3*) the same for unbound fraction (U); (*4*) the same for bound fraction (B), taken in a 4-times excess

In the next step, we performed the binding of telomerase that had already been purified via chromatography on DEAE-cellulose with the affinity resin. We found that active telomerase in fact binds with streptavidin-sepharose, but only partially (Fig. 1d). This could be due to the fact that only part of telomerase complexes contains biotinylated protein. Also, we could not exclude the possibility that, during purification on DEAE-cellulose, some active telomerase complexes lose their biotinylated component.

THE BIOTINYLATED PROTEIN-TELOMERASE SUBUNIT HAS AN APPARENT MASS OF 50 kDa AND IT IS A CONSTITUENT OF ONLY PART OF THE TOTAL AMOUNT OF ACTIVE TELOMERASE We fractionated the yeast S100 extract as well as telomerase purified on DEAE-cellulose in a glycerol density gradient using ultracentrifugation. Centrifugation of both types of samples was done simultaneously and under the same conditions. It is known that yeast telomerase sediments as 19S when ultracentrifugated [30]. We tested the obtained fractions for the presence of TLC1 RNA, telomerase activity, and biotinylated proteins (Figs. 2, 3). The distribution of active telomerase throughout the fractions is shown on Figs. 2a and 2c, and the distribution of TLC1 RNA is shown on Figs. 2b and 2d..

We used Western blotting for the detection of biotinylated proteins in the initial yeast extract (Fig. 3a) and initial DEAE-fraction (Fig. 3b), as well as the distribution of biotinylated proteins throughout the fractions obtained by ultracentrifugation (Figs. 3c, 3d).

The three most intense bands corresponding to 47, 120, and 200 kDa are readily detected in the extract and DEAE-fraction (Figs. 3a, 3b). There are only a few known biotinylated proteins in yeast: Acc1p (250 kDa [31]), Hfa1p (242 kDa [32]), Pyc1p (130 kDa [33]), Pyc2p (130 kDa [33]), Dur1,2p (202 kDa [34]), and Arc1p (42 kDa [35]). In general, the detected bands correspond to those described in the literature [35] and anticipated in accordance with the molecular masses of the known proteins.

In the case of the fractionation of telomerase enriched on DEAE-cellulose, one could see that biotinylated protein with an apparent molecular mass of 50 kDa comigrates and enriches with the telomerase complex. This is obvious from comparing Figs. 2c and 3c. In the case of S100 extract fractionation, we could not find a correlation between the presence of telomerase activity and the presence of biotinylated protein, because a series of bands corresponding to all yeast biotinylated proteins were detected in all fractions like in the initial extract (data not shown).

We have shown that the yeast telomerase complex contains biotinylated protein. We have not managed to establish what protein it is and what its function is. Our attempts to use MALDI-TOF analysis for identifying the protein of interest were unsuccessful due to a small amount of telomerase per cell (approximately 29 molecules of TLC1 RNA per haploid yeast cell [36]) and the fact that only a portion of the total amount of active telomerase contains biotinylated protein. Also, it should be noted that the elution of proteins bound on streptavidin-sepharose by the "biotin-streptavidin" interaction is a difficult task, because, due to the strength of the interaction, it is not quantitative [37].

It is obvious from Figs. 2c and 3c that the detected biotinylated protein comigrates with the lighter portion of telom-

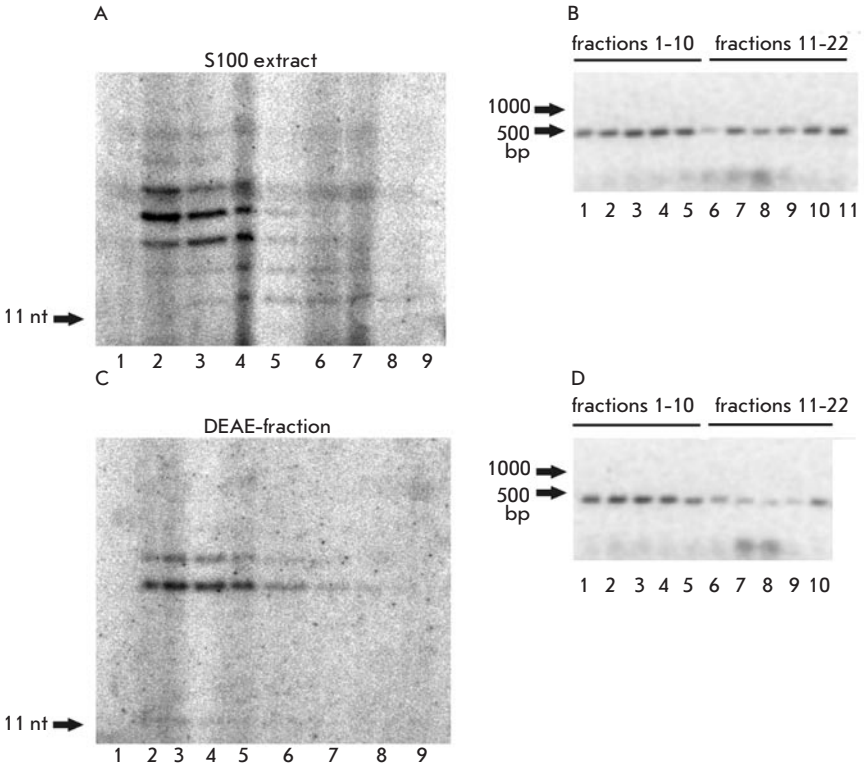

Figure 2. Analysis of fractions obtained by ultracentrifugation in a glycerol density gradient (22 fractions from one gradient). (a) Telomerase activity assay in fractions obtained by ultracentrifugation of S100 extract. (*1–9*) The products of TEL11 elongation by telomerase in fractions 1–9, respectively. (b) RT-PCR analysis of TLC1 RNA in fractions obtained by ultracentrifugation of S100 extract. (*1–9*) RT-PCR products obtained in an analysis of fractions 1–22, respectively, two adjacent fractions in each lane (*1*) 1 and 2 fractions; (*2*) 3 and 4 fractions, etc.). (c) The same as in (a) for fractions obtained by ultracentrifugation of DEAE-fraction. (d) The same as in (b) for fractions obtained by the ultracentrifugation of DEAE-fraction

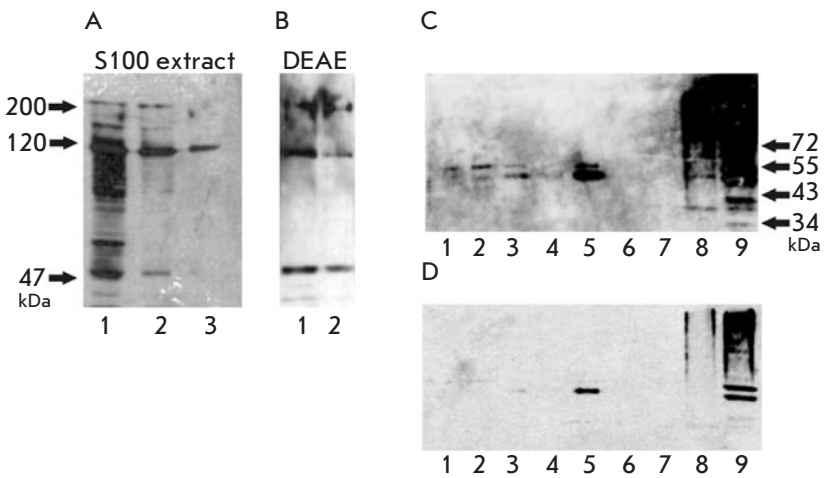

Figure 3. Western blotting analysis of biotinylated proteins in the initial S100 extract, DEAE-fraction and fractions obtained by ultracentrifugation in glycerol density gradient. (a) Western blotting analysis of proteins in the initial S100 extract. (*1–3*) biotinylated proteins from extract (the amount of samples decreases from *1* to *3*). (b) Western blotting analysis of proteins in DEAE-fraction. (*1*, *2*) biotinylated proteins from DEAE-fraction in decreasing amounts (from *1* to *2*). (c) Western blotting analysis of proteins in fractions obtained by the ultracentrifugation of DEAE-fraction. (*1–8*) biotinylated proteins from fractions 1–8, respectively; (*9*) biotinylated proteins from initial DEAE-fraction. (d) The same as in (c) with the quick exposure of a membrane to a film

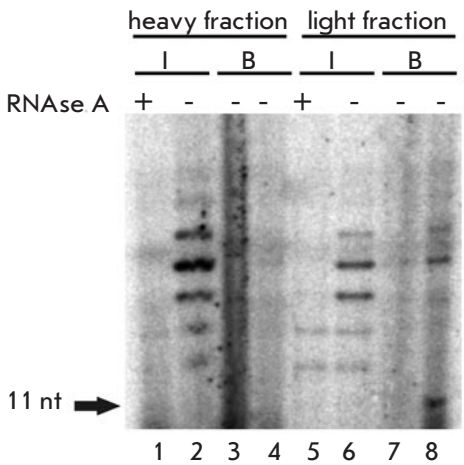

Figure 4. Binding of heavy (2 and 3 fractions) and light (4 and 5 fractions) telomerase complexes obtained by S100 extract ultracentrifugation in glycerol gradient, with streptavidin-sepharose. RNase A(+) and RNase A(–) are the reactions with and without pretreatment with RNase A. (*1*, *2*) the products of TEL11 elongation obtained by the telomerase of the initial heavy fraction (I); (*3*, *4*) the same for bound fraction (B), taken in a 4-times excess and 10-times excess, respectively; (*5–8*) the same as in (*1–4*) for light fraction

erase complexes. An interesting proposition could be made on the basis of this fact and the fact that biotinylated protein is present in less than half of the active telomerase complexes isolated on DEAE-cellulose. We speculated that the biotinylated protein is a constituent of only the light telomerase complexes that may be in the maturation process but already active *in vitro*. We tested this idea for fractions obtained by the ultracentrifugation of the S100 extract. We combined two heavy fractions, and the same was done for two light fractions. Then, we performed the binding of these two samples with streptavidin–sepharose. In fact, one could see that the active telomerase from the heavy fractions does not bind to streptavidin-sepharose, while telomerase from light fractions binds (Fig. 4). So our proposition is proved, and this result disproves the hypothesis that the biotinylated component dissociates during purification on DEAE-cellulose, because, even without this purification step, only a portion of telomerase complexes contains biotinylated protein.

Our data (the molecular mass of a candidate protein is about 50 kDa) and the data existing in the literature allow us to speculate about the nature of biotinylated protein and its function. As was already noted, there are only a few known biotinylated proteins in yeast. These are three types of carboxylases containing biotin as a cofactor: acetyl-CoA carboxylases Acc1p (250 kDa [31]), Hfa1p (242 kDa [32]); piruvate carboxylases Pyc1p (130 kDa [33]), Pyc2p (130 kDa [33]); urea amidolyase Dur1,2p (202 kDa [34]; and protein Arc1p (42 kDa [35]), a cofactor of aminoacyl-tRNA synthetase [38]. Arc1p is also known to bind quadruplex DNA [39]. Of these proteins, only Arc1p is the most similar in molecular mass to the discovered biotinylated protein. It is interesting that Arc1p does not contain a canonical sequence for biotinylation by biotin-protein ligase. Moreover, biotinylation is not functionally important for Arc1p activity [35]. As an RNA-binding protein and a protein that binds quadruplex DNA, Arc1p seems to be a possible candidate for the biotinylated component of telomerase. It is also possible that telomerase contains a protein that is not already known to be biotinylated, interacting as Arc1p with biotin ligase Bpl1p and as Arc1p without a canonical sequence for biotinylation.

An interesting question arises as to the role of biotinylated protein in the telomerase complex. We have found that only the lighter portion of telomerase complexes contains biotinylated protein. It is known that the main components of telomerase crucial for the elongation of telomeric DNA are telomerase reverse transcriptase Est2p and telomerase RNA TLC1 [5]. Other components are necessary for regulation, assembly, biogenesis and degradation of the complex [5]. Some of them join telomerase only transiently at a particular moment in a cell cycle. For example, proteins Est1p and Est3p, crucial for telomerase activity *in vivo*, become part of the complex only in the late S/G2 phase of the cell cycle [18]. Our data indicate that biotinylated protein is not a permanent component of telomerase complex. It joins telomerase only transiently, on a particular step of assembly, biogenesis, regulation or degradation and probably participates in these processes. ●

This work was supported by the Russian Foundation for Basic Research (grants 08-04-01220-a and 07-04-92119-a) and State contract (grant P800).

REFERENCES

1. de Lange T. (2002) *Oncogene*, **21**, 532–40.
2. Greider C.W., Blackburn E.H. (1987) *Cell*, **51**, 887–98.
3. Kim N.W., Piatyszek M.A., Prowse K.R., Harley C.B., West M.D., Ho P.L., Coviello G.M., Wright W.E., Weinrich S.L., Shay J.W. (1994) *Science*, **266**, 2011–5.
4. Cohn M., Blackburn E.H. (1995) *Science*, **269**, 396–400.
5. Cech T.R. (2004) *Cell*, **116**, 273–9.
6. Collins K. (2006) *Nat Rev Mol Cell Biol*, **7**, 484–94.
7. Counter C.M., Meyerson M., Eaton E.N., Weinberg R.A. (1997) *Proc Natl Acad Sci U S A*, **94**, 9202–7.
8. Singer M.S., Gottschling D.E. (1994) *Science*, **266**, 404–9.
9. Zhou J., Hidaka K., Futcher B. (2000) *Mol Cell Biol*, **20**, 1947–55.
10. Hughes T.R., Evans S.K., Weilbaecher R.G., Lundblad V. (2000) *Curr Biol*, **10**, 809–12.
11. Lendvay T.S., Morris D.K., Sah J., Balasubramanian B., Lundblad V. (1996) *Genetics*, **144**, 1399–412.
12. Seto A.G., Zaug A.J., Sobel S.G., Wolin S.L., Cech T.R. (1999) *Nature*, **401**, 177–80.
13. Peterson S.E., Stellwagen A.E., Diede S.J., Singer M.S., Haimberger Z.W., Johnson C.O., Tzoneva M., Gottschling D.E. (2001) *Nat Genet*, **27**, 64–7.
14. Evans S.K., Lundblad V. (1999) *Science*, **286**, 117–20.
15. Ungar L., Yosef N., Sela Y., Sharan R., Ruppin E., Kupiec M. (2009) *Nucleic Acids Res*,
16. Toogun O.A., Dezwaan D.C., Freeman B.C. (2008) *Mol Cell Biol*, **28**, 457–67.
17. Fisher T.S., Taggart A.K., Zakian V.A. (2004) *Nat Struct Mol Biol*, **11**, 1198–205.
18. Osterhage J.L., Talley J.M., Friedman K.L. (2006) *Nat Struct Mol Biol*, **13**, 720–8.
19. Chang M., Arneric M., Lingner J. (2007) *Genes Dev*, **21**, 2485–94.
20. Hector R.E., Shtofman R.L., Ray A., Chen B.R., Nyun T., Berkner K.L., Runge K.W. (2007) *Mol Cell*, **27**, 851–8.
21. Sabourin M., Tuzon C.T., Zakian V.A. (2007) *Mol Cell*, **27**, 550–61.
22. Lue N.F., Peng Y. (1998) *Nucleic Acids Res*, **26**, 1487–94.
23. Laemmli U.K. (1970) *Nature*, **227**, 680–5.
24. Hoja U., Wellein C., Greiner E., Schweizer E. (1998) *Eur J Biochem*, **254**, 520–6.
25. Steiner B.R., Hidaka K., Futcher B. (1996) *Proc Natl Acad Sci U S A*, **93**, 2817–21.
26. Friedman K.L., Cech T.R. (1999) *Genes Dev*, **13**, 2863–74.
27. Green N.M. (1990) *Methods Enzymol*, **184**, 51–67.
28. Srisawat C., Engelke D.R. (2001) *Rna*, **7**, 632–41.
29. Green N.M. (1963) *Biochem J*, **89**, 585–91.
30. Lingner J., Hughes T.R., Shevchenko A., Mann M., Lundblad V., Cech T.R. (1997) *Science*, **276**, 561–7.
31. Hasslacher M., Ivessa A.S., Paltauf F., Kohlwein S.D. (1993) *J Biol Chem*, **268**, 10946–52.
32. Hoja U., Marthol S., Hofmann J., Stegner S., Schulz R., Meier S., Greiner E., Schweizer E. (2004) *J Biol Chem*, **279**, 21779–86.
33. Brewster N.K., Val D.L., Walker M.E., Wallace J.C. (1994) *Arch Biochem Biophys*, **311**, 62–71.
34. Genbauffe F.S., Cooper T.G. (1991) *DNA Seq*, **2**, 19–32.
35. Kim H.S., Hoja U., Stolz J., Sauer G., Schweizer E. (2004) *J Biol Chem*, **279**, 42445–52.
36. Mozdy A.D., Cech T.R. (2006) *Rna*, **12**, 1721–37.
37. Rybak J.N., Scheurer S.B., Neri D., Elia G. (2004) *Proteomics*, **4**, 2296–9.
38. Simos G., Segref A., Fasiolo F., Hellmuth K., Shevchenko A., Mann M., Hurt E.C. (1996) *Embo J*, **15**, 5437–48.
39. Frantz J.D., Gilbert W. (1995) *J Biol Chem*, **270**, 20692–7.

A Comparison of Target Gene Silencing using Synthetically Modified siRNA and shRNA That Express Recombinant Lentiviral Vectors

P.V. Spirin, D. Baskaran, P.M. Rubtsov, M.A. Zenkova, V.V. Vlassov, E.L. Chernolovskaya, V.S. Prassolov*

Engelghardt Institute of Molecular Biology, Russian Academy of Sciences, ul. Vavilova 32, Moscow, 119991

Institute of Chemical Biology and Fundamental Medicine, Siberian Branch, Russian Academy of Sciences, Lavrentiev pr. 8, Novosibirsk, 630090

*E-mail: prasolov@eimb.ru

ABSTRACT RNA-interference is an effective natural mechanism of post-transcriptional modulation of gene expression. RNA-interference mechanism exist as in high eukaryotes both animals and plants as well in lower eukaryotes and viruses. RNA-interference is now used as a powerful tool in study of functional gene activity and many essential for fundamental biology results was obtained with this approach. Also it's widely believed that RNA-interference could be used in working out of new therapeutic medicine against malignant, infectious and hereditary diseases. One of the main problems of these developments is search of effective methods of siRNA transfer into the target cells. At present time for these purpose different sorts of transfect ions or viral transduction are used. At present article the results of comparison of inhibition of expression of oncogene AML-ETO by synthetic siRNA and by recombinant lentiviruses coding for corresponding shRNA are presented.

Keywords: retroviral vectors, RNA interference, embryonic mouse fibroblasts.

Abbreviations: AML – Acute Myeloid Leukemia, CBF – Core Binding Factor, EGFP –Enhanced Green Fluorescent Protein, GTU –GFP Transducing Units, HDAC –Histone deacetylase, IRES –Internal Ribosome Entry Site, NHR –Nervy Homology Region, RHD –Runt Homology Domain, VSV-G –Vesicular stomatitis virus G glycoprotein

INTRODUCTION

The controlled silencing of target genes is important both for molecular biological studies and for related applied sciences: in particular, modern biomedicine.

Among the many gene silencing approaches (which include the use of anti-sense RNA, ribozymes, chemical blockers, and targeted mutagenesis), the most efficient approach is based on RNA-interference.

RNA interference is a highly specific mechanism for the posttranscriptional silencing of target genes. It involves the degradation of the target gene mRNA. The degradation of mRNA occurs in a complex formed by short-interfering RNA oligonucleotides (siRNA) and cellular proteins such as endonucleases. The nucleotide sequence of siRNA is complementary to that of target gene mRNA.

In the past couple of years, the use of siRNA has become widespread in studies of gene functioning and gene interaction. The use of siRNA as next generation therapeutic agents in biomedicine is also being explored. It is possible that, in the near future, siRNA will be used for treating viral and oncological diseases.

Currently, short synthetic 21–22-bp double-stranded siRNA molecules are widely used to silence mammalian genes. A number of commercial firms synthesize siRNA oligonucleotides. These commercial firms have siRNA design tools available on their websites (e.g., www.qiagen.com). Synthetic siRNA oligonucleotides are transferred into cells *in vitro* by lipofection. Since siRNA induces the degradation of mRNA (and not the protein directly), the silencing effect does not occur immediately after cell transfection. The silencing effect is generally noticeable within 18 hours of transfection: however, in the case of stable proteins, the silencing effect may be noticeable only 24–48 hours after transfection. The longevity of siRNA silencing is comparatively short, and different sources claim that the silencing effect lasts for 3–5 cell divisions. It should be noted that the longevity of siRNA silencing may depend on many factors, in particular the nature of the cells being transfected. Approaches have been developed to synthetically modify siRNA oligonucleotides, which enhance the longevity of siRNA silencing in cells. Such synthetically modified siRNA oligonucleotides are useful for the post-transcriptional silencing of genes that encode proteins with a long half-life.

For long-lasting gene silencing, shRNA expressing lenti- and retroviral vectors can be used. Nucleotide sequences encoding the sense and antisense strands of siRNA separated by a spacer sequence can be cloned into lenti- or retroviral vector constructs using standard molecular biological cloning techniques. The transcription of such nucleotide sequences leads to the formation of shRNA molecules. shRNA molecules form a hairpin structure consisting of two complimentary strands separated by a loop (spacer). The cellular endonuclease dicer

is responsible for the cleavage of shRNA molecules. As a result, the loop (spacer) gets removed from shRNA molecules and double-stranded siRNA molecules are formed. These siRNA molecules are capable of initiating the degradation of target gene mRNA.

Within the framework of our project, we were able to silence the expression of activated oncogenes AML1-ETO (t8;21) and RUNX1(K83N) with the help of RNA interference. These activated oncogenes are frequently found in acute myeloid leukemia patients. We were able to compare the efficiency of gene silencing (a) after the lipofection of oncogene-expressing model cell lines with synthetically modified double-stranded siRNA oligonucleotides and (b) after the transduction of oncogene-expressing model cell lines with shRNA-expressing recombinant lentiviral vector particles.

Oncogene-expressing model cell lines were obtained from murine SC1 embryonic fibroblast cell lines after their transduction with bicistronic retroviral vector particles. These retroviral vectors contained a bicistronic expression cassette comprised of the gene of interest and an eGFP marker gene separated by an IRES sequence and driven by a common promoter. The following genes were selected as genes of interest:

(1) The AML1-ETO fusion gene, which is formed as a result of the t(8:21) chromosomal translocation.

(2) The activated RUNX1-K83N oncogene, which is formed as a result of a point mutation in the RUNX1 gene and leads to the substitution of lysine to asparagine in the 83 position of the RUNX1 protein. Since both the gene of interest and eGFP marker gene are driven by a common promoter, the expression levels of the gene of interest in cells can be evaluated based on the intracellular expression of the eGFP marker gene.

The typical results of transduction efficiency and transgene expression are shown in Fig. 1.

Throughout the course of our work, we used the murine SC1 embryonic fibroblast cell line, the HEK 293 cell line, and two transgenic SC1 cell lines expressing either activated oncogene AML1-ETO or RUNX1(K83N). All four cell lines were cultured in standard DMEM medium containing 10% FBS, 4mM L-glutamine, 1mM sodium pyruvate, 100 mkg/ml streptomycin, and 100 units/ml penicillin at 37 °C in a 5% CO2 atmosphere.

The design and synthesis of double-stranded siRNA molecules was carried out in collaboration with the Institute of Chemical Biology and Fundamental Medicine, Siberian Branch of the Russian Academy of Sciences (ICBFM SB RAS). The oligonucleotides were synthesized at ICBFM SB RAS using the phosphamide method. During oligonucleotide synthesis, a unique method was used to methylate the oligonucleotides at certain positions. These modifications significantly increase the lifespan of synthetic siRNA in cells. The nucleotide sequences of siRNA oligonucleotides and the oncogene mRNA zones being targeted by them are shown in Table. 1.

Anti-AML1-ETO and anti-RUNX1 siRNA duplexes were transferred into transgenic SC1 cell lines by lipofection using Lipofectamin2000 (Invitrogen) as per the manufacturers' protocol. The final concentration of siRNA duplexes in the transfection culture medium was 200nM. Four hours after

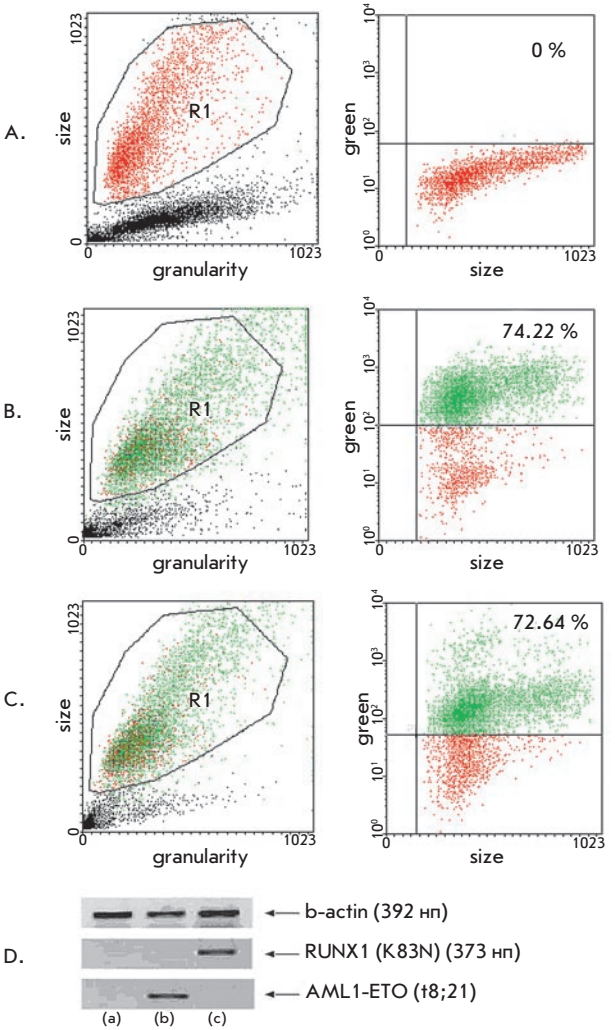

Fig. 1. Efficiency of transgene expression in cell lines transduced with AML1-ETO- and RUNX1-K83N-expressing recombinant retroviral vector particles; (A) Histogram of nontransduced SC-1 murine fibroblast cell line, (B)
Histogram of SC-1 murine fibroblast cell line transduced with RUNX1-K83N expressing retroviral vector particles (74,22 % of the population shows increased fluorescence), (C) Histogram of SC-1 murine fibroblast cell line transduced with AML1-ETO expressing retroviral vector particles (72,64 % of the population shows increased fluorescence). The absolute values of the size of each event analyzed (cell) is shown along the *X* axis, while the absolute values of the intensity of fluorescence of each event (cell) is shown along the *Y* axis. Every third histogram in each row is divided into 4 quadrants; the upper right quadrant contains cells expressing eGFP and AML1-ETO, while the lower right quadrant contains cells that do not express eGFP and AML1-ETO. (D) RT-PCR (from left to right; (a) non transduced SC-1 cell line, (b) SC-1 cell line transduced with RUNX1-K83N expressing retroviral vector particles, (c) SC-1 cell line transduced with AML1-ETO expressing retroviral vector particles)

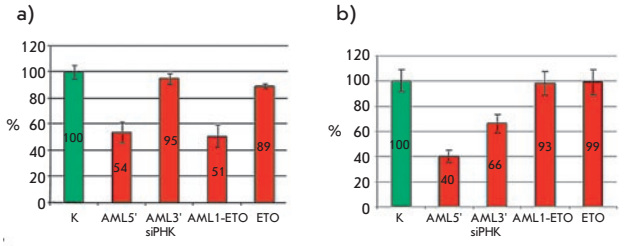

Fig. 2. Results obtained after flow cytometric analysis of cell suspensions. The percentage of fluorescent cells in the population of different siRNA transfected cell lines is shown. A) The percentage of fluorescent cells in the AML1-ETO expressing murine fibroblast cell line 48 hours after transfection with various siRNA duplexes. B) The percentage of fluorescent cells in the RUNX1(K83N) expressing murine fibroblast cell line 48 hours after transfection with various siRNA duplexes

transfection, the culture medium was changed to a fresh medium. The transfected cell lines were cultured at 37 °C in a 5% CO2 atmosphere for 72 hours.

The level of oncogene expression in the cell lines was evaluated by reverse transcription PCR (RT-PCR) and flow cytometry. The total mRNA from the cell lines was extracted using Trizol (Invitrogen) as per the manufacturers' protocol. The extracted mRNA was used to synthesize the first strands of cDNA using the ImProm-II™ Reverse Transcriptase (Promega) kit.

PCR with sequence-specific primers was carried out to identify the nucleotide sequences of the genes of interest and eGFP marker gene in the total cDNA. The following primers were used for RUNX1(K83N): sense-AGTCCTACCAATACCTGGGA; antisense-TCTCAGCTGTGGTGGTGAAG, for AML1/ETO: sense-CATTTCACCCGAGATAGGAG; antisense-AAGTCCTCGGCGTCACTGAT, for eGFP : sense-ACCTACGGCCTGCAGTGCTT; antisense-TGCCGTTCTTCTGCTTGTCG. PCR products were then visualized after 1.5% agarose gel electrophoresis. The results were processed using the Gel-Pro Analyzer 4.0 software, which gives a maximum optical density (maxOD) reading. The results were normalized against β-actin.

Cell fluorescence was measured using an Epics 4XL Beckman Coulter flow cytometer (United States). The WinMDI2.8 software program was used for data collection and data analysis. The diagrams of the percentage of fluorescent cells in the cell populations are shown in Fig. 2. Cell populations transfected with respective siRNA duplexes are shown along the *X* axis, while the percentage of fluorescent cells in the population is shown on the *Y* axis.

Results obtained by flow cytometry correlate well with the results obtained by RT-PCR. The electrophoregram of RT-PCR products is shown in Fig. 4. The reduction of oncogene mRNA is clearly visible in the SC1-AML1/ETO(t8;21) transgenic cell lines transfected with siRNA oligonucleotides targeting the 5'-end of RUNX1 mRNA, ETO mRNA and the site of junction of AML1-ETO mRNA. Oncogene mRNA reduction is also seen in the SC1-RUNX1(K83N) transgenic cell lines transfected with siRNA oligonucleotides targeting the 5'- and 3'-ends of RUNX1 mRNA.

While there is a significant reduction of fluorescence in a portion of the cell population (two times or more) after the addition of synthetic siRNA, there is no such reduction in fluorescence in the rest of the cell population (Fig. 3). This coincides with the results obtained by RT-PCR (Fig. 3). The most likely reason for this is the low efficiency of siRNA delivery into cells. According to the manufacturers of Lipofectamin2000 (Invitrogen), the lipofection efficiency with siRNA oligonucleotides is 50–60% and depends on the nature of the cells being transfected. Apart from this, there is the possibility of a reduction of synthetic siRNA activity due to their enzymatic degradation, which is catalyzed by cellular endonucleases, despite the stabilizing modifications introduced to the siRNA oligonucleotides. According to our data, the maximum interfering activity of synthetically modified siRNA is observed 48–72 hours post transfection.

The gene silencing kinetics of synthetic siRNA oligonucleotides targeting the junction point of AML1-ETO mRNA is illustrated in Fig. 4. The moment of siRNA transfection has been taken as zero-time reference.

It has been shown that the maximum silencing activity of synthetic siRNA is 48–72 hours post transfection, when the percentage of fluorescent cells in the population is around 56%. The percentage of fluorescent cells in the population increases to 67.92 and 74.39% 96 and 120 hours post transfection, respectively. The results shown are averaged from three parallel measurements and are in reference to a control.

The efficiency of RNA-interference can be increased by increasing the efficiency of siRNA delivery into the model cell lines. For this purpose, taking into account the efficiency of the synthetic siRNA duplexes, two shRNA-expressing lentiviral vectors were constructed targeting the junction point of AML1-ETO mRNA and the 5`-end of RUNX1 mRNA, respectively. The lentivectors were constructed by cloning the shRNA-expressing DNA sequence into the pLSLP vector.

DNA sequence which encodes anti AML1-ETO shRNA
AML1-ETO-sense
5'-p-gatccgCCTCGAAATCGTACTGAGGcttcctgtcaTCTCAGTACGATTTCGAGGtttttg-3'
AML1-ETO antisense
5'-p-aattcaaaaaCCTCGAAATCGTACTGAGAtgacaggaagCCTCAGTACGATTTCGAGGcg-3'

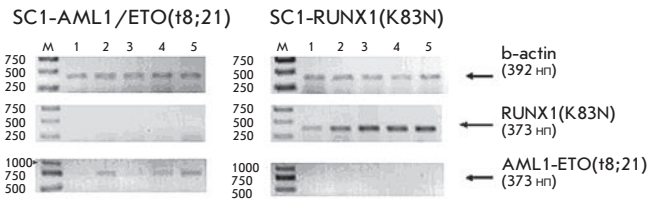

Fig. 3. The electrophoregram of RT-PCR products of total cDNA obtained from oncogene expressing model cell lines transfected with siRNA. 1) siRNA(AML1-5`), 2. siRNA(AML1-3`), 3. siRNA(AML1-ETO), 4. siRNA(ETO), 5. Control (without siRNA)

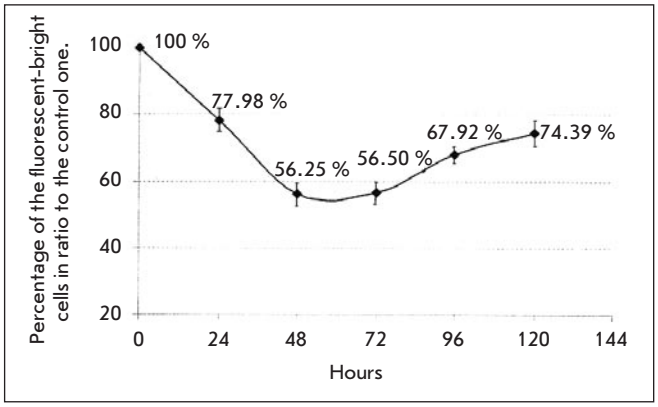

Fig. 4. The gene silencing kinetics of synthetic siRNA oligonucleotides targeting the junction point of AML1-ETO mRNA

DNA sequence which encodes anti-RUNX1 shRNA
AML-5-sense
5'-p-gatccgGAACCAGGTTGCAAGATTCcttcctgt-caAAATCTTGCAACCTGGTTCtttttg-3'
AML-5-antisense
5'-p-aattcaaaaaGAACCAGGTTGCAAGATTTtgacag-gaagGAATCTTGCAACCTGGTTCcg-3'

The design of the shRNA-coding DNA sequences was done through an internet resource (http://gesteland.genetics.utah.edu/siRNA_scales/index.html). Standard genetic engineering techniques were used for all cloning procedures. The vector maps of the constructed shRNA-expressing lentiviral vectors are shown in Fig. 5.

The transient cotransfection of HEK293 T cells with shRNA-expressing lentiviral vectors and packaging plasmids was done for the production of shRNA-expressing lentiviral vector particles. The transfection was carried out using Lipofectamin2000 (Invitrogen) as per the manufacturers' protocol. Viral stocks were harvested for three days and used for the infection/transduction of the transgenic model cell lines expressing the activated oncogenes AML1-ETO and RUNX1(K83N). Forty-eight hours after transduction/infection, the model cell lines were placed in culture media containing puromycin (10mkg/ml) for five days. After selection for puromycin resistance, the shRNA-expressing transduced model cell lines were analyzed by flow cytometry.

The percentage of fluorescent cells in the SC1-AML1/ETO(t8;21) transgenic cell line decreased 6 times after their transduction with shRNA-expressing lentiviral vector particles targeting the junction point of AML1-ETO mRNA (Fig. 6). Similar results were seen when the SC1-AML1/ETO(t8;21) and SC1-RUNX1(K83N) cell lines were transduced with shRNA-expressing lentiviral vector particles targeting the 5`-end of RUNX1 mRNA. The percentage of fluorescent cells in the cell lines decreased 8 and 8.5 times, respectively. It should be noted that the SC1-RUNX1(K83N) cell line showed no reduction in fluorescence when trans-

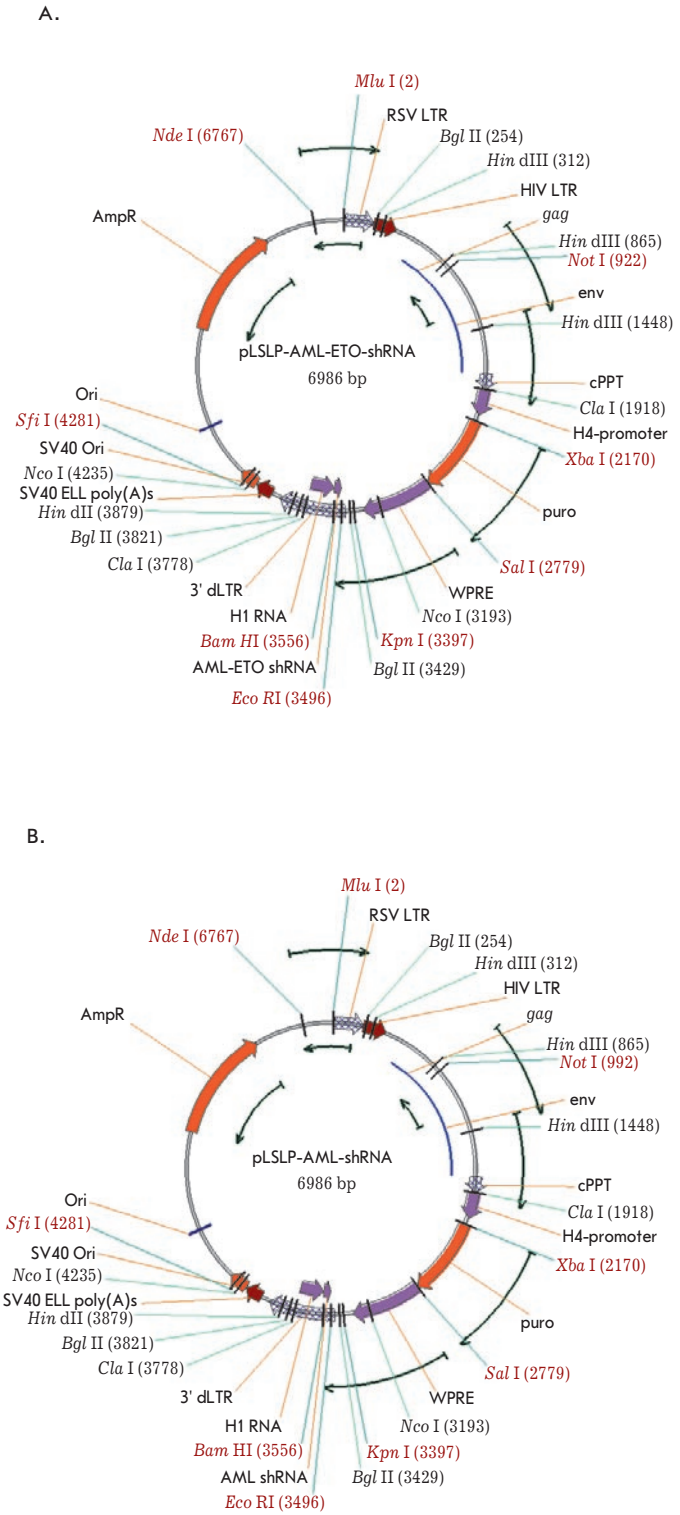

Fig 5. shRNA expressing lentiviral vectors; (A) pLSLP-AML-ETO-shRNA: lentiviral vector expressing shRNA targeting the junction point of AML1-ETO mRNA, (B) pLSLP-AML-shRNA: lentiviral vector expressing shRNA targeting the 5`-end of RUNX1-K83N mRNA

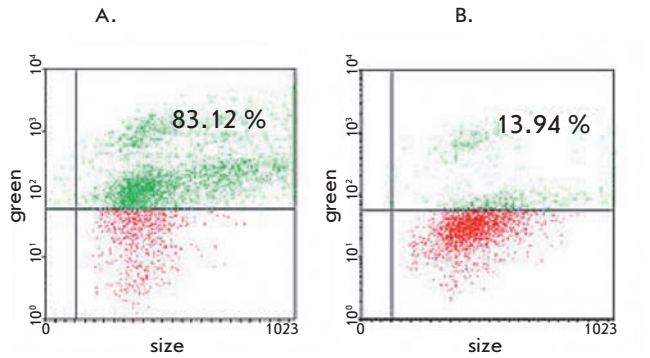

Fig 6. Histogram illustrating the reduction in fluorescence in the AML1-ETO expressing SC-1 murine fibroblast cell line: (A) before transduction, (B) after transduction with shRNA-expressing lentiviral vector particles targeting the junction point of the AML1-ETO mRNA

Table

target	chain	sequence
AML-ETO	sense	5'-CCUCGAAAUCGUmACUmGAG**U**AG-3'
	antisense	5'-UCUCmAGUmACGAUUUCGAGGUU-3'
ETO	sense	5'-GGCCmAGCGGUmACmAGUCCmA**G**AU-3'
	antisense	5'-UUmGGACUmGUmACCGCUmGGCCUG-3'
AML (5')	sense	5'-GAACCmAGGUUmGCmAAGAUU**G**AA-3'
	antisense	5'-AAAUCUUmGCmAACCUmGGUUCUU-3'
AML (3')	sense	5'-AGCCCGGGAGCUUmGUCCU**C**UU-3'
	antisense	5'-AAGGACmAAGCUCCCGGGCUUmG-3'

siPHK
1. AML5'
2. AML3'
3. AML1-ETO
4. ETO

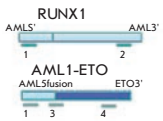

duced with shRNA-expressing lentiviral vector particles targeting the junction point of AML1-ETO mRNA. The results obtained by flow cytometry correlate well with the results obtained by RT-PCR (the electrophoregram is shown in Fig. 7).

CONCLUSIONS

Our results illustrate the high efficiency of stable synthetically modified siRNA duplexes for silencing the activated oncogenes frequently found in acute myeloid leukemia patients.

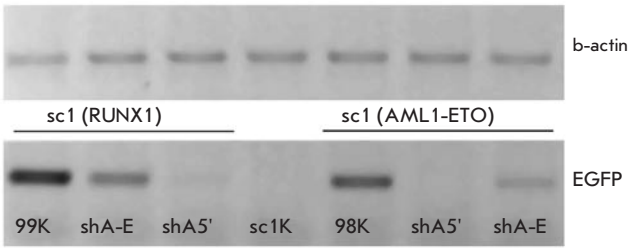

Fig. 7. The electrophoregram of RT-PCR products of total cDNA obtained from RUNX1(K83N) and AML1-ETO oncogene expressing SC1 model cell lines transduced with shRNA expressing lentiviral vector particles: 99K - control (non-transduced RUNX1(K83N) expressing SC1 cell line); shA-E - RUNX1(K83N) expressing SC1 cell line transduced with shRNA expressing lentiviral vector particles targeting the junction point of AML1-ETO mRNA; shA5` - RUNX1(K83N) expressing SC1 cell line transduced with shRNA expressing lentiviral vector particles targeting the 5`-end of RUNX1 mRNA . sc1K - control (non transduced SC1 cell line); last three samples - Analysis of AML1-ETO(t8;21) expressing SC1 cell lines (98k - non transduced control, shA-E, sh5` - transduced with corresponding lentiviral vector particles)

Validated siRNA sequences were used to design and synthesize shRNA-coding DNA sequences. The synthesized DNA sequences were cloned into a recombinant lentiviral vector. The shRNA-expressing lentiviral vector particles targeting the junction point of AML1-ETO mRNA and 5`-end of RUNX1 mRNA were used to transduce the oncogene-expressing model cell lines. The transduced model cell lines were analyzed by RT-PCR and flow cytometry. The analysis revealed a significant reduction in the expression of activated oncogenes in the transduced cell lines. This is indicative of the high efficiency of the constructed lentiviral vector constructs, which can be used for silencing target genes by RNA interference. ●

We would like to thank Prof. P.M. Chumakov for providing us with the pLSLP lentiviral vector.

The experimental work was carried out within the framework of the "Molecular and Cell Biology" project and project No. 27 "Fundamental Research Basics in Nanotechnology and Nanomaterials" of the RAS presidium fundamental research program.

REFERENCES:
1. Vilgelm A.E., Chumakov S.P., Prasolov V.S. // Molecular Biology 2006. Vol. 40. #3 pages 1-18.
2. Volkov A.A., Kruglova N.S., Meschaninova M.I., et al. // Oligonucleotides. 2009. Jun;19(2):191-202.
3. Shuey D.J., McCallus D.E., Giordano T. // Drug Discov. Today. 20027. 1040–1046.
4. Stanisławska J., Olszewski W.L. // Arch. Immunol. Ther. Exp. 200553. 39–46.
5. Elbashir S.M., Harborth J., Weber K., Tuschl T. // Methods. 200226. 199–213.
6. Brummelkamp T.R., Bernards R., Agami R. // Science. 2002296. 550–553.
7. Satake N., Maseki N., Kozu T., et al. // British Journ. of Haemat. 199591: 892-898.
8. Peterson L.F., Zhang D.E. // Oncogene. 2004; 23(24):4255-62.
9. Kravchenko J.E., Ilyinskaya G.V., Komarov P.G., et al. // Proc. Natl. Acad. Sci. USA. 2008. Apr 29;105(17):6302-7.

Derivation and Characterization of Human Induced Pluripotent Stem Cells

M.V. Shutova, A.N. Bogomazova, M.A. Lagarkova, S.L. Kiselev*
Vavilov Institute of General Genetics, Russian Academy of Sciences
*E-mail: kiselev@vigg.ru

ABSTRACT Cell biology is one of the most rapidly developing branches in modern biology. The most interesting stages in early embryonic development for cell biology are those when a large number of cells are pluripotent. Inner-cell mass of blastocyst can be cultivated *in vitro*, and these cells are called embryonic stem cells. They are able to differentiate into different types of cells and tissues. But the greatest interest for practical application is the return (reprogramming) of adult cells into the pluripotent state. In our study for the first time induced pluripotent cells were derived from human umbilical vein endothelial cells by genetic reprogramming. We showed that these cells are similar to embryonic stem cells in their morphology, function, and molecular level. We are the first to show that reprogramming sufficiently changes X-chromosome chromatin state, which is normally inactive in female endothelial cells, towards its activation, providing evidence that endothelial cells are reprogrammed at an epigenetic level.
Keywords: pluripotency, cell reprogramming, X-chromosome reactivation.
Abbreviations: embryonic stem cells (ESC), cells with induced pluripotency (iPS).

A multicellular organism develops from a single cell, a zygote, and becomes a complex of mutually supported tissue types during its individual development. The totipotent zygote cell and the terminally differentiated cell contain the same set of genetic information, but this information is achieved differently. Cellular programs of differentiation happen at the genetic and epigenetic levels. The zygote achieves a specified program and divides, and at a certain stage, cells begin to specialize. A blastocyst (about 3.5 days in mouse and 5.5 days in humans) has two types of cells and is a future embryo which has no physical connection with its mother's organism. The inner cells will develop into the organism and all its tissues, and the outer layer of cells will develop into trophectogerm, which will interact with the mother's organism. *In vitro* (in laboratory conditions) cultivated blastocyst inner-cell mass were called embryonic stem cells (ESC). *In vitro* ESC under appropriate conditions do not continue their program further; they stay in a pluripotent state for an unlimited time [1], but one can induce their controlled differentiation into the tissues of all three germ layers just by changing the culture's conditions [2]. However, in the case of using these type of cells in therapy, the immunologic compatibility between the derived tissues and the recipient remains to be defined. Reprogramming individual somatic cells to a pluripotent state will be a perfect solution to this problem. For this purpose, the technologies of somatic cell nuclear transfer into the oocyte and fusion of the somatic cell with the pluripotent one were developed [3–5]. However, in 2006, S. Yamanaka [6] put forward a method of somatic cell genetic reprogramming to the pluripotent state. For the induction of the pluripotent state, genes which encode the transcriptional factors essential for early embryonal development and maintenance of the pluripotent state Oct3/4 and Sox2, the antiapoptopic transcriptional factor Klf4, and the transcriptional factor, which maintain the cell's proliferation c-Myc, were used. These cells were called induced pluripotent stem (iPS) cells. In the last three years, this technology has been significantly improved and doesn't require obligatory genetic modification [7–9]. But the number of human cell types that were successfully reprogrammed remained very restricted [10, 11].

Cells which are able to generate iPS cells should have some distinct features. First, they should be sensitive to total reprogramming. Second, they should be available. Third, they should not have any accumulated DNA damage, for example, UV or other environmental skin-cell damage. And finally, the number of cells should be sufficient, and the reprogramming effective enough to minimize all possible DNA damage during *in vitro* manipulations. Based on the above-mentioned criteria, our aims were to choose an optimal cell type and genetically reprogram these cells to optimize their further use.

We decided to take human umbilical vein cells for reprogramming. They can be easily obtained; have not accumulated any DNA damage; can be obtained in large amounts without cultivation, proliferate well in culture only in the presence of factors that maintain their growth; and, in con-

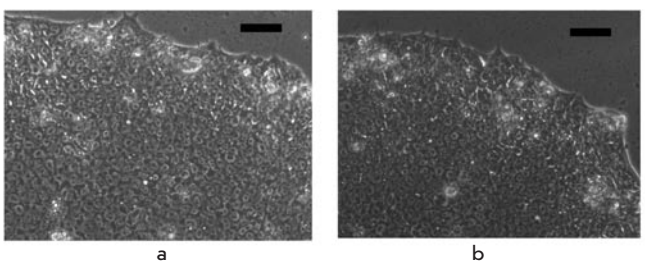

Fig. 1. Morphology of iPS derived from an endothelium, feeder-free culture. A – Bright field image of iPS colony. B – Image of ESC colony. Bar scale – 100 mkm

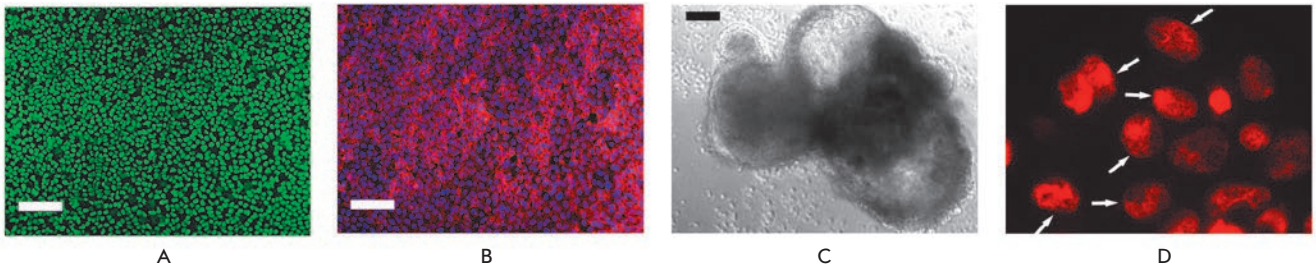

Fig. 2. Feature analysis of human iPS cells derived from human umbilical vein endothelial cells. A, B – immunohistochemical analysis of iPS cells, antibodies stain to specific markers of pluripotency Oct4 (A) and SSEA-4 (B). The specific signals are stained with green (A) and red (B), nuclei in (B) are stained with blue (DAPI). C – embryonic bodies, derived from iPS cultured in suspension. Bar scale – 100 mkm. D – interphase nucleus in iPS cells stained with active chromatin marker H3me2K4 (red). White arrows localize the chromosome region of partly reactivated X – chromosome

junction with the development of umbilical vein banks, they can be stored for a long time. There is no data in the literature about endothelial-cell reprogramming. The reprogramming was achieved by the use of genetic constructs which were tested in earlier experiments [6]. Human umbilical vein endothelial cells (HUVEC) were transducted with retroviral vectors which contained cDNA of Oct3/4, Sox2, KLF4 and cMyc genes. The multiplicity of infection was five viral particles. Six days after infection, the endothelial-cell culture medium was changed to an ESC medium. It is worth noting that endothelial cells do not proliferate in an ESC culture medium; this significantly enabled the selection of iPS cells. Three weeks after viral infection, morphologically identical ESC clones were selected (Fig 1).

The derived iPS cells did not differ in their the proliferative or morphological characteristics from human ESCs (Figs 2a, 2b). We confirmed with fingerprinting that these iPS were generated from human umbilical vein endothelial cells selected for reprogramming and were not the result of cellular culture contamination with human ES cells. To determine the number of integrated pro-virus copies, we used genomic hybridization with specific probes. Copy number varied from two to three copies of each virus per genome in derived iPS lines. These human iPS cells were pluripotent, formed embryonic bodies (Fig 2c), and differentiated into derivatives of all three germ layers. A karyotype analysis demonstrated that reprogrammed cells have a normal karyotype and retain it for at least 22 passages. iPS cells were cultivated in feeder-free conditions in a mTeSR1-defined medium. Thus, we are the first to obtain iPS cells from human endothelium free of animal-derived components. The developed method allows us to obtain clinically applicable iPS cell lines.

Apart from changes in the realization of the genetic, program significant changes in the epigenetic state of somatic cells should take place during reprogramming. Inactivation of one of the two X-chromosomes in female cells occurs during early emryogenesis, although both X-chromosomes can be active in ESCs. Consequently, one can expect that during reprogramming there would be functional changes resulting in the reactivation of the inactive X-chromosome in endothelial cells. We used antibodies to active (H3me2K4) and nonactive (H3me3K27) chromatin to conduct an immunocytochemical analysis of X-chromosomes in derived iPS cell lines. Our data revealed that the marker of active chromatin (H3me2K4) appears on the nonactive X-chromosome in iPS cells (Fig 2d); at the same time, inactive chromosome in endothelial cells lacks an expression of this marker. Therefore, we are the first to show that, during genetic reprogramming, the reactivation of the inactive X-chromosome occurs in human cells. Our findings show that human endothelial cells can be effectively and completely reprogrammed to the pluripotent state, which was confirmed by morphological, molecular, and functional tests.

It is obvious that further experiments should be carried out for iPS cells application: for example, to confirm the reprogrammed state on the genome level and to confirm the oncogenic safety of iPS cells. This kind of research is one of the most promising avenues in the sphere of cell technologies. However, one should not forget that iPS cells are only an artificial analogue of ESCs: therefore, in order to identify their significance for application, two groups of pluripotent cells should be studied. ●

This research was supported by the program of the Russian Academy of Sciences Biodiversity, grant RFBR 09-04-12199 ofi-m and OOO LKT (Moscow).

REFERENCES

1. Thomson J.A., Itskovitz-Eldor J., Shapiro S.S., et al. // Science. 1998. 282(5391): 1145–1147.
2. Lagarkova M.A., Volchkov P.Y., Philonenko E.S., Kiselev S.L // Cell Cycle. 2008. 7: 2929–2935.
3. Kato Y., Tani T., Sotomaru Y., et al. // Science. 1998. 282: 2095–2098.
4. Tada M., Takahama Y., Abe K., Nakatsuji N., Tada T. // Curr. Biol. 2001. 11: 1553–1558.
5. Matveeva N.M., Shilov A.G., Kaftanovskaya E.M., et al. // Mol. Reprod. Dev. 1998. 50: 128–138.
6. Takahashi K., Yamanaka S. // Cell. 2006. 126: 663–676.
7. Aasen T., Raya A., Barrero M.J., et al. // Nat. Biotechnol. 2008. 26: 1276–1284.
8. Zhou H., Wu S., Joo J., Zhu S., Han D., Lin T., Trauger S., Bien G., Yao S., Zhu Y., et al. //. Generation of Induced Pluripotent Stem Cells Using Recombinant Proteins. Cell Stem Cell. doi:10.1016/j.stem.2009.04.005
9. Stadtfeld M., Maherali N., Breault D.T., Hochedlinger K. // Cell Stem Cell. 2008. 2: 230–240.
10. Maherali N., Hochedlinger K. // Cell Stem Cell. 2008. 3: 595–605.
11. Loh Y.H., Agarwal S., Park I.H., et al. // Blood. Prepublished online Mar 18, 2009.

Influence of *pub* Gene Expression on Differentiation of Mouse Embryonic Stem Cells into Derivatives of Ecto-, Meso-, and Endoderm *in vitro*

E.V. Novosadova, E.S. Manuilova, E.L. Arsenieva, A.N. Lebedev, N.V. Khaidarova, V.Z. Tarantul, and I.A. Grivennikov*
Institute of Molecular Genetics, Russian Academy of Sciences, Akad. Kurchatova Square 2, 123182 Moscow, Russia
*E-mail: igorag@img.ras.ru; Tel: +8 (499) 196-00-14; Fax: +8 (499) 196-02-21

ABSTRACT The influence of low and high *pub* gene expression on the initial stages of the differentiation of mouse embryonic stem cells into derivatives of ecto-, meso-, and endoderm *in vitro* was investigated. As follows from the results of a RT-PCR analysis, the expression of the *vimentin, somatostatin, GATA 4,* and *GATA 6* genes, being the markers of endodermal differentiation, does not vary in both the cells with high *pub* gene expression and the cells with low *pub* gene expression, as well as in the corresponding control lines. The cells with high *pub* gene expression are characterized by an increase in the expression of mesodermal differentiation gene-markers (*trI card, trI skel*, *c-kit,* and *IL-7*), whereas the cells with low *pub* gene expression are specified by a decrease in their expression. According to the analyses carried out, the reverse is characteristic of the expression of ectodermal differentiation gene-markers (*nestin, β-III tubulin, gfap,* and *th).* Expression of these genes decreases in cell lines with high *pub* gene expression, whereas their expression increases with the decrease in *pub* gene expression. Hence, it is suggested that the variations in the *pub* gene expression in the embryonic stem cells influence significantly the mesodermal and ectodermal differentiation of these cells.
Keywords: embryonic stem cells, differentiation, polymerase chain reaction, *pub* gene, mesoderm, endoderm, and ectoderm.
Abbreviations: ES - embryonic stem cells, FBS - foetal bovine serum

INTRODUCTION

An embryonic stem (ES) cell is a unique model to use for the investigation of the processes underway at the early stages of embryogenesis [1]. It is well known that in the course of *in vivo* embryo development, ES cells are able to form all three embryonic layers in culture – endoderm, mesoderm, and ectoderm – and, thus, all cell types developing from them. Analysis of gene expression in the process of ES cell differentiation into specialized cell types shows that the succession and efficiency of gene expression in the course of *in vitro* differentiation corresponds, as a whole, to the sequence of these processes *in vivo* [10]. Hence, ES cells may be used as an adequate experimental model for the investigation of molecular mechanisms at the initial stages of differentiation. Moreover, the investigations of ES cell differentiation in this or other directions in response to the action of specific inducers (growth factors, cytokines) or to direct the genetic modification of these cells make it possible to understand the functions of the investigated substances and different genes in this process [1].

In the previous investigations, we obtained and described cDNA clones characterized by intensive transcription in the HIV-associated immunoblastic lymphomas using the method of subtractive hybridization [16, 17]. An analysis of those cDNA allowed us to detect among them, along with the previously described genes (*set*, *calpain, etc.*), several cDNA coding genes with previously unknown functions. One of such lymphoma-specific genes was then termed *pub*. The protein product of the human *pub* gene (hPub) is highly homological to the mouse Pub protein (mPub) [5].

Pub is referred to the TRIM (tripartite motif) protein family [5] characterized by the presence of the so-called TRIM (or RBBC) motive composed of three Zn-binding domains such as RING (R), B-box 1 (B1), and B-box 2 (B2) accompanied by the coiled-coil (CC) region [15]. Currently, 37 representatives of this protein family are known. Some of them are involved in such biological processes as regulation of transcription, formation of cytoskeleton, control of cell proliferation, and differentiation [18]. The functions of the *hpub* gene in the organism are poorly investigated. The mouse-homologue *mpub* plays

an important role in the processes of cell differentiation and influences substantially the transcription activity of the PU.1 factor [5]. PU.1 referred to the ETS family of transcription factors plays a major role in the differentiation and proliferation of macrophages and B-cells in the course of haemopoiesis and controls the functional activity of neutrophiles [11]. The *mpub* gene product inhibits the transcription activity of PU.1 in hemocytes and, thus, plays a very important role in the proliferation and differentiation of myeloid and lymphoid cells [5].

The model of mouse ES cells was used to investigate the influence of the *pub* gene on the initial stages of their development. Earlier on, we obtained stable, transfected cell cultures with a high expression of the *hpub* gene (ES-hPub line) controlled by the CMV promoter, cell cultures with a low expression of the *mpub* gene (ES-RNAi line) caused by the action of interfering RNA, as well as the corresponding control lines (ES-DNA3 and ES-pJneo, respectively) [2]. High expression of the *hpub* gene resulted in an increase, while low expression of the *mpub* gene resulted in a decrease, in the number of embryoid bodies formed by the ES cells. However, gene expression had no influence on the proliferative activity of those cells [2, 3].

In the present paper, we estimate the influence of high and low *mpub* and *hpub* gene expression on the expression of gene-markers of ento-, meso, and ectodermal differentiation in cultures of transfected mouse ES cells using the RT-PCR method (polymerase chain reaction with reverse transcription).

EXPERIMENTS

CULTIVATION OF ES CELLS

Mouse ES cells of the R1 line kindly provided by A. Nagy (Mount Sinai Hospital, Toronto, Canada) were used in the investigation. The ES cells were cultivated at 37°C and 5% CO_2 in a α-MEM medium (Sigma, USA) containing 15% of fetal cow serum (FCS) (Gibco, the USA), 0.1 mM of 2-mercaptoethanol, 2 mM of L-glutamin, replaceable amino acids (Gibco, USA), nucleosides, vitamins, and gentamicin (20 μg/ml). Primary fibroblasts from mice 11-12 days of embryonic development in age with proliferation blocked by mitomycin C (5 μg/ml) were used as a feeding layer for the ES cells. A DMEM medium (Sigma, USA) containing 10% of FCS, 2 mM of L-glutamin, and gentamicin (20 μg/ml) was the growth environment for the primary culture of fibroblasts. When the ES cells were cultivated without the feeding layer, LIF (leukemia inhibitory factor) (Sigma, USA) in a final concentration of 10 ng/ml, which blocked the spontaneous differentiation of those cells, was added to the medium. Cell subculturing and change of the medium were carried out every 3 days.

INDUCTION OF ES CELL DIFFERENTIATION WITH FORMATION OF EMBRYOID BODIES

The ES cells were isolated from the fibroblasts of the feeding layer to induce differentiation, followed by the formation of embryoid bodies. The cells were processed with tripsin, subject to centrifuging, and then the suspension obtained was incubated in a Petri dish (d = 60 mm) (Nunc, Denmark) for 10-20 minutes in the CO_2-incubator. In that period of time, most fibroblasts were attached to the dish bottom, while the ES cells remained in the suspension. To form the embryoid bodies, the suspension with the ES cells was transferred to the Petri dish (d=35 mm) (Nunc, Denmark) in a quantity of 200,000 cells per 2 ml of medium or to the 96-well immunological plate (1,000 cells per 1 well in 1 μl of medium) and then was placed in the CO_2-incubator. On the third day of cultivation, the formed embryoid bodies were transferred to plates coated with gelatin for further differentiation.

EXTRACTION OF TOTAL RNA AND CONDUCTION OF REVERSE TRANSCRIPTION

Total RNA was extracted from the differentiated ES cells and other cell lines and tissues by the phenol-chloroform extraction method using the YellowSolve equipment (Clonogen, Russia) and following the manufacturer's recommendations. The procedure of reverse transcription was carried out using the Sileks equipment (Russia) in accordance with the protocol and the manufacturer's recommendations. cDNA was synthesized with the use of total RNA for 1 hour at 37°C in a 20 μl reaction mixture containing 0.05 μg of randomly selected hexaprimers, and 100 units of MMLV (moloney murine leukemia virus) reverse transcriptase. When the reaction was completed (incubation for 10 minutes at 70°C), the cDNA samples were stored at 20°C.

POLYMERASE CHAIN REACTION

The polymerase chain reaction (PCR) was carried out in a 25 μl reaction mixture containing Taq-buffer, 1.5 mM of dNTP mixture, 1.25 of "colored" Taq-polymerase (Synthol, Russia), 0.5 μl of cDNA samples, and 10 pmole of each primer. The primers selected for the corresponding genes, as well as the PCR conditions and lengths of the products, are presented in Table 1. The PCR products were separated in a 1.5% agarose gel, visualized with the help of ethidium bromide, and then analyzed using the BioDocAnalyze system (Biometra, Germany).

RESULTS AND DISCUSSION

It is known that ectodermal differentiation produces the nervous system and epithelium, endodermal differentiation produces the liver, pancreatic gland, thyroid gland, and lungs, while mesodermal differentiation produces blood, skeletal and cordular muscles (http://stem-cells.ru).

We investigated the infulence of variations in *mpub* and *hpub* gene expression on the differentiation of mouse ES cells in the ectodermal, endodermal, and mesodermal directions.

For that purpose we chose specific gene-markers characterizing different types of cells originating from this or another germ layer (Fig. 1).

Transfected ES cells of four lines (ES-hPub, ES-DNA3, ES-Ineo, and ES-RNAi) were subjected to "spontaneous" differentiation: i.e., we did not add any specific inductors of certain types of cell differentiation. The presence of expression and variations in its level were determined with the help of the RT-PCR method. The cells that underwent endodermal and mesodermal differentiations were analyzed on the 10th day, while the cells that underwent ectodermal differentiation were analyzed on the 21st day of cultivation [6].

INFLUENCE OF HIGH *HPUB* GENE EXPRESSION AND LOW *MPUB* GENE EXPRESSION ON THE ENDODERMAL DIFFERENTIATION OF TRANSFECTED ES CELLS.

GATA 4 and *GATA 6* are referred to the family of transcription factors. They play a definite role in the regulation of genes involved in embryogenesis, as well as in the development of cardiovascular and viscerogenic endoderm. As follows from our investigation of the Zebrafish and Xenopus organisms, the *GATA* 4 and 6 genes play a very important role at the initial stages of the heart's development [7, 8, 12-14]. Moreover, the knockout of mouse *GATA* 4 and 6 genes causes the death of the embryo at the gastrulation stage, due to the interruption of the definitive endoderm formation [19].

The experiments carried out established no difference in the expression of the *vimentin, somatostatin, GATA 4*, and *GATA 6* genes in both the differentiated cells with high *hpub* gene expression and cells with low *mpub* gene expression, as well as in the corresponding control lines (Fig. 2). Hence, it can be suggested that variations in the *pub* gene expression do not influence the endodermal differentiation of ES cells.

INFLUENCE OF HIGH *HPUB* GENE EXPRESSION AND LOW *MPUB* GENE EXPRESSION ON THE MESODERMAL DIFFERENTIATION OF TRANSFECTED ES CELLS.

At the following stage of the investigation, we checked the influence of *hpub* and *mpub* gene expressions on cell differentiation in the mesodermal direction. Taking into consideration the homology of mouse gene *mpub* and human gene *hpub*, we may suggest that the *hpub* gene product will inhibit the transcription activity of PU.1 and, by that, will influence the differentiation of hematopoetic cells. To verify that theory, we investigated the influence of high *hpub* gene expression and low *mpub* gene expression on the differentiation of ES cells in the lymphoid tissue. For that purpose, we chose specific gene-markers for lymphoid cells, such as *c-kit* and *IL-7* [7]. On the 10th day of cultivation, a PCR analysis of transgenic cell lines showed that high *hpub* gene expression led to an increase in

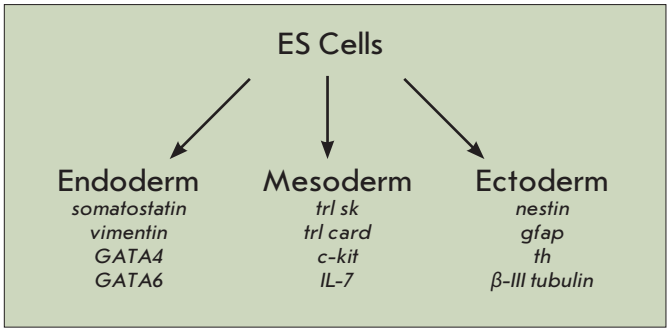

Fig. 1. Gene-markers of the definite directions of ES cell differentiation used in experiments

Table 1. Primers used in polymerase chain reaction

N	Gene	Structure of primers	Annealing temperature (^{0}C)	Number of cycles	Size of product (bps)
1	GAPDH	5'-TCCATGACAACTTTGGCATTGTGG-3'-s 5'-GTTGCTGTTGAAGTCGCAGGAGAC-3'-as	66	27	376
2	pub	5'-CCCATTTGGAAGACGCCG -3' –s 5'-AGGGTGGCTCAGCTCCG -3'-as	70	43	328
3	hpub	5'-GCAGCAGCACATTGACAACA-3'-s 5'-TCCACGAGGCCCTTAAAGAA-3'-as	60	30	382
7	GATA 4	5'-GGTTCCCAGGCCTCTTGCAATGCGG-3'-s 5'-AGTGGCATTGCTGGAGTTACCGCTG-3'-as	65	40	153
8	GATA 6	5'-CCGCGAGTGCGTGAACT-3'-s 5'-CGCTTCTGTGGCTTGATGAG-3'-as	65	40	137
9	trI card	5'-CCACACGCCAAGAAAAAGTC-3'-s 5'-AAGCTGTCGGCATAAGTCCT-3'-as	62	32	204
10	trI skel	5'-CACACTCTGCAGTCTGTGGTGAG-3'-s 5'-CTGAAGGGCACTGAGAGACAGAC-3'-as	64	35	314
12	nestin	5'-CGCTGGAACAGAGATTGGAAGG-3'-s 5'-GTCTCAAGGGTATTAGGCAAG-3'-as	58	30	375
13	gfap	5'-TCCTGGAACAGCAAAACAAG-3'-s 5'-CAGCCTCAGGTTGGTTTCAT-3'-as	61	42	224
14	β-III tubulin	5'-GAGGAGGAGGGGGAGATGTA-3'-s 5'-CCCCCGAATATAAACACAACC-3'-as	65	35	348
15	th	5'-TGCACACAGTACATCCGTCA-3'-s 5'-TCTGACACGAAGTACACCGG-3'-as	60	35	376
16	vimentin	5'-ACCTGTGAAGTGGATGCCCT-3'-s 5'-AAATCCTGCTCTCCTCGCCTT-3'-as	55	30	318
17	somatostatin	5'-CAGACTCCGTCAGTTTCTGC-3'-s 5'-ACAGGATGTGAAAGTCTTCCA-3'-as	56	30	262
18	c-kit	5'-TGTCTCTCCAGTTTCCCTGC-3' -s 5'-TTCAGGGACTCATGGGCTCA-3'-as	58	45	765
19	IL-7	5'-ACATCATCTGAGTGCCACA-3' -s 5'-CTCTCAGTAGTCTCTTTAG-3'-as	57	45	355

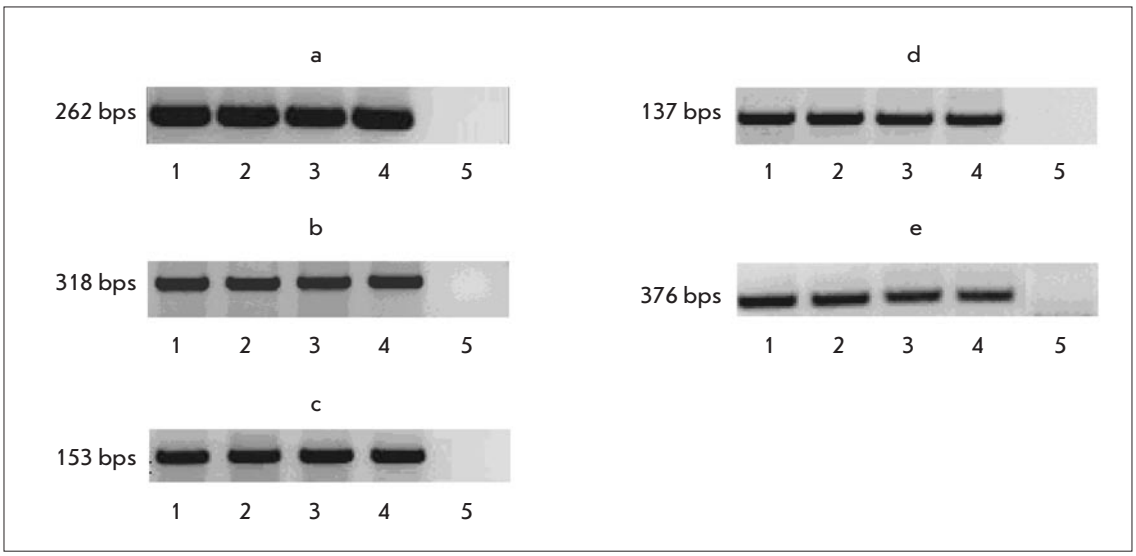

Fig. 2. Expression of genes involved in the endodermal differentiation of stable transfected ES cells (10 days of differentiation *in vitro*). Data of RT-PCR analyses. Genes: a) *somatostatin*, b) *vimentin*, c) *GATA 4*, d) *GATA 6*, e) *GAPDH*, gene for comparison. Cell lines: 1. ES-hPub, 2. ES-DNA3, 3. ES-RNAi, 4. ES-plneo. 5. Negative control (water)

the expression of both gene markers, while inhibition of the endogenic *mpub* gene, on the contrary, caused a decrease in their expression as compared to the corresponding controls (Fig. 3).

Hence, the data obtained testify to the fact that high *hpub* gene expression may lead to ES cell differentiation through the lymphoid way.

Two genes – *trI sk* (skeletal troponin I) and *trI card* (cardiac troponin I) – were selected to determine the influence of a differently directed expression of the *pub* gene on ES cell differentiation into other derivative mesoderms. Both cardiac protein isoform and isoform from slow skeletal fibers are expressed in the heart of a human embryo. After birth, the expression of skeletal-muscular troponin I isoform is blocked, whereas the synthesis of cardiac isoform is stimulated [5].

As follows from Fig. 4, the *trI card* and *trI sk* genes are expressed in different ways. In the transfected cells with superexpression of the *hpub* gene, expression of these genes is also high as compared to the control line, whereas the cells with a repressed expression of the *mpub* gene demonstrate a lower level of expression of the troponin I genes relative to the control line.

The results obtained testify to a possible influence of the *mpub* and *hpub* genes on ES cell differentiation into different derivative mesoderms. Moreover, *hpub* gene superexpression leads to an increase in the level of mRNA for some gene markers of this type of differentiation.

INFLUENCE OF HIGH *HPUB* GENE EXPRESSION AND LOW *MPUB* GENE EXPRESSION ON THE ECTODERMAL DIFFERENTIATION OF TRANSFECTED ES CELLS.

The *nestin*, *β-III tubulin*, *gfap*, and *th* gene markers were used to investigate the influence of the *hpub* and *mpub* genes on the ectodermal differentiation of ES cells. The *nestin* gene is expressed in neural stem cells, young neurons, some glial cells, and ependymal cells. The *nestin* gene is commonly expressed at the initial stages of formation of the central and peripheral nervous sytem. The *β- III tubulin* and *gfap* genes code proteins of the cytoskeleton of neurons and glial cells, respectively. Tyrosine hydroxylase gene *th* is expressed in dopaminergic neurons [19]. Data on the expression of these genes in the experimental and control lines of ES cells are presented in Fig. 5.

CONCLUSIONS

As follows from the results of the PCR analysis, the expression of genes involved in the neural differentiation decreases in cells with high *hpub* gene expression, and the expression of these genes increases in cells with low *mpub* gene expression relative to the controls. This situation is characteristic of three (*nestin*, *β-III tubuli*, and *gfap*) of the four genes analyzed. Expression of the *th* gene does not vary in all four cell lines. This result may be explained by the fact that variations in the *pub* gene expression do not influence the formation of dopaminergic neurons characterized by the presence of *th* gene expression. Hence, according to the experiments performed, the

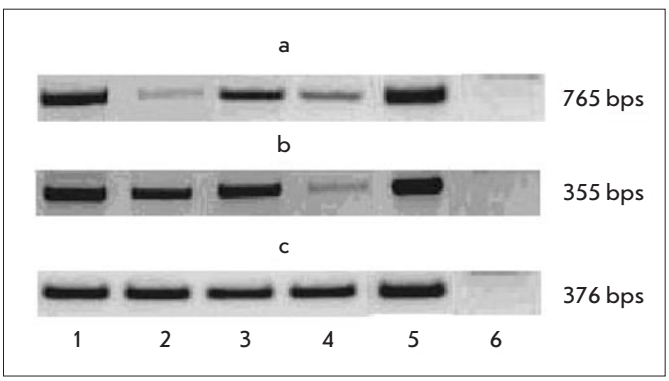

Fig. 3. Expression of *c-kit* and *IL-7* genes in stable transfected ES cells (10 days of differentiation *in vitro*). Data of RT-PCR analyses. Genes: a) *c-kit*, b) *IL-7*, c) *GAPDH*, gene for comparison. Cell lines: 1. ES-hPub, 2. ES-DNA3, 3. ES-RNAi, 4. ES-plneo, 5. Positive control (mouse thymus). 6. Negative control (water)

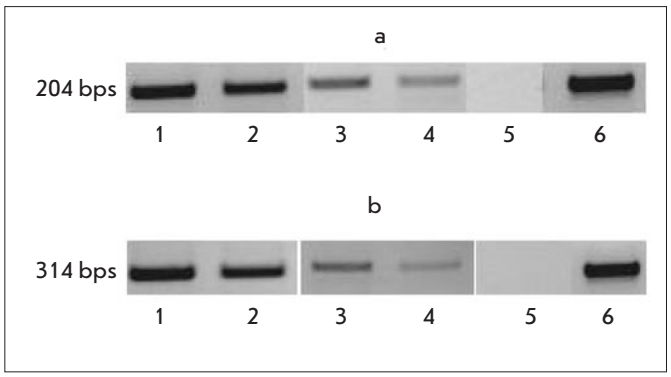

Fig. 4. Expression of cardiac (*trl card)* and skeletal (*trl sk)* troponin I genes in stable transfected ES cells (10 days of differentiation *in vitro*). Data of RT-PCR analyses. a) *trl card* gene. Cell lines: 1. ES-hPub, 2. ES-DNA3, 3. ES-plneo, 4. ES-RNAi, 5. Negative control (water), 6. Positive control (heart of adult mouse). b) *trl sk* gene. Cell lines: 1. ES-hPub, 2. ES-DNA3, 3. ES-plneo, 4. ES-RNAi, 5. Negative control (water), 6. Positive control (heart of mouse embryo)

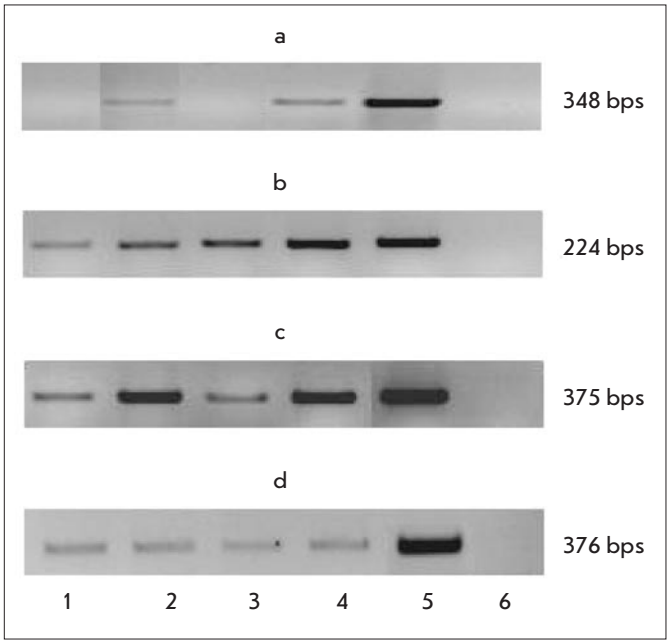

Fig. 5. Expression of genes involved in the ectodermal differentiation of stable transfected ES cells (21 days of differentiation *in vitro*). Genes: a) *β-III tubulin*, b) *gfap*, c) *nestin*, d) *th*. Cell lines: 1. ES-hPub, 2. ES-DNA3, 3. ES-plneo, 4. ES-RNAi, 5. Positive control (mouse hippocampus), 6. Negative control (water)

hpub gene superexpression or the repression of *mpub* gene expression in mouse ES cells causes significant variations in the expression of gene markers in derivatives of some germ layers and, thus, has a definite, differently directed influence on the differentiation of cells in the meso- and ectodermal directions. ●

This work was partially supported by Grants from the Ministry of Education and Science of the Russian Federation (project no. 02.512.12.2013) and the Russian Foundation for Basic Research (project no. 09-04-01117).

REFERENCES

1. Grivennikov I.A. // Progress in Biological Chemistry. 2008. V. 48. P. 181-220.
2. Novosadova E.V., Manuilova E.S., Arsenieva E.L., et al. // Cell Technologies in Biology and Medicine. 2005. N 3. P. 174-179.
3. Novosadova E.V., Manuilova E.S., Arsenieva E.L., et al. // Yu.A. Ovchinnikov Bulletin of Biotechnology and Physicochemical Biology. 2005. V. 1. N 2. P. 14-21.
4. Novosadova E.V., Manuilova E.S., Arsenieva E.L., et al. // Medical Genetics. 2008. N 8. P. 43-46.
5. Dhoot G., Perry S. // Exp. Cell. Res. 1978. V. 117. P. 357–370.
6. Fraichard A., Chassande O., Bilbaut G., et al. // J. Cell Sci. 1995. V. 108. P. 3181-3188.
7. Holtzinger A., Evans T. // Development. 2005. V. 132. P. 4005–4014.
8. Holtzinger A., Evans T. // Dev. Biol. 2007. V. 312. P. 613–622.
9. Jiang Y., Henderson D., Blackstad M., et al. // Proc. Natl. Acad. Sci. U.S.A. 2003. V. 18. P. 11854-11860.
10. Keller G. // Genes & Dev. 2005. V. 19. P. 1129-1155.
11. Lloberas J., Solier C., Celada A. // Immunol. Today. 1999. V. 20. P. 184-189.
12. Peterkin T., Gibson A., Patient R. // EMBO J. 2003. V. 22. P. 4260–4273.
13. Peterkin T., Gibson A., Patient R. // Dev. Biol. 2007. V. 311. P. 623–635.
14. Reiter J., Alexander J., Rodaway A., et al. // Genes Dev. 1999. V. 3. P. 2983–2995.
15. Reymond A., Meroni G., Fantozzi A., et al. // EMBO J. 2001. V. 20. P. 2140-2151.
16. Tarantul V.Z., Nikolaev A.I., Martynenko A., et al. //AIDS Res. Hum. Retroviruses. 2000. V. 16. P. 173-179.
17. Tarantul V., Nikolaev A., Hannig H., et al. // Neoplasia. 2001. V. 3. P. 132-142.
18. Torok M., Etkin L. // Differentiation. 2000. V. 67. P. 63-71.
19. Zhao R., Watt A.J., Battle M.A., Li J., Bondow B.J., Duncan S.A. // Dev. Biology. 2008. V. 317. P. 614-619.

Cell Phenotypes in Human Amniotic Fluid

D.A. Davydova[a,*], E.A.Vorotelyak[a], Yu.A. Smirnova[a], R.D. Zinovieva[a], Yu.A. Romanov[b], N.V. Kabaeva[b], V.V. Terskikh[a], and A.V. Vasiliev[a]
[a] Koltzov Institute of Developmental Biology, Russian Academy of Sciences, Moscow
[b] Russian Cardiology Research-and-Production Complex, Moscow
*E-mail: davydovad@gmail.com

ABSTRACT Stem cells capable of long-term proliferation and differentiation into different cell types may be a promising source of cells for regenerative medicine. Recently, much attention has been paid to fetal stem cells, among which are cells from amniotic fluid (AF). We have isolated amniotic stem cells from 3 AF samples. Flow cytometry, RT-PCR and immunohistochemistry have shown that these cells express mesenchymal (CD90, CD73, CD105, CD13, CD29, CD44, and CD146), neural (β_3-tubulin, Nestin, and Pax6), epithelial (keratin 19 and p63) markers and also markers of pluripotency (*Oct4, Nanog, and Rex-1).* Transplantation of the cells to nude mice does not lead to tumor formation. Thus, putative stem/progenitor cells from AF are capable of long-term proliferation *in vitro* and the profile of gene expression led us to speculate that they have greater differentiation potential than mesenchymal stem cells and may be useful for cell therapy.
Keywords: amniotic fluid, cell culture, epithelial markers, mesenchymal stem cells, neural markers, stem cells.
Abbreviations: amniotic fluid (AF); mesenchymal stem cells (MSCs); embryonic stem cells (ESCs).

INTRODUCTION

AF has been used in prenatal diagnosis of genetic diseases for more than 70 years (Baranov and Kuznetsova, 2007). It contains a heterogeneous population of cells, which includes cells from fetal skin, respiratory, digestive, and urinary tracts, as well as cells from the amniotic membrane. Most of these cells are differentiated and have a low proliferative potential (Siddiqyi and Atala, 2004; Tsai *et al.*, 2006). Recent data seem to indicate that AF contains cells which can proliferate for extended periods of time and can differentiate *in vitro* into different cell types. Based on the fact that these cells express such markers as CD73, CD90, CD105, CD44, and CD29, several researchers consider them as MSCs (Tsai *et al.*, 2004; Sessarego *et al.*, 2008). Interestingly, cells isolated from AF express neural markers, such as Nestin, β_3-tubulin, GFAP, NEFH, as well as several markers of ESCs, such as SSEA-4, Oct4, and Nanog (Prusa *et al.*, 2003; Siddiqyi and Atala, 2004; Tsai *et al.*, 2006). These cells exhibit osteogenic, adipogenic, myogenic and neural differentiation; they can also differentiate into hepatocytes and endothelial cells (Tsai *et al.*, 2004; Delo *et al.*, 2006; Tsai *et al.*, 2006; De Coppi *et al.*, 2007; Perin *et al.*, 2008; You *et al.*, 2008; Zheng *et al.*, 2008). Thus, the available data suggest, on the one hand, that cells from AF are intermediate in their differentiation potential (between embryonic and adult stem cells) and, on the other hand, the possibility that AF culture contains several distinct cell types (i.e. population heterogeneity). In order to assess this possibility, a further detailed investigation of the population structure is needed, which implies extensive data on the gene expression profile.

Obtaining AF is a very simple and safe procedure; the cells from AF are relatively easy to isolate and cultivate, and they show little immunogenicity and higher proliferative potential than that of adult stem cells. Also, AF cells can differentiate into the derivatives of the three germ layers and do not form teratomas after transplantation. All these facts suggest that AF can be an alternative source of stem cells for cell therapy (Prusa *et al.*, 2003; Delo *et al.*, 2006; Trounson, 2007). Also, the possibility of obtaining cells which express several pluripotency markers evade the ethical concerns arising in human ESCs research.

The goal of this study was to investigate the proliferative potential of cells isolated from AF and to analyze the expression of certain tissue-specific genes and stem cell markers.

MATERIALS AND METHODS

AF CELL CULTURE

Samples of AF (10 ml) were obtained from three donors via amniocentesis performed at 16–20 weeks of pregnancy in Snegirev Obstetrics and Gynaecology Clinic, Moscow. The cells were collected by centrifugation (10 min, 1100 rpm) and cultured in α-MEM medium (Gibco, United States) supplemented with 15% ES-FBS (HyClone, United States), 1% glutamine (Invitrogen, United States), 18% Chang B and 2% Chang C (Irvine Scientific, United States), and 1% penicillin/streptomycin (Sigma, United States) at 37 °C with 5% humidified CO_2. Cells were replated at 1:3 every 2nd or 3rd day, when they grew to confluence.

FLOW CYTOMETRY

Expression of the surface antigens in AF cells (passage 7) was assessed using a flow cytometer (Becton Dickinson FACSCalibur, United States). The cells were trypsinzed and stained with fluorescein isothiocyanate- (FITC) or phycoerythrin- (PE) conjugated antibodies against CD13, CD29, CD44, CD106, CD73, CD54, CD45, CD34, CD146, CD90, CD105, CD71, HLA-A,B,C, and HLA-DR,DP,DQ (BD Pharmingen, United States). FITC- or PE-conjugated immunoglobulins of the same isotype were used as controls.

Mouse antibodies against keratin 19 (Millipore, United States) with secondary Alexa Fluor 488 (Molecular Probes, United States) antibodies were used to assay keratin expression. Staining without primary antibodies and isotypic controls were also performed.

RT-PCR

Total RNA extraction was performed with TRI® Reagent (Sigma, United States) in accordance with the manufacturer's protocol. mRNA was isolated by using magnetic beads (Sileks, Russia). The first cDNA strand was synthesized with the M-MLV reverse transcriptase (Sileks, Russia). cDNA libraries were normalized to the housekeeping gene RPL19. The PCR primers were constructed with DNAStar software and located in different exons. Information on the structure of the studied genes was obtained from the National Center for Biotechnology Information (NCBI, GeneBank, United States). Primer sequences are listed in Table 1. PCR with specific primers was performed with ColoredTaq-polymerase (Sileks, Russia) on a Mastercycler (Eppendorf, Germany). PCR fragments were separated by electrophoresis in 1% agarose gels and analyzed on a UV gel analyzer (®BIO RAD, United States).

IMMUNOHISTOCHEMISTRY

Cells for immunohistochemistry were taken at the 11th passage, fixed with 4% paraformaldehyde and incubated overnight at +4°C with antibodies against CD34 (mouse, 1:200, Millipore, United States), CD105 (mouse, 1 : 50; Millipore, United States), CD49d (mouse, 1 : 50, Millipore, United States), STRO-1 (rabbit, 1 : 100, R&D Systems, United States), keratin 14 (mouse, 1:20, Novocastra, Germany), keratin 19 (mouse, 1 : 50; Millipore, United States), p63 (mouse, 1 : 50; BD Pharmingen, United States), β_3-tubulin (mouse, 1:300, Millipore, United States), NF (Neurofilament) (mouse, 1:10, ICN, United States), Pax6 (mouse, 1:100, Millipore, United States). After that, the cells were washed with PBS and incubated with secondary Alexa Fluor 488 or Alexa Fluor 546 antibodies (Molecular Probes, United States) at room temperature for 1 h. Cell nuclei were stained with DAPI (VECTASHIELD mounting medium for fluorescence with DAPI, Vector Laboratories, United States).

IMMUNODEFICIENT ANIMAL TRANSPLANTATION

In order to study the ability of AF cells to form teratomas, immunodeficient Nude mice were used (Pushino animal nursery). The animals were subcutaneously injected with 3×10^6 5th passage cells suspended in 100 microliters of serum-free α-MEM medium (suspension concentration 30×10^6 cells/ml). Control animals were injected with 100 microliters of suspension of 2nd passage stem cells from human adipose tissue (45×10^6 cells/ml) (negative control) and 100 microliters of 65th passage mouse ESCs suspension (20×10^6 cells/ml) (positive control). Each group consisted of three animals. Animals were withdrew from the experiment when tumors were detected (positive control) or 11 weeks after injection (experimental group and negative control). Tumors and animal organs (liver, kidney, spleen, heart, lung, and testicle) were analyzed histologically.

RESULTS AND DISCUSSION

AF CELL CULTURE

Three samples of AF from three donors were used in this study. Cultivation was performed in 24-well plates in Chang medium, following the previously described protocol (De Coppi *et al.*, 2007) with modifications.

Centrifugation of AF yielded a heterogeneous population of cells, most of which were flat epithelial cells. Small round cells were a minority. The flat epithelial cells did not adhere to plastic and were eliminated from the culture after the first medium change on day 5-7. However, round cells did adhere to plastic and formed small colonies differing in size and morphology (Fig. 1). Most colonies consisted of fibroblastic cells; however some consisted of epithelioid cells. After the first medium change, the fibroblastic cell colonies started to proliferate actively, while the colonies with epithelioid cells did not change noticeably. Four to six days after the medium change, when the cells formed a subconfluent layer, the culture was replated; this did not lead to the formation of colonies. Cells distributed evenly on the bottom of the well and grew to confluence in 2–3 days. After passaging, the culture comprising only fibroblastic and epithelioid cells were no longer observed.

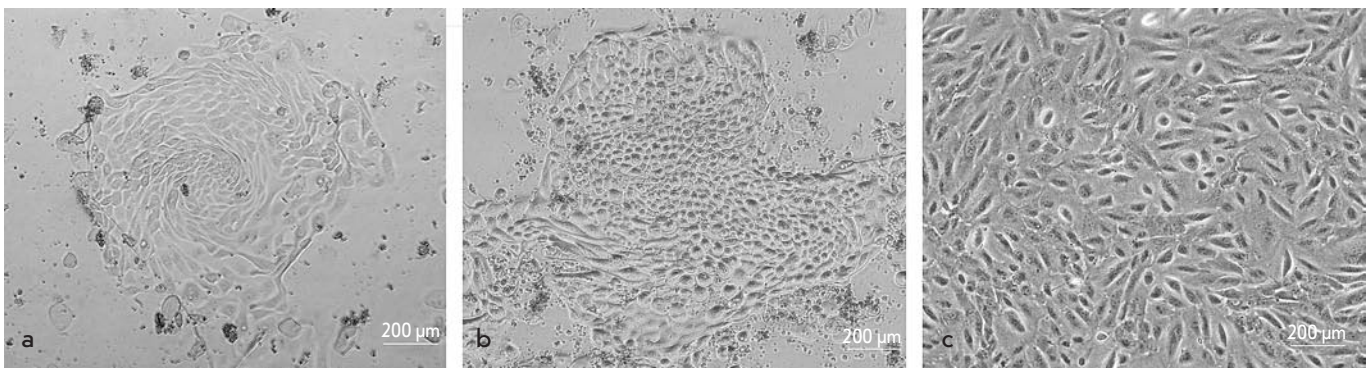

Fig. 1. AF cells in culture. (a) Primary fibroblastic cell colony on day 9 of culture. (b) Primary epithelioid cell colony on day 9 of culture. (c) Cells grew to confluence in the 8th-passage culture. (a, b, c) Light field

Table 1. Primers

Gene	Primer sequence
Rpl19	5' agggtacagccaatgcccga 3' 5' ccttggataaagtcttgatgatc 3'
CD90	5'acctggccatcagcatcgct3' 5'gaaatccgtggcctggagga 3'
β_3-tubulin	5'cagtgcggcaaccagatcgg 3' 5'caggtcagcgttgagctggc 3'
Nestin	5' aggaggatgtaccaccagtgc 3' 5' caccaatgatgtctgcccct 3'
Nucleostemin	5'gcatgacctgccataagcgg3' 5'ctgtccactctggacaatggc3'
Pax6	5' gtcatcaataaacagagttcttc 3' 5' cgattagaaaaccatacctgtat 3'
Keratin 19	5'gatcgaaggcctgaaggaag3' 5'atgctcagctgtgactgcag3'
p63	5'gagccgtgaattcaacgagg3' 5'tccgaaacttgctgctttctg3'
CD117 (c-kit)	5'gtgggcgacgagattaggctg3' 5'cgcgtttcacactttgatcatg3'
Oct4	5'cgaccatctgccgctttgag3' 5'ccccctgtcccccattccta3'
Nanog	5'gtgtggatccagcttgtccc 3' 5'ctgcgtcacaccattgctattc 3'
Rex1	5'gctggagcctgtgtgaacag3' 5'atcacataaggcccacaccg3'
Stella	5'gcctagtgttgtgtcaagac3' 5'ggtgcaagaataagatttatggc3'
Sox2	5'acagcccggaccgcgtcaag 3' 5'tctgcgagctggtcatggag 3'

Table 2. Flow cytometry analyses of marker expression in AF cells

Marker	Flow cytometry[a]
CD 90 (Thy-1)	83% - 58% - 70%
CD 73 (SH3,SH4)	99% - 99% - 96%
CD 105	85% - 89% - n/s
CD 13	99% - 98% - 87%
CD 29 (integrin β_1)	99% - 99% - 99%
CD 44	99% - 99% - 98%
CD 106 (VCAM-1)	- - -
CD 54 (ICAM-1)	43% - 60% - n/s
CD 146	99% - 98% - 90%
CD 71	36% - 32% - n/s
CD 34	- - -
CD 45	- - -
Keratin 19	92% - 70% - 88%
HLA-A,B,C	95% - 87% - 65%
HLA- DR,DP,DQ	- - -

[a] *This column quotes the percentage of cells positive for this marker in the three cultures, respectively; (-) no expression; and (n/s) was not studied .*

Three groups of AF cells may be distinguished according to their morphology: epithelioid, amniotic fluid-specific, and fibroblastic cells (Prusa and Hengstschlager, 2002; Tsai *et al.*, 2004). The first group and the second one appear at the beginning of cultivation, and the third one appears later. The epithelioid cells quickly disappear, while the other two types persist in the culture. Many authors believe that the fibroblastic cells are stem cells and, taking into account the expression of mesenchymal markers and the spectrum of possible differentiations, place them into the MSCs category. However, other cells besides the fibroblastic cells can remain in the culture. These amniotic fluid-specific cells produce estrogen, progesterone, and chorionic gonadotropin. It seems that these cells originate from the trophoblast and the amniotic membrane. Thus, the question of amniotic stem cells origin is still unresolved (Prusa and Hengstschlager, 2002; Tsai *et al.*, 2004).

It is worth noting that we analyzed fast-adherent cells, as well as cells with delayed adhesion, because the first medium change was performed only 5–7 days after inoculation. Other researchers report slowly adhering cells (Tsai *et al.*, 2004) and a mixed population, which was later selected for c-kit expres-

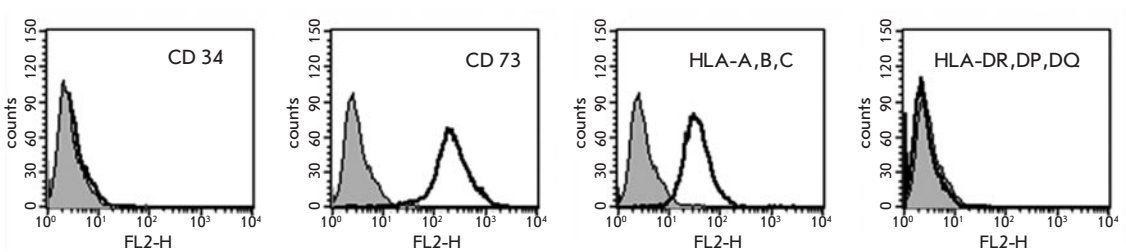

Fig. 2. The results of flow cytometry analyses of CD34, CD73, HLA-A,B,C and HLA-DR,DP,DQ expression

sion (Delo *et al.*, 2006; De Coppi *et al.*, 2007; Perin *et al.*, 2008). Some authors suggest that just c-kit positive cells in AF are pluripotent. Nevertheless, slowly adhering cells are also characterized by a wide range of markers and can differentiate into different types of cells.

It has been demonstrated that stem cells isolated from AF can undergo 350 population doublings maintaining their undifferentiated state, high proliferative potential, clonogenicity, and telomere length (Siddiqyi and Atala, 2004; Delo *et al.*, 2006; Perin *et al.*, 2008). The maximum number of passages can reach 42 (Wang *et al.*, 2008). We have obtained three cultures from three donors. Currently, they have been cultivated to 20, 18, and 15 passages. According to a karyological analysis performed in a genetic laboratory, the fetuses did not exhibit any karyotype abnormality.

PHENOTYPE CHARACTERIZATION ACCORDING TO MOLECULAR MARKER EXPRESSION

Flow cytometry shows that cells from AF express the mesenchymal markers CD90, CD73, CD105, CD13, CD29, CD44, CD146, CD54, and CD71 (weak expression) and do not express CD106, CD34, or CD45 (Table 2, Fig. 2). These data suggest that fetal MSCs are present in our cultures. Judging by flow cytometry, the absence of CD34 and CD45 expression shows that there are no hemopoietic stem/progenitor cells in the culture. These results are in accordance with other authors, who report that hemopoietic stem cells are numerous in AF at the beginning of pregnancy (7–12 weeks). It seems that these cells get there through the thin wall of the yolk sac, where hemopoiesis is active at that time (Torricelli *et al.*, 1993). At the usual time of amniocentesis (16–20 weeks), these cells are no longer present in AF (Siddiqyi and Atala, 2004; De Coppi *et al.*, 2007; Perin *et al.*, 2008; Sessarego *et al.*, 2008). Keratin 19 was one of the epithelial markers discovered by flow cytometry and immunohistochemistry. Of the antigens of the major histocompatibility complex, (MHC), HLA-A,B,C were present and HLA-DR,DP,DQ were not, which is in accordance with the expression profiles of MSCs and AF cells (In't Anker *et al.*, 2004; Tsai *et al.*, 2004; Sessarego *et al.*, 2008; Zheng *et al.*, 2008).

Immunohistochemical analysis shows that AF cells express not only mesenchymal markers such as CD105, STRO-1, and CD49d, but also neural (neuronal cytoskeleton marker β_3-tubulin, mature neuron neurofilament NF, and transcription factor Pax6) and epithelial markers (keratin 19, transcription factor p63) (Table 3, Fig. 3). Keratin 14, which is a marker of cornified epidermis, was not found in AF cells. Notably, more than 70% of the cells express keratin 19, and 80% also express the mesenchymal CD105 marker, and more than 95% express CD73. This suggests that a major portion of the cell population can express both mesenchymal and epithelial markers simultaneously. These data must be proven by alternative methods. It was demonstrated earlier that AF cell clones can express neural and mesenchymal markers simultaneously (Tsai *et al.*, 2006). On the other hand, expression of neural markers in MSCs is also found (Corti *et al.*, 2003; Wislet-Gendebien *et al.*, 2004; Bertani *et al.*, 2005). However, keratin 19 expression is not character-

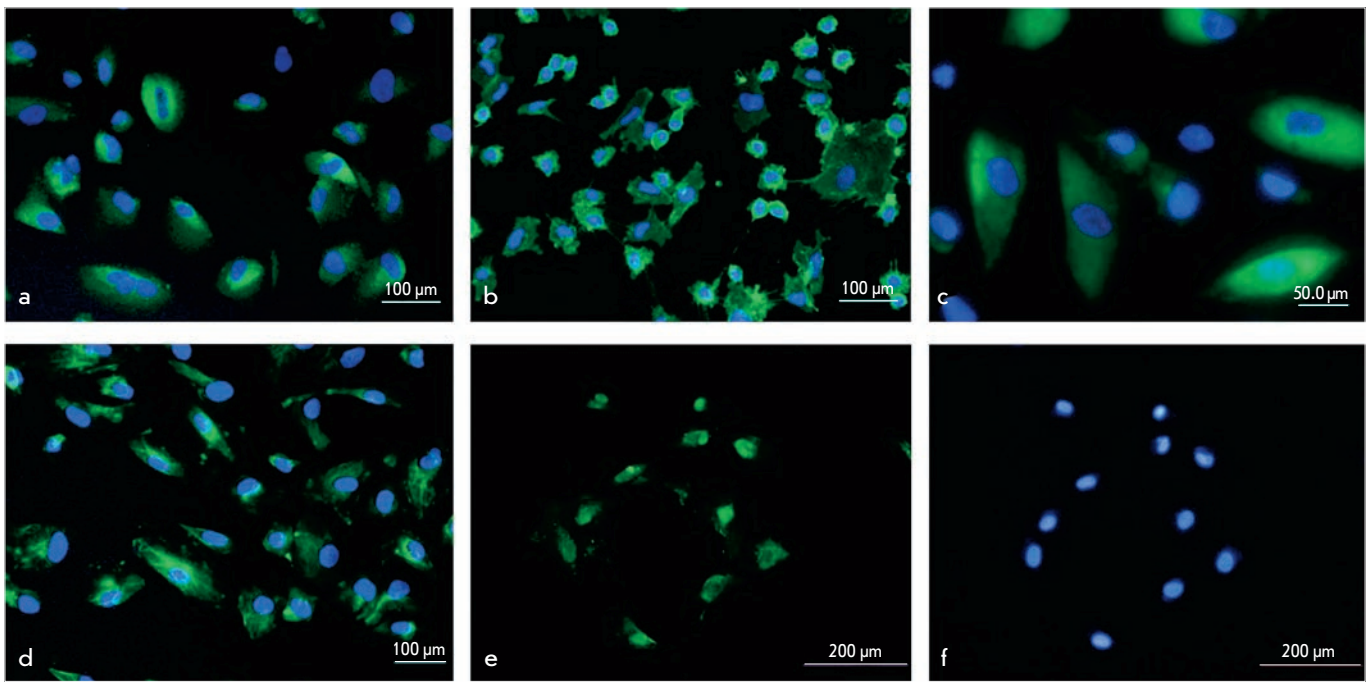

Fig. 3. Immunohistochemical analyses of mesenchymal, neural and epithelial markers expression in cultured AF cells. Stained with antibodies against (a) CD105; (b) CD49d; (c) β_3-tubulin; (d) keratin 19; (e) p63; (f) the same field, nuclei stained with DAPI. (a, b, c, d) Merge, nuclei stained with DAPI

stic of mesenchymal cells. Thus, our data do not support the opinion that AF cells are fetal MSCs.

RT-PCR data confirm that AF cells express the markers of mesenchymal (CD90), neural (β_3-tubulin, Nestin, Nucleostemin, Pax6), and epithelial (keratin 19, p63) lineages (Fig. 4). Also, RT-PCR detects the surface marker *c-kit*, homeobox gene *Pitx2*, and several ESCs markers (*Oct4*, *Nanog*, and *Rex-1)*. These results and previous data (Siddiqyi and Atala, 2004; Tsai *et al.*, 2006; De Coppi *et al.*, 2007) suggest a more primitive status of amniotic stem cells when compared to adult stem cells, as well as their wide differentiation potential. However, pluripotency markers such as *Sox2* and *Stella* were not detectably expressed in AF cells. These data probably suggest that the potential of the studied cells is less than that of ESCs, and this might be the reason why AF cells do not form teratomas after *in vivo* transplantation.

TRANSPLANTATION OF CELLS INTO IMMUNODEFICIENT ANIMALS

Teratomas were not observed even 11 weeks after transplantation of cultured human AF cells into immunodeficient mice. Under the same conditions, human ESCs caused teratoma formation after 3–4 weeks. These results are in agreement with data, which show that the *in vivo* transplantation of a large number (up to 8×10^6) of AF cells does not cause teratoma formation (De Coppi *et al.*, 2007; Trounson, 2007). Furthermore, it was shown that even seven months after the intravenous injection of these cells, experimental animals had no detectable tumors (Carraro *et al.*, 2008).

Animals in the experimental group had no detectable organ abnormalities upon histological examination.

Thus, we have obtained cell cultures from three AF donors. These cells are characterized by a wide spectrum of marker expression, including mesenchymal, neural, epithelial, and pluripotency markers.

Taking into account their morphology, cell culture behavior, and expression of multiple mesenchymal cell markers, one would assume that AF is a source of MSCs which are currently being discovered in many tissues (Campagnoli *et al.*, 2001; Hu *et al.*, 2003; Romanov *et al.*, 2003). There is data showing that MSCs can also express neural markers. On the other hand, the data obtained on the expression of epithelial markers suggests that the culture may either be heterogeneous or that AF cells may have a special differentiation status, which seems to be confirmed by the expression of pluripotency markers. We plan to investigate these possibilities in the future.

Current data on marker expression, differentiation potential of AF cells, and the absence of teratoma formation after *in vivo* transplantation leads us to the opinion that these cells are promising in the field of cell therapy. We suggest that AF cells can be useful for restoring spinal cord damage, treating diabetes, Alzheimer's disease, heart attack damage, etc. (Hampton, 2007). These cells can be used not only for autografts, but also for allografts, because the cells are only mildly immunogenic and donor-recipient pairs can be matched. Also, as opposed to other extraembryonic tissues (placenta, amniotic membrane, and umbilical blood) which are available only postnatally, AF cells can be obtained at 16–20 weeks of pregnancy. This suggests the possibility of treating developmental defects *in utero* or immediately after birth (Marcus, Woodbury, 2008; Ye *et al.*, 2009). ●

Table 3. Immunohistochemistry analyses of marker expression in AF cells

Marker	Immunohistochemistry
CD 49d (integrin α_4)	+
CD 105	+
STRO-1	+
CD 34	-
Pax6	+
NF	+
β_3-tubulin	+
Keratin 19	+
Keratin 14	-
p63	+

(+) marker expression detected; (–) marker expression not detected.

This work was supported by Grant from Russian Foundation for Basic Research (project 09-04-12132-ofi-m).

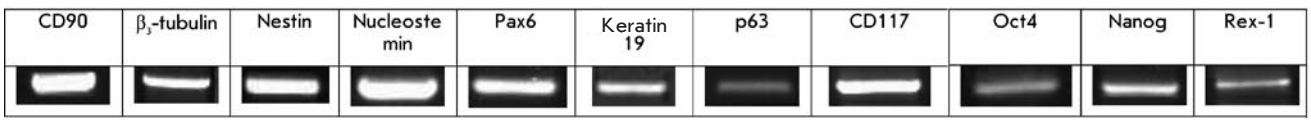

Fig. 4. Expression of differentiation and stem cell markers determined by RT-PCR

REFERENCES

1. Baranov V. S., Kuznetsova T. V. 2007. Cytogenetics of Human Embryonic Development. St. Petersburg, *N-L*, 639 p.
2. Bertani N., Matatesta P., Volpi G., Sonego P., Perris R. 2005. Neurogenic Potential of Human Mesenchymal Stem Cells Revisited: Analysis by Immunostaining, Timelapse Video and Microarray. *Journal of Cell Science*. 118: 3925-3936.
3. Campagnoli C., Roberts I. A., Kumar S., Bennett P. R., Bellantuono I., Fisk N. M. 2001. Identification of Mesenchymal Stem/Progenitor Cells in Human First-Trimester Fetal Blood, Liver and Bone Marrow. *Blood*. 98: 2396-2402.
4. Carraro G., Perin L., Sedrakyan S., Giuliani S., Tiozzo C., Lee J., Turcatel G., De Langhe S. P., Driscoll B., Bellusci S., Minoo P., Atala A., De Filippo R. E., Warburton D. 2008. Human Amniotic Fluid Stem Cells Can Integrate and Differentiate into Epithelial Lung Lineages. *Stem Cells*. 26 (11): 2902-2911.
5. Corti S., Locatelli F., Strazzer S., Guglieri M., Corni G. P. 2003. Neuronal Generation from Somatic Stem Cells: Current Knowledge and Perspectives on the Treatment of Acquired and Degenerative Central Nervous System Disorders. *Curr. Gene Ther.* 3: 247-272.
6. De Coppi P., Bartsch G., Jr, Siddiqui M. M., Xu T., Santos C. C., Perin L., Mostoslavsky G., Serre A. C., Snyder E. Y., Yoo J. J., Furth M. E., Soker S., Atala A. 2007. Isolation of Amniotic Stem Cells with Potential for Therapy. *Nature Biotechnology*. 25 (1): 100-106.
7. Delo D. M., De Coppi P., Bartsch G., Jr, Atala A. 2006. Amniotic Fluid and Placental Stem Cells. *Methods in Enzymology*. 419: 426-438.
8. Hampton T. 2007. Stem Cells Obtained from Amniotic Fluid. *JAMA*. 297 (8): 795.
9. Hu Y., Liao L., Wang Q., Ma L., Ma G., Jiang X., Zhao R.C. 2003. Isolation and Identification of Mesenchymal Stem Cells from Human Fetal Pancreas. *J. Lab. Clin. Med.* 141: 342-349.
10. In't Anker P. S., Scherjon S. A., Kleijburg-van der Keur C., de Groot-Swings G. M.J. S., Claas F. H. J., Fibbe W. E., Kanhai H. H. H. 2004. Isolation of Mesenchymal Stem Cells of Fetal or Maternal Origin from Human Placenta. *Stem Cells*. 22: 1338-1345.
11. Marcus A. J., Woodbury D. 2008. Fetal Stem Cells from Extra-Embryonic Tissues: Do Not Discard. *J. Cell. Mol. Med.* 12 (3): 730-742.
12. Perin L., Sedrakyan S., Da Sacco S., De Filippo R. 2008. Characterization of Human Amniotic Fluid Stem Cells and Their Pluripotential Capability. *Methods in Cell Biology*. Burlington, Elsevier Academic Press, 86: 85-99.
13. Prusa A-R., Hengstschlager M. 2002. Amniotic Fluid Cells and Human Stem Cell Research – A New Connection. *Med. Sci. Monit.* 8 (11): 253-257.
14. Prusa A-R., Marton E., Rosner M., Bernaschek G., Hengstschlager M. 2003. Oct4-Expressing Cells in Human Amniotic Fluid: A New Source for Stem Cell Research? *Human Reproduction*. 18 (7): 1489-1493.
15. Romanov Y. A., Svintsitskaya V. A., Smirnov V. N. 2003. Searching for Alternative Sources of Postnatal Human Mesenchymal Stem Cells: Candidate MSC-Like Cells from Umbilical Cord. *Stem Cells*. 21: 105-110.
16. Sessarego N., Parodi A., Podestà M., Benvenuto F., Mogni M., Raviolo V., Lituania M., Kunkl A., Ferlazzo G., Bricarelli F. D., Uccelli A., Frassoni F. 2008. Multipotent Mesenchymal Stromal Cells from Amniotic Fluid: Solid Perspectives for Clinical Application. *Haematologica*. 93 (3): 339-346.
17. Siddiqui M.M., Atala A. 2004. Amniotic Fluid-Derived Pluripotential Cells. *Handbook of Stem Cells*. Burlington, Elsevier Academic press, 2: 175-179.
18. Torricelli F., Brizzi L., Bernabei P. A., Gheri G., Di Lollo S., Nutini L., Lisi E., Di Tommaso M., Cariati E. 1993. Identification of Hematopoietic Progenitor Cells in Human Amniotic Fluid before the 12th Week of Gestation. *Ital. J. Anat. Embryol.* 98 (2): 119-126.
19. Trounson A. 2007. A Fluid Means of Stem Cell Generation. *Nature Biotechnology*. 25 (1): 62-63.
20. Tsai M-S., Lee J-L., Chang Y-J., Hwang S-M. 2004. Isolation of Human Multipotent Mesenchymal Stem Cells from Second-Trimester Amniotic Fluid Using a Novel Two-Stage Culture Protocol. *Human Reproduction*. 19 (6): 1450-1456.
21. Tsai M-S., Hwang S-M., Tsai Y-L., Cheng F-C., Lee J-L., Chang Y-J. 2006. Clonal Amniotic Fluid-Derived Stem Cells Express Characteristics of Both Mesenchymal and Neural Stem Cells. *Biology of Reproduction*. 74: 545-551.
22. Wang H., Chen S., Cheng X., Dou Z., Wang H. 2008. Differentiation of Human Amniotic Fluid Stem Cells into Cardiomyocytes through Embryonic Body Formation. *Chinese Journal of Biotechnology*. 24 (9): 1582-1587.
23. Wislet-Gendebien S., Bruyère F., Hans G., Leprince P., Moonen G., Rogister B. 2004. Nestin-Positive Mesenchymal Stem Cells Favour the Astroglial Lineage in Neural Progenitors and Stem cells by Releasing Active BMP4. *BMC Neuroscience*. 5: 33.
24. Ye L., Chang J.C., Lin C., Sun X., Yu J., Kan Y.W. 2009. Induced Pluripotent Stem Cells Offer New Approach to Therapy in Thalassemia and Sickle Cell Anemia and Option in Prenatal Diagnosis in Genetic Diseases. *Proc. Natl. Acad. Sci.* United States. 106 (24): 9826-9830.
25. You Q., Cai L., Zheng J., Tong X., Zhang D., Zhang Y. 2008. Isolation of Human Mesenchymal Stem Cells from Third-Trimester Amniotic Fluid. *Int. J. Gynecol.* Obstet.103 (2): 149-152.
26. Zheng Y.B., Gao Z.L., Xie C., Zhu H.P., Peng L., Chen J.H., Chong Y.T. 2008. Characterization of Hepatogenic Differentiation of Mesenchymal Stem Cells from Human Amniotic Fluid and Human Bone Marrow: A Comparative Study. *Cell Biology International*. 32 (11): 1439-1448.

Rules for authors

GENERAL PROVISIONS

Journal «Acta Naturae» publishes experimental research papers and reviews, and also discussion papers, mini-reviews, short communications, which are related to most topical problems of the fundamental and practical life sciences and biotechnologies.

Journal is published by Park Media Publishing Company in Russian and English languages.

Edition board of the journal «Acta Naturae» would like to ask authors to follow the following rules. Manuscripts, which are not consistent with those rules, will be sent back to authors without consideration.

The maximal size of review together with tables and references should not be more than 60 000 character (it is about 40 pages of A4 format and with 1.5 lines interval, Times New Roman, size 12), and 16 figures.

The size of experimental research paper should not exceed 30 000 characters, (20 pages of A4 format, including tables and references). The number of figures should not exceed 10. Papers of larger size could be accepted only in case of preliminary agreement with the editors.

Short communication should include task design, experimental data and conclusions. The size of short communication should not exceed 12 000 characters (8 pages of A4 format, including tables and references, no more than 12 references). Number of figures should not exceed 4.

Manuscript should be presented as a set of files: main test, summary, list of references, comments to figures, tables must be in Microsoft Word 2003 for Windows format, figures must be in JPG or TIF format, each figure should represented as a separate file.

Manuscript should be sent to editor board as an electronic version; it is possible to do it on a CD-ROM.

MANUSCRIPT DESIGN

Manuscript should have:

Title of the manuscript. It must not be very long or very short or low-informative. It should represent the main result, the essence and the novelty of the work.

Authors initials and surnames with the references to the organisations in which authors work. Author, which is responsible for the communication with the editorial board and correction, should be indicated by the reference, and his correspondent e-mail should be represented on the bottom of the first page.

Full name of the scientific organisation and agency.

Summary. Structure of summary must be very clear and reflect following: task design; experimental methods, possibility of the practical application, new possible tasks and problems. 20 lines.

Key words. Key words should reflect: the subject of research, method, object, specificity of this work.

Abbreviations.

Introduction.

Chapter «Experimental part».

Chapter «Results and discussion».

Chapter «Conclusions». At the end of this chapter names of organisations, that provided financial support, should be indicated (and in brackets number of grants should be indicated).

Chapter «References». References in text should be given in square brackets, for example [1].

RECOMMENDATION ABOUT TEXT FORMATTING:

We recommend using Microsoft Word 2003 for Windows editor.

Font should be Times New Roman, and standart size is 12.

Interval between lines is 1.5

We do not recommend using more that one space between words.

Strictly do not use automatic reference option, automatic hyphenation or automatic block of hyphenation, automatic list, automatic indention etc.

It is recommended to use Word for making tables (Table – Add Table) or MS Excel. Tables, which are created manually (by using a lot of empty spaces, but not cells), should not be used.

Always, it must be an empty space between surnames and initials: A.A. Ivanov (except from the names of authors in the title of the manuscript, in this situation empty spaces must be between initials as well, i.e A. A. Ivanov).

Everywhere in the text, except the date of manuscript's arrival, all dates should be in format "date. month.year", according the examples: 02.05.1991, 26.12.1874 and so on.

Do not use full stop after title of the manuscript, authors names, addresses, headings and subheading, titles of tables, comments to figures, dimensionalities (s for second, g for gram, min for minute, h for hours, d for days, º for degrees).

Full stop must be after: footnotes (and particularly in tables), comments to the table, short annotations, abbreviations (y. for years, t. melt. for the temperature of melting, but not for inferior indexes: T_{melt} for temperature of melting, $T_{ph.tr}$ for temperature of phase transition). Exception: mln for million does not need full stop.

For decimal fractions use full stops, but not commas (0.25, but not 0,25).

Dash «-» must be between two empty spaces, symbols for «minus», «interval» or «chemical bound» do not need to be between two empty spaces.

Use only «×» as a symbol for multiplication. Use symbol «×» only in case if there is a number in the right from his symbol. Symbol «·» is used for the complex compounds in chemical formulas, and also for the non-covalent complexes (DNA·RNA and so on)

Do not use inverted commas for quotes.

All numerical data should be represented as tables.

In formulas, use the letters of Latin and Greek alphabets.

Latin names of genera and species must be in italic font, for higher taxons use regular font. For the names of viruses and bacteriophages in Latin transcription use regular font.

Names of genes (except the yeast genes) should be in italic font, for names of proteins use regular font.

Names of nucleotides (A, T, G, C, U), amino acid residues (Arg, Ile, Val etc.) and phosphates (ATP, AMP etc) should be written in Latin transcription using regular font.

Numeration of nucleotides and amino acid residues should be written without hyphen (T34, Ala89).

Use international system of units SI for measurement units.

For molecular mass, use daltons (da, kda, mda).

For the number of nucleotide pair, use abbreviations (b.p, t.b.p.).

Biochemical terms (and particularly, names of enzymes) should be according the international rules of IUPAC.

Using of abbreviations of terms in the text should be minimized.

Repetition of the same data in text, tables and graphs is not allowed.

RULES FOR ILLUSTRATIONS

Figures for manuscripts should be represented as separate files.

The resolution of illustrations must be 300 dpi or higher for the colourful or halftone pictures, and 600 dpi for the black-white illustrations.

It is not allowed to keep in files the ways of clipping paths that are not in use, and also to keep additional channels (Path and Alpha Channel), and also to use additional layers.

File's formats should be in Adobe Photoshop up to version 7.0. (including this version), TIFF, JPG.

REVIEWING, PREPARATION TO PUBLISHING, AND THE QUEUE FOR PUBLICATION

Papers will be published accordingly to the process of receiving. The queue for the publications will be established accordingly to the date of approval for publication. Members of Editorial Board have a right to recommend the papers, which were classified as a high priority and had high marks of reviewers, to the faster publication. Manuscripts, which arrived to Editorial Board, are reviewed by the experts from Editorial Board, and, if it is required, could be sent to the external review.

The prerogative of Editorial Board is to choose the reviewer. The manuscript will be sent to the review of the experts in this area of research, and the Editorial Board will make a decision about the fate of this manuscript: it could be accepted as it is, it could need an improvement and it could be rejected.

If manuscript does not fit to the above requirements, it could be rejected by the decision of Editorial Board.

If manuscript was sent back to authors for improvement as a decision of reviewers and editors, it will be reviewed second time, and after that Editorial Board will consider the possibility of the publication of this manuscript again. The date of the arrival of manuscript and the date of the acceptance of this manuscript to publishing will be indicated at the beginning of the paper.

Returning of the manuscript for improvement back to the authors does not mean that this manuscript is accepted to publishing. After improvement, this manuscript will be considered by Editorial Board again. The author should return back the text after improvement together with the original variant of manuscript and also with the answers to all of the comments. The date of arrival of the final version of the manuscript to Editorial Board is considered as date of arrival of the manuscript.

The improved manuscript should arrive back to Editorial Board during 1 week after author accepted comments; otherwise this manuscript will be considered as a newly arrived.

Editorial Board uses e-mail on the all of the steps of the communication with authors; authors must be very careful with the e-mail that is indicated in the manuscript, and in case of any changes immediately provide the information about changes to the Editorial Board.

After the approval of the layout of the journal, Editorial Board will send the proofreading to authors via e-mail in the PDF file.

On the step of correction, it is not possible to change the text, figures of tables. If it is necessary, this question will be considered by Editorial Board.

REFERENCES FORMAT

For books: author's surname and initials, full name of the book, the place og publishing, publishing company, year of publication, volume or issue and total number of pages.

For periodical issues: author's surname and initials, the name of the journal, year of publication, volume, number, firs and last page of the paper.

Bressanelli S., Tomei L., Roussel A., et al// Proc. Natl. Acad. Sci. USA. 1999. V. 96. P,13034–13039 (if there are more than 5 authors), and all authors, if there are less than 5 authors.

References to the author's abstracts of the dissertations should contain author's surname and initials, title of the dissertation, the place were work was done, year of the dissertation's defence.

References to patents should contain surnames and initials of authors, the type of the patent's document (certificate of recognition or patent), number, the name of the country in which document was issued, index of international classification of inventions, year of the patent's issue.

The list of references should be represented on the separate page.

Tables should be represented on the separate page.

Comments to figures should be represented on the separate page.

For the communication with Editorial Board, use e-mail addresses: rpetrov@strf.ru, vera.knorre@gmail.com, vsychev@strf.ru, tel.: (495) 727-38-60, (495) 930-80-05